Targeted Sensors to Monitor Oxidative Stress in the Endoplasmic Reticulum

A thesis submitted to the University of Glasgow for the degree of Ph.D

Rachel E. Martin

Institute of Molecular, Cell and Systems Biology
College of Medical, Veterinary and Life Sciences
University of Glasgow

2014

Abstract

Hydrogen peroxide has a diverse array of functions in cells. Not only as a mediator of oxidative stress, it is also involved in signalling in many pathways including tyrosine phosphorylation, sumoylation, proliferation and differentiation and cysteine oxidation [1]. There are a number of different producers of hydrogen peroxide in the cell including the NADPH oxidase (Nox) family of enzymes [2], the electron transport chain in the mitochondria [3] and disulfide bond formation in the endoplasmic reticulum (ER) [4]. In order to prevent a toxic build-up of hydrogen peroxide the cell also deploys a range of antioxidant enzymes including catalase, the glutathione peroxidases (GPxs) and the peroxiredoxins (Prxs) [5]. Therefore at all times a balance must be maintained to allow enough hydrogen peroxide production to allow for signalling to occur but at the same time ensuring the concentration does not increase enough to cause any oxidative damage.

Oxidative damage is associated with aging in general and diseases including cancer, cardiovascular disorders and neurodegenerative diseases. For such diseases to occur the balance of hydrogen peroxide production and removal must be tipped and it is the elucidation of these processes with regards to the ER that we hope to achieve.

We present the development and use of a novel sensor, BGB, which specifically detects hydrogen peroxide in the ER. BGB works in conjunction with the SNAP-tag system to allow specific targeting of a small molecule probe to the ER. BGB is selective for hydrogen peroxide over other reactive oxygen species due to the use of a boronic acid group as the reactive moiety. We have developed MALDI-TOF mass spectrometry methods for quantitative analysis of this probe when used both *in vitro* and *in cellulo*.

Also included is the development of Pep-B, a probe which was designed to measure hydrogen peroxide in the ER, but using a peptide targeting system rather than SNAP-tag, an investigation into the synthesis of a fluorophore based probe and the development of an alternative method of analysis of BGB using an antibody based system which negates the requirement of MALDI-TOF.

Contents

1.0 Lists of Figures, Tables and Equations

2.0 Acknowledgements

3.0 Declaration

I declare that, except where explicit reference is made to the contribution of others, that this thesis is the result of my own work and has not been submitted for any other degree at the University of Glasgow or any other institution.

4.0 List of Abbreviations

AGT - O^6-Alkylguanine-DNA-alkyltransferase

APQ8 - Mammalian aquaporin 8

ASK-1 - Signal regulating kinase-1

AtTIP1 - Arabidopsis aquaporin

ATR - Attenuated total reflectance

BGB - Benzylguanine-boronate

BG-Fura-A – Benzylguanine-Fura-amine

BG-Fura-B – Benzylguanine-Fura-boronate

BG-Fura-P - Benzylguanine-Fura-phenol

BG-NBD-X - Benzylguanine-NBD-X

BGP - Benzylguanine-phenol

BiFC - Bimolecular fluorescence complementation

BSA - Bovine serum albumin

CDCl$_3$ - Deuterated chloroform

CHCA - α-Cyano-4-hydroxycinnamic acid

CNBr - Cyanogen bromide

ConA - Concanavalin A

DABCO - 1,4-diazabicyclo[2.2.2]octane

DCF - Dichlorofluorescein

DCFH - Reduced dichlorofluorescein

DCM - Dichloromethane

DHB - 2,5-Dihydroxybenzoic acid

DMEM - Dulbecco's Modified Eagle medium

DMSO - Dimethylsulfoxide

DTT - Dithiothrietol

Duox - Dual oxidase

ELISA - Enzyme-linked immunosorbent assay

EndoH - Endoglycosidase H

ER - Endoplasmic Reticulum

Ero1 - ER oxidoreductin 1

EtOAc - Ethyl acetate

EtOH - Ethanol

GFP - Green fluorescent protein

GPx - Glutathione peroxidase

GSH - Glutathione

GSSG - Glutathione disulfide

HA - Hemagglutinin

HPLC - High performance liquid chromatography

IEF - Isoelectric focussing

IPTG - Isopropyl β-D-1-thiogalactopyranoside

IR - Infra-red

ISC - Intersystem crossing

KLH - Keyhole limpet hemocyanin

LB - Luria broth

MALDI-TOF - Matrix-assisted laser desorption ionisation - time of flight

MeOD - Deuterated methanol

MeOH - Methanol

MS - Mass spectrometry

NBD-X - 6-(*N*-(7-Nitrobenz-2-oxa-1,3-diazol-4-yl)amino) hexanoate

NMR - Nulcear magnetic resonance

Nox - NADPH oxidase

OST - Oligosaccharyltransferase

PBS - Phosphate buffered saline

PDI - Protein disulfide isomerase

PEG - Polyethyleneglycol

PEI - Polyethyleneimine

PF1 - Peroxyfluor-1

PG1- Peroxy green 1

PR1 - Peroxyresorufin-1

PTP - Protein tyrosine phosphatase

PX1 - Peroxyxanthone-1

Prx - Peroxiredoxin

SDS-PAGE - Sodium dodecyl sulfate polyacryalamide gel electrophoresis

SNAP-B - BGB conjugated to SNAP-tag

SNAP-Fura-A - BG-Fura-B conjugated to SNAP-tag

SNAP-Fura-B – BG-Fura-B conjugated to SNAP-tag

SNAP-Fura-P – BG-Fura-P conjugated to SNAP-tag

SNAP-NBD-X – BG-NBD-X conjugated to SNAP-tag

SNAP-P - BGP conjugated to SNAP-tag

SOH - Sulfenic acid

SO₂H - Sulfinic acid

SO₃H - Sulfonic acid

SPG1 - SNAP-Peroxy Green 1

SPG2 - SNAP-Peroxy Green 2

SUMO - Small ubiquitin-like modifier

TC - Tetracysteine

TCA - Trichloroacetic acid

TetR - Tetracycline repressor protein

Tris - 2-Amino-2-hydroxymethyl-propane-1,3-diol

TFA - Trifluoroacetic acid

THF - Tetrahydrofuran

TPP - Triphenylphosphonium

5.0 Introduction

5.1 The Role of Hydrogen Peroxide in the Cell

Hydrogen peroxide is one of a group of chemicals in cells described as reactive oxygen species. These include radicals such as superoxide ($O_2^{\bullet-}$), hydroxyl ($^{\bullet}OH$) and peroxyl ($RO_2^{\bullet}$) and non-radicals that are oxidising themselves or that are converted into radicals including ozone (O_3), singlet oxygen ($^1O_2$) and hydrogen peroxide (H_2O_2). The production of reactive oxygen species generally begins with the production of superoxide which rapidly dismutates to hydrogen peroxide and molecular oxygen, spontaneously or catalysed by superoxide dismutase [6]. Other sources of reactive oxygen species in cells include the Fenton reaction which is the iron-catalysed generation of the hydroxyl radical and the reaction of superoxide with nitric oxide leading to the production of peroxynitrite [7].

Hydrogen peroxide has long been viewed as a dangerous and toxic free radical compound which damages proteins and DNA in cells, leading to apoptosis and cell death. Only in more recent times has the importance of hydrogen peroxide as a signalling molecule, which acts as a stimulus for a huge range of processes, come to be appreciated. These processes include cysteine oxidation, cell proliferation and differentiation, modification by the small ubiquitin-like modifier (SUMO), tyrosine phosphorylation and oxidative stress [8]. Intracellular levels of hydrogen peroxide must be tightly controlled as left unchecked this chemical will lead to cell death. Antioxidant proteins, therefore, play a vital role in maintaining the hydrogen peroxide levels high enough for signalling events but low enough to prevent damage. The Jekyll and Hyde nature of hydrogen peroxide is what makes it such a fascinating molecule to study and one which the more is known of, the more will be understood about what happens when the hydrogen peroxide balance tips the scale and aging and disease occur.

5.2 Production of Hydrogen Peroxide by NADPH Oxidases

One of the main sources of hydrogen peroxide in cells are the Nox enzymes [2]. The Nox family is composed of seven catalytic subunits termed Nox 1-5 and Dual Oxidases 1 and 2 (Duox 1 and 2). All of the members of the Nox family are transmembrane proteins that transport electrons across membranes for the reduction of oxygen to superoxide [9]. They have been shown to be capable of

producing millimolar concentrations of hydrogen peroxide [10]. They were first discovered when it was noted that cells were capable of producing a respiratory burst which resulted in the production of superoxide. It was then determined that the main substrate for this production was NADPH [11]. Nox enzymes can assemble at the plasma membrane for the production of hydrogen peroxide. They are found in a range of different tissue and cell types including endothelial cells, vascular smooth muscle cells, macrophages and fibroblasts. Nox enzymes work towards the production of hydrogen peroxide for a number of reasons. These include specific functions such as differentiation and angiogenesis [12].

There are a number of conserved features within the complex. These include the NADPH binding domain situated at the C-terminus, FAD-binding site, six conserved transmembrane domains and four conserved heme-binding histidine residues. The first member of the Nox family to be discovered was Nox2 which once activated uses NADPH to reduce molecular oxygen to superoxide and in particular is used by phagocytes to destroy microorganisms [13]. Nox enzymes differ from other reactive oxygen species producing proteins in that other proteins produce reactive oxygen species as a by-product, whereas the sole purpose of Nox enzymes is to produce hydrogen peroxide.

Nox enzymes are stimulated by a wide variety of substrates to produce superoxide. Both inorganic and organic chemicals have the ability to stimulate. Heavy metals such as lead have been shown to stimulate Nox proteins, as a response to the toxicity of such metals [14]. With regards to organic chemicals, ethanol has been shown to be a stimulator of Nox [15]. Oxidised lipoproteins, known to have a role in atherosclerosis, have been shown to cause an up-regulation in Nox activity and consequently an increase in hydrogen peroxide. Other stimulators include physical factors such as ionizing radiation, adverse environmental factors such as low nutrition and oxygen level changes, inflammatory stimuli such as the bacterial endotoxin lipopolysaccharide and stress response hormones have all been shown to influence the levels of reactive oxygen species produced from Nox enzymes [16].

As well as having a range of stimuli, the downstream effects of reactive oxygen species production by Nox enzymes is also far reaching. Signal regulating kinase-1 (ASK-1) is activated as a response to cellular stresses and regulates apoptosis

[17]. Reactive oxygen species produced by Nox enzymes are also known to down-regulate protein tyrosine phosphatases (PTPs) [18]. Interestingly, dependant on the Nox isoform involved and the intensity and type of stimulus, there can either be a cell survival or an apoptotic response, once again highlighting the complexities involved with hydrogen peroxide as a signalling molecule.

5.3 Production of Hydrogen Peroxide in Mitochondria

One of the other main cellular sources of hydrogen peroxide is the mitochondria. Within the mitochondria there is a highly reducing environment. The reduction potential required to reduce molecular oxygen to superoxide is -0.16 V. Various parts of the respiratory chain within mitochondria have the thermodynamic capability to service this reduction potential. There are, therefore, various sources of superoxide and consequently hydrogen peroxide in the mitochondria [19].

Complex IV within the mitochondrial respiratory chain does not produce superoxide as it does not release any intermediates until full reduction from oxygen to water has been achieved (Fig.1). Other complexes within the respiratory chain are not so efficient however and leak electrons, resulting in the partial reduction of oxygen and consequently superoxide. Superoxide dismutase within the mitochondria can go on to convert these sources of superoxide to hydrogen peroxide. It is believed that most of the superoxide produced in the mitochondrial matrix is converted within the matrix; superoxide produced within the intermembrane space may be allowed to travel to the cytosol via voltage dependant ion channels [20]. Monoamine oxidases are bound to the outer membrane of mitochondria and are also capable of producing hydrogen peroxide during the catalytic oxidative deamination of monoamines such as noradrenaline and adrenaline [21].
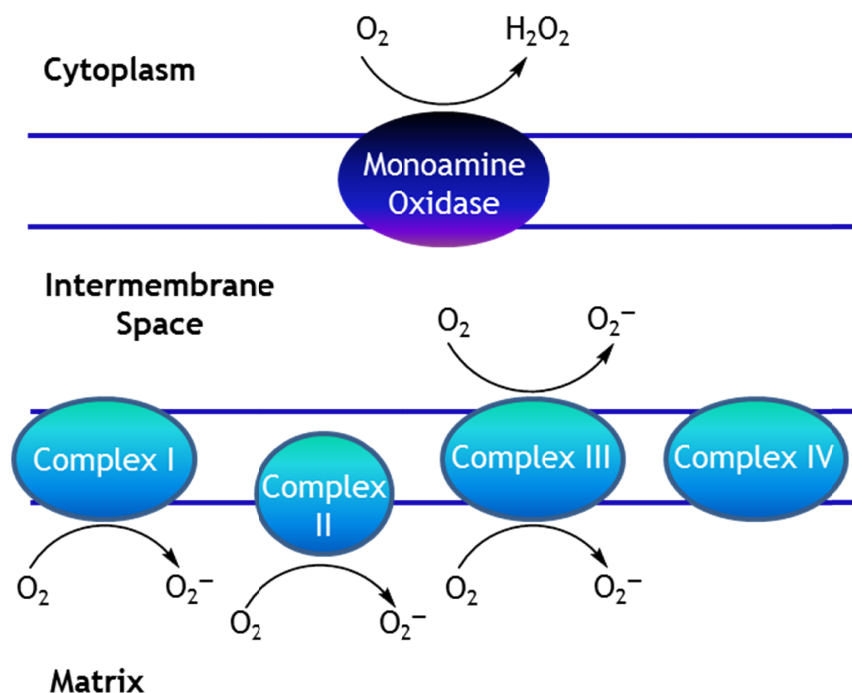
Figure 1 – Sources of superoxide in the mitochondria. Complexes I-III leak electrons as a by-product of the respiratory chain causing the partial reduction of molecular oxygen. Superoxide dismutase is then capable of converting this superoxide to hydrogen peroxide. Complex IV is more efficient with no leakage, so is different from other mitochondrial complex proteins in that it does not result in the production of superoxide. Monoamine oxidase, situated on the outer mitochondrial membrane is also capable of producing hydrogen peroxide as a by-product of the oxidative deamination of monoamines.

Other than the respiratory chain, hydrogen peroxide can be produced in the mitochondria as a result of oxidative folding that occurs in the intermembrane space. Newly synthesised proteins can be imported into the mitochondria and are trapped in the intermembrane space by a disulfide relay. Imported proteins are in the reduced state and require disulfide bond formation. The protein Mia40 contains a disulfide bond within the active site which it can pass onto the substrate in a method analogous to that of PDI. Mia40 is in the reduced state after this process and is reoxidised by the protein Erv1. The electrons are then passed onto the FAD moiety of Erv1 and after this onto Cytochrome C peroxidase. The final electron acceptor is oxygen as with the PDI-Ero1 relay in the ER and results in the production of hydrogen peroxide [22].

5.4 Production of Hydrogen Peroxide in the ER

Hydrogen peroxide is produced in the ER as a result of disulfide bond formation. It is known that most secretory proteins which pass through the ER contain disulfide bonds. As a newly synthesised polypeptide chain crosses the ER membrane it comes into contact with a whole host of proteins whose function it is to guide the polypeptide chain into its native conformation. One of the most important groups of enzymes that exist within the ER is the protein disulfide isomerases (PDIs). Within a thioredoxin-like domain of PDI there exists a catalytic disulfide within a CXXC motif, the intermediate amino acids (X) contributing to the redox potential [23]. This catalytic disulfide is transferred onto the client protein as a step in the folding process (Fig. 2). As a result, PDI is left in the reduced thiol form. The PDI family members do not show specificity for forming native disulfides within the client protein and so often non-native disulfides will also be formed. PDI is however an isomerase so is capable of reducing non-native disulfides. During the folding process it is possible that many native and non-native disulfides are formed and removed until the native conformation is achieved, guided by the potential energy.

Once PDI has passed on its catalytic disulfide to the client protein it is in the reduced thiol form and so must be reoxidised to carry on its catalytic role in protein folding [24]. Originally, it was believed that glutathione was responsible for the reoxidisation of the PDI proteins. The environment within the ER is an oxidising one, with the ratio of glutathione disulfide (GSSG) to glutathione (GSH) around 1:3, higher than that of the cytosol, suggesting GSSG is capable of oxidising PDI [25]. It has been shown, however, that in the ER the protein ER oxidoreductin 1 (Ero1) is actually the main source of oxidising equivalents for PDI [26].

Ero1 is a flavoprotein which contains a number of disulfide bonds, including one which reoxidises PDI. Once this action has been performed Ero1 uses the newly reduced thiols in the reduction of molecular oxygen to produce hydrogen peroxide [27]. Ero1 also contains a number of regulatory disulfides which act to control its activity [28], [29]. This is important as some PDI must be maintained in the reduced form for reduction of non-native disulfides in newly synthesised

proteins and also to prevent the ER concentration of hydrogen peroxide from becoming too great.
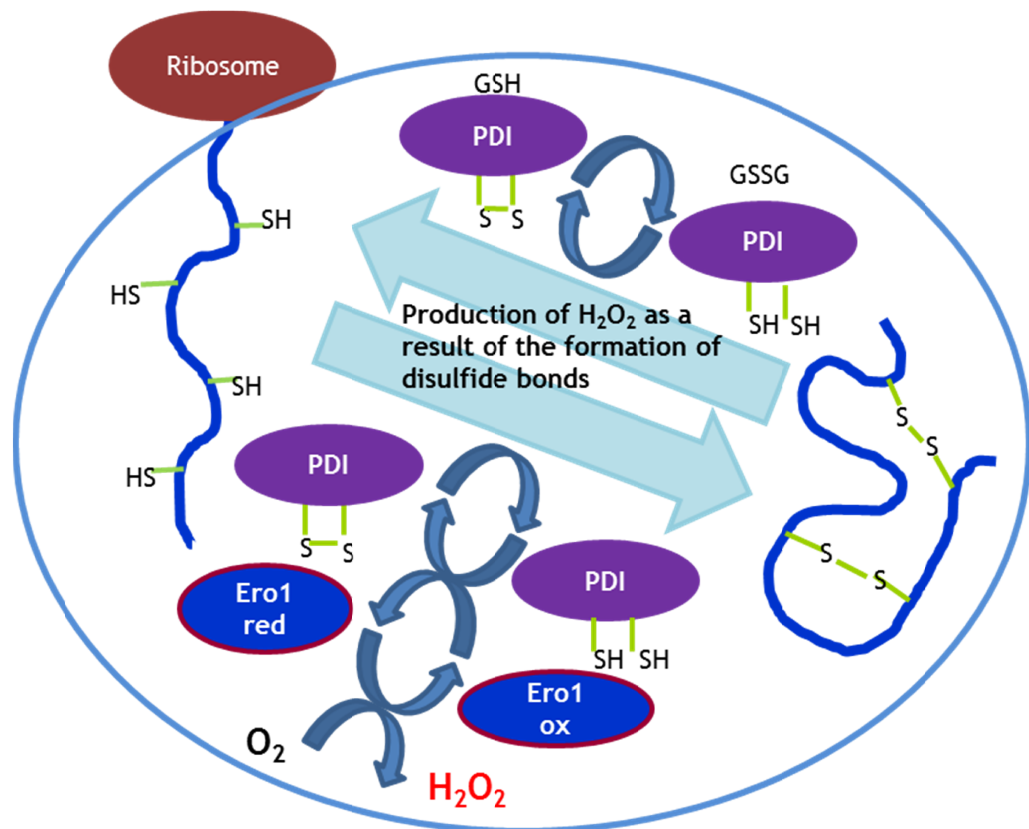
Figure 2 – Production of H_2O_2 in the ER as a result of disulfide bond formation. PDI passes its catalytic disulfide to newly synthesised proteins and as a result becomes reduced. Ero1 combines the reoxidation of PDI with the reduction of molecular oxygen to produce hydrogen peroxide.

5.5 Removal of Hydrogen Peroxide in Cells

With all the hydrogen peroxide being produced in cells, there must be methods of removing this molecule as the toxicity would soon cause severe damage to cells if left unchecked.

The most well-known enzyme capable of removing hydrogen peroxide in cells is catalase (Fig. 3). Catalase is a heme protein and is found in nearly all organisms exposed to oxygen. It reacts with two molecules of hydrogen peroxide to produce two molecules of water and molecular oxygen [30]. Catalase is an incredibly efficient enzyme with a high turnover number and therefore plays a

vital role in protecting cells from the toxic effect of too much hydrogen peroxide.

When catalase reacts with the first molecule of hydrogen peroxide it is oxidised to a high valent iron intermediate known as Compound [I] [31]. This is characterized by an oxoferryl porphyrin cation radical. After compound [I] is formed it rapidly reacts with a further molecule of hydrogen peroxide to produce water and oxygen.

Most catalase found in mammalian cells is found in the peroxisomes. This is an organelle whose main function is the degradation of long chain fatty acids through oxidation. As a result a lot of hydrogen peroxide is produced in the peroxisomes, requiring catalase for removal. There is a high concentration of catalase found in the liver of mammals. This is due to the fact that peroxisomes in the liver are responsible for the degradation of various toxic substances that are in the blood of the mammal. Catalase activity can also be regulated by tyrosine phosphorylation, which is suggestive of a mechanism specifically for high levels of hydrogen peroxide [32].

Another group of enzymes which are capable of removing hydrogen peroxide is the glutathione peroxidases (GPxs) (Fig. 3). In humans there are eight members of the family of GPx family and they can be found in most parts of the cell [33]. Gpx proteins contain either a cysteine or selenocysteine which can be oxidised by hydrogen peroxide or lipid peroxides to form cysteine sulfenic acid or selenenic acid. Glutathione then reacts with the oxidised residue to form a disulfide or Se-S bond and a molecule of water. The bond formed can then be resolved by a further molecule of glutathione.

GPxs 7 and 8 are localised to the ER. It was shown in a bimolecular fluorescence complementation (BiFC) experiment that they are capable of interacting with Ero1 [34]. This means that hydrogen peroxide produced by Ero1 as a result of the oxidation of PDI can be directly removed by GPx 7 and 8, therefore preventing a build-up that could cause toxicity. It has also been shown that GPx 7 and 8 are capable of oxidising PDI directly, a mechanism which could aid the folding process.

The third class of enzymes which is capable of utilising hydrogen peroxide in cells are the peroxiredoxins (Prxs) (Fig. 3). The typical 2-Cys Prxs are composed of 5 or 6 dimers [35]. Each Prx monomer contains two cysteine residues within the active site. One of these is known as the peroxidatic cysteine and the other is the resolving cysteine. The peroxidatic cysteine reacts with hydrogen peroxide and forms the sulfenic acid intermediate. The resolving cysteine then reacts with the sulfenic acid forming a disulfide and a molecule of water. The disulfide can be reduced by thioredoxin which in turn is reduced by thioredoxin reductase. When the Prx intermediate sulfenic acid has been formed further reaction with hydrogen peroxide is also possible. This leads the enzyme to form sulfinic acid (SO_2H) or sulfonic acid (SO_3H) [36]. Once in these forms the enzyme is inactivated as the resolving cysteine cannot form a disulfide.

PrxIV is the only Prx resident in the ER. PrxIV is different from other Prx enzymes in that it contains extra residues at the N-terminus. Within these residues there is a third cysteine residue which forms a disulfide between the dimeric units of the Prx structure. PrxIV has shown to be capable of metabolising hydrogen peroxide produced by Ero1 and can play a role in *de novo* disulfide formation by the direct oxidation of PDI [37].
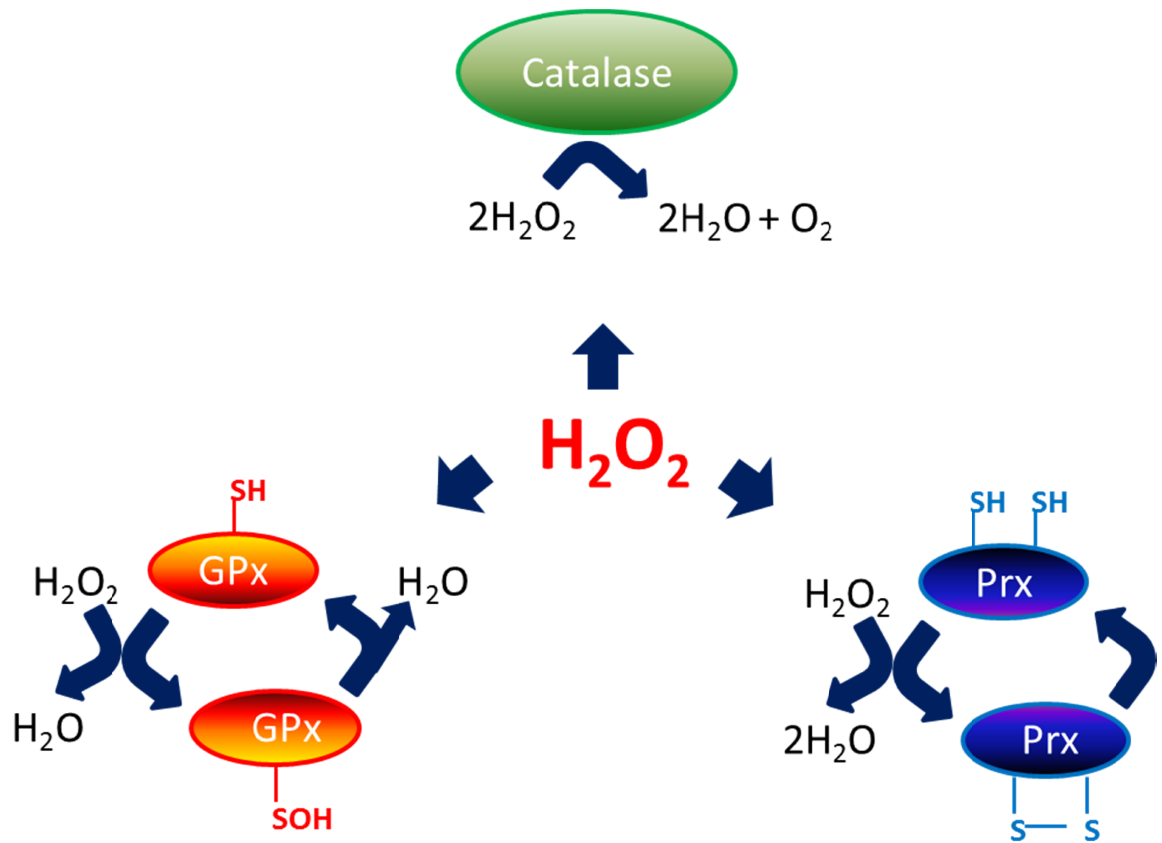
Figure 3 – Removal of hydrogen peroxide in cells. Catalase is a heme protein that reacts with hydrogen peroxide to from a high-valent iron intermediate. A second molecule of hydrogen peroxide can then react forming two molecules of water and oxygen. The GPx group of enzymes containing a cysteine residue which forms sulfenic acid after reaction with hydrogen peroxide. This forms a disulfide with glutathione, releasing a molecule of water. The disulfide can be reduced by a second molecule of glutathione. The Prxs contain two cysteines in the active site. The peroxidatic cysteine reacts with hydrogen peroxide forming sulfenic acid. This is resolved by the resolving cysteine which forms a disulfide. The disulfide can be reduced by thioredoxin.

5.6 Hydrogen Peroxide Movement in Cells

Previously it was believed that hydrogen peroxide was free to move around cells and that all membranes were permeable to hydrogen peroxide. It has now been discovered that different membranes have different hydrogen peroxide permeability and some are fairly impermeable [38]. This suggests that the

concentration of hydrogen peroxide inside cells is tightly regulated, a fact which is also suggested by the presence of antioxidant proteins. The concentration of hydrogen peroxide in a cell can be calculated as the amount entering the cell plus the amount being produced in the cell minus the amount being removed by antioxidant enzymes and the amount leaving the cell. It is believed that variations in membrane permeability to hydrogen peroxide could be due to differences in lipid composition or the presence of hydrogen peroxide selective channels or a combination of both [39].

Antunes et al. made an estimate of hydrogen peroxide permeability via measurement of the enzyme latencies of catalase and GPx. They showed that hydrogen peroxide gradients were formed when membranes separated the site of hydrogen peroxide production and consumption [38]. The time taken for hydrogen peroxide to diffuse was measured by the delay in the reaction of the enzyme. They found significant gradients which were attributed to the capacity of the enzymes consuming hydrogen peroxide and the permeability of the membranes involved.

Hydrogen peroxide permeability of membranes has been shown to have some dependence on the lipid composition of membranes. Experiments in yeast have shown that hydrogen peroxide permeability is five times higher when the yeast are actively growing compared to when the cells are in stationary phase [40]. This difference is suggestive of different membrane composition during different phases in the life cycle. Though it is likely that membrane composition does affect the diffusion of hydrogen peroxide it is unlikely to be the main influencer in the process. Changing membrane lipid composition is a slow process and is more of a long term strategy. Also if cells were to rely on this as the only method of hydrogen peroxide diffusion regulation then it is likely that many other cellular processes would be affected as well.

Aquaporins are diffusion channels situated in cellular membranes that allow diffusion of water and other small non-charged solutes including carbon dioxide and ammonia [41]. Water can of course diffuse through membranes but the diffusion rates of water through aquaporins are far greater. Aquaporins have, therefore, been studied as a potential mechanism for hydrogen peroxide transport. One factor which suggests that hydrogen peroxide also is capable of

entering aquaporins is that on a molecular level it has very similar properties to water. These properties include dipole moment and hydrogen bond forming capacity. The mean diameter of a hydrogen peroxide molecule is around 0.25-0.28 nm [42]. Some typical aquaporins have pore diameters of between 0.3 and 0.4 nm suggesting size is not a barrier to the transport of hydrogen peroxide through aquaporins [43].

Yeast mutants expressing various aquaporins from plants and mammalian systems were created to investigate the differential selectivity of aquaporins to hydrogen peroxide [44]. A total of 24 mutants were created but only two saw increases in hydrogen peroxide sensitivity. The increase was found to be up to 10-fold. The aquaporins which showed sensitivity were AtTIP1, an Arabidopsis aquaporin and APQ8, a mammalian aquaporin. APQ8 is found in the plasma membrane but also in the inner mitochondrial membrane [45]. This suggests that aquaporins are certainly capable of transporting hydrogen peroxide but that they are selective and there may be aquaporins which have the specific role of hydrogen peroxide transport.

5.7 Hydrogen Peroxide in Signalling

One of the main responses to increased levels of hydrogen peroxide in the cell is increased expression of antioxidant enzymes such as peroxiredoxins and glutathione peroxidases. However, hydrogen peroxide is also an important signalling molecule and a wide variety of responses is produced. With regards to multicellular organisms the responses can include differentiation [46], proliferation [47], migration [48] and apoptosis [49]. The fact that one compound can generate such a range of responses is intriguing and the ability to do so is due to the careful control of the hydrogen peroxide concentration inside cells.

In mammalian cells it has been shown that low levels of hydrogen peroxide stimulate the expression of antioxidant enzymes whereas high levels stimulate the expression of pro-oxidant enzymes which encourage apoptosis [50]. It seems that at levels where the cellular antioxidant enzymes will not be able to cope and damage is inevitable the cell propels itself towards apoptosis by the further production of hydrogen peroxide and other reactive oxygen species.

One process where hydrogen peroxide concentrations are important and can change the response is modification of proteins by SUMO proteins. SUMO proteins are small proteins around 12 kDa that can be covalently attached or removed from other proteins, leading to a change in action of the substrate protein. They are indicated in a wide range of processes including cell cycle progression, stress response, protein stability, transcriptional regulation, nuclear cytosolic transport and apoptosis. It has been found that in lower concentrations of hydrogen peroxide then the conjugation of SUMO proteins to substrates is reduced whereas in high concentrations the removal of SUMO proteins from substrates is inhibited [51].

Another important process affected by hydrogen peroxide is that of protein tyrosine phosphorylation. All protein tyrosine phosphatases (PTPs) contain a cysteine residue within the active site. Importantly this cysteine residue is predominantly in the thiolate anion form at pH 7.4. It is normally part of a thiol-phosphate intermediate, formed as part of the catalytic cycle, but when free it is predominantly in the thiolate form and so it is easily oxidised by hydrogen peroxide or other reactive oxygen species [52]. The thiolate anion forms sulfenic acid after reaction with hydrogen peroxide as in the cases of the peroxiredoxins and glutathione peroxidases. The oxidised PTP which is inactivated can be reduced by glutathione back to the active form.

It has been shown that when a high level of tyrosine phosphorylation is required in a cell, the activation of receptor protein tyrosine kinases by substrates such as epidermal growth factor may not be enough to allow the required amount of phosphorylation to occur [53]. As receptor protein tyrosine kinases are stimulated then PTPs may also be inactivated by oxidation of the cysteine thiolate within the active site which prevents the thiol-phosphate reaction intermediate being formed and hence no removal of phosphate groups.

5.8 Hydrogen Peroxide in Cell Death

A range of factors can cause a cell to undergo apoptosis. These include a loss of nutrients required for cell survival, oxidative stress, radiation and infection by a virus. Due to the well characterized toxicity of hydrogen peroxide and other reactive oxygen species, it has long been known that too much can cause cell

damage and eventually death. However, the mechanism by which this occurs and the concentrations required have not always been so well studied.

A study was carried out by Clément et al. which aimed to determine the mechanisms by which hydrogen peroxide caused cell death [54]. They found that upon addition of hydrogen peroxide to mammalian cells the amount of cell death increased as the concentration of hydrogen peroxide increased. When the concentration of hydrogen peroxide was between 0.25 mM and 0.5 mM then the cells went into apoptosis, whereas if the concentration was above 1 mM the cells went into necrosis, suggesting two different mechanisms. It was found that hydrogen peroxide mediated apoptosis also required caspase activity. Caspase proteins have been termed "executioner" proteins due to their role in apoptosis and are a form of protease [55].

The level of intracellular superoxide was measured when cells were treated with apoptotic concentrations of hydrogen peroxide. It was found that the intracellular concentration of superoxide dropped as much as 50% when cells were treated. It was also shown that necrotic concentrations of hydrogen peroxide caused no alteration to the intracellular superoxide concentration. To further correlate the hydrogen peroxide and superoxide levels cells were again treated with the apoptotic concentration of hydrogen peroxide along with an inhibitor of superoxide dismutase, the main superoxide scavenging protein. It was found that the levels of superoxide did not decrease as much as when the cells were treated with hydrogen peroxide alone. The amount of caspase activity and apoptotic cell death was also reduced due to the maintenance of higher superoxide levels [54].

The effect of reduced levels of superoxide on the intracellular redox state was also investigated. In the cytosol the GSH:GSSG ratio is usually between 100 and 200:1 [56]. Any increase in cellular superoxide would be expected to cause an increase in the amount of GSSG compared to GSH and conversely any decrease in superoxide would be expected to cause a decrease in the amount of GSSG compared to GSH. It was found that when high concentrations of hydrogen peroxide were added to cells and necrosis was caused then the amount of GSSG relative to GSH increased whereas when apoptotic concentrations of hydrogen peroxide were added to cells then the amount of GSSG decreased relative to

GSH. An acidification of the cell was also associated with apoptotic cell death, in comparison to necrotic cell death which was associated with an increased alkalinity.

These results are not, however, without any contradiction. Tochigi et al. found that treatment of mammalian cells with concentrations of hydrogen peroxide between 30 μM and 100 μM stimulated apoptotic cell death and activation of caspase enzymes, in agreement with Clément et al., but they found that this caused an increase in intracellular superoxide [57]. It was found that the increase in superoxide caused by apoptosis activated the ER stress response and ER associated cell death.

What can be deduced is that at lower concentrations hydrogen peroxide can cause apoptotic cell death and that at concentrations of 1 mM or above the cells will undergo necrotic cell death. The mechanism of how hydrogen peroxide causes apoptosis is unclear but almost certainly involves activation of caspase enzymes amongst others. The contradiction in the discussed results is a further testimony to the complex nature of the role of hydrogen peroxide in cells.

5.9 Measuring Hydrogen Peroxide in Cells

As has been shown, hydrogen peroxide is undoubtedly an interesting molecule, but the roles it plays within cells have not been fully deduced. With regards to the ER in particular, the measurement of hydrogen peroxide is a particularly fascinating prospect. It is known that Ero1 is a producer of hydrogen peroxide in the ER and PrxIV, Gpx7 and Gpx8 are capable of reacting with this source [58]. What is unknown is what happens to the levels of hydrogen peroxide in the ER if conditions are stressful, for example during the unfolded protein response (UPR) when changes within the ER occur to cope with the extra load of protein folding required [59].

There have been previous probes created to measure hydrogen peroxide inside cells. A number of these have been small molecule probes but there has also been protein based methods.

The commercially available Amplex Red is an organic compound that is not fluorescent but becomes fluorescent after reaction with hydrogen peroxide (Fig. 4). Amplex Red will only work in the presence of a peroxidase enzyme. Amplex

Red reacts in a stoichiometric manner to produce resorufin, a highly fluorescent compound. The reliance of Amplex Red upon the presence of a peroxidase enzyme is where the disadvantage of the method lies. The requirement for a peroxidase makes analysis of complex biological samples and analysis in cells difficult as the enzyme activity can be affected by many factors, resulting in an effect on the resorufin fluorescence [60]. Amplex Red has also been shown to be susceptible to photo oxidation [61]. Nevertheless Amplex Red is used for a range of applications including microwell plate based assays.
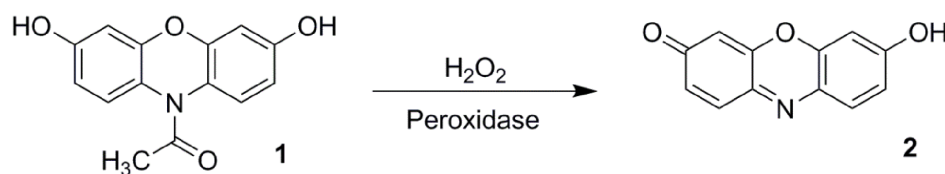
Figure 4 – The reaction of Amplex Red. Amplex Red 1, a commercially available sensor reacts with hydrogen peroxide in the presence of peroxidase to form Resorufin 2, a highly fluorescent compound.

Another of the earlier methods of measuring hydrogen peroxide used the small molecule probe dichlorofluorescein (DCF) as a reporter (Fig. 5). The reduced form of DCF, DCFH, is not strongly fluorescent is used as an oxidation sensitive probe. After reaction there is an increase in fluorescence up to 20-fold at 525 nm [62]. It was first used to study the reactive oxygen species released from neutrophils and has gone on to be used in neutrophil disease diagnosis [63]. It is important to note that oxidation sensitive DCFH is not a hydrogen peroxide specific probe and it has a number of disadvantages.
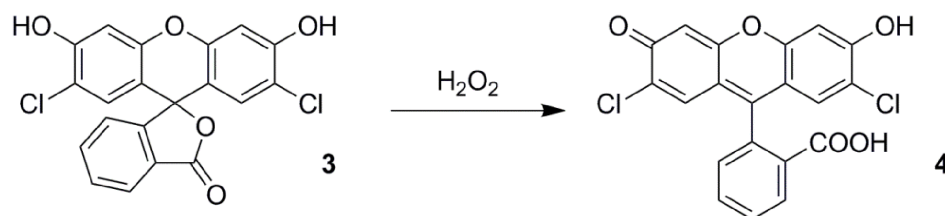
Figure 5 – The reaction of DCFH. DCFH 3 is an oxidation sensitive probe that reacts with hydrogen peroxide and to give DCF 4 and so displays a fluorescence increase after reaction.

DCFH is capable of photo-oxidation which can lead to a false signal or a more intense signal than what is real. One of the main issues is that hydrogen peroxide does not directly react with DCFH. It requires a transition metal catalyst which can be found in proteins such as peroxidases [64]. There is consequently a correlation between catalyst availability and level of oxidation. Upon autooxidation of DCF by molecular oxygen the superoxide radical is generated which is readily converted to hydrogen peroxide, resulting in a self-amplification of signal. It has also been shown the cytochrome c and other factors are capable of oxidising DCFH [65]. Though several factors must be taken into account when using DCFH as an oxidative stress indicator, it is suitable for use in a simple or first-look assay.

Since the reliance of DCF and Amplex Red on enzymes acts as a disadvantage to their use as probes, further probes have been developed which use the fluorescence of fluorescein but do not require any enzyme activity to do so. Once such example is a fluorescein derived probe that is modified as a perfluorobenzenesulfonate ester (Fig. 6) [66]. This acts to quench the fluorescence until after reaction with hydrogen peroxide. The probe is cell permeable but the reaction is strongly dependent upon pH. If the pH rises above the optimum of pH 7.4 then hydrolysis of the probe that is independent of hydrogen peroxide can occur, leading to a false signal. The reaction was also found to be a rather slow one, around 60 min. It was also found that cleavage of the perfluorobenzenesulfonate ester is not specific to hydrogen peroxide and will reactive with other reactive oxygen species. Therefore the probe is useful as an oxidation sensor, as long as the limitations are taken into account in the design of the experiment.
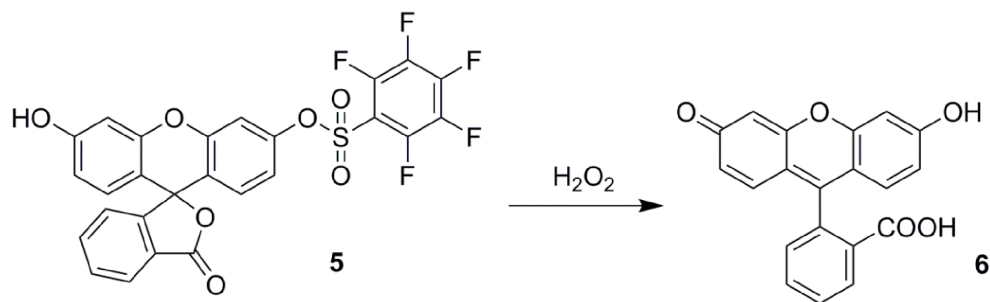
Figure 6 – The reaction of of 2',7'-dichlorofluorescein pentaflurobenzenesulfonate ester. Perhydrolysis of 2',7'-dichlorofluorescein pentaflurobenzenesulfonate ester by hydrogen peroxide results in the release of the fluorophore.

Another issue of the previously discussed small molecule probes is that they are not ratiometric. They function purely as ON-OFF probes which are only able to show a relative increase. This makes determination of concentration of hydrogen peroxide nigh on impossible. HyPer was developed as a ratiometric genetically encoded protein based method for hydrogen peroxide measurement in cells. HyPer is based on a fusion of the regulatory domain of OxyR, an *E.coli* protein sensitive to hydrogen peroxide, and a circularly permuted yellow fluorescent protein (cpYFP) [67].

OxyR has two key cysteine residues, Cys199 and Cys208. Cys199 can react with hydrogen peroxide and goes on to form cysteine sulfenic acid. This causes a conformational change whereby Cys199 moves into the proximity of Cys208 and a disulfide bond is formed [68]. Circularly permuted proteins such as cpYFP have been found to be particularly sensitive to conformational change, and display this sensitivity in fluorescence changes. HyPer therefore consists of cpYFP inserted into OxyR with an excitation peak at 420 nm and emission at 500 nm. As HyPer becomes oxidised the peak at 420 nm decreases in intensity and the intensity of the peak at 500 nm increases, giving the probe a ratiometric quality. It was shown that HyPer was selective for hydrogen peroxide over other reactive oxygen species and the sensitivity was shown to be in the nanomolar range *in vitro*. HyPer was also expressed in *E.coli* and mammalian cells and can be targeted to different organelles by incorporating targeting sequences (Fig. 7). In both *E.coli* and mammalian cells the lowest hydrogen peroxide concentration detectable was 5 µM.
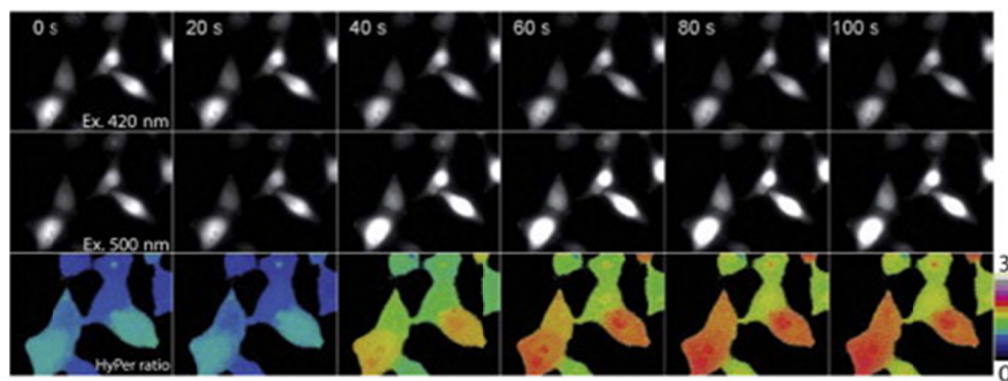
Figure 7 – The ratio change of HyPer in HeLa cells. The upper images are those measured at 420 nm, the middle images are those measured at 500 nm and the lower images show the ratio change. The times indicated are measured after the addition of hydrogen peroxide to the cells. The ratio change indicates the probe becomes more oxidised after the addition of hydrogen peroxide (reproduced from [69]).

Criticism of HyPer as a method for measuring intracellular hydrogen peroxide has been due to the fact that most cpYFP proteins are sensitive to pH, as HyPer has been shown to be. There has also been debate about whether HyPer is sensitive to superoxide as well as hydrogen peroxide [70]. Taking this information into account, as with DCFH, HyPer can certainly give an indication of hydrogen peroxide level changes although the results must be interpreted with care due to the other possible influences on the fluorescence of the probe.

As discussed, both DCFH and HyPer can offer an indication of hydrogen peroxide levels but have issues with regards to specificity. For this reason boronic acids recently have been exploited as tools for measuring hydrogen peroxide.

Boronic acids are organic compounds containing a trivalent boron atom. There is one boron-carbon bond and two boron-oxygen bonds. Boronic acids have a trigonal planar geometry with six valence electrons. This two-electron deficit results in a vacant p orbital. Interestingly boronic acids are not found in nature but the first synthesis was reported in 1860 [71].

Due to the presence of the vacant p orbital boronic acids have the properties of a mild Lewis acid, a Lewis acid being any substance that can accept a pair of non-bonding electrons [72].

In water the trigonal planar boronic acid is in equilibrium with the anionic tetrahedral form produced by formal reaction with a hydroxide anion. Thus, boronic acids have acidic character in water with the pKa of phenylboronic acid in water being 8.8 (Fig. 8). This is similar to the acidity of a phenol [73].
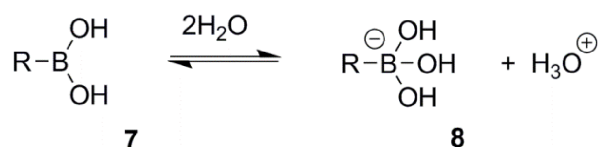
Figure 8 - The ionization of a boronic acid in water. The boronic acid 7 is ionized to the borate anion 8, showing the acidic character.

Boronic acids are commonly synthesised as the ester derivatives to make handling and purification easier due the reduction in polarity caused by caging the acid [74]. In aqueous systems, however, the ester form is in equilibrium with the acid.

Aryl boronic acids are known to react with hydrogen peroxide forming the corresponding phenol (Fig. 9) [75]. This has been exploited as a selective reaction to measure hydrogen peroxide in biological systems. The boron atom first acts as an electrophile to form a tetrahedral complex with the peroxide. The C-B bond then acts as a nucleophile and an oxygen atom is inserted between the carbon and boron. The final step is loss of boric acid and production of the corresponding alcohol.
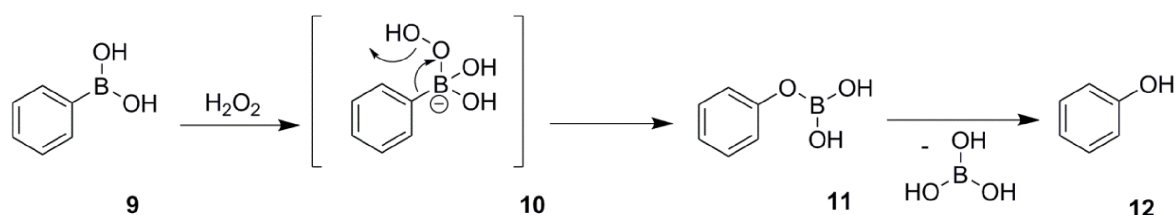
Figure 9 - Reaction of phenylboronic acid with hydrogen peroxide. Boric acid is lost from the boronic acid 9 after ⁻OOH inserts and phenol 12 is produced.

This molecular feature has been utilised in the production of hydrogen peroxide sensitive probes for use in cells. A range of intensity based fluorescent probes incorporating a boronic acid have been developed. The response of boronic acids

to hydrogen peroxide has been shown to be selective over other reactive oxygen species [76].

Fluorescence is the rapid emission of energy converted from absorbed radiation. After absorption of energy by a molecule, the molecule reaches an excited state. The excited molecule is eager to give up this energy. Collisions with nearby molecules result in non-radiative decay and the energy drops down vibrational levels. When the energy reaches the lowest vibrational level of the excited state, if the nearby molecules are not capable of accepting the larger energy difference between the excited state and the ground state, then the emission of a photon may occur (Fig. 10). Fluorescence is emitted at longer wavelengths than the absorption of energy occurs due to the fact that it happens after the non-radiative decay resulting from collisions with surrounding molecules. This explains why solvent choice can affect the fluorescence of a compound, as if the solvent molecules are capable of receiving the large energy difference between the lowest vibrational level of the excited state and the ground state then the fluorescence is quenched [77].
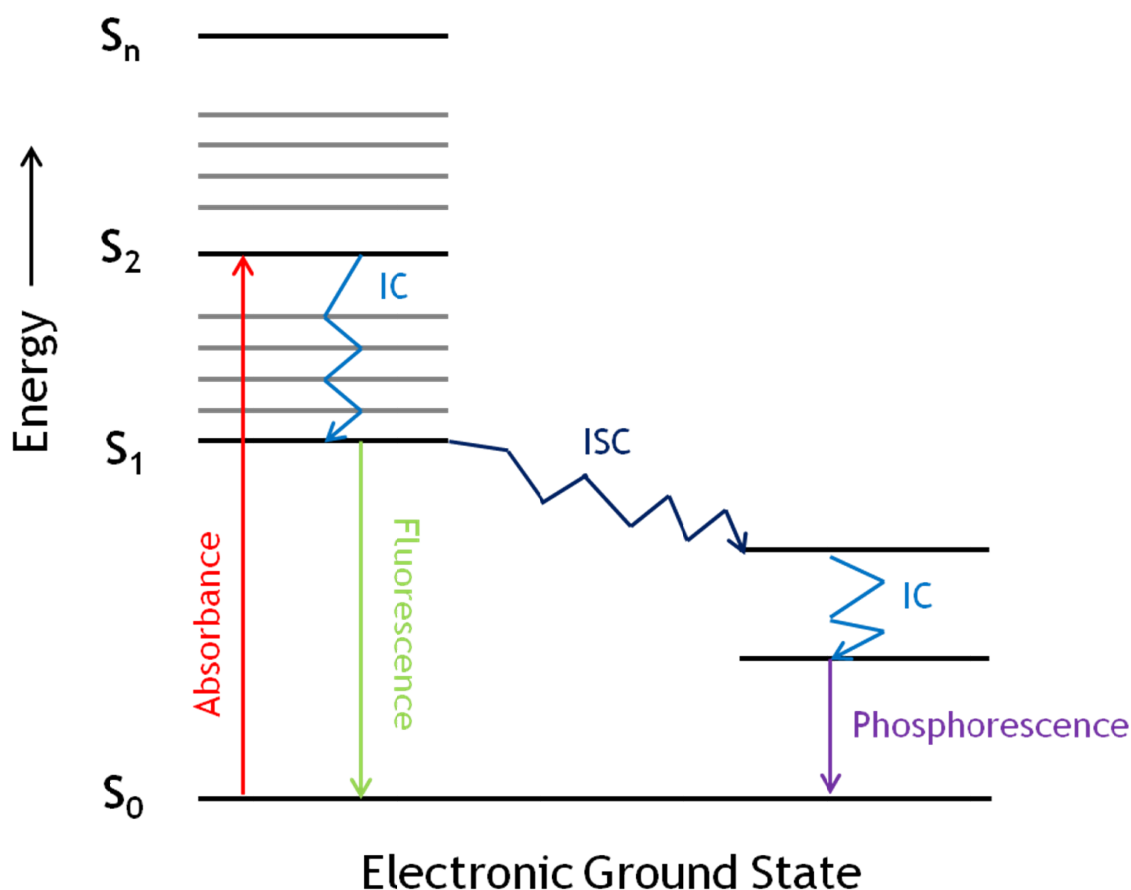
Figure 10 – Jablonski Diagram showing a molecule's absorbance of energy leading to an excited singlet state. Internal conversion (IC) occurs which is a radiationless procedure between energy levels in the same spin state. When the photon is emitted in the same spin state fluorescence is produced. If intersystem crossing (ISC) occurs and the photon is released from a different spin state, the triplet state, then it is termed phosphorescence.

Fluorescence microscopy is a key technique in biology used for studying a whole range of cellular processes. Therefore, to incorporate this fluorescence various fluorescent proteins and probes are used. In the design of small molecule fluorescent probes various criteria must be fulfilled. It is generally desired that a fluorophore has some lipophilic character so that it is capable of easily diffusing through the cell membrane. For probes without lipophilicity, techniques to encourage membrane permeability can include the addition of ester groups which are hydrolysed after entry, or the use of electroporation or patch clamping of single cells [78].

The ability and efficiency with which a compound fluoresces is measure by the quantum yield (Φ), defined as the ratio of photons absorbed to photons emitted via fluorescence [79]. Quantum yields can be sensitive to environmental factors such as solvent, something which must be considered when designing a fluorescent probe. A common problem facing the use of fluorescent probes is photobleaching. This is irreversible removal of the fluorophore under high intensity light by chemical reactions of the excited fluorophore.

The Stokes shift of a fluorophore is the difference between the absorption and emission wavelengths. If this difference is small it becomes impossible to achieve the optimum excitation of the probe while differentiating the fluorescence emission from any scattered light from the absorption. The ideal fluorophore must have a large Stokes shift along with high quantum yield and low incidence of photobleaching [80].

One of the early boronic ester incorporating probes was Peroxyfluor-1 (PF1) [81], which relies on reaction of two boronic esters to produce fluorescein (Fig. 11). This is highly fluorescent, however due to the quenching nature of boron; it is an off-on probe and cannot be used ratiometrically. It has been shown to have selectivity for hydrogen peroxide over most other reactive oxygen species [82].

The sensitivity of PF1 was improved upon by the design of a second generation of probes which incorporated only one boronic ester. Peroxy Green 1 (PG1) (Fig. 11) contains only one boronic ester group and showed a greater fluorescence response to hydrogen peroxide than that of PF1 [83]. As a result of only having one boron atom it also showed measurable fluorescence before reaction, though at the same wavelength as the reacted form so it cannot be said to be truly ratiometric.
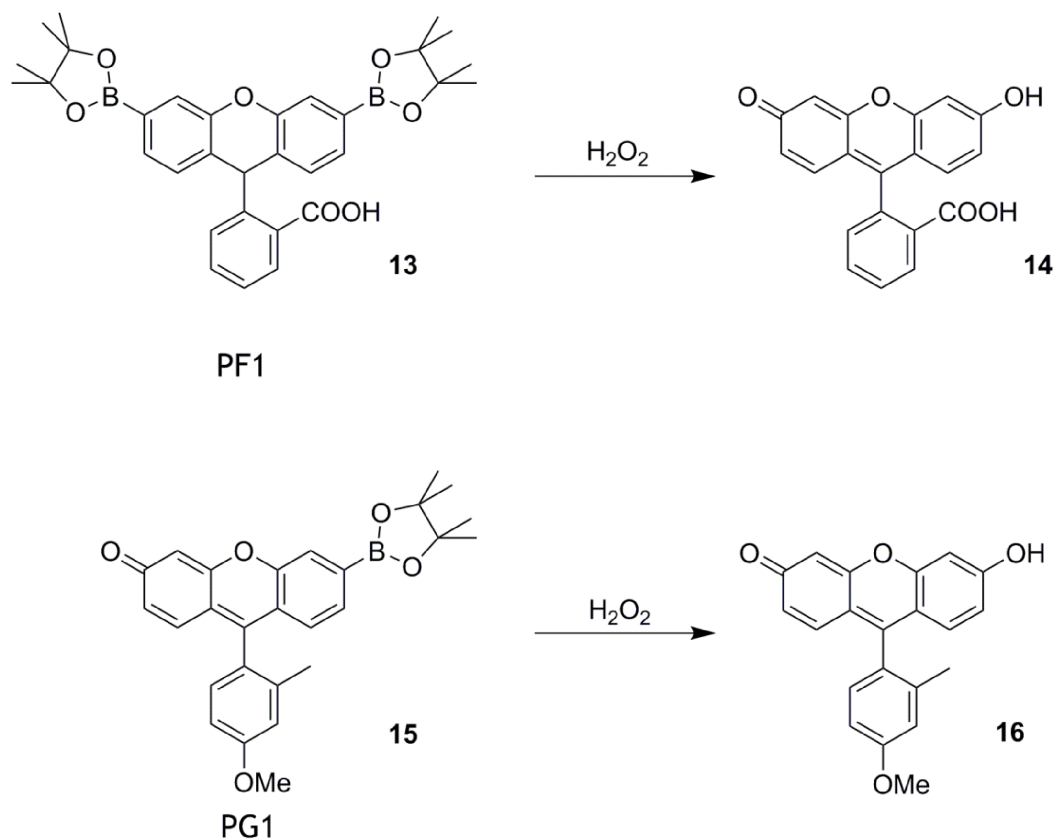
Figure 11 – PF1 and PG1, two boronate ester based probes for hydrogen peroxide. PF1 13 relies on the deprotection of two boronate ester groups to release fluorescein 14. Due to the quenching nature of boron this probe gives an OFF-ON response. PG1 15 only contains one boronate ester group. This means it does display some fluorescence before reaction with hydrogen peroxide but at the same wavelength as after reaction when Tokyo Green 16 is released.

5.10 Targeting of Probes within Cells

All the probes discussed have various advantages and disadvantages and with the exception of HyPer, none are targeted to specific areas of the cell, though they are cell permeable.

For a probe to be targeted there must be a feature of the structure that determines the organelle or locale of the cell to which it is directed. Various methods have been designed which allow small molecules to have such a homing device incorporated into the structure. There is an electrochemical gradient across the mitochondrial inner membrane as a result of the movement of protons

out of the matrix by the electron-transport chain in the inner mitochondrial membrane. Thus there is charge separation with a build up of negative charge on the inside (matrix side) of the inner membrane, and this corresponds to a voltage. The triphenylphosphonium (TPP) cation has been used to great effect in the mitochondria because it is positively charged and so partitions across this membrane in accordance with the Nernst equation resulting in a several hundred fold accumulation on the negatively charged side at normal operating voltages (120-180 mV) [84]. The TPP cation is lipophilic and therefore easily crosses the phospholipid bilayer. Any small probe or chemical group attached to the TPP cation is selectively taken-up into the mitochondria as a consequence. One probe which uses this technology is MitoSox™, a TPP-containing mitochondria-targeted fluorescent probe for superoxide [85]. However, this electrochemical gradient is a unique feature of the mitochondria and so different methods of targeting are required for other organelles.

Recombinant proteins are commonly expressed with an extra peptide or tag. These extra peptides or tags are often used as an aid for purification or for detection of the protein. The most common examples being the use of the hexahistidine tag for purification [86] and green fluorescent protein (GFP) for detection [87]. Tag technology has expanded to allow a much wider range of chemistry to occur. This means that proteins can be imparted with properties which cannot be provided by genetic manipulation alone.

One of the major developments has involved systems which allow site-specific incorporation of unnatural amino acids into proteins and can be used in living cells [88]. Other methods have involved the covalent modification of a tag with a range of molecules [89]. Covalent modification of a tag often involves the use of a chemical probe. The efficiency of expressing a tag inside a living cell in conjunction with the infinite number of possibilities provided by synthetic chemistry makes this a very powerful technique.

To be successful, the reaction that occurs between the peptide or fusion tag and the synthetic compound must hold certain qualities. The reaction must be highly specific and fast, the synthetic probe must have bio-orthogonal properties [90] as any interference with the biochemical processes inside a living cell could be detrimental to the overall aim of the experiment. Also the substrate which

reacts with the peptide or fusion tag should not be affected by the probe or small molecule to which it is conjugated as the system must be universal.

The incorporation of a tetracysteine (TC) tag allows for the specific binding of biarsenical compounds. An example is FlAsH, a fluorescein derivative (Fig. 12) [91]. The TC tag has the main advantage of being small and so is unlikely to have any adverse effects on the folding or processes of the protein in which the tag is incorporated. The main disadvantage of the TC tag is the risk of unspecific binding of the biarsenical compounds. This can be circumvented to some extent by co-incubation with dithiols.
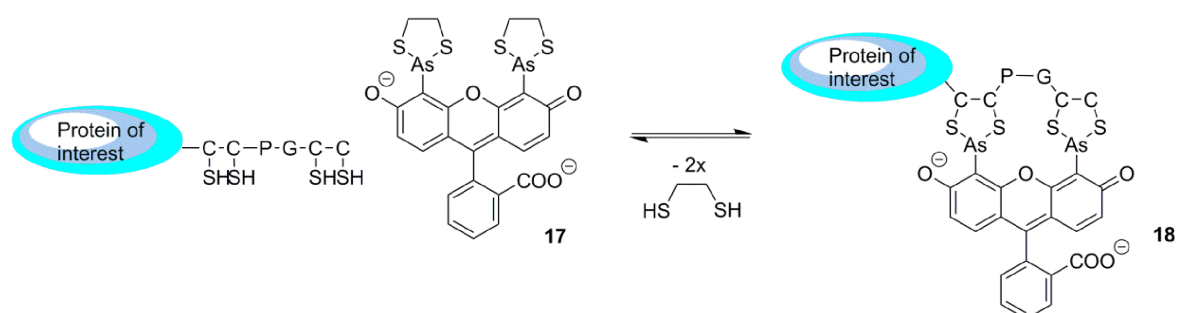
Figure 12 - The tetracysteine (TC) tag. Conjugation of FlAsH 17, a biarsenical substrate with a fluorescein derived fluorophore to a protein of interest which has been genetically manipulated to express the TC tag resulting in the conjugate 18.

The issues associated with the TC tag have been overcome with the development of folded protein tags. Human O^6-alkylguanine-DNA-alkyltransferase (AGT) repairs the damage incurred by alkylation of guanine to form O^6-methyl guanine. The process of repair involves the transfer of the O^6-alkyl group from O^6-methyl guanine to the active site cysteine of AGT. This process is both irreversible and stoichiometric.[92] AGT is not hugely specific regarding its substrate choice and is also known to react with O^6-benzylguanine derivatives [93].

AGT provides protection from alkylating agents such as dacarbazine and temoxolomide which are used in chemotherapy treatments [94]. O^6-Benzylguanine was found to be an inhibitor of AGT that sensitized tumours towards alkylating agents and so was researched as an agent to aid the success of chemotherapy compounds [95]. It was found that there was some natural resistance of AGT to the use of O^6-benzylguanine in this treatment strategy.

Further investigation found that this natural resistance was due to natural polymorphism in the AGT gene. Various mutants of AGT were expressed in *E.coli* to determine the effects of such polymorphism. The mutant that was of most interest was G160R. G160R exists naturally in some individuals and causes AGT to be resistant to O^6-benzylguanine. Interestingly it was found that the mutation G160W actually made AGT far more sensitive to O^6-benzylguanine and caused enzyme inactivation [96].

Due to the targeting of AGT in anti-cancer therapy it was reasoned that if there was a simple method for studying the activity of AGT it would be of great use. Oligonucleotides were developed that used O^6-benzylguanine and O^6-alkylated guanine derivatives to bind to AGT. It was demonstrated that probes for AGT using the described derivatives could be used successfully and quantitatively to study the activity of AGT [97].

The knowledge garnered from the studies of probes investigating AGT activity and the effects of different mutants at the G160 position were utilised in the development of the SNAP-tag system. This lack of specificity with regards to substrates of AGT lead to this development [89]. SNAP-tag is a 23.5 kDa monomeric protein developed from the AGT mutant G160W which has a greater specificity for O^6-benzylguanine derivatives and also accepts substrates with substituted benzyl rings (Fig. 13).
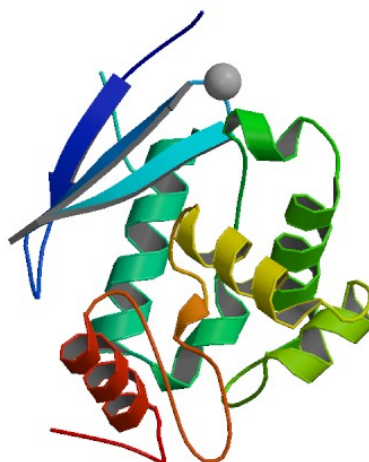
Figure 13 - The structure of SNAP-tag.

The kinetics of the binding reaction of [W160]AGT with O^6-benzylguanine derivatives *in vitro* have been studied and have a second order rate constant of 600 s^{-1} M^{-1}. It is possible to express [W160]AGT as a fusion protein and it has been demonstrated *in cellulo* that it is completely labelled after the addition of an O^6-benzylguanine derivative to the medium of the cells expressing the fusion protein [93]. SNAP-tag substrates consist of an O^6-benzylguanine derivative with a probe, fluorophore or other synthetic compound conjugated via a substituted benzyl ring (Fig. 14).
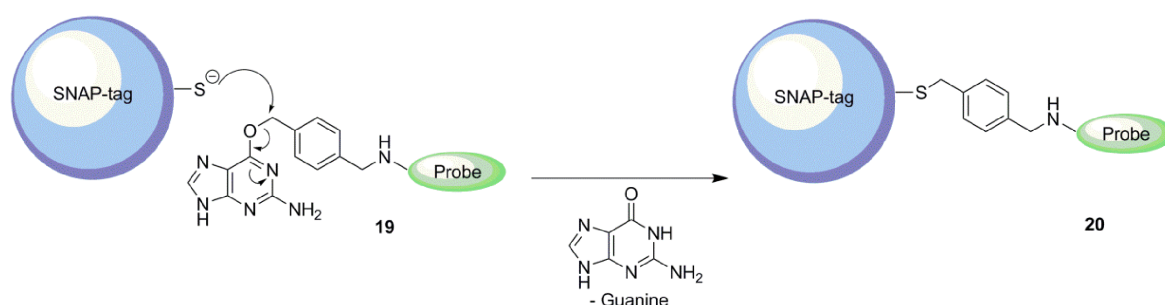
Figure 14 - Probe conjugation to SNAP-tag. The active site cysteine of SNAP-tag performs a nucleophilic displacement specifically with benzylguanine derivatives 19. Guanine is released as a harmless by-product and the synthetic probe is covalently bound to the protein forming conjugate 20.

The SNAP-tag technology has been used widely and for varied purposes including protein distribution studies [98], protein immobilization [99], protein-protein interaction studies [100] and as a tool for locating a synthetic compound to a particular area or organelle of the cell [101].

SNAP-tag has been used in conjunction with a hydrogen peroxide sensor to target it to various areas of the cell, including the ER [101]. HEK293 cell lines were created which expressed SNAP-tag in regions including the plasma membrane, mitochondria, ER and nucleus. There are two different possible SNAP-tag substrates, O^6-(4-aminomethyl)benzylguanine and benzyl-2-chloro-6-aminopyrimidine, which were both synthesised in preparation for coupling to the fluorophore containing probe. The probes, SNAP-Peroxy Green 1 (SPG1) and SNAP-Peroxy Green 2 (SPG2), were a development on the previously discussed PG1 (Fig. 10) and so contained the same fluorophore and boronate ester group for hydrogen peroxide reactivity, but were conjugated to the SNAP-tag substrates to allow specific organelle localisation (Fig. 15).
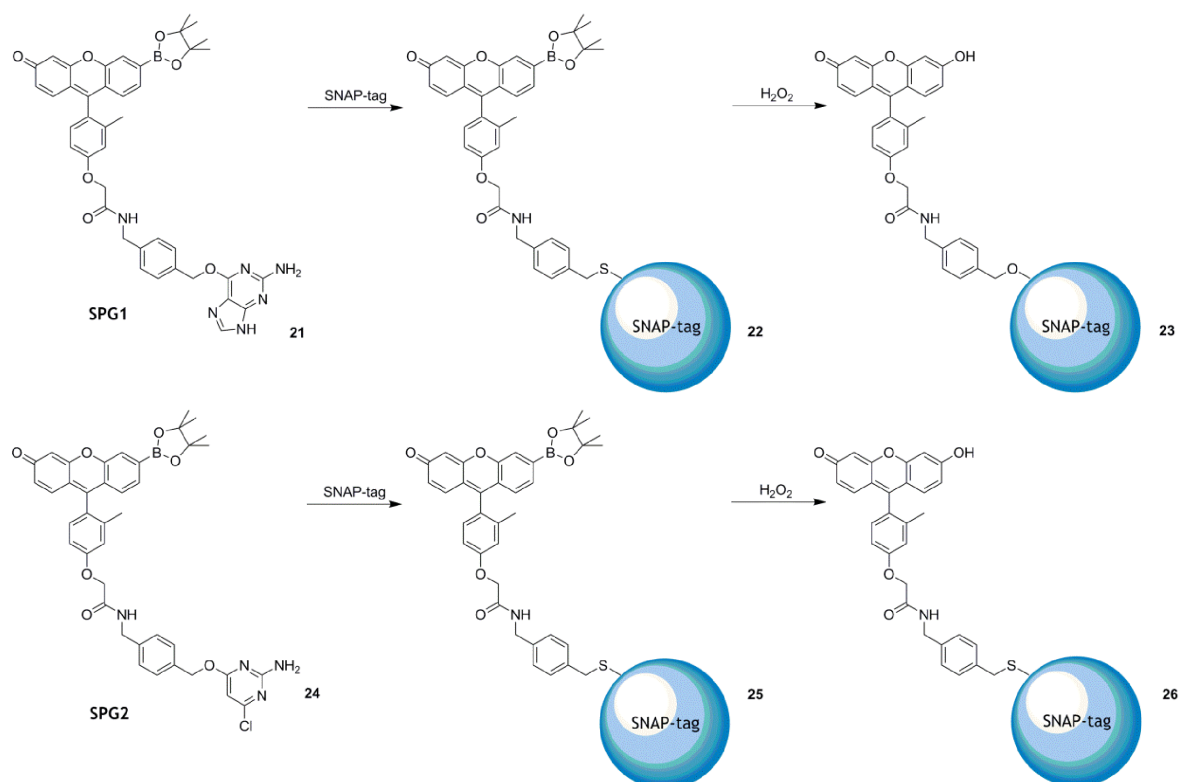
Figure 15 – Two hydrogen peroxide sensors targeted to the ER. SPG1 21 and SPG2 24 are based on the fluorophore Tokyo Green and incorporated a boronate ester for hydrogen peroxide reactivity and SNAP-tag substrates to allow for intracellular localisation. Both probes diffuse into the cell and reacted with SNAP-tag wherever expressed. The probes are mildly fluorescent before reaction with hydrogen peroxide. After reaction the fluorophore is uncaged leading to an increase in fluorescence.

Both SPG1 and SPG2 showed mild fluorescence before reaction with hydrogen peroxide but far more noticeable fluorescence after reaction, when the fluorophore had been uncaged. When the fluorescence of the probes was studied *in vitro*, without any SNAP-tag present, the O^6-(4-aminomethyl)benzylguanine moiety was found to cause quenching, whereas the benzyl-2-chloro-6-aminopyrimidine did not. These moieties are of course removed when the sensors bind to SNAP-tag and any extra quenching before then should not be an issue. When used in cells, a binding time was allowed before any excess probe washed out. Both probes showed reaction and localisation inside cells, though SPG2 was found to be more cell permeable. When used inside cells, the lowest

concentration of hydrogen peroxide detected was 100 μM, when added exogenously.

SPG1 and SPG2 confirm the ability of SNAP-tag to be a useful tool on the localisation of small molecule sensors to different organelles of the cell, however, the use of the Tokyo Green fluorophore offers no significant improvement as the fluorescence is at the same wavelength before and after reaction with hydrogen peroxide and, therefore, is not a ratiometric readout.

HaloTag is a 34 kDa monomeric protein labelling system which is based on a similar theory to SNAP-tag [102]. HaloTag employs a modified bacterial haloalkane dehalogenase. Haloalkane dehalogenases remove halides, such as chlorine, from alkanes by a nucleophilic displacement [103]. This involves nucleophilic attack of the haloalkane by an aspartate residue within the active site. This forms a covalent bond to the substrate. The enzyme is recycled by histidine mediated hydrolysis of the aspartate-alkane intermediate. In HaloTag the histidine is mutated to a phenyalanine preventing the hydrolysis, so that the alkane stays covalently bound to the protein. HaloTag can be expressed in mammalian cells as with SNAP-tag and the use of a bacterial system prevents cross-reactivity from occurring.

HaloTag substrates can therefore be any small molecule as long as it is conjugated to a chloroalkane to provide reactivity (Fig. 16).

27
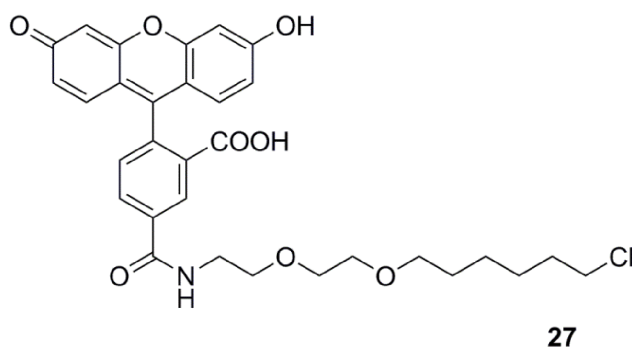
Figure 16 – An example of a HaloTag substrate 27. The fluorophore is conjugated to the haloalkane for reactivity towards HaloTag. A nucleophilic displacement causes loss of the chlorine atom and leaves the fluorophore covalently bound to the protein.

Another possible method of targeting synthetic probes to different cellular locations is the use of targeting peptides. Targeting peptides are short sequences of amino acids that act as a method of directing a protein to a particular area of the cell such as the nucleus, ER, mitochondria or plasma membrane. Almost all proteins that traverse the secretory pathway contain N-terminal signal sequences and proteins destined specifically for the ER often carry the C-terminal ER retention sequence, KDEL [104]. The KDEL receptor exists within the Golgi apparatus with the function of binding to proteins with the retention sequence and retrotransporting them back to the ER [105].

The advantage of using a peptide targeting method over a protein based one, such as SNAP-tag, is that no transfection of cell lines is required. This can be a slow process with varying efficiency. Peptides have been used extensively in therapeutics and molecular imaging techniques [106]. The advances in combinatorial chemistry have meant that a hugely diverse array of peptides can be created.

Peptides have been used successfully with small molecule probes. The zinc sensors Palm-ZP1 and Palm-ZQ make use of a peptide containing a palmitoyl moiety which mimics palmitoylation [107]. Palmitoylation is a post-translational modification of residues such as cysteine with the fatty acid, palmitic acid, which directs proteins to be membrane associated.

The majority of ER targeted probes that use peptide based systems incorporate the ER retention sequence; however Hwang et al. made use of the peptide NYTC [108]. The analyte involved was glutathione and this was studied by the disulfides it formed with the cysteine residue of the short peptide, so strictly the peptide itself was the probe, but a local concentration of the peptide did build up in the ER since the peptide contained an acceptor site for *N*-linked glycosylation. Once glycosylated the peptide did not leave the ER, because the hydrophilic oligosaccharide prevented diffusion across the ER membrane.

The majority of proteins that travel through the secretory pathway undergo N-linked glycosylation on Asn residues that are part of an Asn-X-Ser/Thr sequence [109]. These hydrophilic modifications can dramatically alter the properties of the protein. Glycosylation usually occurs co-translationally once the polypeptide chain is at least 12-14 amino acids in length and extends into the lumen of the

ER. This acts to align the amino acids with the oligosaccharyltransferase (OST). The OST attaches a ready-made carbohydrate which consists of three glucoses, nine mannoses and two N-acetylglucosamines to the Asn residue of the Asn-X-Ser/Thr sequence (Fig. 17).
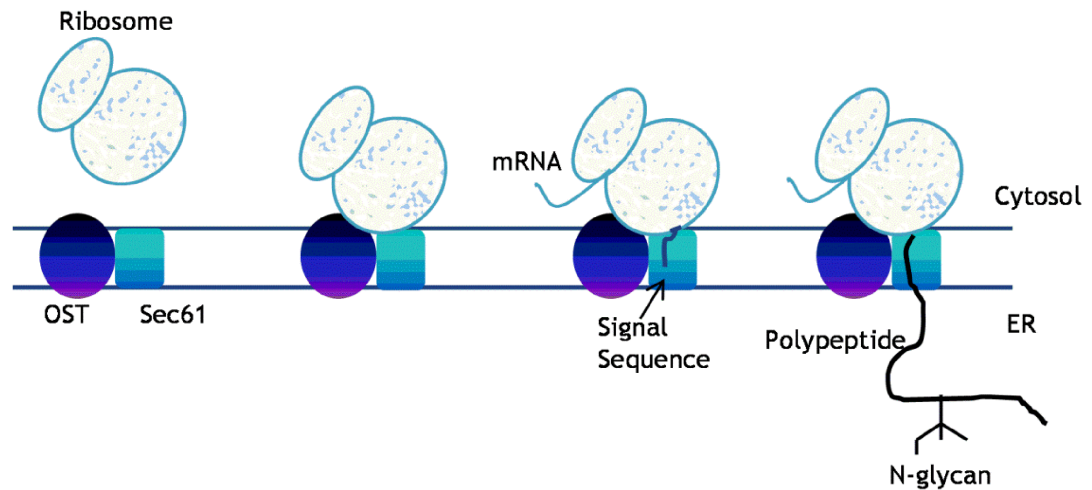
Figure 17 - The glycosylation process. The ribosome comprised of large and small subunit, binds to the ER membrane at the Sec61 complex. The mRNA is translated into the polypeptide chain which passes through the Sec61 complex into the ER lumen. The signal sequence is cleaved and the OST glycosylates at Asn residues that are part of the Asn-X-Ser/Thr sequence.

The main part of the OST consists of a dimer and within each dimeric subunit, there are numerous different parts [110]. Studies have shown that glycosylation is more likely to occur on flexible regions of the polypeptide [111]. This is due to the fact that during the process of N-glycosylation, the hydroxyl group on either the Ser or Thr must be mobile enough to move into a position whereby it increases the nucleophilic properties of the Asn residue.

6.0 Aims

- To synthesise a novel sensor for hydrogen peroxide.
  - Inclusion of a moiety to allow the sensor to be targeted to the ER specifically and a moiety to give the sensor hydrogen peroxide reactivity.
- Incorporate hydrogen peroxide reactivity that causes a structural change in the molecule
  - If fluorescence was to be used as the detection method then the sensor would also require the incorporation of a fluorophore within the structure.
- *In vitro* testing of the probe to give an indication of the reactivity of the sensor to hydrogen peroxide.
  - Assess the sensor for ratiometricity.
- Use of the probe *in cellulo*
  - Show the probe can be selectively targeted to the ER.
  - Show the probe can react with hydrogen peroxide in the ER
  - Develop a simple and robust method of use of the sensor *in cellulo*.

7.0 Materials and Methods

All general chemicals sourced from Sigma-Aldrich unless stated otherwise.

Antibodies

Antibody	Animal of Origin	
Anti-FLAG-tag	Mouse	Sigma-Aldrich
Anti-GAPDH	Mouse	Abcam
Anti-Mouse-FITC	Rabbit	Sigma-Aldrich
Anti-PDI	Rabbit	Abcam
Anti-Rabbit-Texas Red	Mouse	Abcam
Anti-SNAP-P	Rabbit	Pierce Antibodies
Anti-SNAP-tag	Rabbit	New England Biolabs
Anti-Tubulin	Mouse	Santa Cruz Biotechnology
IR Dye 800 Secondary	Rabbit	Li-Cor
IR Dye 800 Secondary	Mouse	Li-Cor
IR Dye 680 Secondary	Rabbit	Li-Cor
IR Dye 680 Secondary	Mouse	Li-Cor

Expression and purification of SNAP-tag

A pET 28a His-tagged SNAP-tag construct was transformed into BL21 DE3 *E. coli* cells. Colonies were grown on LB agar containing kanamycin at a concentration of 20 µg/mL overnight at 37ºC.

A colony was picked and used to inoculate 5 mL Luria Broth (LB) containing kanamycin at a concentration of 10 µg/mL. This culture was incubated at 37ºC overnight, shaking at 180 rpm. The 5 mL culture was used to inoculate 500 mL LB also containing kanamycin, which was left to grow until the OD_{600} reached between 0.5 and 1. At this point the culture was induced using 0.5 mM isopropyl-ß-D-thiogalactopyranoside (IPTG, Bioline), returned to incubation at 37ºC and shaken at 180 rpm for 3 h.

Cells were then pelleted by centrifugation at 5000 *x g* for 20 min at 10ºC before resuspending in 20 mL ice-cold lysis buffer (50 mM Tris-HCl, pH 8.0 containing

200 mM NaCl, 0.5% Triton X-100, 100 µg/mL lysosyme, 10 µg/mL DNAse) containing one complete EDTA free protease inhibitor tablet (Roche). Cells were lysed by freeze-thawing in liquid nitrogen and a 37ºC water bath twice. The solution was rocked for 20 min at room temperature then centrifuged for 30 min at 5000 *x g*. The supernatant was mixed with Ni-NTA agarose resin (Qiagen) which had been equilibrated in 50 mM Tris-HCl pH8.0 buffer containing 500 mM NaCl and 20 mM imidazole. The suspension of supernatant and Ni-NTA agarose was rocked at room temperature for 30 min then centrifuged at 4000 × *g* for 5 min. The resin was resolubilised with 10 mL equilibration buffer and left to rock at room temperature for 5 min. This suspension was centrifuged at 4000 × *g* for 5 min and the process repeated. Elution buffer (5 mL) containing 50 mM Tris-HCl pH8.0, 500 mM NaCl, 0.5 mM EDTA and 500 mM imidazole was then added to the resin, the solution rocked at room temperature for 5 min. The resin solution was poured into a disposable chromatography column (Bio-Rad) and the eluate collected. The resin was washed with a further 5 column volumes of dH$_2$O and 1 mL factions collected. Presence of SNAP was confirmed by running 20 µL of each fraction on a reducing 12.5% SDS-PAGE and visualising the proteins with Colloidal Coomassie (10% w/v ammonium sulfate, 0.1% w/v Coomassie G-250, 5% ortho-phosphoric acid, 20% v/v methanol).

The fractions containing SNAP-tag were then pooled and purified further via a GE healthcare Mono-Q anion exchange column on an ÄKTA purifier system. The binding buffer contained 50 mM Tris-HCl pH7.5, 50 mM NaCl and 1 mM DTT. The protein was eluted using a gradient with buffer containing 50 mM Tris-HCl pH7.5, 1M NaCl and 1 mM DTT. The protein was desalted using a PD-10 column (GE healthcare) according to manufacturer's instructions. The concentration was determined by measuring the absorbance of the solution at 280 nm on a Cary 300-bio UV-visible spectrophotometer and using the extinction coefficient of SNAP-tag.

SDS-PAGE and Western Blotting

Samples for SDS-PAGE analysis were resuspended in SDS sample buffer (25 mM Tris-HCl pH 6.8, 25% glycerol, 7.5% w/v SDS and 0.004% w/v bromophenol blue). Samples were boiled in the presence or absence of 50 mM DTT for 2 min prior to loading on the gel. Gels used were either 10% or 12.5% SDS-PAGE gels

Gels were then either stained with colloidal Coomassie or transferred onto a nitrocellulose membrane. Membranes were blocked for 1 h with 8% skimmed milk powder in TBST buffer (10 mM Tris-HCl pH8.0, 150 mM NaCl, 0.05% Tween-20). Membranes were incubated with primary antibodies in TBST containing 3% skimmed milk powder for 1 h at dilutions between 1 in 500 and 1 in 10000. Blots were washed 3 × with TBST for 5 min before incubation with fluorescently-labelled secondary antibodies at a 1 in 10000 dilution for 1 h in TBST. Blots were washed 2 × with TBST with a H_2O rinse in between washes. Blots were stored in the dark in H_2O for 10 min before being scanned with an Odyssey Sa quantitative fluorescence imaging system.

Tissue Culture

Experiments used an HT1080 human fibrosarcoma cell line. Cells were passaged in a sterile hood according to normal tissue culture practice and incubated at 37°C with 5% CO_2. Cells were grown in Dulbecco's modified eagle medium (DMEM, Gibco) supplemented with 10% foetal calf serum (Gibco), 1% v/v L-glutamine (200 mM stock, Gibco) and 1% v/v penicillin/streptomycin (5000 units/mL penicillin, 5000 µg/mL streptomycin stock, Gibco). Cells were washed with Dulbecco's Phosphate Buffered Saline (PBS, Gibco) and passaged with 0.05% Trypsin-EDTA (Gibco).

For the creation of the stable cell line HT SNAP ER the SNAP plasmid containing a KDEL sequence and ER targeting sequence was linearised using 20 µg DNA, 5µL restriction enzyme 10 x buffer H (Promega), 20 units restriction endonuclease SSP (Roche) and made up to 50 µL with H_2O and incubated at 37°C for 2 h. TE buffer (250 µL, 10 mM Tris-HCl pH7.5 and 1 mM EDTA) and 300 µL phenol/chloroform/isoamylalcohol 25:24:1 were added, the solution vortexed and centrifuged for 2 min at 16162 × g. The upper phase was removed, 300 µL chloroform added and the solution vortexed and centrifuged at 16162 × g for 5 min. The upper phase was then transferred to a new eppendorf tube and precipitation induced by the addition of an excess of ethanol. The solution was then centrifuged at 16162 × g for 10 min. The supernatant was disposed of and the pellet washed with 1 mL 70% ethanol. This was centrifuged for 5 min at 16162 × g. The supernatant was removed again and the pellet left to air dry before being resuspended in 10 µL H_2O.

For transfection 0.5 mL DMEM and 10 μL polyethyleneimine (PEI) were added to each to two 15 mL falcon tubes. Linearised DNA solution (4 μL) was then added to one of the tubes. These were vortexed and left at room temperature for 10 min. A further 3.5 mL of DMEM were then added to each tube and each solution was added to a 6cm dish with good cell coverage. The pCI vector was used which carries neomycin resistance. G418 was used as the selection agent at a concentration of 800 μg/mL.

The stable cell line, HT SNAP Cyto was created by M. Pringle (University of Glasgow) and carries Hygromycin B (Roche) resistance (250 μg/mL).

Confocal Microscopy

Immunofluorescence Staining of HT SNAP ER cells

Coverslips were dipped in ethanol then left to air dry in a sterile hood. Coverslips were placed in the wells of a 6-well dish and 50 μL of poly-D-lysine HBr pipetted on top of each coverslip. After 5 min poly-D lysine HBr was removed and HT1080, HT SNAP ER cells in medium were seeded. Cells seeded onto coverslips were left overnight. The next morning cover slips were washed with PBS × 2 and fixed with -20ºC methanol for 10 min. The methanol was removed and cells washed twice with PBS. A solution of 0.2% bovine serum albumin (BSA, Sigma Aldrich) in PBS was then left on the coverslips for 30 min. The primary antibody solutions were then left on the coverslips for 1 h at a dilution of 1 in 200 in 0.2% BSA in PBS. Antibodies used were anti-FLAG (Sigma-Aldrich) and anti-PDI (Abcam). The coverslips were then washed with PBS twice and the secondary antibody solutions were placed on the coverslips for 1 h, again in 0.2% BSA in PBS. The secondary antibody for anti-FLAG was anti-mouse-FITC (Sigma-Aldrich) and for anti-PDI, anti-rabbit-Texas red (Abcam). The coverslips were then washed with PBS and H_2O. The coverslips were adhered onto slides using a solution of 25 mg/mL1,4-diazabicyclo[2.2.2]octane (DABCO) in Mowiol 4.88. A Zeiss LSM confocal microscope was used to collect images of fixed cells.

Treatment of HT SNAP ER and Cyto with BG-NBD-X and Fluorescence

Coverslips were dipped in ethanol then left to air dry in a sterile hood. Coverslips were placed in the wells of a 6-well dish and 50 μL of poly-D-lysine

HBr pipetted on top of each coverslip. After 5 min poly-D lysine HBr was removed and HT1080, HT SNAP ER and HT SNAP Cyto cells in medium were seeded. G418 and Hygromycin B were added accordingly. The following day cells were washed with PBS and either medium or medium with 5 μM BG-NBD-X added to the wells. After 30 min incubation cells were washed with PBS twice and fixed for 10 min with -20°C methanol. Coverslips were removed from wells and washed with PBS then H_2O and adhered to slides using 7 μL 25 mg/mL DABCO in Mowiol 4.88. Images of cells were taken using a Zeiss LSM confocal microscope.

Fluorescein Maleimide Binding Assay

Hemocyanin from *Megathura crenulata* (Keyhole limpet, KLH) (1 μg, 0.4 μL KLH 3.0 mg-7.0 mg in PBS, Sigma-Aldrich) either untreated or treated with hapten, was mixed with 10 μL 5 mM fluorescein maleimide in DMSO and 19.6 μL denaturing buffer (6M urea, 200 mM Tris-HCl pH 8.0, 0.5% SDS), and rocked at room temperature for 30 min in the dark. The reaction was stopped by precipitating the mixture with 150 μL of -20°C acetone. The solution was stored at -20°C for 1 h then centrifuged for 10 min at 16162 × *g*. Supernatant was removed and samples resuspended in 5 × SDS sample buffer with 50 mM DTT. After boiling, samples were run on a 6% polyacrylamide gel with no stacking gel for 3 h. The gel was fixed in 5% acetic acid with 10% methanol and scanned using a GE healthcare Typhoon FLA 9500.

HPLC Purification of Peptides

Peptides were purified by HPLC on a GE healthcare ÄKTAmicro system. An ACE 5 C4-300 column was used. Flow rate was run at 0.2 mL/min. Gradient was 0-90% MeCN with 0.1% TFA in H_2O over a volume of 2 mL.

Sample Preparation of Purified SNAP Samples for MALDI-TOF

A stock of SNAP-B was prepared by adding 222 μL of a 1 mg/mL solution of BGB in buffer (100 mM Tris-HCl pH7.5) to 120 μL of a 351 μmol solution of SNAP in buffer (50 mM Tris-HCl pH7.5 with 150 mM NaCl). The solution was kept at 37°C for 30 min. Excess unbound BGB was removed by buffer exchange using Bio-Rad Micro Bio-Spin chromatography columns resulting in a stock of SNAP-B in 100 mM Tris-HCl pH 7.5 buffer at a concentration of 123 μmol.

For each sample 2 μL of SNAP-B was added to an eppendorf tube containing 7 μL of buffer (100 mM Tris-HCl pH7.5) and 1 μL of H_2O_2 at the desired concentration. After allowing samples to react for a particular time period reaction was stopped by the addition of 50 μL -20°C acetone. Samples were kept at -20°C for 1 h to precipitate protein. Samples were then centrifuged at 16162 *x g* for 10 min and resuspended in trypsin solution (10 ng/μL in 100 mM Tris-HCl pH 7.5). Samples were kept overnight at 37°C then the next day 10 μL acetonitrile containing 0.4% formic acid added. Samples were kept at room temperature for 30 min before analysis.

Sample Preparation of HT SNAP Samples for MALDI-TOF

HT SNAP cells were seeded into 10 cm dishes. The following day, cells at confluency of 70-90% cells were washed with PBS then DMEM containing 5 μM BGB added and cells placed back in incubator for 30 min. Cells were washed with PBS to remove unbound probe then medium containing H_2O_2 or other treatment was added to cells. Cells were then placed back in the incubator for the desired time. Medium was then removed and cells washed with PBS, then fresh PBS containing 25 mM iodoacetamide left on for 5 min to block free thiols. Cells were then lysed in 200 μL lysis buffer (50 mM Tris-HCl pH 8.0, 1% Triton X-100 and 150 mM NaCl). Lysates were left on ice for 10 min then centrifuged at 14167 *x g* for 5 min.

Supernatants were added to 20 μL anti-FLAG M2 affinity gel (Sigma-Aldrich) which had been equilibrated using TBS buffer (50 mM Tris-HCl pH 7.5, 150 mM NaCl) according to manufacturer's instructions. SNAP expressed in mammalian cells has a FLAG tag incorporated to allow immunoaffinity purification. Total volume was made up to 1 mL with lysis buffer (50 mM Tris-HCl pH 7.5, 200 mM NaCl, 0.5% Triton X-100). Samples were immunoisolated for 2 h at 4°C on a roller shaker. Samples were centrifuged at 8000 x *g* for 30 seconds and supernatant removed. Affinity gels were washed three times with 400 μL TBS buffer and resuspended in 10 μL 8 M urea in 50 mM Tris-HCl pH8.0. Samples were incubated at 60 °C for 45 min then diluted with 70 μL 100 mM Tris-HCl pH 7.5 containing 100 ng trypsin. Samples were stored overnight at 37°C. Supernatants were transferred into fresh Eppendorf tubes and peptides purified using C18 ZipTips (Millipore). Use of ZipTips differed from manufacturer's instructions as wetting

solution was isopropanol: H_2O: TFA 1:1:0.1, equilibrating solution was H_2O: TFA 1:0.1 as recommended and elution solution was isopropanol: TFA 1:0.1.

MALDI-TOF

Samples were analysed using either a Bruker Ultraflex MALDI-TOF/TOF or a Shimadzu AXIMA Performance MALDI-TOF/TOF. A Bruker MTP 384 ground steel target plate was used. Matrices used were either 5 mg/mL α-cyano-4hydroxycinnamic acid (CHCA) in 50% acetonitrile and 0.1% trifluoroacetic acid (TFA) or 5 mg/mL 2,5-dihyroxybenzoic acid (DHB) with 2.5 mg/mL CHCA in 50% acetonitrile and 0.1% TFA. Sample solution (0.5 µL) was mixed with matrix solution (0.5 µL), spotted on the target and allowed to air dry completely before analysis.

In Vitro **Translation**

Peptide NYTCKDEL (AnaSpec) was solubilised in H_2O at a concentration of 25 mM. Peptide NYTC (Cambridge peptides) was solubilised in 10% acetonitrile in dH_2O at a concentration of 25 mM. In each reaction tube was added 16.5 µL rabbit reticulocyte lysate, 0.4 µL KCl, 0.5 µL methionine free amino acid mix, 1 µL influenza virus hemagglutinin RNA and 1 µL ^{35}S methionine. If included, peptides were added to a final concentration of 5 mM and 1 µL of dog pancreas microsomes were used. Samples were incubated for 60 min at 30 °C then centrifuged at $16162 \times g$ for 5 min. Supernatants were removed and samples prepared for SDS-PAGE. After electrophoresis, gels were fixed for 30 min at room temperature in 10% acetic acid and 10% methanol. Gels were then dried for 1 h at 80°C using a Hoefer Scientific DryGel. Phosphor plates were prepared by illumination on a lightbox for 10 min prior to exposure overnight to the dried gel. Phosphor plates were analysed using a phosphorimager (Fujifilm FLA-7000).

ELISA

SNAP, SNAP-B and SNAP-P were bound to 96-well plates at a concentration of 10 µg/mL in 100 µL of 50 mM sodium carbonate buffer pH 9.6. Plates were incubated overnight at 4°C. Wells were then washed with 1% w/v BSA (bovine serum albumin, Melford), 0.5 Tween20 in PBS. Non-specific binding was blocked by incubation for 1 h at 37°C with 200 µL per well of 1% w/v BSA in PBS. A 1:500 dilution anti-SNAP-P (100 µL, Pierce) in 1% w/v BSA in PBS was added to each

well and plates incubated for 1 h at 37°C. Wells were then washed twice with 200 µL 1% w/v BSA, 0.5 Tween20 in PBS. 100 µL of 1:10000 Goat anti-Rabbit HRP conjugate was added to each well and incubated for 1 h at 37°C. Wells were then washed twice with 200 µL 1% w/v BSA, 0.5 Tween20 in PBS. One *O*-phenylenediamine dihydrochloride tablet (10 mg) was dissolved in 25 mL 50 mM phosphate-citrate buffer pH5.0 with 10 µL 30% H_2O_2. 100 µL of substrate was added to each well and incubated for 20 min at room temperature. The reaction was stopped by the addition of 25 µL of 3 M HCl to each well. Absorbance was read at 490 nm using a BMG Labtech Pherastar FS plate reader.

Use of Peptides in HT1080 Cells

Confluent HT1080 cells in 6 cm dishes were first washed with PBS then treated with either 1 mM Ac-NYTCKDEL (AnaSpec) or Ac-NYTC (Cambridge Peptides) in medium, or medium only for the control. Cells were incubated with peptides for 1 h. After incubation medium was removed and cells were washed with PBS. 100 µL of cold 10% trichloroacetic acid (TCA) was added to each dish to precipitate proteins. The lysates were centrifuged for 10 min at 14167 *x g* at 4°C. Supernatants were purified using C18 ZipTips (Millipore) according to manufacturer's instructions. Samples were analysed by MALDI-TOF using a matrix with CHCA (5 mg/mL in 50% acetonitrile, 0.1% TFA).

Antibody Purification

A stock of SNAP-P was first prepared by mixing 600 µL of 351 µM purified SNAP, 360 µL 100 mM Tris-HCl pH 7.5 and 40 µL of 10 mg/mL benzylguanine-phenol (BGP) in DMF and incubating the solution at 37 °C for 30 min. Excess BGP was removed and SNAP-P buffer exchanged into 0.1 M $NaHCO_3$ pH 8.3 with 0.5 M NaCL using a PD10 column (GE healthcare) according to manufacturer's instructions. The fraction collected from the PD10 column was concentrated to a volume of 1.5 mL using a Sartorius Vivaspin 20 centrifugal concentrator. Cyanogen bromide (CNBr) activated Sepharose (0.3 g, Amersham) was suspended in 2 mL 1 mM HCl and placed on a glass sinter attached to a conical flask with a side arm. This was placed under vacuum and the Sepharose washed with 200 ml 1 mM HCl. The concentrated SNAP-P and the prepared CNBr-Sepharose were mixed and left on a rocker at 4 °C overnight. Prior to mixing with the Sepharose, the absorbance at 280 nm of the SNAP-P stock was measured.

The next day supernatant was removed from the Sepharose and the absorbance at 280 nm measured. The drop in absorbance indicated coupling of the protein to the Sepharose had occurred. The SNAP-P Sepharose washed with 5 × gel volume of coupling buffer (0.1 M NaHCO$_3$ pH 8.3, 0.5 M NaCl). Tris-HCl pH8.0 (0.1 M) was added to the gel and it was left to stand for 2 h to block any remaining unreacted groups. The gel was washed 3 × with alternating pH buffers.

1. 0.1 M NaOAc/acetic acid, 0.5 M NaCl, pH 4.0
2. 0.1 M Tris-HCl, 0.5 M NaCl, PH 8.0

The gel was packed into a disposable chromatography column (Bio-Rad) and flushed with PBS (Gibco). Crude antibody serum (1 mL) was placed on the gel bed and the flow-through reapplied three times before washing with seven times column volumes of PBS (Gibco). The antibody was eluted with 10 mL 0.1 M glycine.HCl pH 2.8. Fractions (1 mL) were collected into eppendorf tubes containing 70 µL 1 M Tris-HCl to raise the pH. The absorbance of the fractions at 280 nm was measured to assess which ones contained antibody. The purification was assessed by using the eluate in an ELISA experiment to gauge the affinity of the sera to SNAP, SNAP-B and SNAP-P.

8.0 Chemistry Experimental

All reactions under an inert atmosphere were carried out using flame dried glassware. Solutions were added *via* syringe. Acetonitrile, diethyl ether, tetrahydrofuran, dichloromethane, and toluene were dried where necessary using a solvent drying system, Puresolv™, in which solvent is pushed from its storage container under low nitrogen pressure through two stainless steel columns containing activated alumina and copper. Triethylamine was dried via distillation with calcium hydride. Reagents were obtained from commercial suppliers and used without further purification. ^{1}H, ^{13}C NMR spectra were obtained on a Bruker DPX/400 spectrometer operating at 400 and 100MHz respectively or on a Bruker AVIII spectrometer operating at 500, and 126 MHz respectively. All coupling constants are measured in Hz. DEPT was used to assign the signals in the ^{13}C NMR spectra as C, CH, CH$_2$ or CH$_3$. Mass spectra (MS) were recorded on a Jeol JMS700 (MStation) spectrometer except ESI$^+$, ESI$^-$ and certain CI$^+$ analyses, which were recorded on a Thermofisher LTQ Orbitrap XL. Infra-red (IR) spectra were obtained on a Shimadzu FTIR-8400S spectrometer using attenuated total reflectance (ATR) so that the IR spectrum of the compound (solid or liquid) could be directly detected (thin layer) without any sample preparation. Fluorescence spectra were collected on a Shimadzu RF-5301PC spectrofluorophotometer. MALDI-TOF MS spectra were collected out on a Shimadzu AXIMA Performance MALDI-TOF/TOF mass spectrometer. High performance liquid chromatogpraphy (HPLC) was carried out on a GE healthcare ÄKTAmicro chromatography system.

4-(Aminobenzyl)methanol (34)
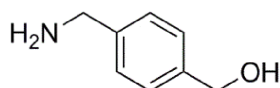
Methyl 4-cyanobenzoate **33** (3.00 g, 18.6 mmol, 1.0 eq) was dissolved in anhydrous THF (100 mL) and cooled to 0 °C. To the stirred solution, lithium aluminium hydride (1.90 g, 50.0 mmol, 2.7 eq) was added slowly, leading to a change of colour to from yellow to blue/dark green and formation of a slurry, out of which hydrogen gas evolved. The reaction mixture was heated to reflux for 12h, then cooled to 0 °C and H$_2$O (50 mL) was added slowly to quench the reaction. The mixture was treated with aqueous NaOH (10%, 50 mL), and then

extracted into DCM (5 × 40 mL). The combined organic layers were washed twice with brine, dried over magnesium sulfate and evaporated to dryness *in vacuo* yielding amine **34** as a cream solid (1.67 g, 12.2 mmol, 66%). δ_H (CDCl$_3$, 400 MHz): 7.31 (2H, d, *J* = 8.1 Hz, H2 and H6), 7.26 (2H, d, *J* = 8.1 Hz, H3 and H5), 4.6 (2H,s, OCH$_2$), 3.82 (2H, s, NCH$_2$), 1.98 (1H, br s). δ_C (CDCl$_3$, 100 MHz): 142.28 (C), 139.84 (C), 127.27 (CH), 127.23 (CH), 64.79, (CH$_2$), 46.09 (CH$_2$).

Agrees with literature [93].

N-[4'-(Hydroxymethyl)benzyl]2,2,2-trifluoro-acetamide (35)
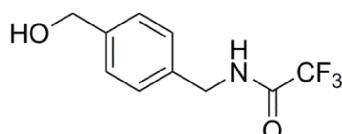
To a solution of amine **34** (693.0 mg, 5.10 mmol, 1.0 eq) and triethylamine (0.8 mL, 6.60 mmol, 1.3 eq) in anhydrous MeOH (10 mL), ethyl trifluoroacetate (0.7 mL, 5.1 mmol, 1.0 eq) was added dropwise. The reaction mixture was stirred for 45 min, diluted with EtOAc (150 mL) and H$_2$O (150 mL). The combined organic layers washed with brine and dried over Na$_2$SO$_4$. After removal of solvent *in vacuo*, column chromatography (0-20% EtOAc in cyclohexane) yielded amide **35** (0.70 g, 3.0 mmol, 59 %). R_f[SiO$_2$, EtOAc: cyclohexane (1:1)]:0.26. δ_H (CDCl$_3$, 400 MHz): 7.36 (2H, d, *J* = 8.1 Hz, H3' and H5'), 7.27 (2H, d, *J* = 8.1 Hz, H2' and H6'),6.70 (1H, br s, NH), 4.68 (2H, s, OCH$_2$), 4.51 (2H, d, *J* = 5.9 Hz, NCH$_2$), 1.84 (1H, br s). δ_C (CDCl$_3$, 100 MHz): 141.04 (C), 135.21 (C), 128.18 (CH), 127.57 (CH), 117.00 (C), 114.71 (C), 64.80 (CH$_2$), 43.64 (CH$_2$).

Agrees with literature [93].

1-(2'-Amino-9*H*-purin-6'-yl)-1-methylpyrrolidinium chloride (37)
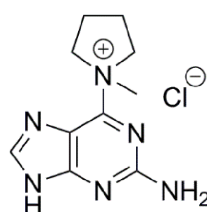
6-Chloro-guanine **36** (5.0 g, 29.4 mmol, 1.0 eq) was dissolved in 100 mL anhydrous DMF at 40˚C. After cooling to room temperature, 1-methyl-pyrrolidine (7.0 mL, 65.8 mmol, 2.2 eq) was added and the reaction mixture stirred

overnight at rt. Acetone (10 mL) was added to complete precipitation and the solid was filtered, washed with Et_2O (50 mL) and dried yielding chloride **37** as a beige solid (3.54 g, 13.8 mmol, 47%). δ_H (d6-DMSO, 500 MHz): 13.38 (1H, br s, 13.38, NH), 8.35 (1H, s, H8'), 7.12 (2H, br s, NH_2), 4.62-4.58 (2H, m, H2/H5), 3.98-3.95 (2H, m, H2/H5), 3.65 (3H, s, Me), 2.27-2.21 (2H, m, H3/H4), 2.06-2.01 (H3/H4). δ_C (d6-DMSO, 100 MHz): 159.52 (C), 159.03 (C), 152.12 (C), 143.42 (CH), 116.50 (C), 64.52 (CH_2), 52.04 (Me), 21.92 (CH_2).

Agrees with literature [93].

O^6-(4-Aminomethyl-benzyl)guanine (39)
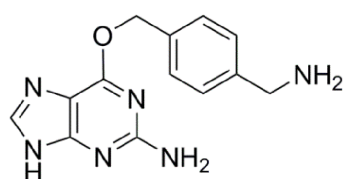
Amide **35** (473 mg, 2.00 mmol, 1.0 eq) was dissolved in anhydrous DMF under argon and sodium hydride (0.24 g, 6.10 mmol, 3.0 eq) was added forming a blue solution. 4-Dimethylaminopyridine (25.0 mg, 0.20 mmol, 0.1 eq) was added to the mixture then chloride **37** (0.50 g, 2.00 mmol, 1.0 eq) and the solution warmed to 40 °C and stirred under argon for 3h. A few drops of H_2O were added to quench any excess sodium hydride and solvent removed *in vacuo*. Column chromatography (MeOH 0-10% in DCM) yielded amine **39** at 75% purity (341.6 mg, 0.958 mmol, 48%). R_f[SiO_2, MeOH-DCM (1:5)]: 0.07. Not purified further to prevent loss of material. Selected data from crude**:** δ_H (DMSO, 400 MHz): 7.82 (1H, s, H6), 7.39 (4H, m, Ar), 6.27 (2H, s, NH_2, guanine), 5.45 (2H, s, CH_2O), 3.71 (2H, s, CH_2NH_2).

Agrees with literature [93].

N-(4-[(2'-Amino-9H-purin-6'-yl)oxymethyl]benzyl)-6''-[(7'''-nitro-2''',1''',3'''-benzoxadiazol-4'''-yl)amino]hexanamide (BG-NBD-X) (41)
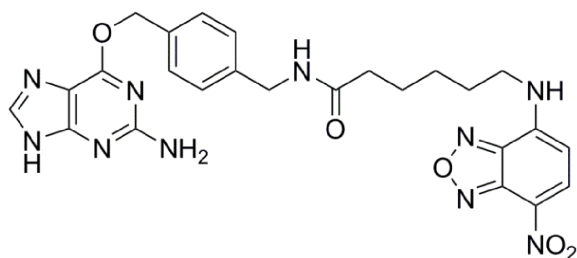
Triethylamine (7 µL, 0.048 mmol, 3.0 eq.) was added to a solution of O^6-(4-aminomethyl)benzylguanine **39** (75% pure, 11.3 mg, 0.031 mmol, 2.0 eq.) in anhydrous DMF (0.1 mL). NBD-X-succinimidyl ester (6.1 mg, 0.0165 mmol, 1.0 eq.) was added and the mixture stirred at room temperature under argon for 24 h. Solvent was removed *in vacuo*. Column chromatography (0-20% MeOH in DCM) yielded BG-NBD-X **41** as an orange solid (6.5 mg, 0.012 mmol, 74%). δ_H (MeOD, 400 MHz): 8.42 (1 H, d, J = 8.8 Hz, H-6'''), 7.78 (1H, br s, H-8), 7.48 (2 H, d, J = 8.2 Hz, H-3' and H-5'), 7.30 (2H d, J = 8.2 Hz, H-2' and H-6'), 6.19 (1 H, d, J = 8.8 Hz, H-5'''), 5.50 (2H, s, CH_2O), 4.35 (2H, s, PhCH_2NH), 3.45 (2H, br s, H-6), 2.26 (2H, t, J = 7.2 Hz, H-2), 1.76-1.66 (4H, m, H-4 and H-5), 1.47-1.41 (2H, m, H-3). LRMS (EI$^+$): m/z 569 ([M+Na]$^+$ 8%), 481 (instrument background 100%). HRMS (ESI$^+$): m/z 569.1964. $C_{25}H_{26}N_{10}O_5$ requires [M+Na]+ 569.1980.

2,3-Dihydro-2-(3'-hydroxyphenyl)-1H-isoindole-1,3-dione (43)
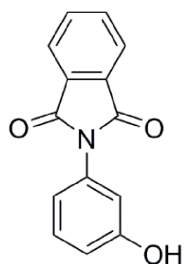
3-Aminophenol **42** (15.00 g, 137 mmol, 1.0 eq) was mixed with phthalic anhydride (20.29 g, 137 mmol, 1.0 eq) and heated to 150 °C to form a melt. This was left for 48 h before acidification with 10% HCl (200 mL) and extraction into EtOAc (3 × 250 mL). The organic layers were combined, dried over MgSO$_4$ and concentrated *in vacuo* to yield phthalimide **43** as a lilac solid (25.99 g, 109 mmol, 79%). Mp: 219-220 °C. v_{max} (ATR): 3327 (OH), 1699 (C=O), 1609 (Ar) cm^{-1}. δ_H (CDCl$_3$, 400 MHz): 7.96 (2H, dd, J = 3.1, 5.5 Hz, H5 and H6), 7.80 (2H, dd, J =

3.1, 5.5 Hz, H4 and H7), 7.37 (1H, t, J = 8.1 Hz, H5'), 7.04, (1H, ddd, J = 0.8, 1.9, 8.0 Hz, H4'), 6.96 (1H, t, J = 2.2 Hz, H2'), 6.88 (1H, ddd, J = 0.8, 2.5, 8.2 Hz, H6'). δ_C (CDCl$_3$, 100 MHz): 167.22 (C), 156.03 (C), 134.49 (CH), 131.70 (C), 130.10 (CH), 123.84 (CH), 120.99 (C) 118.90 (CH), 115.34 (CH), 113.78 (CH). LRMS (CI$^+$): m/z 240 [(M+H)$^+$, 100%]. HRMS (CI$^+$): m/z [M+H]$^+$ 240.0659. C$_{14}$H$_{10}$O$_3$N requires 240.0661.

4-(2',3'-Dihydro-1',3'-dioxo-1*H*-isoindol-2'-yl)-2-hydroxybenzaldehyde (44)
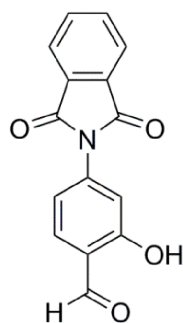
Magnesium chloride (2.97 g, 31.0 mmol, 1.5 eq), triethylamine (11 mL, 79.0 mmol, 3.8 eq) and paraformaldehyde (4.18 g, 139 mmols, 6.7 eq) were added to a stirring solution of phthalimide **43** (4.95 g, 20.7 mmol, 1.0 eq.) in MeCN (100 mL). The reaction was heated to reflux and stirred overnight under argon. The reaction mixture was acidifed with 10% HCl (50 mL), extracted into DCM (3 × 100 mL), dried over MgSO$_4$ and concentrated *in vacuo*. Column chromatography (0-10% EtOAc in DCM) yielded aldehyde **44** as needles (2.82 g, 10.6 mmol, 51%). R_f[SiO$_2$, EtOAc-DCM (1:20)]: 0.89. Mp: 197-198 °C. v_{max} (ATR): 3051 (OH), 2872 (CHO), 1735 (C=O), 1628 (Ar) cm^{-1}. δ_H (CDCl$_3$, 400 MHz): 11.16 (1H, s, H1), 9.94 (1H, s, OH), 7.98 (2H, J = 3.1, 5.5 Hz, H5' and H6'), 7.83, (2H, dd, J = 3.0, 5.5 Hz, H4' and H7'), 7.69 (1H, dd, J = 1.0, 7.6 Hz, H5), 7.20 (2H, m, H6 and H3). δ_C (CDCl$_3$, 100 MHz): 195.81 (CH), 166.42 (C), 162.02 (C), 139.31 (C), 138.84 (CH), 134.19, (CH), 131.48 (C), 124.09 (CH), 119.56 (C), 117.31 (CH), 115.00 (CH). LRMS (CI$^+$): m/z 268 [(M+H)$^+$, 100%]. HRMS (CI$^+$): m/z [M+H]$^+$ 268.0611. C$_{15}$H$_{10}$O$_4$N requires 268.0610.

4-(2',3'-Dihydro-1',3'-dioxo-1*H*-isoindol-2'-yl)-2-(prop-2''-en-1''-yloxy)benzaldehyde (45)
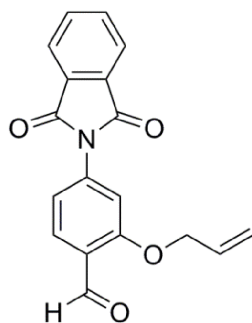
Potassium carbonate (5.91 g, 42.8 mmol, 1.1 eq.) and allyl bromide (3.70 mL, 42.8 mmol, 1.1 eq.) were added to a stirring solution of aldehyde **44**(10.4 g, 38.9 mmol, 1.0 eq.) in MeCN (250 mL). The solution was heated to reflux and left overnight. The reaction was quenched into H_2O (100 mL) and extracted into DCM (3 × 100 mL). The organic layers were dried over $MgSO_4$ and concentrated *in vacuo* to yield allyl ether **45** as a white amorphous solid (11.4 g, 37.1 mmol, 95%). Mp: 158-160°C. v_{max} (ATR): 1724 (C=O), 1688 (C=C) cm^{-1}. δ_H (CDCl$_3$, 400 MHz): 10.54 (1H, s, CHO), 8.00-7.98 (3H, m, H6, H5' and H6'), 7.83 (2H, dd, J = 3.0, 5.4 Hz, H4' and H7'), 7.23 (1H, ddd, J = 0.6, 1.8, 8.4 Hz, H5), 7.19 (1H, d, J = 1.8 Hz, H3), 6.15-6.05 (1H, m, H2''), 5.48 (1H, dd, J = 1.5, 17.5 Hz, H3''), 5.37, (1H, dd, J = 1.5, 10.6 Hz, H3''), 4.71 (2H, dt, J = 1.5, 5.3 Hz, CH$_2$). δ_C (CDCl$_3$, 100 MHz): 188.77 (CH), 166.63 (C), 161.05 (C), 138.32 (C), 134.82 (CH), 131.94 (CH), 131.45 (C), 129.00 (CH), 123.98 (CH), 118.57 (CH$_2$), 118.27 (CH), 110.67 (CH), 69.54 (CH$_2$). LRMS (EI$^+$): *m/z* 307 [(M)$^{•+}$, 55%] 267 [(M - C$_3$H$_5$) $^{•+}$, 100%]. HRMS (EI$^+$): *m/z* [M]$^{•+}$ 307.0844. C$_{18}$O$_4$NH$_{13}$ requires 307.0845.

6-(2',3'-Dihydro-1',3'-dioxo-1*H*-isoindol-2'-yl)-1-benzofuran-2-carbaldehyde (46)
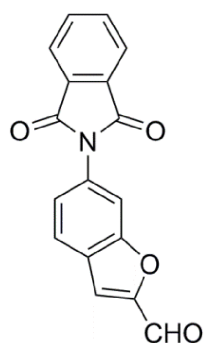
Methyl morpholine *N*-oxide (5.97 g, 51.0 mmol, 2.8 eq.) and osmium tetroxide (2.5% in propanol, 6.2 mL, 0.6 mmol, 0.03 eq.) were added to a stirring solution of allyl ether **45** in THF (70 mL). The solution was stirred at room temperature overnight under argon. Solvent was then removed *in vacuo* and the residue produced dissolved in EtOAc (100 mL) and H_2O (100 mL). The aqueous layer was washed with further EtOAc (100 mL) and the organic layers were combined and dried over magnesium sulphate and concentrated *in vacuo*. The residue produced was dissolved in MeOH (40 mL) and H_2O (20 mL), sodium metaperiodate (8.56 g, 40.0 mmols, 2.2 eq.) added and the mixture stirred at room temperature overnight. The solvent was removed *in vacuo* and the residue produced was dissolved in EtOAc (100 mL) and H_2O (100 mL). The organic layers were combined, washed with H_2O, dried over $MgSO_4$ and concentrated *in vacuo*, yielding a beige solid. The beige solid was dissolved in acetic acid (100 mL) and heated to reflux overnight. Solvent was removed *in vacuo* and column chromatography (0-10% EtOAc in DCM) yielded benzofuran **46** as an amorphous solid (2.58 g, 8.86 mmol, 89%). R_f[SiO2, EtOAc-DCM(1:20)]: 0.87. Mp: 274 – 276 °C. v_{max} (ATR): 1719 (C=O), 1705 (C=O), 1676 (alkene C) cm^{-1}. δ_H (CDCl$_3$, 400 MHz): 9.91 (1H, s, CHO), 8.00 (2H, dd, *J* = 3.1, 5.4 Hz, H5' and H6'), 7.88 (1H, d, *J* = 8.4 Hz, H4), 7.84 (2H, dd, *J* = 3.1, 5.4 Hz, H4' and H7'), 7.78 (1H, s, H5), 7.61 (1H, d, *J* = 0.7 Hz, H7), 7.50 (1H, dd, J = 1.65, 8.50 Hz, H5) . δ_C (CDCl$_3$, 100 MHz): 179.63 (CH), 166.99 (C), 155.92 (C), 153.84 (C), 134.71 (CH), 132.39 (C), 131.58 (C), 126.20 (C), 123.99 (CH), 123.88 (CH), 122.85 (CH), 116.93 (CH), 111.20 (CH). LRMS (CI$^+$): *m/z* 292 [(M+H)$^+$, 80%], 268 [C$_{15}$H$_9$NO$_4$ + H)$^+$, 100%]. HRMS (CI$^+$): *m/z* [M+H]$^+$ 292.0607. C$_{17}$H$_{10}$O$_4$N requires 292.0610.

3-Azidoprop-1-ylamine (48)

$N_3 \overset{\frown}{\diagup} NH_2$
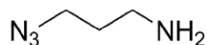
Sodium azide (13.9 g, 214 mmol, 2.8 eq) was added to a stirring solution of 3-chloroprop-1-yl-aminium chloride **47** (10.0 g, 77.0 mmol, 1.0 eq) in H_2O (150 mL) and heated to 80 °C overnight. The mixture was cooled to −10 °C and potassium hydroxide added until the pH reached 14. The mixture was extracted to Et_2O (3 × 150 mL). The organic layers were combined, dried over $MgSO_4$ and concentrated *in vacuo* to yield amine **48** as a colourless oil (6.65 g, 66.4 mmol, 86%). v_{max} (ATR): 2938 (CH), 2090 (N_3) cm^{-1}. δ_H (CDCl$_3$, 400 MHz): 3.38 (2H, t, J = 6.8 Hz, NCH$_2$), 2.80 (2H, t, J = 6.8 Hz, N_3CH$_2$), 1.73 (2H, quintet, J = 6.8 Hz, CH$_2$CH$_2$CH$_2$). δ_C (CDCl$_3$, 100 MHz): 49.04 (CH$_2$), 39.18 (CH$_2$), 32.25 (CH$_2$). LRMS (CI$^+$): m/z 101 [(M+H)$^+$, 72%], 75 [(C$_3$H$_{10}$N$_2$ + H)$^+$, 100%]. HRMS (CI$^+$): m/z [M+H]$^+$ 101.0827. C$_3$H$_9$N$_4$ requires 101.0825.

3-Isothiocyanatoprop-1-ylamine (49)

$N_3 \overset{\frown}{\diagup} N{=}C{=}S$
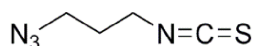
1,1'-Thiocarbonyldiimadazole (5.35 g, 30.0 mmol, 1.5 eq) was added slowly to a stirring solution of amine **48** (2.00 g, 20.0 mmol, 1 eq) and potassium carbonate (5.80 g, 42.0 mmol, 2.1 eq) in DCM (25 mL) and H_2O (25 mL). The mixture was stirred under argon for 90 min then quenched into H_2O (50 mL) and extracted to DCM (3 × 50 mL). The combined organic layers were washed with 20% HCl (100 mL), dried over $MgSO_4$ and concentrated *in vacuo* to yield isothiocyanate **49** (1.84 g, 12.9 mmol, 65%), which was not purified due to instability. Selected data from crude. δ_H (CDCl$_3$, 400 MHz): 3.66 (2H, t, J = 6.3 Hz, SCNCH$_2$), 3.49 (2H, t, J = 6.3 Hz, N_3CH$_2$), 1.94 (2H, quintet, J = 6.4 Hz, CH$_2$CH$_2$CH$_2$).

3-(3'-Azidopropyl)-2-sulfanylideneimidazolidin-4-one (50)
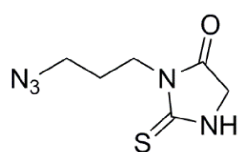
Glycine methyl ester hydrochloride (1.81 g, 14.5 mmol, 1.1 eq) was added to a stirring solution of isothiocyanate **49** (1.84 g, 12.9 mmol, 1.0 eq) and

triethylamine (2.0 mL, 14.5 mmol, 1.1 eq) in EtOAc (20 mL). The reaction was heated to reflux and stirred overnight. The mixture was then cooled, H_2O (20 mL) added to quench and extracted to DCM (3 × 20 mL). The combined organic layers were dried over $MgSO_4$ and concentrated *in vacuo* to yield thiohydantoin **50** as a red solid (2.13 g, 11.4 mmol, 88%). Mp: 73 - 75 °C. v_{max} (ATR): 2092 (N_3), 1717 (C=O) cm^{-1}. δ_H (CDCl$_3$, 400 MHz): 7.05 (1H, s, NH), 4.09, (2H, s, 2 × H5), 3.93 (2H, t, *J* = 6.9 Hz, NCH$_2$), 3.40 (2H, t, *J* = 6.7 Hz, N$_3$CH$_2$), 1.98 (2H, quintet, *J* = 6.7 Hz, CH$_2$CH$_2$CH$_2$). δ_C (CDCl$_3$, 100 MHz): 184.80 (C), 171.54 (C), 49.05 (CH$_2$), 48.46 (CH$_2$), 38.87 (CH$_2$), 27.07 (CH$_2$). LRMS (CI$^+$): *m/z* 200 [(M+H)$^+$, 100%]. HRMS (CI$^+$): *m/z* [M+H]$^+$ 200.0606. C$_6$H$_9$N$_5$OS requires 200.0609.

2-(4'-Bromobenzyloxy)tetrahydrofuran (52)
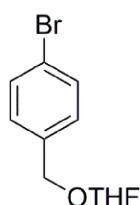
A solution of 4-bromobenzyl alcohol **51** (13.0 g, 69.5 mmol, 1.0 eq), 2,3-dihydrofuran (6.3 mL, 84 mmol, 1.2 eq) and *para*-toluene sulfonic acid monohydrate (20.0 mg, 0.11 mmol, 0.0016 eq) in DCM (50 mL) was stirred at room temperature for 90 min. The reaction mixture was then washed with H_2O (2 × 100 mL) and saturated aqueous NaHCO$_3$ (100 mL). Organics were dried over $MgSO_4$ and concentrated *in vacuo* to yield THF ether **52** as a yellow oil (17.2 g, 66.9 mmol, 96%). δ_H (CDCl$_3$, 400 MHz): 7.45 (2H, d, *J* = 8.3 Hz, H3' and H5'), 7.20 (2H, d, *J* = 8.3 Hz, H2' and H6'), 5.19 (1H, dd, *J* = 3.7 and 2.6 Hz, H2), 4.65 (1H, d, *J* = 12.4 Hz, ArC*H*^{A}H^B), 4.42 (1H, d, *J* = 12.4 Hz, ArCH^A*H*^{B}), 3.95-3.84 (2H, m, 2 × H5), 2.07-1.80 (4H, m, 2 × H3 and 2 × H4). δ_C (CDCl$_3$, 100 MHz): 137.44 (C), 131.41 (CH), 129.43 (CH), 121.29 (C), 103.17 (CH), 67.97 (CH$_2$), 67.08 (CH$_2$), 32.34 (CH$_2$), 23.44 (CH$_2$).

Data agree with literature [112].

2-[4'-(4'',4'',5'',5''-Tetramethyl-1'',3'',2''-dioxaborolan-2''-yl)benzyloxy] tetrahydrofuran (53)
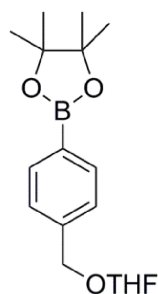
A solution of THF ether **52** (12.00 g, 46.7 mmol, 1.0 eq) in anhydrous THF (130 mL) was cooled to –78 °C and degassed with argon for 15 min. Under argon, ^{n}BuLi (1.68 M in hexanes, 31.7 mL, 56.0 mmol, 1.2 eq) was added dropwise over three hours and the mixture allowed to stir for 15 min. 2-Isopropoxy-4,4,5,5-tetramethyl-1,3,2-dioxaborolane (11.4 mL, 56.0 mmol, 1.2 eq) was added dropwise and the resulting solution allowed to stir for 2h. The reaction was quenched with H_2O (100 mL) and the product extracted with DCM (3 × 100 mL). Combined organics were washed with brine (100 mL), dried over $MgSO_4$ and concentrated *in vacuo* to give a yellow oil. Impurities were removed by Kugelrohr distillation to yield boronate ester **53** as a residual yellow oil, which solidified on standing (11.9 g, 39.1 mmol, 84%). δ_H (CDCl$_3$, 400 MHz): 7.78 (2H, d, *J* = 7.7 Hz, H-3' and H-5'), 7.34 (2H, d, *J* = 7.7 Hz, H-2' and H-6'), 5.20 (1H, dd, *J* = 4.2 and 1.2 Hz, H-2), 4.72 (1H, d, *J* = 12.4 Hz, ArC*H*^{A}H^B), 4.50 (1H, d, *J* = 12.4 Hz, ArCH^A*H*^{B}), 3.97-3.86 (2H, m, 2 × H-5), 2.09-1.83 (4H, m, 2 × H-3 and 2 × H-4), 1.34 (12H, s, 4 × CH$_3$). δ_C (CDCl$_3$, 100 MHz): 141.60 (C), 134.86 (CH), 126.99 (CH), 103.09 (CH), 83.73 (C), 68.60 (CH$_2$), 67.02 (CH$_2$), 32.33 (CH$_2$), 24.84 (CH$_3$), 23.44 (CH$_2$).

Data agree with literature [112].

[4-(4',4',5',5'-Tetramethyl-1',3',2'-dioxaborolan-2'-yl)phenyl]methanol (54)
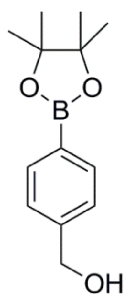
Aluminium trichloride (40 mg, 0.30 mmol, 0.1 eq) was added to a stirring solution of boronate ester **53** (1.00 g, 3.29 mmol, 1 eq) in anhydrous EtOH (10 mL) under argon. The mixture was stirred overnight at room temperature and then concentrated under reduced pressure. The residue was dissolved in Et$_2$O (40 mL) and filtered. The filtrate was concentrated under reduced pressure and redissolved in EtOH (10 mL) under argon. Aluminium chloride (30.0 mg, 0.22 mmol, 0.07 eq) was added and the solution was stirred overnight at room temperature. The residue was concentrated *in vacuo*, dissolved in Et$_2$O (40 mL) and filtered. The filtrate was concentrated *in vacuo* to yield benzylic alcohol **54** as an oil (517 mg, 2.21 mmol, 67%). δ_H (CDCl$_3$, 400 MHz): 7.79 (2H, d, *J* = 7.7 Hz, H-3' and H-5'), 7.39 (2H, d, *J* = 7.7 Hz, H-2' and H-6'), 4.49 (2H, s, CH$_2$), 1.34 (12H, s, 4 × CH$_3$). δ_C (CDCl$_3$, 100 MHz): 144.07 (C), 134.99 (CH), 126.06 (CH), 83.82 (C), 65.05 (CH$_2$), 24.83 (CH$_3$).

Data agree with literature [112].

Benzyl *N*-(4-iodophenyl)carbamate (56)
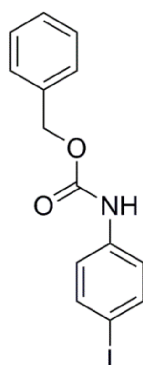
A mixture of benzyl alcohol **55** (0.2 mL, 1.9 mmol, 1.0 eq) and anhydrous pyridine (0.16 mL, 2.0 mmol, 1.1 eq) was slowly added to a stirring solution of phosgene (20% in toluene, 5.1 mL, 9.7 mmol, 5.1 eq) in anhydrous THF (10 mL)

under argon. The mixture was stirred for 3 h at room temperature. The white precipitate formed was filtered off and washed with further anhydrous THF (10 mL). The filtrate was concentrated *in vacuo*. The residue produced was redissolved in anhydrous THF (10 mL) and 4-iodoaniline (0.42 g, 1.9 mmol, 1.0 eq) was added. The mixture was stirred for a further 24 h under argon. THF was then removed *in vacuo* and the residue dissolved in EtOAc (20 mL) and washed with H_2O (20 mL). The aqueous layer was extracted with further EtOAc (20 mL). Combined organic layers were washed with brine and dried over $MgSO_4$ before concentration *in vacuo* to yield carbamate **56** as a beige solid (681 mg, 1.92 mmol, 100%). Mp: 124 °C. v_{max} (ATR): 1703 (C=O), 1532 (Ar), 1233 (CO). δ_H (CDCl$_3$, 400 MHz): 7.59 (2H, d, *J* = 8.9 Hz, H5 and H3), 7.40-7.33 (5H, m, 5 × ArH), 7.17 (2H, d, *J* = 8.8 Hz, H2 and H6), 6.62 (1H, s, NH), 5.19 (2H, s, CH$_2$). δ_C (CDCl$_3$, 100 MHz): 153.04 (C), 138.98 (CH), 137.62 (C), 135.82 (C), 128.68 (CH), 128.49 (CH), 128.38 (CH), 120.54 (CH), 86.41 (C), 67.26 (CH$_2$). LRMS (CI$^+$): *m/z* 354 [(M+H)$^+$, 100%]. HRMS (CI$^+$): *m/z* [M+H]$^+$ 353.9998. C$_{14}$O$_2$ H$_{12}$NI requires 353.9991.

N-[4'- (2''-Amino-9*H*-purin-6''-oxymethyl)benzyl]pent-4-ynamide (57)
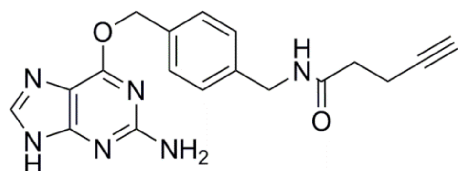
EDCI.HCl (38.0 mg, 0.20 mmol, 1.1 eq), HOBt.H$_2$O (27 mg, 0.2 mmol, 1.1 eq) and 4-pentynoic acid (20 mg, 0.20 mmol, 1.1 eq) were added to a stirring solution of amine **39** (75% pure, 64.8 mg, 0.18 mmol, 1 eq) in anhydrous DMF (5 mL). The reaction was stirred under argon at room temperature overnight then quenched with H_2O (5 mL) and extracted into DCM (3 × 20 mL). The organic extracts were washed with brine (10 mL) and dried over $MgSO_4$ before concentration *in vacuo*. The residue was washed with EtOAc (50 mL) to remove excess HOBt.H$_2$O to yield alkyne **57** (49.0 mg, 0.14 mmol, 78%). Mp: 151 °C. v_{max} (ATR): 1775 (C≡C), 1700 (C=O), 1271 (CN), 607 (alkyne CH). δ_H (MeOD, 400 MHz): 8.40, (1H, t, *J* = 5.6, H6''), 7.45 (2H, d, *J* = 8.1, H2' and H6'), 7.28 (2H, d, *J* = 8.1, H3' and H5'), 6.28 (2H, s, NH$_2$), 5.45 (2H, s, OCH$_2$), 4.28 (2H, d, *J* = 5.9, NHCH$_2$), 2.79 (1H, t, *J* = 2.6, H1), 2.36 (4H, m, 2 × CH$_2$). δ_C (MeOD, 100 MHz): 173.95 (C), 161.69 (C), 139.91 (C), 136.92 (C), 129.64 (CH), 128.68 (CH), 126.27 (CH), 125.91 (C),

118.69 (CH), 112.10 (C), 83.57 (C), 70.38 (C), 68.68 (CH$_2$), 43.88 (CH$_2$), 36.05 (CH$_2$), 15.75 (CH$_2$). LRMS (FAB/NOBA): m/z 351 [(M+H)$^+$, 15%]. HRMS (FAB/NOBA): m/z [M+H]$^+$ 351.1569. C$_{18}$H$_{18}$N$_6$O$_2$ requires 351.1564.

2-(2'-[1''-(3'''-Azidopropyl)-2''-oxo-5''-sulfanylideneimidazolidin-4''-ylidene]methyl-1'-benzofuran-6'-yl)-2,3-dihydro-1*H*-isoindole-1,3-dione (58)
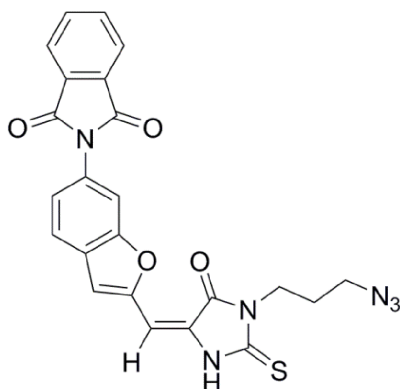
Aldehyde **46** (1.92 g, 6.59 mmol, 1.1 eq) was dissolved in EtOH (30 mL). Piperidine (1.3 mL, 13.2 mmol, 2.2 eq) and thiohydantoin **50** (1.20 g, 6.02 mmol, 1.0 eq) were added and the solution heated to reflux overnight. The reaction was then quenched with H$_2$O (20 mL) and extracted to EtOAc (3 × 30 mL). The combined organic layers were washed with brine (30 mL), dried over MgSO$_4$ before concentration *in vacuo* to give crude azide 8. Column chromatography (0-5% EtOAc in DCM) yielded azide **58** as a yellow solid (1.02 g, 2.20 mmol, 36%). R_f[SiO2, EtOAc-DCM(1:20)]: 0.70. Mp: 209 °C. v_{max} (ATR): 2926 (CH), 2101 (N$_3$), 1727 (C=O) cm^{-1}. δ_H (CDCl$_3$, 400 MHz): 9.49 (1H, s, NH), 8.01 (2H, dd, J = 3.1 Hz, 5.4, H5 and H6), 7.84 (2H, dd, J = 3.0, 5.4 Hz, H4 and H7), 7.71 (2H, m, H4' and H7'), 7.43 (1H, dd, J = 1.5, 8.4 Hz, H5'), 7.06 (1H, s, H3'), 6.61 (1H, s, methylidene), 4.04 (2H, t, J = 6.9 Hz, NCH$_2$), 3.42 (2H, t, J = 6.6 Hz, N$_3$CH$_2$), 2.03 (2H, quintet, J = 7.0 Hz, CH$_2$CH$_2$CH$_2$). δ_C (CDCl$_3$, 100 MHz): 176.72 (C), 167.19 (C), 163.27 (C), 154.38 (C), 152.83 (C), 134.69 (CH), 131.65 (C), 130.29 (C), 127.65 (C), 126.28 (C), 124.01 (CH), 122.69 (CH), 121.99 (CH), 111.93 (CH), 109.96 (CH), 99.20 (CH), 49.00 (CH$_2$), 38.96 (CH$_2$), 27.29 (CH$_2$). LRMS (CI$^+$): m/z 473 [(M+H)$^+$, 15%], 441 (100%). HRMS (CI$^+$) m/z: [M+H]$^+$ 473.1024. C$_{23}$H$_{21}$O$_4$N$_6$S requires 473.1027.

5-[(6''-Amino-1''-benzofuran-2''-yl)methylidene]-3-(3'-azidopropyl)-2-sulfanylideneimidazolidin-4-one (59)
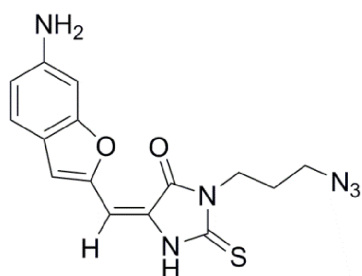
58 (20.0 mg, 0.04 mmol, 1 eq) was dissolved in MeOH (0.5 mL) and hydrazine hydrate added (3 µL, 0.06 mmol, 1.5 eq). The mixture was stirred at room temperature for 3 h. Solvent was removed *in vacuo* to yield amine **59** as a red solid (13.5 mg, 0.04 mmol, 97%). Selected data from crude. δ_H (CDCl$_3$, 400 MHz): 7.36 (1H, d, J = 8.4 Hz, H4''), 6.93 (1H, s, H7''), 6.80 (1H, s, H3''), 6.66 (1H, dd, J = 2.0, 8.4 Hz, H5''), 6.56 (1H, s, H2''), 4.03 (2H, t, J = 6.9 Hz, NCH$_2$), 3.41 (2H, t, J = 6.7 Hz, N$_3$CH$_2$), 2.03 (2H, quintet, J = 6.9 Hz, CH$_2$**CH$_2$**CH$_2$). Degradation occured before further characterisation could be carried out.

3-[4'-(4'',4'',5'',5''-Tetramethyl-1'',3'',2''-dioxabrolan-2''-yl)phenyl]propanoic acid (70)
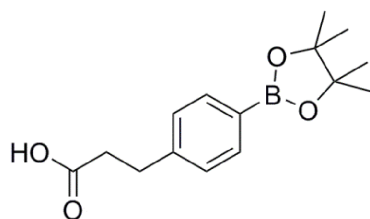
Pinacol (120 mg, 1.03 mmol, 1 eq.) was added to a solution of 4-(2-carboxyethyl)benzeneboronic acid **69** in CHCl$_3$ (10 mL). The mixture was stirred at room temperature of 30 min and solvent removed in vacuo yielding boronate ester **70** as a white solid (280 mg, 1.03 mmol, 100%). δ_H (400 MHz. CDCl$_3$): 7.75 (2H, d, J = 8.1 Hz, H-3' and H-5'), 7.23 (2H, d, J = 8.1 Hz, H-2' and H-6'), 2.98, t, J = 7.7 Hz, ArC**H$_2$**), 2.68 (2H, t, J = 8.1 Hz, C**H$_2$**COOH), 1.34 (12H, s, 4 × Me). δ_C (CDCl$_3$, 100 MHz): 177.61 (C), 143.47 (C), 135.11 (CH), 127.71 (CH), 83.74 (C), 35.17 (CH2), 24.86 (Me).

Data agree with literature [113].

2''',5'''-Dioxopyrrolidin-1'''-yl   3-[4'-(4",4",5",5"-tetramethyl-1",3",2"-dioxaborolan-2"-yl)phenyl]propanoate (71)
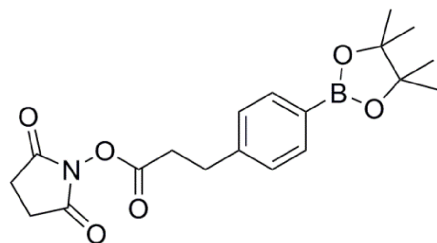
A mixture of *N,N*-dicyclohexylcarbodiimide (208 mg, 1.01 mmol, 1.4 eq.) in anhydrous DMF (12 mL) was added to a flask containing boronate ester **70** (200 mg, 0.720 mmol, 1.0 eq.) and *N*-hydroxysuccinimide (99.0 mg, 860 µmol, 1.2 eq.) which had been dried by azeotrope with toluene. The reaction mixture was stirred at room temperature overnight under argon the added to deionized H_2O (10 mL) and extracted into Et_2O (3 × 20 mL). The combined organic layers were washed with H_2O and brine and dried over $MgSO_4$, before concentration *in vacuo*. Column chromatography (0-30% hexane in EtOAc) yielded succinimidyl ester **71** as a white solid (163 mg, 0.51 mmol, 70%). R_f[SiO$_2$, hexane:EtOAc(3:10)]: 0.62. Mp: 137 °C. ν_{max} (ATR): 1738 (C=O), 1072 (C-O). δ_H (CDCl$_3$, 400 MHz): 7.76 (2H, d, *J* = 8.1 Hz, H-3' and H-5'), 7.24 (2H, d, *J* = 8.1 Hz, H-2' and H-6'), 3.07 (2H, t, *J* = 8.0 Hz, COC*H*$_2$), 2.92 (2H, t, *J* = 8.0 Hz, ArC*H*$_2$), 2.82 (4H, s, 2 × CH2), 1.33 (12H, s, 4 × Me). δ_C (CDCl$_3$, 100 MHz): 169.06 (C), 167.84 (C), 142.33 (C), 135.24 (CH), 127.66 (CH), 83.75 (C), 32.45 (CH$_2$), 30.63 (CH$_2$), 25.59 (CH$_2$), 24.87 (Me). LRMS (ESI$^+$): *m/z* 396 [(M+Na [^{11}B])$^+$, 100%]. HRMS (ESI$^+$) *m/z*: 395.1614 and 396.1590. C$_{19}$H$_{24}$O$_6$N^{10}B requires [M+Na]$^+$ 395.1625 and C$_{19}$H$_{24}$O$_6$N^{11}B requires [M+Na]$^+$ 396.1625.

***N*-[4'''-(2'''''-Amino-9*H*-purin-6'''''-yloxymethyl)benzyl]-3-[4'-(tetramethyl-1''',3''',2'''-dioxaborolan-2'''-yl)phenyl]propanamide (BGB) (61)**
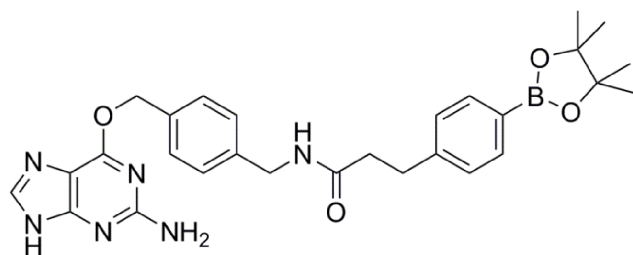
Triethylamine (0.04 mL, 0.27 mmol, 3.0 eq.) was added to a solution of *O*^{6}-(4-aminomethyl)benzylguanine **39** (75% pure, 32.0mg, 0.09 mmol, 1.0 eq.) in

anhydrous DMF (0.5 mL). Boronate ester **71** (50.0 mg, 0.10 mmol, 1.1 eq) was added and the reaction mixture stirred at room temperature under argon for 24 h. Solvent was removed *in vacuo* and the mixture purified by HPLC (12 mL/min, 20% - 50% MeCN in 0.1% formic acid in H_2O over 45 min, using a Phenomenex Gemini NX C18 110A 250 x 4.60 mm, BGB retention time: 27 min) yielding BGB **61** as a white solid (10.4 mg, 0.019 mmol, 21%). Mp: 66 °C. v_{max} (ATR): 1620 (C=O), 1581 (NH) cm^{-1}. δ_H (MeOD, 400 MHz): 7.85 (1H, s, H-8''''), 7.68 (2H, d, *J* = 8.1 Hz, H-3''' and H-5'''), 7.39 (2H, d, *J* = 8.1 Hz, H-3'' and H-5''), 7.23 (2H, d, *J* = 8.1 Hz, H-2''' and H-6'''), 6.98 (2H, d, *J* = 8.1 Hz, H-2'' and H-6''), 5.50 (2H, s, CH_2O), 4.31 (2H, s, NHCH_2), 2.97 (2H, t, *J* = 7.4 Hz, NHCOCH$_2$CH_2), 2.57 (2H, t, *J* = 7.3 Hz, NHCOCH_2CH$_2$), 1.33 (12H, s, 4 × Me). δ_C (MeOD, 100 MHz): 173.55 (C), 160.00 (C), 144.10 (C), 138.48 (C), 135.15 (C), 134.60 (CH), 128.22 (CH), 127.71 (CH), 127.42 (CH), 127.11 (CH), 83.64 (C), 67.34 (CH$_2$), 42.22 (CH$_2$), 37.13 (CH$_2$), 31.48 (CH$_2$), 23.78 (Me). LRMS (ESI$^+$): *m/z* 551 [(M+Na [^{11}B])$^+$, 100%]. HRMS (ESI$^+$): *m/z* 550.2559 and 551.2539. $C_{28}H_{33}O_4N_6{}^{10}B$ requires [M+Na]$^+$ 550.2549 and $C_{28}H_{33}O_4N_6{}^{11}B$ requires [M+Na]$^+$ 551.2549.

3-(4'-Acetoxyphenyl)propanoic acid (73)
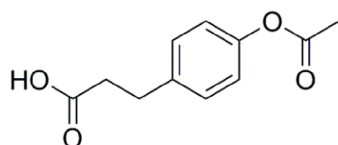
Sodium hydroxide (0.920 g, 22.9 mmol, 3.8 eq.) was added to a suspension of 3-(4'-hydroxyphenyl)propanoic acid **72** (1.00 g, 6.02 mmol, 1.0 eq.) in deionised H_2O (10 mL) at 0°C. Acetic anhydride (2.10 mL, 22.3 mmol, 3.7 eq.) was added and the mixture allowed to warm to room temperature and stirred for 48 h. 1M HCl (5 mL) was added and the organics extracted into EtOAc (3 x 15 mL). The organic layers were combined, washed with H_2O and brine, dried over MgSO$_4$ and concentrated *in vacuo* to yield acetate **73** as a white solid (1.14 g, 5.43 mmol, 90%). δ_H (CDCl$_3$, 400 MHz): 7.25 (2H, d, *J* = 8.7 Hz, H-2' and H-6'), 7.05 (2H, d, *J* = 8.6 Hz, H-3' and H-5'), 2.80 (2H, t, *J* = 7.8 Hz, ArCH_2), 2.71 (2H, t, *J* = 7.8 Hz, CH_2COOH), 2.32 (3H, s, Me). δ_C (CDCl$_3$, 100 MHz): 178.86 (C), 169.67 (C), 149.18 (C), 137.74 (C), 129.28 (CH), 121.62 (CH), 35.50 (CH$_2$), 29.94 (CH$_2$), 21.13 (Me).

Data agree with literature [114].

2",5"-Dioxopyrrolidin-1"-yl 3-(4'-acetoxyphenyl)propanoate (74)
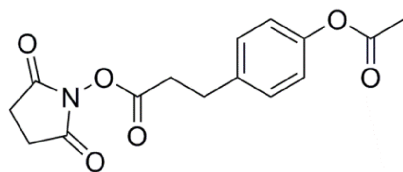
N-Ethyl-N'-(3-dimethylaminoprop-1-yl)carbodiimide (1.38 g, 7.20 mmol, 1.5 eq.) was added to a solution of acetate **73** (1.00 g, 4.80 mmol, 1.0 eq.) and *N*-hydroxysuccinimide (0.94 g, 8.16 mol, 1.7 eq.) in anhydrous DMF (15 mL). The reaction mixture was stirred at room temperature under argon for 48 h. H_2O (15 mL) was added and the mixture extracted to DCM (3 x 30 mL). The combined organic layers were washed with H_2O and brine and dried over $MgSO_4$. Column chromatography (0-20% MeOH in DCM) yielded succinimidyl ester **74** as a white solid (1.40 g, 4.60 mmol, 96%). R_f[SiO_2, methanol-dichloromethane (1:10)]:0.68. Mp: 94 °C. ν_{max} (ATR): 1734 (C=O), 1200 (CN) cm^{-1}. δ_H ($CDCl_3$, 400 MHz): 7.23 (2H, d, J = 8.6 Hz, H-2' and H-6'), 7.01 (2H, d, J = 8.6 Hz, H-3' and H-5'), 3.03 (2H, t, J = 8.0 Hz, ArCH_2CH$_2$), 2.89 (2H, t, J = 7.9 Hz, ArCH$_2$CH_2), 2.75 (4H, s, 2 × succinimidyl CH_2), 2.25 (3H, s, Me). δ_C ($CDCl_3$, 100 MHz): 169.52 (C), 169.36 (C), 167.92 (C), 149.39 (C), 136.76 (C), 129.33 (CH), 121.75 (CH), 32.46 (CH$_2$), 29.76 (CH$_2$), 25.54 (CH$_2$), 21.04 (CH3). LRMS (EI$^+$): m/z 305 ([M$^{\bullet+}$] 70%), 263 ([M$^{\bullet+}$ - CH$_2$CO$^{\bullet}$] 100%), 107 [HOC$_6$H$_5$CH$_2$$^+$]. HRMS (EI$^+$): m/z 305.0903. $C_{15}H_{15}O_6N$ requires [M$^{\bullet+}$] 305.0899.

N-[4"-(2'''-amino-*9H*-purin-6'''-yloxymethyl)benzyl]-3-(4'-hydroxyphenyl)propanamide (BGP) (68)
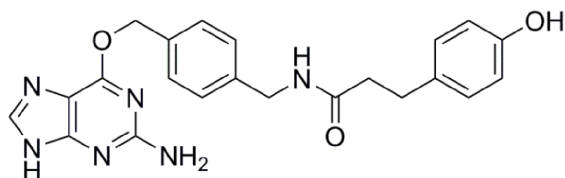
Triethylamine (50 μL, 360 μmol, 3.0 eq.) was added to a solution of O^6-(4-aminomethyl)benzylguanine **39** (43.0 mg, 120 μmol, 1.0 eq.) in anhydrous DMF (0.6 mL). Succinimidyl ester **74** (40.0 mg, 0.13 mmol, 1.0 eq) was added to the reaction mixture stirred at room temperature under argon for 24 h. Solvent was removed *in vacuo* and the crude gum produced was dissolved in anhydrous MeOH (1.0 mL). K_2CO_3 (33.0 mg, 240 μmol, 2.0 eq.) was added to the solution and it

was stirred at room temperature for 2 h under argon. The mixture was concentrated *in vacuo* and purified by HPLC (12 mL/min 20% - 50% MeCN in 0.1% formic acid in H_2O over 45 min, using a Phenomenex Gemini NX C18 110A 250 x 4.60 mm, BGP retention time: 5 min) yielding BGP **68** as a white solid (4.00 mg, 9.56 µmol, 8%). δ_H (MeOD, 00 MHz): 7.68 (1H, s, H-8'''), 7.45 (2H, d, J = 8.1 Hz, H-3'' H-5''), 7.14 (2H, d, J = 8.1 Hz, H-2'' and H-6''), 6.91 (2H, d, J = 8.5 Hz, H-2' and H-6'), 6.61 (2H, d, J = 8.5 Hz, H-3' and H-5'), 5.51 (2H, s, CH_2O), 4.32 (2H, s, H Hz, $NHCH_2$), 2.79 (2H, t, J = 7.6 Hz, $NHCOCH_2CH_2$), 2.46 (2H, t, J = 7.6 Hz, $NHCOCH_2CH_2$). LRMS (ESI$^+$): m/z 441 ([M + Na]$^+$ 100%). HRMS (ESI$^+$): m/z 441.1639. $C_{22}H_{22}N_6O_3$ requires [M + Na]$^+$ 441.1646.

2-(3'-bromobenzyl)-4,4,5,5-tetramethyl-1,3,2-dioxaborolane (80)
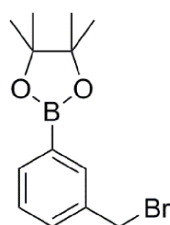
Pinacol (165 mg, 1.40 mmol, 1.0 eq) was added to a solution of 3-bromobenzyl boronic acid **79** (0.30 g, 1.40 mmol, 1.0 eq) in EtOAc (5 mL). The reaction was stirred for 30 min at room temperature then solvent was removed *in vacuo*. Crude material was recrystallised from EtOH yielding boronate ester **80** as a white solid (416 mg, 1.40 mmol, 100%). Mp: 84 °C. v_{max} (ATR): 607 (C-Br), 1356 (C-H) cm^{-1}. δ_H (400 MHz, CDCl$_3$): 7.82 (1H, s, H-2), 7.74 (1H, d, J = 7.4 Hz, H-4), 7.52-7.48 (1H, m, H-6), 7.36 (1H, t, J = 7.5 Hz, H-5), 4.50 (2H, s, CH_2), 1.35 (12H, s, 4 × Me). δ_C (100 MHz, CDCl$_3$): 137.15 (C), 135.22 (CH), 134.83 (CH), 131.96 (CH), 128.28 (CH), 83.99 (C), 33.49 (CH_2), 24.89 (CH_3). LRMS (ESI$^+$): m/z 318 [M+Na(^{79}Br, ^{10}B)]$^+$, 319 [M+Na(^{79}Br, ^{11}B)]$^+$, 320 [M+Na(^{81}Br, ^{10}B)]$^+$, 321 [M+Na(^{81}Br, ^{11}B)]$^+$. HRMS (ESI$^+$): m/z 318.0517, 319.0470, 320.0499 and 321.0451. $C_{13}H_{18}NaO_2{}^{10}B^{79}Br$ requires [M+Na]$^+$ 318.0512. $C_{13}H_{18}NaO_2{}^{11}B^{79}Br$ requires [M+Na]$^+$ 319.0476. $C_{13}H_{18}NaO_2{}^{10}B^{81}Br$ requires [M+Na]$^+$ 320.0492. $C_{13}H_{18}NaO_2{}^{11}B^{81}Br$ requires [M+Na]$^+$ 321.0456.

Data agrees with literature [115].

Pep-B (77)

Ac-NYTCKDEL-NH$_2$
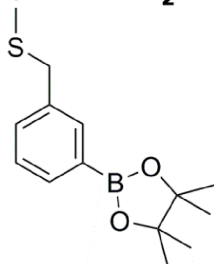
Ac-NTYCKDEL (0.005 g, 5.00 µmol, 1.0 eq, AnaSpec) and boronate ester **80** (15.0 mg, 0.05 mmol, 10 eq) were dissolved in a mixture of phosphate buffered saline (0.5 mL) and acetonitrile (1.0 mL). The reaction was stirred overnight at room temperature then purified by HPLC (0.2 mL/min 0-90% MeCN with 0.1% TFA in dH$_2$O over a volume of 2 mL, ACE 5 C4-300 column). Binding was confirmed by MALDI-TOF with DHB matrix. [M+H]$^+$ 1279.78.

3-(Bromomethyl)phenol (82)
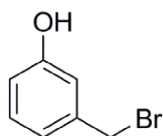
Triphenylphosphine (1.06 g, 4.03 mmol, 2.5 eq) and carbon tetrabromide (1.34 g, 4.03 mmol, 2.5 eq) were dissolved in anhydrous THF (6 mL). 3-(hydroxymethyl)phenol **80** (0.20 g, 1.61 mmol, 1.0 eq) was added and the reaction was stirred overnight at room temperature under argon. The reaction was quenched with H$_2$O (4 mL) and extracted to DCM (3 × 10 mL). Organic layers were combined, washed with brine, dried over MgSO$_4$ and concentrated *in vacuo*. Column chromatography (0-10% EtOAc in DCM) yielded benzyl bromide **81** as a white solid (149 mg, 0.80 mmol, 50%). R_f[SiO$_2$, EtOAc-DCM (1:10)]:0.75. Mp: 61-62 °C. ν_{max} (ATR): 694 (C-Br), 3246 (O-H) cm^{-1}. δ_H (400 MHz, CDCl$_3$): 7.19 (1H, t, *J* = 8.0 Hz, H-3), 6.95 (1H, d, *J* = 7.6 Hz, H-4), 6.86 (1H, t, *J* = 2 Hz, H-2), 6.76 (1H, ddd, *J* = 8.4 Hz, 2.8 Hz, 0.8 Hz, H-6), 5.19 (1H, br s, O*H*), 4.41, (2H, s, C*H*$_2$). δ_C (100 MHz, CDCl$_3$): 155.54 (C), 139.48 (C), 130.15 (CH), 121.61 (CH), 116.01 (CH), 115.65 (CH), 33.27 (CH$_2$). LRMS (ESI$^-$): *m/z* 185 ([M-H (^{79}Br)]$^-$ 100%), 187 [M-H (^{81}Br)]$^-$. HRMS (ESI$^-$): *m/z* 184.9604 and 186.9584. C$_7$H$_6$O^{79}Br requires [M-H]$^-$ 184.9608 and C$_7$H$_6$O^{81}Br requires [M-H]$^-$ 186.9588.

Data agrees with literature [116].

Pep-P (83)

Ac-NYTCKDEL-NH₂
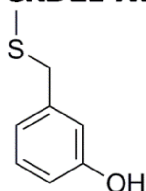
Ac-NTYCKDEL (0.005 g, 5.00 μmol, 1.0 eq) and benzyl bromide **81** (0.009 g, 0.05 mmol, 10 eq) were dissolved in a mixture of phosphate buffered saline (0.5 mL) and acetonitrile (1.0 mL). The reaction was stirred overnight at room temperature then purified by HPLC (0.2 mL/min 0-90% MeCN with 0.1% TFA in dH$_2$O over a volume of 2 mL, ACE 5 C4-300 column). Binding was confirmed by MALDI-TOF with DHB matrix. [M+H]$^+$ 1133.76.

***N*-[4'-hydroxymethyl(benzyl)]-3-(4'-acetoxyphenyl)propanamide (84)**
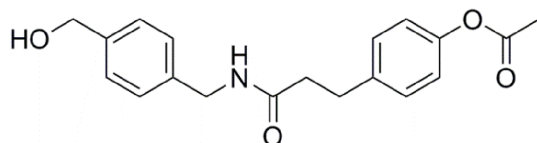
Triethylamine (1.8 mL, 12.9 mmol, 3.0 eq) was added to a solution of 4-(hydroxymethyl)benzylamine **34** (590 mg, 4.30 mmol, 1.0 eq) in anhydrous DMF (14 mL). Succinimidyl ester **74** (1.44 g, 4.73 mmol, 1.1 eq) was added and the reaction mixture was stirred overnight under argon then quenched with H$_2$O (10 mL) and extracted into EtOAc (3 × 40 mL). Organic layers were combined, washed with brine (40 mL), dried over MgSO$_4$ and concentrated *in vacuo*. The crude mixture was purified by column chromatography (0-10% MeOH in DCM) then recrystallised from EtOAc and hexane yielding amide **83** as a cream solid (0.760 g, 2.32 mmol, 54%). R_f[SiO2, MeOH-DCM (1:10)]:0.48. Mp: 126 °C. v_{max} (ATR): 1628 (amide CO), 1758 (ester CO) cm^{-1}. δ$_H$ (400 MHz, CDCl$_3$): 7.29 (2H, d, *J* = 8.4 Hz, H-2'' an H-6''), 7.18 (2H, d, *J* = 8.8 Hz, H-2' and H-6'), 7.14 (2H, d, *J* = 8.4 Hz, H-3'' and H-5''), 6.97 (2H, d, *J* = 8.8 Hz, H-3' and H-5'), 5.60 (1 H, br t, N*H*), 4.67 (2H, d, *J* = 6.0 Hz, HOC*H*$_2$Ar) 4.39 (2H, d, *J* = 6.0 Hz, ArC*H*$_2$NH), 2.97 (2H, t, *J* = 7.6 Hz, ArC*H*2CH2), 2.48 (2H, t, *J* = 7.6 Hz, ArCH2C*H*2), 2.29 (3H, s, M*e*), 1.75 (1H, t, *J* = 6.0 Hz, O*H*). δ$_C$ (100 MHz, CDCl$_3$): 171.80 (C), 169.69 (C),

149.09 (C), 140.22 (C), 138.31 (C), 137.50 (C), 129.39 (CH), 127.96 (CH), 127.35 (CH), 121.56 (CH), 64.99 (CH_2), 43.33 (CH_2), 38.38 (CH_2), 31.02 (CH_2), 21.15 (CH_3). LRMS (ESI$^+$): m/z 350 ([M+Na]$^+$ 100%). HRMS (ESI$^+$): m/z 350.1362. $C_{19}H_{21}NO_4$ requires [M+Na]$^+$ 350.1363.

N-[4'-4''-(hydroxymethyl)benzyl]-3-(4''-4'-hydroxyphenyl)propanamide (85)
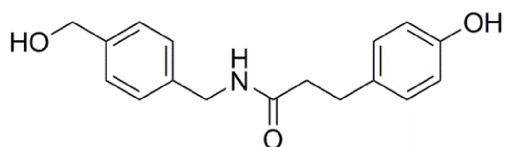
Potassium carbonate (2.10 g, 15.2 mmol, 2.0 eq) was added to a solution of amide **83** (2.49 g, 7.61 mmol, 1.0 eq) in anhydrous MeOH (25 mL). The reaction was stirred at room temperature for 2.5 h then filtered and solvent removed *in vacuo*. The crude material was flushed through a column (10% MeOH in DCM) to remove residual inorganics yielding phenol **84** as white needles (2.16 g, 7.57 mmol, 99%). R_f[SiO2, EtOAc-DCM (1:5)]:0.03. Mp: 139 °C. v_{max} (ATR): 1649 (amide CO) cm^{-1}. δ_H (400 MHz, MeOD): 7.25 (2H, d, J = 8.1 Hz, H-2'' and H-6''), 7.06 (2H, d, J = 8.1 Hz,H-3'' and H-5''), 7.00 (2H, d, J = 8.5 Hz, H-2' and H-6'), 6.67 (2H, d, J = 8.5 Hz, H-3' and H-5'), 4.56 (2H, s, HOCH_2Ar), 4.29 (2H, s, ArCH_2NH), 2.83 (2H, t, J = 7.4 Hz, ArCH_2CH$_2$), 2.47 (2H, t, J = 7.4 Hz,ArCH$_2$CH_2). δ_C (100 MHz, MeOD): 175.25 (C), 156.82 (C), 141.53 (C), 138.91 (C), 132.84 (C), 130.49 (CH), 128.49 (CH), 128.18 (CH), 116.27 (CH), 65.01 (CH_2), 43.77 (CH_2), 39.30 (CH_2), 32.14 (CH_2). LRMS (ESI$^-$): m/z 284 ([M-H]$^-$ 100%). HRMS (ESI$^-$): m/z 284.1280. $C_{17}H_{18}NO_3$ requires [M-H]$^-$ 284.1292.

N-[4'-4''-(bromomethyl)benzyl]-3-(4''-hydroxyphenyl)propanamide (78)
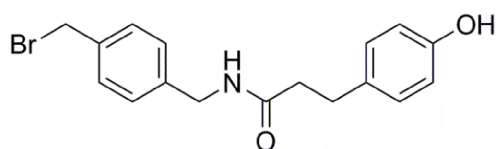
Triphenylphosphine (4.59 g, 17.5 mmol, 2.5 eq) and carbon tetrabromide (5.80 g, 17.5 mmol, 2.5 eq) were dissolved in anhydrous tetrahydrofuran (25 mL). Phenol **84** (2.00 g, 7.00 mmol, 1.0 eq) was added and the reaction was stirred overnight at room temperature under argon. The reaction was quenched with H_2O (20 mL) and extracted into EtOAc (3 × 40 mL). Organic layers were combined, washed with brine, dried over $MgSO_4$ and concentrated *in vacuo*.

Crude material was purified by column chromatography (0-50% EtOAc in DCM) then recrystallised from DCM yielding benzyl bromide **78** as white needles (312 mg, 0.89 mmol, 13%). R_f[SiO2, ethyl acetate-dichloromethane (1:5)]:0.55. Mp: 148 °C. v_{max} (ATR): 610 (C-Br), 1626 (amide CO) cm^{-1}. δ_H (400 MHz, MeOD): 7.31 (2H, d, J = 8.2 Hz, H-2'' and H-5''), 7.04 (2H, d, J = 8.2 Hz, H-3'' and H-5''), 7.01 (2H, d, J = 8.6 Hz, H-2' and H-6'), 6.69 (2H, J = 8.6 Hz , H-3' and H-5'), 4.53 (2H, s, BrCH_2Ar), 4.29 (2H, s, ,ArCH_2NH), 2.84 (2H, t, J = 7.4 Hz, ArCH_2CH$_2$), 2.49 (2H, t, J = 7.4 Hz, ArCH$_2$CH_2). δ_C (100 MHz, MeOD): 175.37 (C), 156.89 (C), 140.06 (C), 138.52 (C), 132.69 (C), 130.51 (CH), 130.28 (CH), 128.74 (CH), 116.25 (CH), 43.67 (CH$_2$), 39.18 (CH$_2$), 33.81 (CH$_2$), 32.09 (CH$_2$). LRMS (ESI$^+$): m/z 370 ([M+Na(^{79}Br)]$^+$ 65%), 372 ([M+Na(^{81}Br)]$^+$ 65%), 325 ([X+Na]$^+$ 100%). HRMS (ESI$^+$): m/z 370.0406 and 372.0387. C$_{17}$H$_{18}$NNaO$_2$^{79}Br requires [M+Na]$^+$ 370.0413 and C$_{17}$H$_{18}$NNaO$_2$^{81}Br requires [M+Na]$^+$ 372.0393.

KLH conjugated *N*-[4'-(bromomethyl)benzyl]-3-(4''-hydroxyphenyl)propanamide (79)
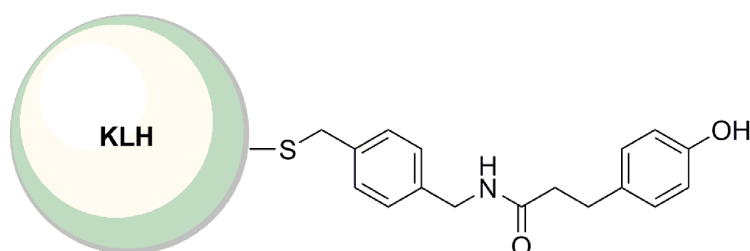
Hemocyanin from *Megathura crenulata* (keyhole limpet) (2.0 mL of a 5.0 mg/mL solution in phosphate buffered saline, 2.5×10^{-8} mmol, 1.0 eq) was stirred with benzyl bromide **78** (10.0 mg, 0.028 mmol, 1000.0 eq) in phosphate buffered saline (1.0 mL) and DMSO (3.0 mL) for 24 h at room temperature. Reaction mixture was buffer exchanged into 50 mM ammonium bicarbonate using a GE healthcare PD10 desalting column according to manufacturer's instructions. Solution was freeze-dried producing the KLH-hapten conjugate as a fluffy white solid. Binding was confirmed by reaction with fluorescein maleimide and fluorescence scan of protein on an SDS-PAGE gel.

9.0 Results I

9.1 Introduction

It has been shown that hydrogen peroxide plays an enormously important role in cells, and what was once thought of as just a toxic and damaging by-product is now considered a far more dynamic compound. In recent years hydrogen peroxide's role as a signalling molecule and vital part of homeostasis has started to become more understood. As a signalling molecule, hydrogen peroxide is known to play a role in many events including tyrosine phosphorylation, proliferation and differentiation and cell stress [1].

In the ER it has been found that hydrogen peroxide plays a vital role in the formation of disulfide bonds. When PDI catalyses the formation of a new disulfide bond in a substrate protein, the catalytic disulfide of PDI is reduced and therefore must be reoxidised to maintain its enzymatic role. Originally it was believed that glutathione was responsible for oxidising PDI, however it was discovered that in cells this role is performed by Ero1, a flavoprotein [26]. The result of the recycling of PDI is a reduced disulfide in Ero1. The disulfide in Ero1 is reoxidised by the parallel reduction of oxygen, producing hydrogen peroxide [27].

The PDI-Ero1 relay results in one molecule of hydrogen peroxide for every disulfide formed in a newly formed protein. Although Ero1 activity is tightly controlled by regulatory disulfides, there also exist within the ER mechanisms for removing hydrogen peroxide. One such example is PrxIV which is localized to the ER and contains a peroxidatic cysteine (Cys124) capable of reacting with hydrogen peroxide to form sulfenic acid and a molecule of water. The resolving cysteine (Cys245) in PrxIV then forms a disulfide with the peroxidatic cysteine [4]. Other proteins which are involved in removal of hydrogen peroxide in the ER are GPx7 and GPx8.

It is this balance of hydrogen peroxide production and removal that we wanted to investigate. Under what conditions does it change from a signalling molecule to a destructive force, particularly with regards to the ER.

The key aim of the project was to develop an effective, ratiometric and user-friendly method of measuring hydrogen peroxide in the ER in order to be able to

study the intricate balance with regards to protein folding and disulfide formation. We decided that the best method to tackle this would be the use of a synthetic probe that could be targeted specifically to the ER, which would react with hydrogen peroxide and which would display a measurable change as this reaction occurred.

During the design of the probe several factors had to be considered. From the previous literature we concluded there were two main options for ER targeting. One was to use a peptide targeting system, and the other to use the SNAP-tag system.

SNAP-tag is the G160W mutant of human AGT. It specifically reacts with O^6-(4-aminomethyl-benzyl)guanine derivatives and has been shown to be a useful tool for conjugating synthetic probes to various cellular locales [93]. SNAP-tag can be expressed in mammalian cells with targeting and retention sequences for the ER and has previously been shown to do so [101]. The advantages of SNAP-tag include that it can be expressed in any cellular locale, which would mean the probe structure would not have to be altered if we later wished to compare and contrast hydrogen peroxide levels, for example between the cytosol and the ER. There is good literature precedent for synthetic probes conjugated to O^6-(4-aminomethyl)benzylguanine being able to cross not only the cell membrane but also the ER membrane.

A peptide targeting system would involve conjugating the synthetic probe to a peptide scaffold. This scaffold would likely include the ER retention sequence, KDEL [117] and an NYTC glycosylation site which once glycosylated prevents the peptide from diffusing back out of the ER. The main advantage the peptide system has is that it does not require any transfection, unlike for SNAP-tag which must be transfected either transiently or by the creation of a stable cell line, which can be a slow process. A probe conjugated to a peptide system could therefore be used in any cell line and the levels of hydrogen peroxide could be compared between cell lines.

Cell permeability cannot be predicted; however it can be prepared for. Generally the larger a compound is the less likely it will be cell permeable. It was also considered that the probe has to cross both the cell membrane and the ER membrane. It was decided that adding a bulky peptide onto the probe would

be too high risk and since previously, fluorophores had been conjugated to the SNAP-tag substrate, O^6-(4-aminomethyl-benzyl)guanine, and been shown to be capable of reaching the ER, the SNAP-tag system was chosen as the most likely to be successful.

We chose to incorporate a fluorophore into the probe to provide a method of measuring the change as the probe reacts with hydrogen peroxide. The advantage of a fluorophore is that live cell experiments can be performed. With all other methods, cells must first be lysed before analysis.

The fluorophore we chose was based on Fura-Red™ (Fig. 18). Fura-Red™ is a commercially available calcium sensor [118]. One of the major advantages of Fura-Red™ is that it absorbs in the visible region, meaning the wavelength of irradiation used will not be harmful to the cells being examined.

28
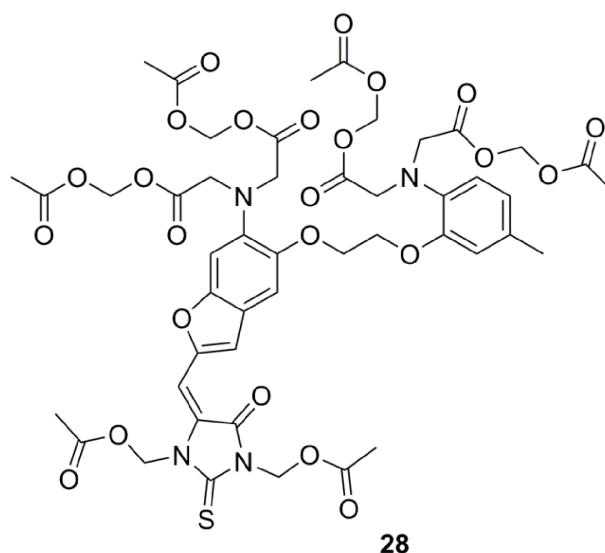
Figure 18 - Fura-Red™, a commercially available calcium sensor. Inspiration was taken from the calcium sensor 28 when designing the fluorophore of BG-Fura-B.

Fura-Red™ has a large Stokes shift of 200 nm and the excitation and emission are red-shifted so there is little interference from any cellular autofluorescence (Fig.19). It is the only truly ratiometric calcium sensor excited in the visible spectrum that is commercially available. This is because it is fluorescent both when free and when binding calcium and the large Stokes shift in the absorption allows excitation at different frequencies for the two forms and fluorescence to be detected at a single frequency [119].
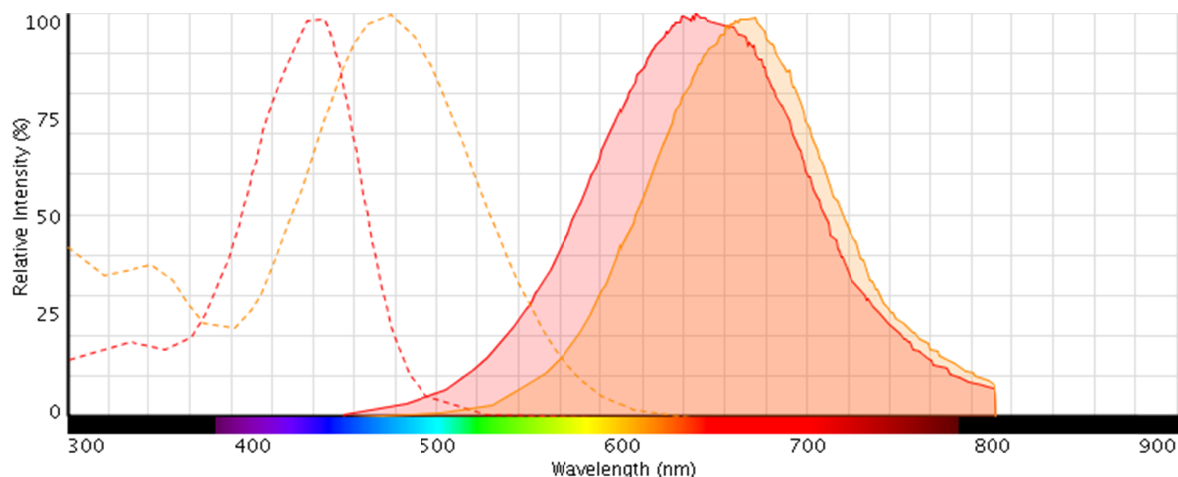
Figure 19 – The absorption and emission spectra of Fura-Red™. The orange trace is calcium free and the red trace is calcium bound.

Fura-Red™ undoubtedly has the most ideal properties of the known fluorescent calcium sensors. It was decided it is better to use an already known fluorophore as designing a completely novel fluorophore is a challenging task and the rules on how to do so form an interesting debate in current literature [120].

It has been well documented in the literature that boronic acids are the only chemical moiety that selectively react with hydrogen peroxide over other reactive oxygen species and have been shown to be highly successful when incorporated in probes [76]. The structure of our proposed probe is shown in Fig 19. For ease of synthesis and stability the boronic acid was designed in the pinacol ester form, which does not affect the reactivity of the probe to hydrogen peroxide once in use. The phenyl ring on which the boronic acid is situated is connected to the fluorophore via a carbamate linkage. This creates enough space between boron and the fluorophore to prevent any fluorescence quenching from the empty p orbital of boron.

A linker was put in place between the SNAP-tag substrate, benzylguanine and the fluorophore (Fig. 20). This is a precautionary measure to place distance between the fluorophore and any biological residues in the SNAP-tag protein which may cause fluorescence quenching. The fluorophore and boronic acid are linked to the SNAP-tag substrate via a 1,2,3-triazole Click linkage. "Click chemistry" is a term coined to describe a group of reactions that are simple, can be conducted in benign or easily removed solvents, are high yielding and that create by-products which do not require chromatography for removal [121].

These properties are advantageous, particularly in the synthesis of complex and sensitive compounds. BG-Fura-B was designed to permeate cells and react with SNAP-tag to give SNAP-Fura-B, which upon reaction with hydrogen peroxide should give SNAP-Fura-A.

- Boronate gives H_2O_2 reactivity and selectivity
- Carbamate results in complete uncaging of the fluorophore

- Benzylguanine derivative to allow specific reaction with SNAP-tag

- Fluorophore is based on FuraRed, which has a large Stokes shift and absorbs in the visible region of the spectrum

- Linker to allow conjugation of probe to SNAP substrate via Click chemistry

29

Figure 20 - The design of the probe BG-Fura-B 29. The structure incorporates SNAP reactivity, fluorescence and hydrogen peroxide reactivity and selectivity.

Between the boronic ester and fluorophore of BG-Fura-B was incorporated a carbamate grouping (Fig. 20). There is evidence in the literature that after the boronic acid has reacted with hydrogen peroxide, forming the phenol, the cascade of electrons generated will result in fragmentation with the loss of a quinone methide and a molecule of carbon dioxide (Fig. 21) [122]. This leaves the free amine of the fluorophore in SNAP-Fura-A. Conversion of the mildly electron-donating amide of SNAP-Fura-B into the strongly donating hydroxyl group should lead to a red-shift in the excitation frequency. Such a large structural change before and after reaction was designed into the probe in the belief that the fluorescence before and after reaction would be at sufficiently different wavelengths to provide a ratiometric analysis.
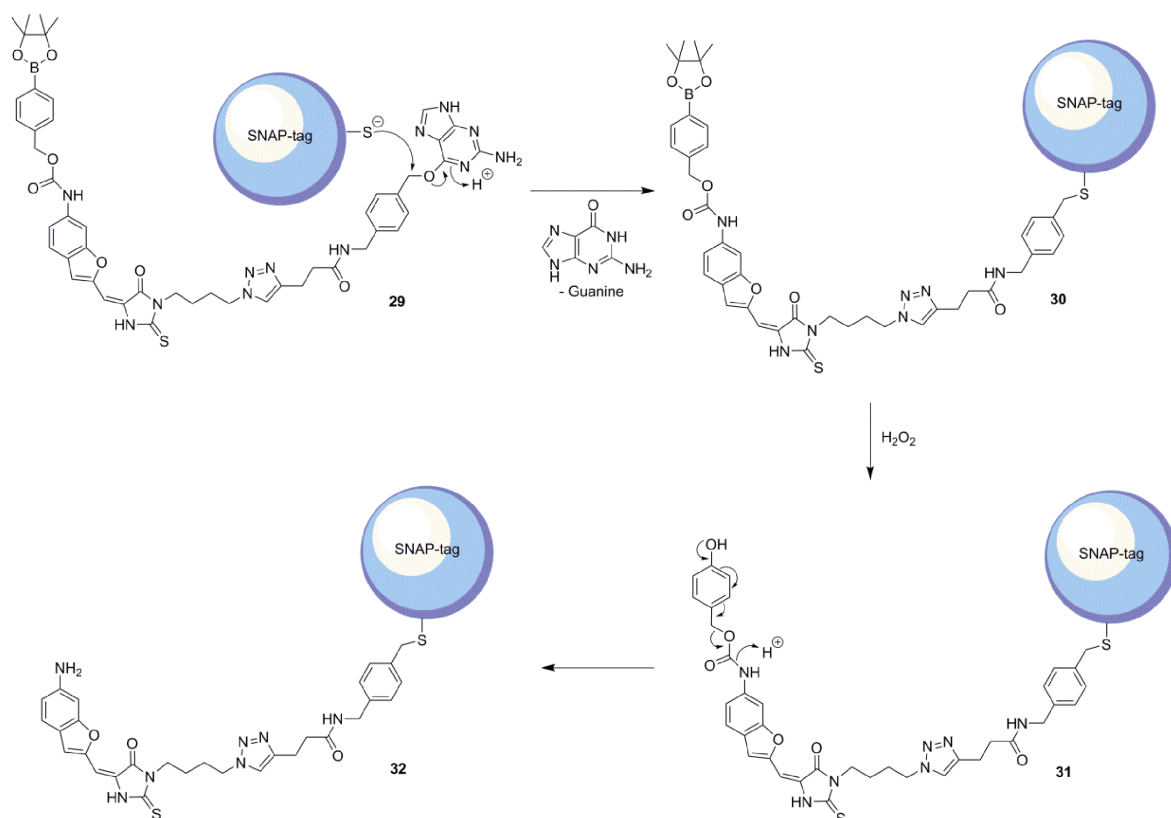
Figure 21 - Probe conjugation to SNAP-tag. BG-Fura-B 29 binds to SNAP-tag with the release of guanine forming SNAP-Fura-B 30. After hydrogen peroxide reacts, the boronate ester is converted into a phenol 31. A quinone methide and carbon dioxide are lost producing the final amine, SNAP-Fura-A 32.

BG-Fura-B was designed to perform live cell imaging experiments. To prepare for these studies, mammalian cell lines were stably transfected to express SNAP-tag localised to the ER. This construct included the ER retention sequence KDEL. Once stably expressed this cell line could be treated with BG-Fura-B which would bind irreversibly to SNAP-tag. Any excess probe could then be washed out. The aim was to then image cells. In the first experiments, cells would be treated with hydrogen peroxide to assess the efficiency of the probe and in later experiments, other stressors such as dithiothrietol (DTT) would be used [123]. DTT is a powerful reducing agent and it has been shown that upon the addition of DTT to cells, disulfide formation in the ER is prevented. DTT acts as a substrate for Ero1, which catalyses the formation of disulfide bonds in PDI [124]. The result of the stimulation of Ero1 by DTT is the *in situ* production of hydrogen peroxide as Ero1 reoxidises by reaction with oxygen.

9.2 Results

9.2.1 SNAP-tag Overexpression and Purification

To allow for *in vitro* testing of both the SNAP-tag binding capabilities and fluorescence measurements of BG-Fura-B, SNAP-tag was first expressed in *E.coli*. The bacterial cells were transformed with a pET 28a vector encoding his-tagged SNAP-tag. Colonies were first grown on LB agar then picked and grown in LB broth with induction by IPTG. The expressed protein was harvested and purified (Fig. 22).
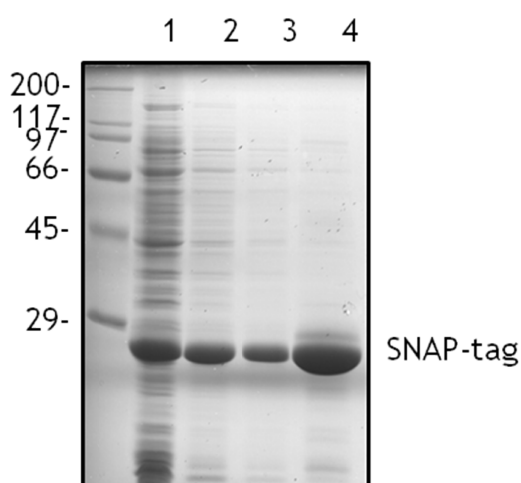
Figure 22 – SNAP-tag expression in *E.coli* and purification. This was carried out by affinity chromatography, ion-exchange chromatography and de-salting. 1. Supernatant from the crude *E.coli* lysate. 2. SNAP-tag after purification from the lysate by affinity chromatography for the His-tag it was expressed with. 3. SNAP-tag after ion exchange chromatography, which removed some of the contamination still seen after the affinity chromatography. 4. SNAP-tag after de-salting which separates the protein from the concentrated salt solution that it is eluted in after ion-exhange.

To follow the purification of SNAP-tag we separated samples from individual stages of the purification by SDS-PAGE (Fig. 22). Lane 1 shows the *E.coli* cell lysate. The cells were pelleted and lysed 3 hours after induction with IPTG. The molecular mass of SNAP-tag is approximately 23.5 kDa which corresponds to the position of an intensely stained band just below the 29 kDa marker. Lane 2 shows SNAP-tag after the first step of the purification which used Ni-NTA agarose

resin to bind to the His-tag of the protein. The most intense band present in the cell lysate was partially purified with some weak background bands being visible. It was decided a second purification step would be undertaken to remove these bands. Ion exchange chromatography was chosen as the second purification step. Lane 3 shows the protein sample after ion-exchange. The background bands seen in the sample after the Ni-NTA agarose affinity were deemed to be reduced to a sufficient level. The final step involved de-salting of the protein to remove the high salt in from the ion-exchange elution buffer, shown in lane 4.

9.2.2 Creation of HT SNAP Cell Lines

SNAP-tag was expressed and purified in *E.coli* to prepare for *in vitro* testing with BG-Fura-B. In addition, mammalian cell lines expressing SNAP were created for the *in cellulo* testing.

The mammalian fibroblastic cell line, HT1080 was chosen to be transfected as it had been extensively used within the group previously to study disulfide formation in newly synthesised proteins. The plasmid, which encoded FLAG-tagged SNAP-tag with ER targeting and retention sequences, was linearised and transfected into cells using PEI as the transfection reagent. The pCI mammalian expression vector was used and carries neomycin resistance. After transfection and selection with neomycin, colonies that grew were isolated and expanded. A killing curve was carried out to determine the most suitable concentration of G418 to remove untransfected cells. This was found to be 800 µg/mL. Cells from individual isolated clonal cell lines were lysed and lysates tested for SNAP-tag expression using Western blot probed with anti-FLAG-tag and anti-tubulin as a control (Fig. 23).
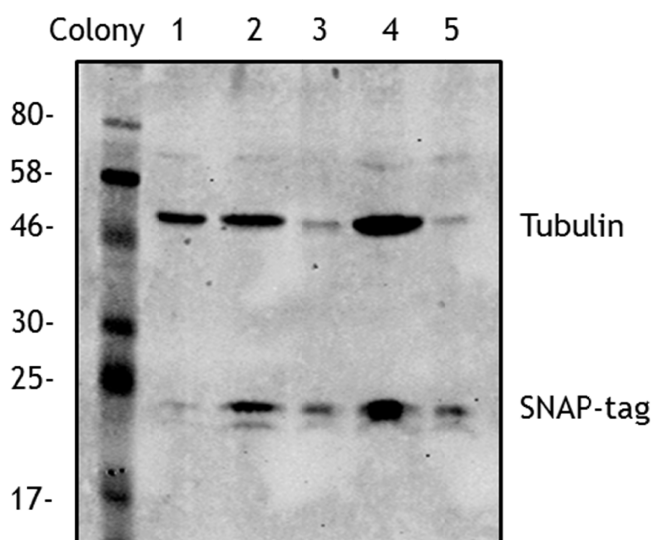
Figure 23 - Western blot from a 12.5% SDS-PAGE showing positive colonies grown from stable transfection. HT1080 cells were transfected with SNAP-tag containing an ER retention sequence. Tubulin was used as a loading control. The weaker tubulin bands for colony 3 and 5 suggest that far less material was loaded in these lanes. Colony 1 shows very weak SNAP-tag expression. Colonies 2, 3, 4 and 5 show stronger SNAP-tag expression. The SNAP-tag bands for colonies 3 and 5 look weaker however the weaker loading control for these bands shows that less material was loaded onto the gel.

The HT SNAP Cyto cell line was created in the lab by M. Pringle and carried hygromycin resistance at a concentration of 250 µg/mL (Fig. 24). The HT SNAP Cyto cell line expressed SNAP-tag in the cytosol of HT1080 cells and so the protein did not contain any targeting or retention sequences unlike HT SNAP ER.
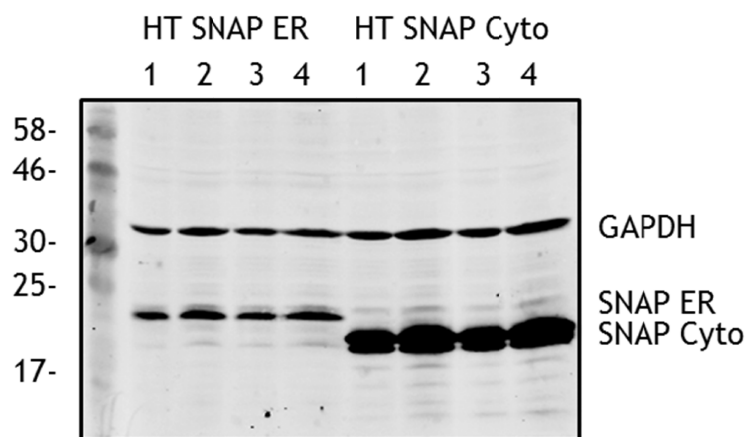
Figure 24 - Western blot from a 12.5% SDS-PAGE showing expression of SNAP-tag. Lysates from HT SNAP ER and HT SNAP Cyto cell lines were analysed with tubulin blotted for as a loading control. The expression is higher for the HT SNAP Cyto cell line.

9.2.3 Confocal Microscopy to Confirm HT SNAP ER Localisation

To confirm that HT SNAP ER only expressed SNAP-tag in the ER a colocalisation study was carried out using confocal microscopy. HT SNAP ER cells were grown on coverslips and fixed with methanol before being probed with both mouse anti-FLAG-tag and rabbit anti-PDI primary antibodies (Fig. 25). Colocalisation with PDI was investigated as PDI is an endogenous ER localised enzyme, therefore SNAP-tag should be expressed in the same regions of the cell as PDI. The fixed cells were then probed with anti-mouse FITC and anti-rabbit IgG Texas Red secondary antibodies to provide a fluorescent marker for protein locations.
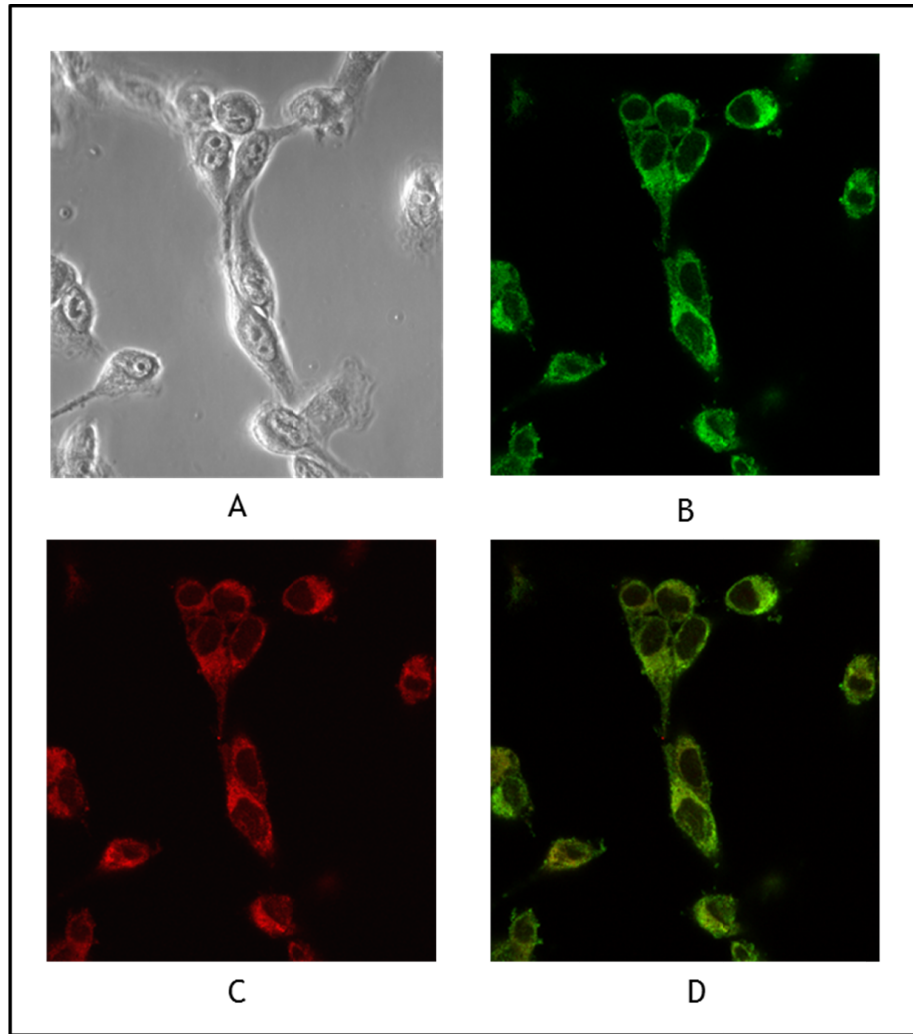
Figure 25 - Immunofluorescence showing HT SNAP ER localisation. A. Brightfield image showing HT SNAP ER cells. B. HT SNAP ER cells treated with anti-FLAG mouse primary antibody (Sigma-Aldrich) and anti-mouse-FITC (Sigma-Aldrich) rabbit secondary antibody. C. HT SNAP ER cells treated with anti-PDI rabbit primary antibody and anti-rabbit-IgG Texas Red mouse secondary antibody. D. Overlay of B. and C. showing SNAP and PDI co-localisation.

The colocalisation experiment confirmed the expression of SNAP-tag in the ER. When overlaid, the cells can clearly be seen to express SNAP-tag in the same location as PDI. PDI is expressed constitutively and retained in the ER by the retention sequence KDEL. It acts as the source of disulfide bonds for newly formed proteins in the secretory pathway. The expression pattern seen in Fig. 25 B, C and D is also typical of the ER. The dark area inside the cells is the nucleus with the ER surrounding.

9.2.4 O^6-(4-Aminomethyl)benzylguanine Synthesis

After preparing purified SNAP-tag for *in vitro* experiments and mammalian cells expressing SNAP-tag in the ER and the cytosol, the next task was to synthesise the O^6-(4-aminomethyl)benzylguanine substrate of SNAP-tag. This synthesis had already been published by Keppler et al. (Fig. 26) [93].
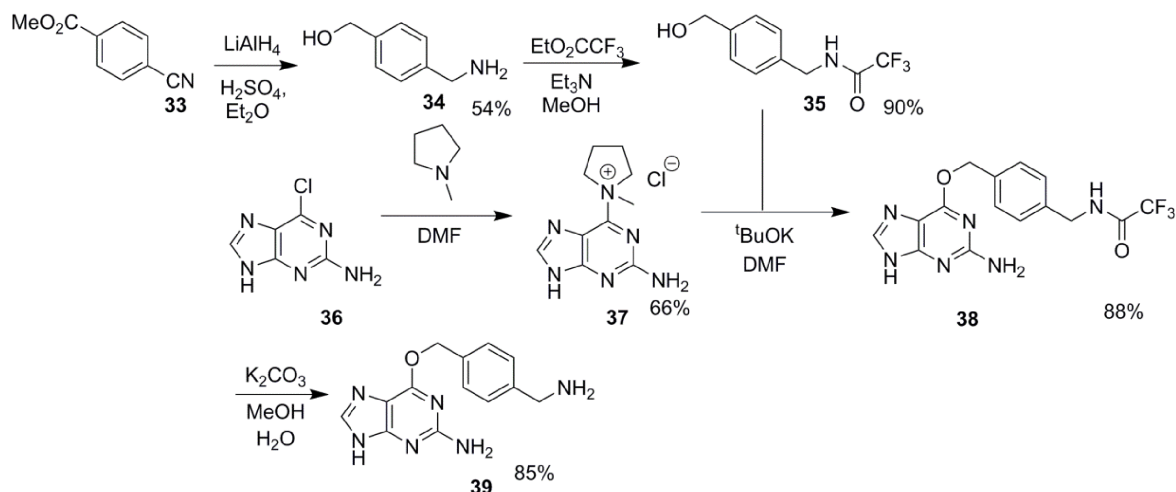
Figure 26 – The synthesis and yields of O^6-(4-Aminomethyl)benzylguanine 39 designed by Keppler et al.

Keppler et al. first performed a reduction on methyl 4-cyanobenzoate **33** using lithium aluminium hydride which produced 4-(aminobenzyl)methanol **34** in a moderate yield. The amine was then protected with ethyl trifluoroacetate in a high yield. With regards to the guanine functionality of the molecule, 2-amino-6-chloropurine **36** was first reacted with *N*-methylpyrrolidine in a moderate yield in order to create a better leaving group for the coupling with the protected 4-(aminobenzyl)methanol **35**. The coupling of the two halves **35** and **37** was then performed with potassium *tert*-butoxide acting as the base producing amide **38** in a high yield. The final step was then deprotection of the amine with potassium carbonate yielding O^6-(4-aminomethyl)benzylguanine **39**, also in a high yield.

When planning our own synthesis of O^6-(4-aminomethyl)benzylguanine we aimed to follow the procedure of Keppler et al., apart from the lithium aluminium reduction of methyl 4-cyanobenzoate **33** for which we decided to forgo the addition of sulphuric acid. When this step was first attempted we also changed the solvent to THF which gave better solubility. This gave a yield of 66% for

amine **34**, an improvement on the published method and required no purification (Fig. 27). For the protection of the amine **34** with ethyl trifluoroacetate to yield amide **35**, we followed the method of Keppler at al; however the yield was reduced, though still moderate at 59%. Again no purification was required. To create the *N*-methylpyrrolidine leaving group on 2-amino-6-chloropurine **36** we also followed the published method and this also gave a lower yield of 47%. No purification was required for this step. The reaction relies on the product cleanly precipitating from the reaction mixture. It was possible that the product did not precipitate in its entirety, even when it was left for an extended period of time. To force the precipitation further may have resulted in any unreacted starting material precipitating. With regards to the guanine containing products, column chromatography is often best avoided as solubility is very low in all the common solvents used in chromatography.
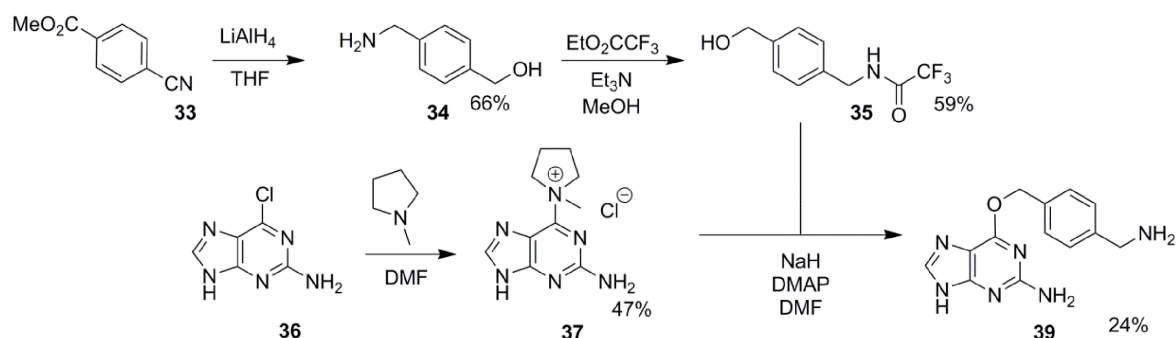
Figure 27 – Our altered synthesis of O^6-(4-Aminomethyl)benzylguanine 39.

The next step was to perform the coupling of the two halves **35** and **37** of the target, **39**. Keppler et al performed this step with potassium *tert*-butoxide in DMF and purified the product by column chromatography. We found when we attempted this step that often a mixture of compounds was produced but most of the starting materials remained. It was not possible to locate more than trace amounts of the desired reaction product. The utmost care was taken to ensure the reaction was completely dry; however we could not produce a yield anywhere close to the published data of 88%. We decided to look at other ways of performing this reaction and attempted the step with sodium hydride as the base and catalytic 4-dimethylaminopyridine. From the crude ^{1}H NMR spectrum it could be seen that starting materials did remain, however there clearly was desired product as well. Column chromatography proved difficult due to a

combination of poor solubility, high polarity and very similar polarities of the desired product **39** and guanine starting material **37**. It was also found that the compound deprotected on the column, which was not a significant issue as it negated having to perform another step in the synthesis. Unfortunately a considerable amount of the product did not elute from the column. We also found that on some occasions what did elute still contained some of the guanine starting material. On those occasions we decided to use the O^6-(4-aminomethyl)benzylguanine **39** without purifying it as if we attempted another purification it would result in the loss of even more material and we anticipated that addition of the masked fluorophore later in the sequence should alter the polarity sufficiently that separation would not be an issue. On the occasions that the purification was successful the yield was low, though an improvement on what we had achieved when using the method of Keppler et al.

9.2.5 BG-NBD-X

We decided to test the functionality of the purified SNAP-tag and the HT SNAP mammalian cell lines before attempting the synthesis of the fluorescent probe, BG-Fura-B. The main test of functionality would be to ensure the SNAP substrate, O^6-(4-aminomethyl)benzylguanine, could successfully react with SNAP-tag both *in vitro* and *in cellulo*. To do this we required a method that would be able to show the binding of the small molecule substrate to the protein.

It was decided that the simplest method to study the binding of O^6-(4-aminomethyl-benzyl)guanine to SNAP-tag would be to conjugate a fluorophore, commercially available if possible, to O^6-(4-aminomethyl)benzylguanine and to visualise the binding by fluorescence scanning of an SDS-PAGE gel to confirm the *in vitro* binding and by confocal microscopy for the *in cellulo* binding.

We first decided on the fluorophore to use. 6-(*N*-(7-Nitrobenz-2-oxa-1,3-diazol-4-yl)amino)hexanoic acid (NBD-X) (Fig. 28) is a commercially available fluorophore with an absorption maximum of 466 nm and an emission maximum of 539 nm.
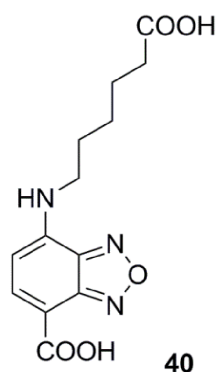
Figure 28 - The structure of NBD-X. NBD-X 40 was the fluorophore chosen to conjugate to O^6-(4-aminomethyl)benzylguanine to test the functionality of SNAP-tag.

NBD-X was found to be available as the succinimidyl ester, which is amine reactive and so would be easily conjugated to O^6-(4-aminomethyl)benzylguanine. The maximum absorption of 466 nm was also particularly suitable for use as the available confocal microscope contained a laser of 488 nm, meaning the fluorescence recorded from the probe should be strong (Fig. 29).
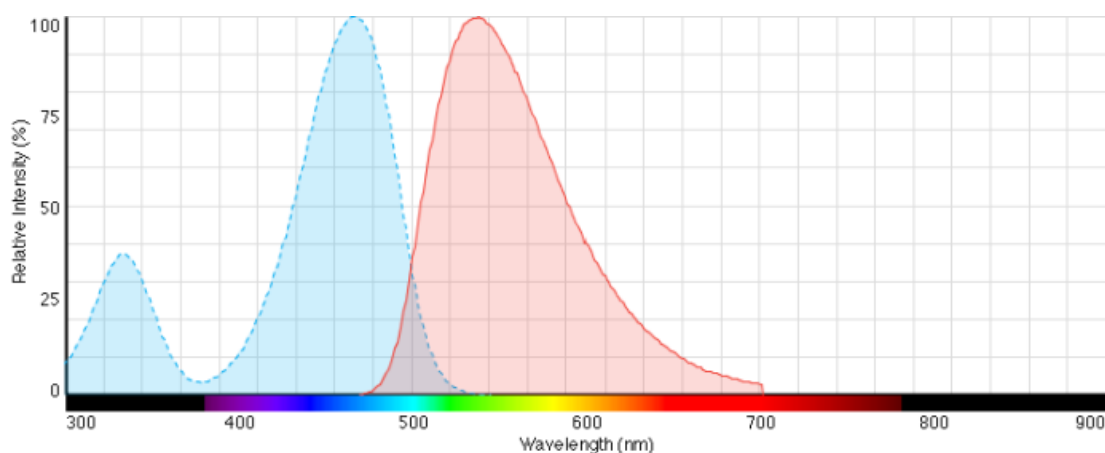
Figure 29 - Absorption (blue) and emission (red) spectra of NBD-X.

The synthesis of benzylguanine-NBD-X (BG-NBD-X) **41** involved the coupling of O^6-(4-aminomethyl-benzyl)guanine **39** to the succinimidyl ester of NBD-X. This proceeded in a moderate yield and did not require any purification (Fig. 30).
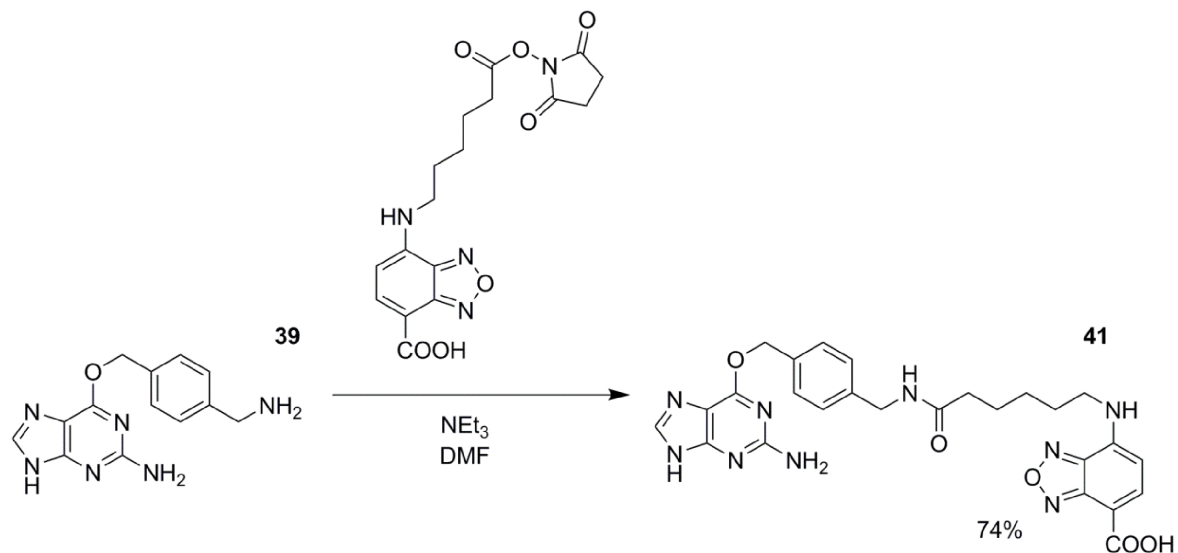
Figure 30 - The synthesis of BG-NBD-X 41. O^6-(4-Aminomethyl)benzylguanine 39 was coupled to the succinimidyl activated NBD-X via an amide bond.

With the test fluorophore, BG-NBD-X in hand, we progressed to testing of SNAP-tag functionality. SNAP-tag which had been expressed in *E.coli* and purified was mixed with a 100 times excess of BG-NBD-X and incubated at 37 °C for 30 min to allow binding to occur. The reaction was stopped by precipitating all the protein in solution with -20 °C acetone. The protein pellet produced was washed with further acetone to remove any excess unbound BG-NBD-X. The pellet was resuspended in SDS-PAGE sample buffer with DTT and subsequently run on a 12.5% SDS-PAGE gel. The gel was scanned by a GE healthcare Typhoon fluorescence scanner then stained with colloidal Coomassie (Fig. 31).
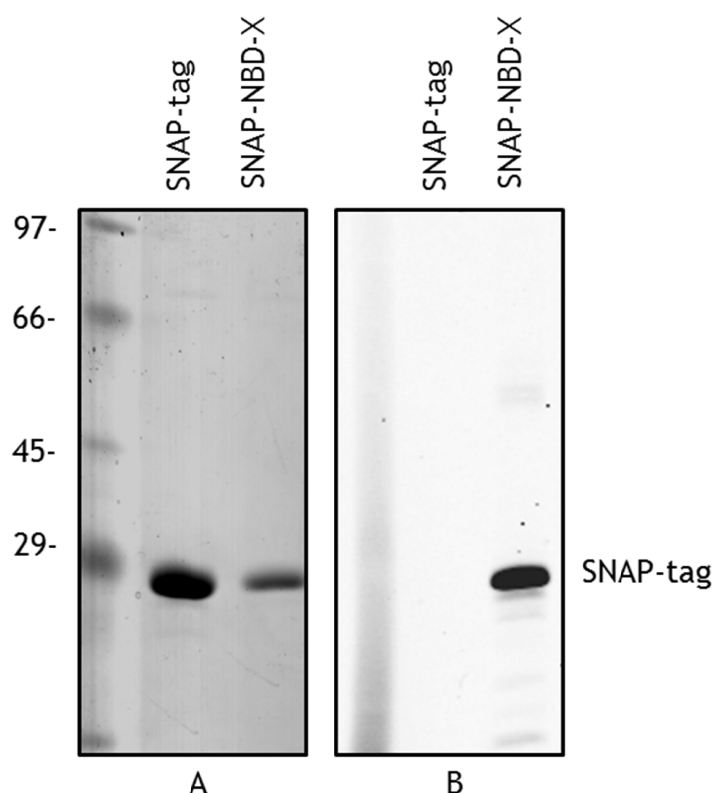
Figure 31 - Confirmation of recombinant SNAP-tag functionality. A. Coomassie stained 12.5% SDS-PAGE showing a band for SNAP-tag and a band for SNAP-NBD-X. B. Gel scanned by a GE healthcare Typhoon fluorescence scanner showing only the sample treated with BG-NBD-X is fluorescent; therefore the conjugation between probe and protein was successful.

The results demonstrated that the SNAP-tag which was reacted with BG-NBD-X is highly fluorescent and SNAP-tag alone is not. This confirms that the SNAP-tag produced in *E.coli* is fully functional and capable of reacting with O^6-(4-aminomethyl-benzyl)guanine derivatives. We then went on to examine the functionality of the protein expressed in mammalian cells.

HT SNAP ER cells were harvested, lysed and treated with 5 µM BG-NBD-X post lysis for 30 min, to allow binding. The protein in the lysates was then precipitated with -20 °C acetone. The pellet produced was washed with further acetone to remove any excess unbound BG-NBD-X. The protein was resuspended in SDS-PAGE sample buffer with DTT, prepared for SDS-PAGE as normal, and run

on a 12.5% SDS gel. After the gel had run it was scanned with a GE healthcare Typhoon fluorescence scanner, and subsequently stained with colloidal Coomassie (Fig. 32).
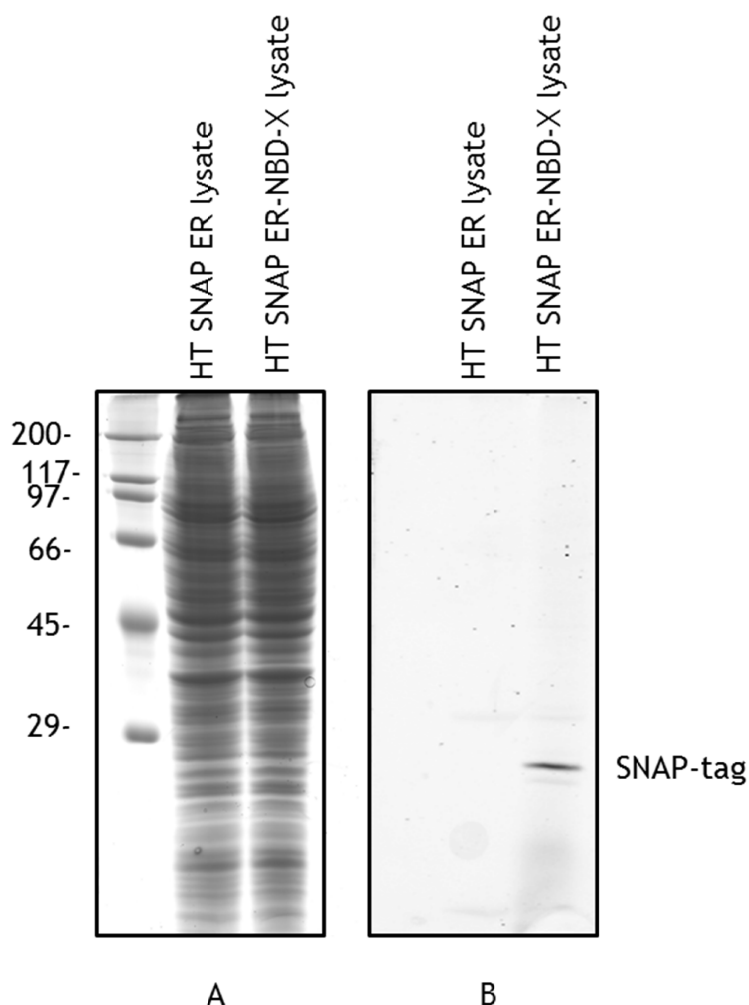
Figure 32 –Confirmation of mammalian cell SNAP-tag functionality. A. HT SNAP ER lysate and HT SNAP ER-NBD-X run on a 12.5% SDS-PAGE and stained with colloidal Coomassie. B. HT SNAP ER lysate and HT SNAP ER-NBD-X run on a 12.5% SDS-PAGE and scanned with a Typhoon FLA 9500 scanner (GE healthcare).

The fluorescent image (Fig. 32) shows a band at the correct height for SNAP-tag, only in the sample that was treated with BG-NBD-X, showing the conjugation of the probe to SNAP-tag was successful and confirming that the SNAP-tag was functional. This confirms that the benzylguanine moiety of the probe is capable of binding to SNAP-tag expressed in mammalian cells and, therefore, that the SNAP-tag expressed in these cells is folded correctly and fully functional;

however, it does not confirm that BG-NBD-X is capable of passing through both the cell and ER membrane to reach this SNAP-tag.

In order to confirm that SNAP-tag was capable of binding to the probe *in cellulo*, confocal microscopy was required. HT SNAP ER and HT SNAP Cyto cells were seeded onto coverslips and then treated with a solution of 5 µM BG-NBD-X in DMEM for 30 min. Cells were washed twice with PBS after the treatment to wash out any excess unbound probe and subsequently fixed with methanol. Cells were then imaged using a Zeiss 510 LSM microscope (Fig. 33)
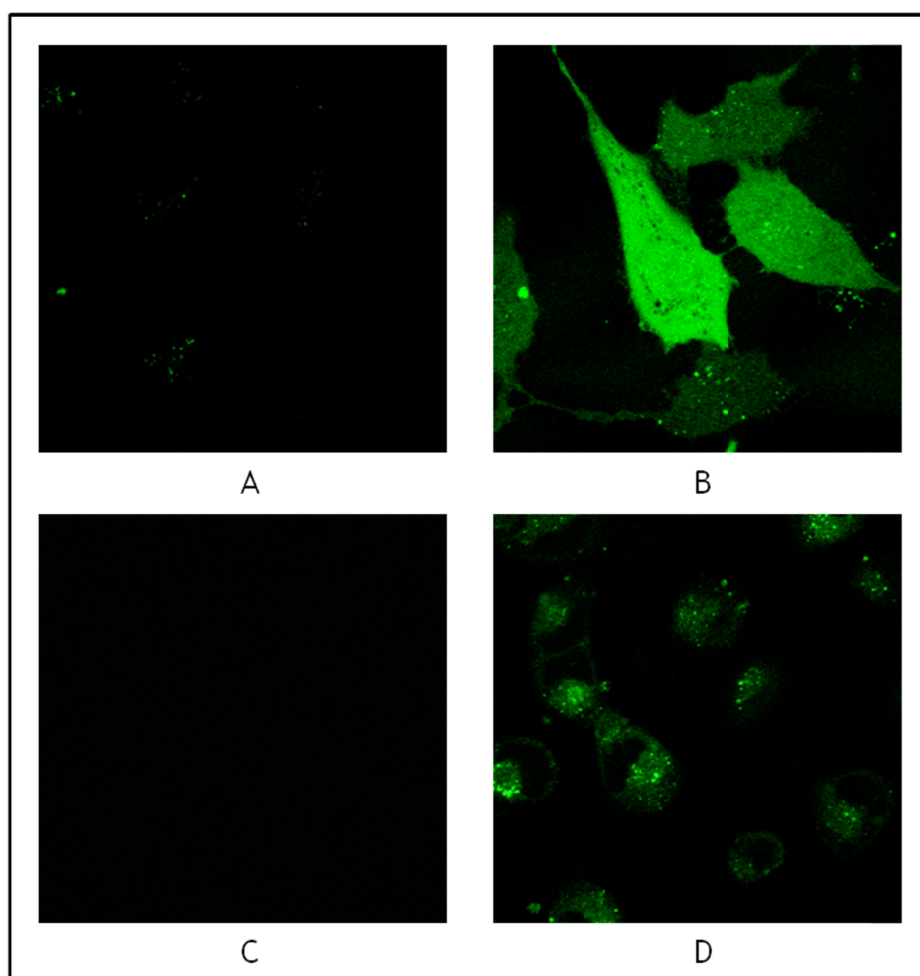
Figure 33 - Confocal microscopy showing cells treated with BG-NBD-X. A. HT SNAP Cyto scanned with an Argon 488 FITC laser in a Zeiss 510 LSM. B. HT SNAP Cyto which had been treated with 5 µM BG-NBD-X scanned with an Argon 488 FITC laser in a Zeiss 510 LSM. C. HT SNAP ER scanned with an Argon 488 FITC laser in a Zeiss 510 LSM. D. HT SNAP ER Cyto which had been treated with 5 µM BG-NBD-X scanned with an Argon 488 FITC laser in a Zeiss 510 LSM.

The images collected from the confocal microscope show fluorescence produced by SNAP-NBD-X. The fluorophore was excited with the 488 nm laser that is traditionally used for fluorescein but works with NBD-X as it has a similar absorbance. For the cells that had not been treated with BG-NBD-X (Fig. 33.A and C) there is no fluorescence compared to the cells that had been treated with BG-NBD-X (Fig. 33.B and D). In Fig.33.B the fluorescence is strong and appears to be throughout the whole cell, the expected result for the HT SNAP Cyto cell line. In Fig.33.D, the fluorescence shows perinuclear staining that is typical of ER expression. We previously confirmed the ER localisation of SNAP-tag in the cell line in the immunofluorescence experiment which showed that SNAP-tag colocalised with PDI (Fig. 25). Fig. 33 confirms that BG-NBD-X is capable of diffusing though the cell membrane and the ER membrane and conjugating to SNAP-tag in live cells when expressed in either the ER or the cytosol.

9.2.6 BG-Fura-B

With a stock of purified SNAP-tag for *in vitro* experiments, cell lines expressing SNAP-tag in both the cytosol and ER and having confirmed the functionality of both the purified SNAP-tag and the SNAP-tag in mammalian cells using a SNAP-tag substrate BG-NBD-X, the next step was to synthesise the hydrogen peroxide reactive probe.

The synthesis was first designed by separating the target molecule into the various functional components in a rational manner. These included the fluorophore core of the molecule, the boronate ester for hydrogen peroxide reactivity and the benzylguanine moiety for SNAP-tag reactivity (Fig. 20).

The synthesis of BG-Fura-B began with the dehydrative protection of the amine **42** with phthalic anhydride (Fig. 34). The planned method using phthalic anhydride in DMF was not successful; however, it was reasoned that the reaction may be possible as a melt. The melting point of phthalic anhydride is 131-132 °C [125] and the melting point of 3-aminophenol is 123-124 °C [126]. As the melting points are relatively close to each other it is possible to melt both compounds and consequently drive water off the reaction. This was found to be a successful method and produced phthalimide **43** in a clean and high yielding manner (Fig. 33). With the amine protected, the next step was to formylate the phenyl ring.

The original plan had been to utilise the Vilsmeier-Haack reaction; however, again this step was found to be unsuccessful [127]. There are other methods for formylation, one being the use of magnesium chloride and paraformaldehyde [128]. Magnesium chloride coordinates through the oxygen of the phenol to form a phenoxymagnesium chloride salt or possibly diphenoxymagnesium and acts to direct the formylation in the *ortho* position only [129]. This method was used and gave aldehyde **44** in a moderate yield. Following the formylation the original plan had involved deprotonating the phenol of **44** and performing a nucleophilic substitution on 2-bromo-1,1-diethoxyethane in preparation for the cyclisation [130]. It was found that the nucleophilic substitution only proceeded with very low yield. Alternatives were studied and a nucleophilic substitution with allyl bromide was instead chosen as it was found to be a much better reaction and produced allyl ether **45** with a yield of 95%. This did essentially mean an extra step was required as the vinyl group of compound **45** then had to be oxidised to the aldehyde prior to the cyclisation. The Lemieux-Johnson oxidation can be used for this purpose and involves the dihydroxylation of a carbon-carbon double bond using sodium periodate-osmium tetroxide, followed by cleavage of the carbon-carbon single bond; however it creates a lot of side-products and can result in a low yield [131]. A similar procedure which first dihydroxylated using catalytic osmium tetroxide and *N*-methylmorpholine *N*-oxide and subsequently oxidatively cleaved by sodium periodate was used instead [132]. This reaction was then combined with the cyclisation in acid to give benzofuran **46** and in an overall high yield of 89%.
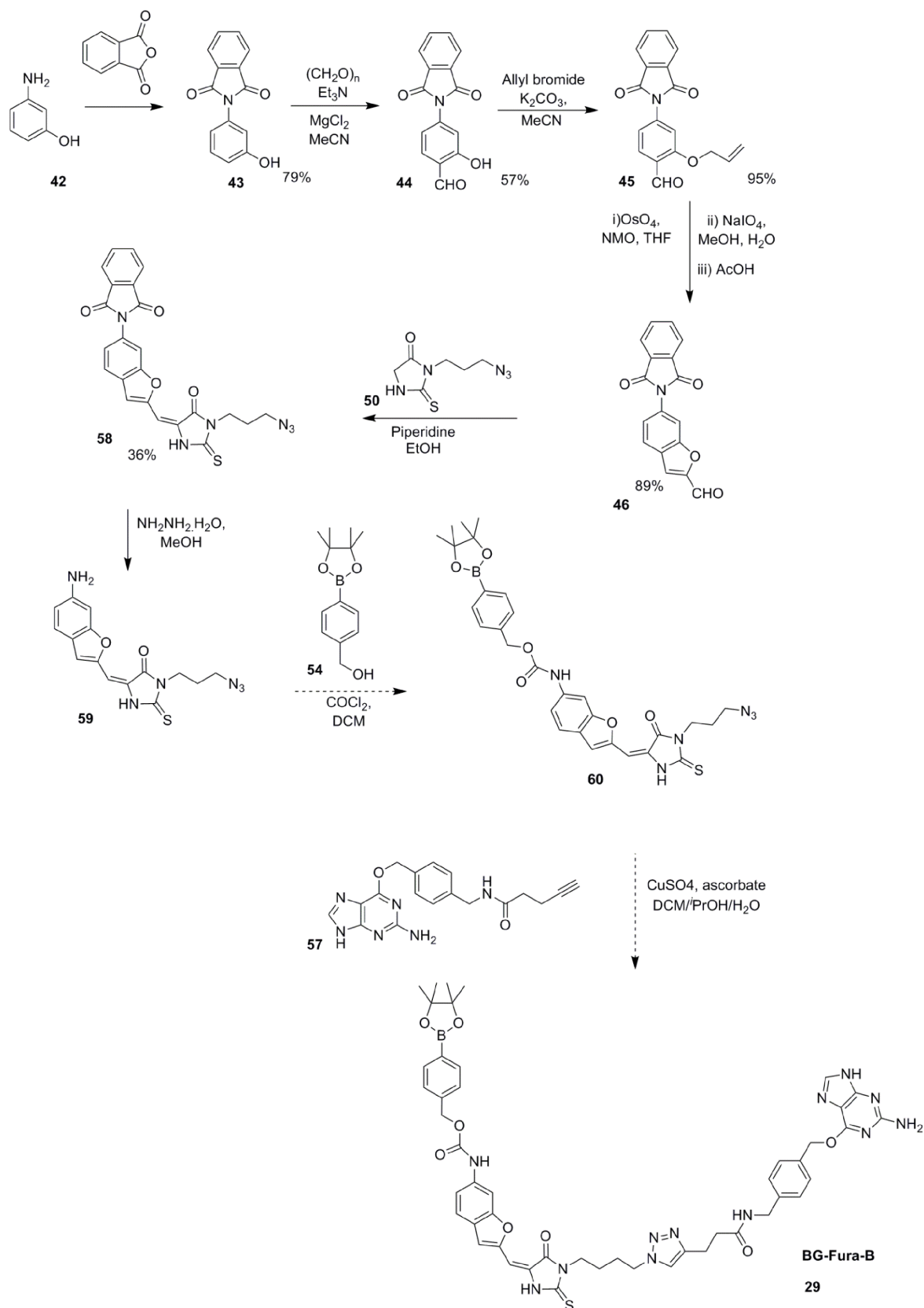
Figure 34 - The synthesis of BG-Fura-B.

The thiohydantoin ring, which makes up the other section of the fluorescent core of the probe was then synthesised (Fig. 35). This synthesis began with the formation of the azide, functionality which was to later perform the Click

chemistry as the final step in the synthesis (Fig. 34). Azidealkylamine **48** was formed using sodium azide and 3-chloroprop-1-yl-aminium chloride **47** in a high yield. This was then reacted with 1,1'-thiocarbonyldiimidazole to form the somewhat unstable isothiocyanate **49** in a moderate yield. This compound was not purified due to its instability. Finally, a cyclisation using the methyl ester of glycine produced the thiohydantoin **50** in a high yield.
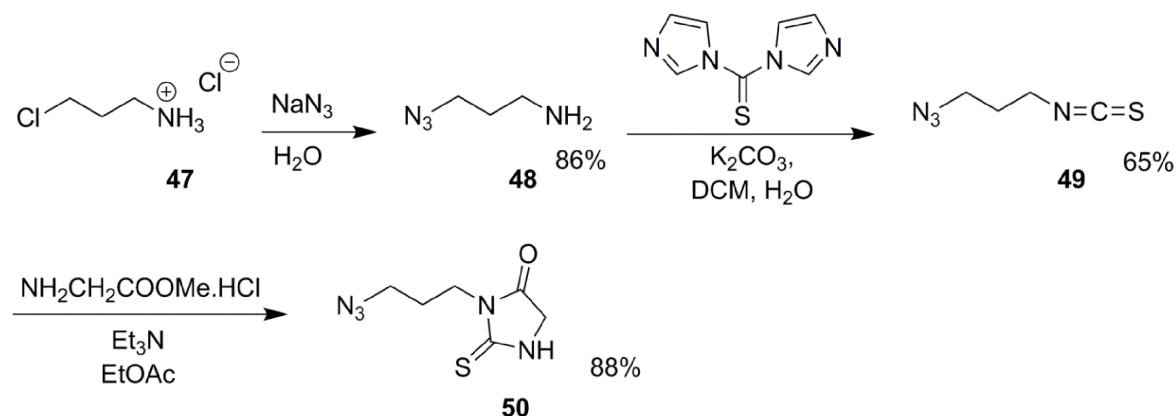
Figure 35 - The synthesis of the thiohydantoin ring.

At this point other components of BG-Fura-B were prepared. The boronic ester moiety **54** was prepared according to literature procedures (Fig. 36) [112]. 4-Bromobenzyl alcohol **51** was first protected with 2,3-dihydrofuran to give the tetrahydrofuranyl ether **52** in excellent yield. This was followed by the use of *n*-butyl lithium in a halogen-lithium exchange reaction followed by borylation to give boronate ester **53** in a high yield. Deprotection using aluminium chloride converted the acetal **53** into benzyl alcohol **54** in a moderate yield.
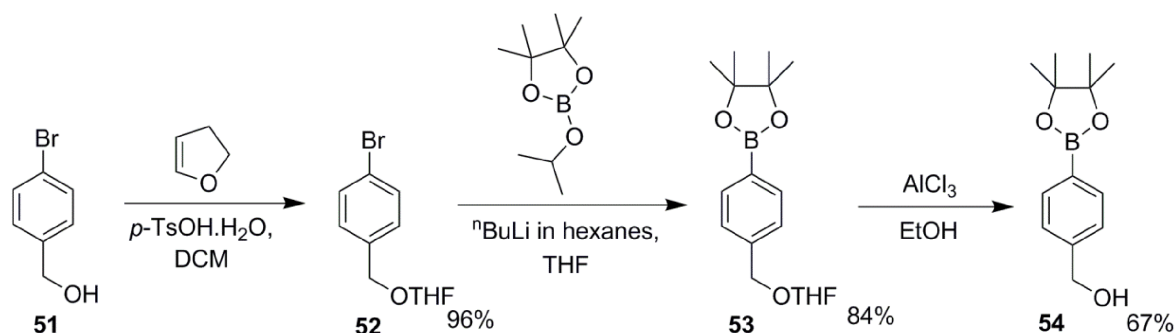
Figure 36 - The synthesis of the boronic acid moiety of BG-Fura-B.

It was decided that a test reaction would be used to check the efficacy of the reaction which would be required to form the carbamate bond (Fig. 37). Benzyl alcohol **55** and 4-iodoaniline were chosen as the substrates. Benzyl alcohol was

first reacted with pyridine and phosgene to form the intermediate benzyl chloroformate. Attack on the carbonyl by the nitrogen atom of 4-iodoaniline yielded carbamate **56** in a quantitative yield. This was promising for the formation of the carbamate for BG-Fura-B as it was important that we did not suffer big losses in yield near the end of the synthesis. It is also possible to form the carbamate by starting with the aniline and going via an intermediate isocyanate.
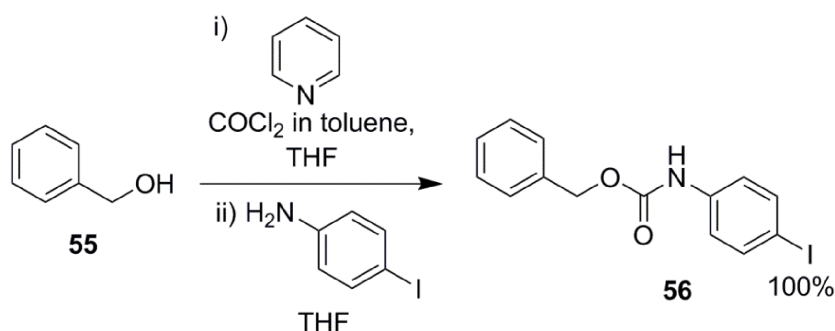
Figure 37 - The synthesis of the carbamate test compound.

The final part of the probe to be incorporated was the SNAP-tag reactivity. A carbodiimide coupling was to be used to create the amide bond via which the alkyne would be incorporated (Fig. 38). The azide-alkyne Huisgen cycloaddition which would bring all parts of BG-Fura-B together, is a 1,3-dipolar cycloaddition and an example of Click chemistry. To be classed as Click chemistry, a reaction must fulfil a number of criteria including high yield, able to work with a wide range of substrates, stereospecific, able to work with benign solvents and require little in the way of purification. The azide-alkyne cycloaddition does fulfil a number of these requirements, but only if copper is included as a catalyst or a strained alkyne is used [133] [90] . Traditionally the azide-alkyne cycloaddition is a thermal reaction requiring high temperatures and produces mixtures of regioisomers, thus preventing it from being classed as a Click reaction. The copper catalysed version however, can be conducted in water, at room temperature and produces only the 1,4-disubstituted regioisomer. This reaction is then particularly suited to the final step of the synthesis, as at this stage gentle conditions and a high yield of the correct product are extremely desirable.

The previously synthesised O^6-(4-aminomethyl)benzylguanine **39** was modified with an alkyne in preparation for the Click chemistry step (Fig. 38). The carbodiimide coupling reagent, EDCI was chosen to form the amide bond between the alkyne and O^6-(4-aminomethyl)benzylguanine **39**. EDCI was used in conjunction with 1-hydroxybenzotriazole to form the alkyne **57** in a high yield, ready for the Click reaction.
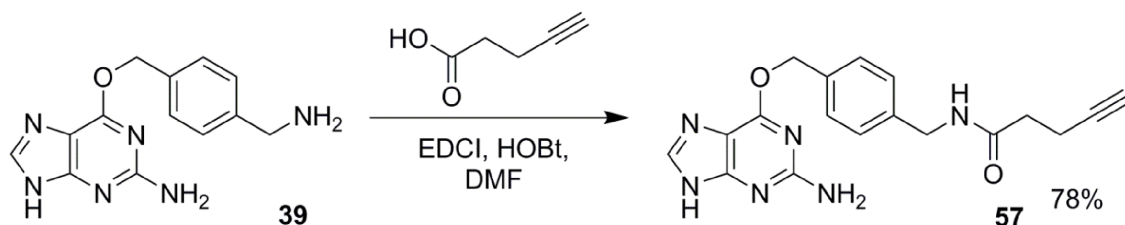
Figure 38 - The synthesis of the alkyne conjugated O^6-(4-aminomethyl-benzyl)guanine.

With the carbamate reaction successfully tested and the hydrogen peroxide reactive boronate ester **54** and the click-ready SNAP-tag substrate **57** prepared, the synthesis of the BG-Fura-B core was continued (Fig. 34). The thiohydantoin and the aldehyde benzofuran underwent a Knoevenagel condensation which involved the nucleophilic addition of the thiohydantoin to the carbonyl, followed by a dehydration to produce the double bond [134]. This produced azide **58** in a low 36% yield. A large proportion of the product was thought to be lost during column chromatography. The product was highly fluorescent, but failed to produce distinct bands on the silica column. Various solvent systems and stationary phases were investigated; however no improvement was found.

Nevertheless the synthesis was continued. The next step was deprotection of azide **58** by removal of the phthalimide group using hydrazine to give amine **59** [135]. There was some evidence that the reaction was successful, however after attempts at column chromatography to purify this, very little was recovered. It was also noticed that the compound degraded very quickly, even when stored at -20 °C in the dark. What material we had was used to investigate whether a particular degradation product was being produced, however there was no one compound but many different species, which were impossible to distinguish from each other. The fluorescence of the material produced was recorded, however full characterisation data was unfortunately never collected due to the degradation (Fig. 39).
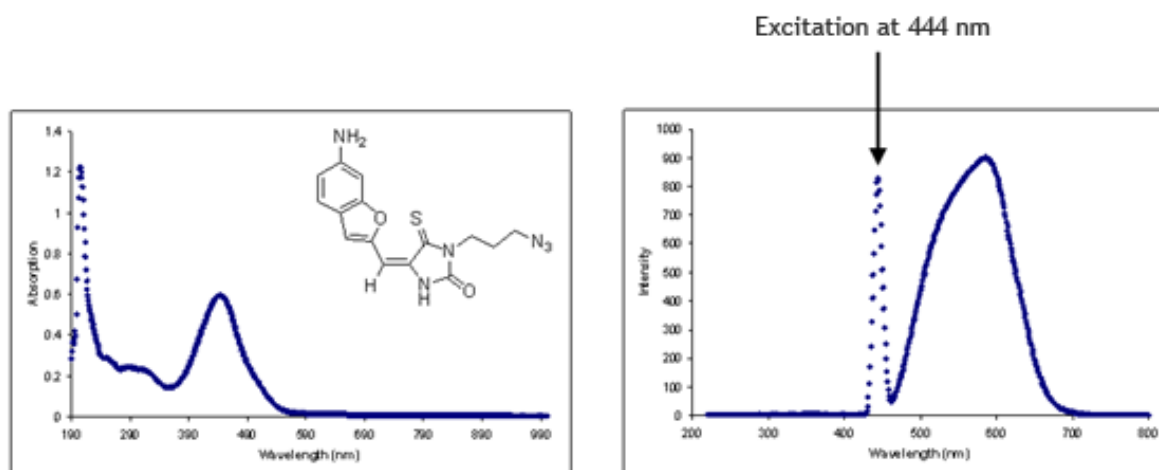
Figure 39 - Absorption and fluorescence spectra of amine 59.

The absorption and fluorescence spectra are as expected and show the core of BG-Fura-B would have had the desired fluorescent properties, particularly the large band gap of almost 200 nm. This would have helped towards the goal of a ratiometric probe for hydrogen peroxide. The instability, however, proved fatal to the project as there was no obvious solution or structural change which could be applied. Another option was to completely redesign the fluorophore but it would have been unlikely that the fluorescent properties required for a ratiometric probe could have been achieved. This coupled to the fact that such a synthesis requires a great deal of time confirmed the decision that the project would take a lower-risk change of direction.

9.3 Conclusions

9.3.1 SNAP-tag Expression and Purification

The SNAP-tag expression and purification was successful with a high yield of protein. When the protein was first expressed an intense band was seen in the SDS-PAGE of the supernatant after cell lysis. This showed that the protein was soluble and not retained in the cell pellet so minimal protein was lost during the lysis procedure. As the SNAP-tag expression vector contained a His-tag this allowed for a simple and effective first step in the purification. This removed most of the other *E.coli* proteins however a few remained. These were then removed in the ion exchange purification. This led to a pure and high yielding stock of protein. The yield produced was 50.5 mg of protein per litre of culture.

9.3.2 HT SNAP Cell Lines

HT SNAP ER and HT SNAP Cyto were stably transfected using the pCI expression vector. Both cell lines showed positive colonies. The expression of HT SNAP Cyto was notably higher than that of HT SNAP ER, as can be seen in the western blot (Fig. 24). In mammalian cells the volume of the cytoplasm is believed to be around 70% of the whole cell, with the ER taking up a much smaller volume. The larger band seen in the western blot could simply be due to the fact that there is more of the cytosol in each cell. It is also possible that SNAP-tag is less stable in the ER or is simply expressed at a lower level. The band seen for the HT SNAP Cyto cell line also runs lower than that of the HT SNAP ER cell line. This is due to the fact that it does not contain the ER targeting and retention sequences and so is a slightly smaller protein.

Both cell lines were transfected successfully and were maintained under selection at all times in culture. However it was found, particularly with regards to the HT SNAP ER cell line that on a number of occasions, expression reduced and was lost fairly quickly after bringing cells into culture, often at a passage number below 20. The consequence was that cells were regularly frozen at low passage number in order to maintain sufficient stocks to enable new cells to be brought into culture as and when required.

The cell lines were stably transfected as this offers a number of advantages over transient transfection. In transient transfection it can be difficult to achieve a

high level of gene expression, the conditions for transfection must be optimized, the transfection must be performed for every experiment and gene expression can vary between each experiment depending on transfection efficiency. Since SNAP-tag was the only protein to be expressed, the time invested in creating stably transfected cell lines was deemed to be acceptable and, therefore, repeated transient transfections would offer no advantage.

Stably transfected cell lines do occasionally lose their expression. This is thought to happen in cases where the protein being expressed has some kind of detrimental effect on the overall health of the cell. In such fast growing cell lines as are used in cell biology, mutations as cells divide are not uncommon and, therefore, any cells which mutate so that they do not express SNAP-tag but do retain the selection resistance will have a selective advantage over those which still express the protein. This can lead to a population of cells in which all have selection resistance but most do not express the desired protein anymore and so appear to have lost expression when the lysates are analysed by western blot.

It is not possible to know whether this is the case for SNAP-tag so we can only assume, but a recommendation for the future may be to stably transfect SNAP-tag as an inducible cell line. The tetracycline repressor protein (TetR) taken from the *E.coli* tetracycline resistance operon can be used to generate tight control over expression in mammalian cell systems. In the most commonly used system TetR blocks transcription by binding to the Tet-operator in the promoter region unless tetracycline is added in which case transcription occurs [136]. This would help reduce any loss of expression since the cells would spend far less time actually expressing any protein which may be inhibiting or damaging to them.

9.3.3 BG Synthesis

The synthesis by Keppler et al. [5] was used as a basis; however, minor adjustments were made, namely the altered lithium aluminium hydride reduction which yielded amine **34** in an improved yield compared to the published method. The other alteration made was to the conjugation of the two halves **35** and **37** of the universal BG precursor **39**. Sodium hydride and catalytic DMAP was used instead of potassium carbonate. This reduced the number of

steps as O^6-(4-aminomethyl-benzyl)guanine **39** was produced directly, since the intermediate deprotected under the reaction conditions. The yields for all the steps other than that of the reduction were lower than those published, however enough of the universal BG precursor **39** was made for the uses required.

9.3.4 BG-NBD-X

BG-NBD-X was successfully synthesised and did not require any purification. BG-NBD-X showed that SNAP-tag was functional when expressed and purified in *E.coli* and in HT SNAP lysates through the use of a fluorescent scan of the protein after being run on a 12.5% SDS-PAGE gel. With regards to this method the probe was very effective.

When BG-NBD-X was added to HT SNAP cells, which were then fixed and visualised by confocal microscopy, the fluorescence recorded was indicative of the probe being able to diffuse into the cells and bind to SNAP-tag whether in the ER or cytosol; however, there were issues with the fluorophore itself. NBD-X bleaches very quickly, even with the addition of Mowiol 4-88, an anti-fade compound used in immunofluorescence. NBD-X is known to be environmentally sensitive [137] and so though it allowed the aims of the experiment to be achieved it perhaps does not have the best attributes for confocal microscopy.

9.3.5 BG-Fura-B

The design of BG-Fura-B (Fig. 19) encompassed all the moieties necessary. The SNAP-tag substrate and boronate ester both had good literature precedence and Fura-red is used as a commercially available sensor. It would not, therefore, have been possible for us to foresee the stability issues that we encountered. The fluorescence which was recorded suggests that the probe would have had at least the desired fluorescent properties.

Since the fluorescent properties had to be very specific to be successful as a ratiometric probe, synthesis of a newly designed or different fluorophore was not altogether appealing. The aim of the project was to make a probe which can get into mammalian cells and to use this to look at hydrogen peroxide levels inside cells when they are placed under various stresses. The aim of the project did not include synthesis of a novel fluorophore or advanced method development for synthesis.

The main learning outcomes were that SNAP-tag was a very effective system and would be ideal for a probe to be targeted to the ER but perhaps the fluorescent system designed was not the most appropriate. It was decided that the next part of the project would keep the use of SNAP-tag but simplify the probe. This would allow the most important aim of the project, to perform experiments in mammalian cells, to occur sooner.

10.0 Results II

10.1 Introduction

Due to the lack of success with regards to BG-Fura-B it was decided to reassess the probe design. In theory BG-Fura-B was the perfect probe as it had the desired fluorescent properties, successful targeting method and hydrogen peroxide reactivity. However, in practice this did not work out. Due to the complexity of the structure of BG-Fura-B, a lot of time was invested in the synthesis and in attempting to create solutions for the synthetic problems. After concluding the lack of stability of BG-Fura-B was too great a hurdle to overcome it was decided that the next step in the project must include a lower risk solution for chemical synthesis.

It was clear that SNAP-tag was the best method for targeting a synthetic probe to the ER. The synthesis and use of BG-NBD-X confirmed that the method was successful both *in vitro* and in mammalian cells. It was, therefore, concluded that the next probe design would incorporate the benzylguanine structure. From the numerous uses previously published it was also concluded that a boronate ester would also have to be included in the structure [138]. The boronate being the only biologically validated group that irreversibly reacts with hydrogen peroxide in a selective manner. The boronate ester rather than the boronic acid was chosen as it makes the compound easier to handle in the synthetic setting [73].

The final decision involved changing the method of detection and analysis. Fluorescence microscopy was previously chosen as it has the advantage of the power to analyse events taking place in live cells. However, since the attempt to incorporate the desired fluorescent properties into a probe had been unsuccessful a different approach was chosen. MitoB previously synthesised in the Hartley group is a successful probe to measure hydrogen peroxide in the mitochondria [115]. Importantly, this provides an accurate and ratiometric assessment since the analysis is carried out by mass spectrometry. This led to the conclusion that a new probe design would allow for analysis also by mass spectrometry.

The final probe (BGB, Fig. 40) therefore incorporates the benzylguanine moiety for SNAP-tag reactivity, an aryl-boronic acid caged as the pinacol ester and a short linker holding the two functionalities together.
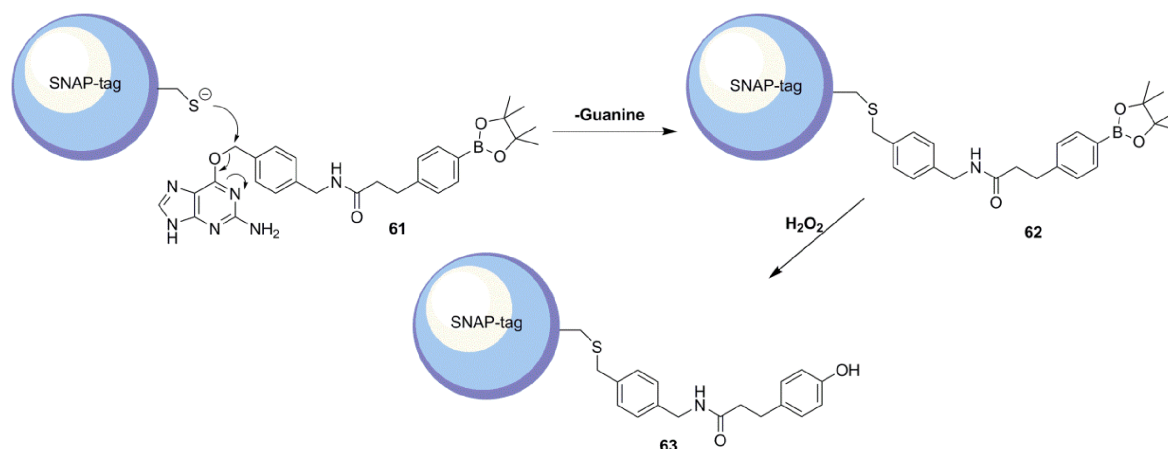
Figure 40 - Design of the probe BGB. After the benzylguanine substrate, BGB 61, reacts with cysteine in the active site of SNAP-tag, forming SNAP-B 62 and releasing guanine. When SNAP-B reacts with a molecule of H_2O_2, the boronate ester is converted into a phenol and SNAP-P 63 is produced.

After designing BGB the method of detecting reactivity was considered. After BGB enters the cell and comes into contact with SNAP-tag the irreversible reaction between the benzylguanine moiety and the cysteine in the active site will occur, releasing guanine and covalently binding the probe to the protein, resulting in the SNAP-B conjugate. The experimental plan then involved stressing the cells to cause an increase in hydrogen peroxide. The next step would involve recovery of the SNAP-tag conjugated probe to measure the ratio of SNAP-B (unreacted) to SNAP-P (reacted). It is possible to recover a specific protein from a cell lysate using immunoisolation. This is a process which allows the isolation of a particular protein from a mixture of many thousands of proteins, such as would exist in a cell lysate mixture, by the use of an antibody which recognises the desired protein and which is conjugated to a solid support such as agarose beads. SNAP-tag was expressed in cells with a FLAG-tag to allow easy detection and to act as a handle for the immunoisolation. FLAG-tag has the sequence DYKDDDDK and is an example of epitope tagging.

There exists a range of different types of mass spectrometry, each suited to a particular type of analyte molecule. Electrospray ionisation, for example, is particularly suited to the analysis of polar molecules [139]. When choosing the type of mass spectrometry for analysis of BGB samples the important point for consideration was that the probe would be conjugated to a protein. MALDI-TOF is generally the mass spectrometry method of choice for biochemical molecules including proteins, peptides and glycopeptides. MALDI-TOF uses a gentle ionisation process which creates singly charged ions and is usually coupled to a time of flight analyser. This means the interpretation of spectra is simpler than for mass spectrometry methods which create multiply charged ions and also allows any modifications to stay intact during the procedure [140]. Consequently it was decided to analyse the SNAP-B to SNAP-P ratio by MALDI-TOF.

The SNAP-tag probe conjugate was digested into its component peptides by trypsin prior to analysis. MALDI-TOF is capable of analysing whole proteins, however the greater the mass being analysed the broader the peaks produced in the spectrum. By instead studying the peptides, the mass peaks produced are more accurate and therefore unambiguous. An *in silico* digest can be used to calculate theoretical peptides masses (Table.1).

Mass	Peptide sequence
6437.1763	GTSAADAVEVPAPAAVLGGP EPLMQATAWLNAYFHQPEAI EEFPVPALHHPVFQQESFTR
2791.4442	LCIPQVLLALFLSMLTGPGE GSASMDK
2390.2714	FGEVISYQQLAALAGNPAAT AAVK
1687.9312	TALSGNPVPILIPCHR
1636.8540	VVSSSGAVGGYEGGLAVK
1555.7784	LELSGCEQGLHEIK
1513.8372	LGKPGLGPAGIGADYK
1247.6279	EWLLAHEGHR
931.5095	TTLDSPLGK
673.4031	QVLWK
625.2320	DCEMK
607.2205	DDDDK

Table 1 – Masses and sequences of peptides derived from SNAP-tag. The masses were calculated using an *in silico* digest with trypsin. The active site peptide (highlighted) has a mass of 1688.

A standard enzyme used for creation of peptides for MALDI is trypsin which cleaves at the carboxyl side of arginine and lysine residues. Trypsin was consequently chosen as the starting point for the digestion. The calculated mass for the active site peptide is [M+H]$^+$ 1688. The active site peptide from unreacted SNAP-B has a mass of [M+H]$^+$ 2066 with the boron in the boronate ester form, however, since the boronate ester is in an equilibrium with the boronic acid in aqueous solutions, it is far more likely to be in the boronic acid form and have a mass of [M+H]$^+$ 1984. The mass of the active site peptide from the product of reaction with hydrogen peroxide, SNAP-P is [M+H]$^+$ 1955 (Fig. 41).

TALSGNPVPILP<u>C</u>HR = 1688   TALSGNPVPILPCHR = 1955

64

65
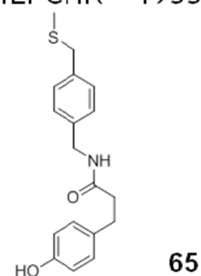
TALSGNPVPILPCHR = 1984   TALSGNPVPILPCHR = 2066
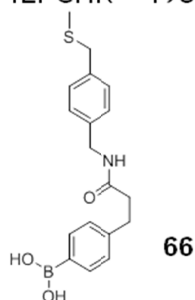
66   **67**
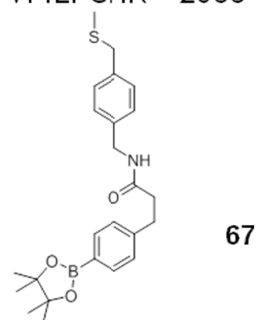
Figure 41 - Modified peptides. The masses of SNAP-tag derived peptide containing the active site 64 and modified with BGB (boronate ester) 65, BGB (boronic acid) 66 and BGP (phenol) 67, which is produced when SNAP-B reacts with hydrogen peroxide.

In MALDI-TOF the intensity of a peak correlates to the abundance of that ion. Therefore by comparing the intensities of the boronic acid to the phenol product the change of that ratio over time or other variable will represent the reaction of the SNAP-B with hydrogen peroxide.

10.2 Results

10.2.1 Syntheses of BGB and BGP

The structures of the designed molecular probes are shown in Fig. 41. BGB, is the boronate probe and BGP, is a reagent that would produce the phenol product SNAP-P directly from unmodified SNAP-tag. BGP is necessary for use in control experiments. The structures were based on the derivatised O^6-(4-aminomethyl)benzylguanine.
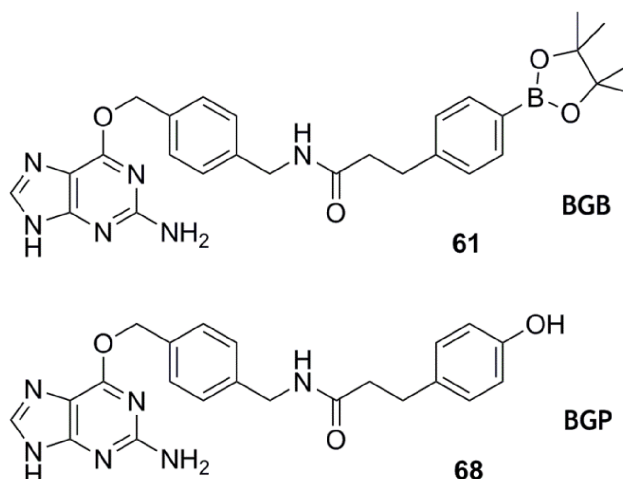
Figure 42 – The structures of BGB 61 and BGP 68. The probes were based on the derivatised O^6-(4-aminomethyl)benzylguanine.

With the universal SNAP-tag substrate precursor **39** previously synthesised, the task of producing BGB and BGP was a relatively simple one. This had of course, been the focal point of the design process of the probe. The design of the fluorescent probe BG-Fura-B, had been in theory the perfect probe, however, unforeseen synthetic difficulties prevented its realisation. With the simplified structure of BGB it meant the concept of a mass spectrometry probe for the ER could be tested quickly and so provide some proof of concept. Once this reassurance had been gained, then if required the structure could be tweaked and more synthesis carried out.

The syntheses of BGB and BGP are shown in Fig. 43.
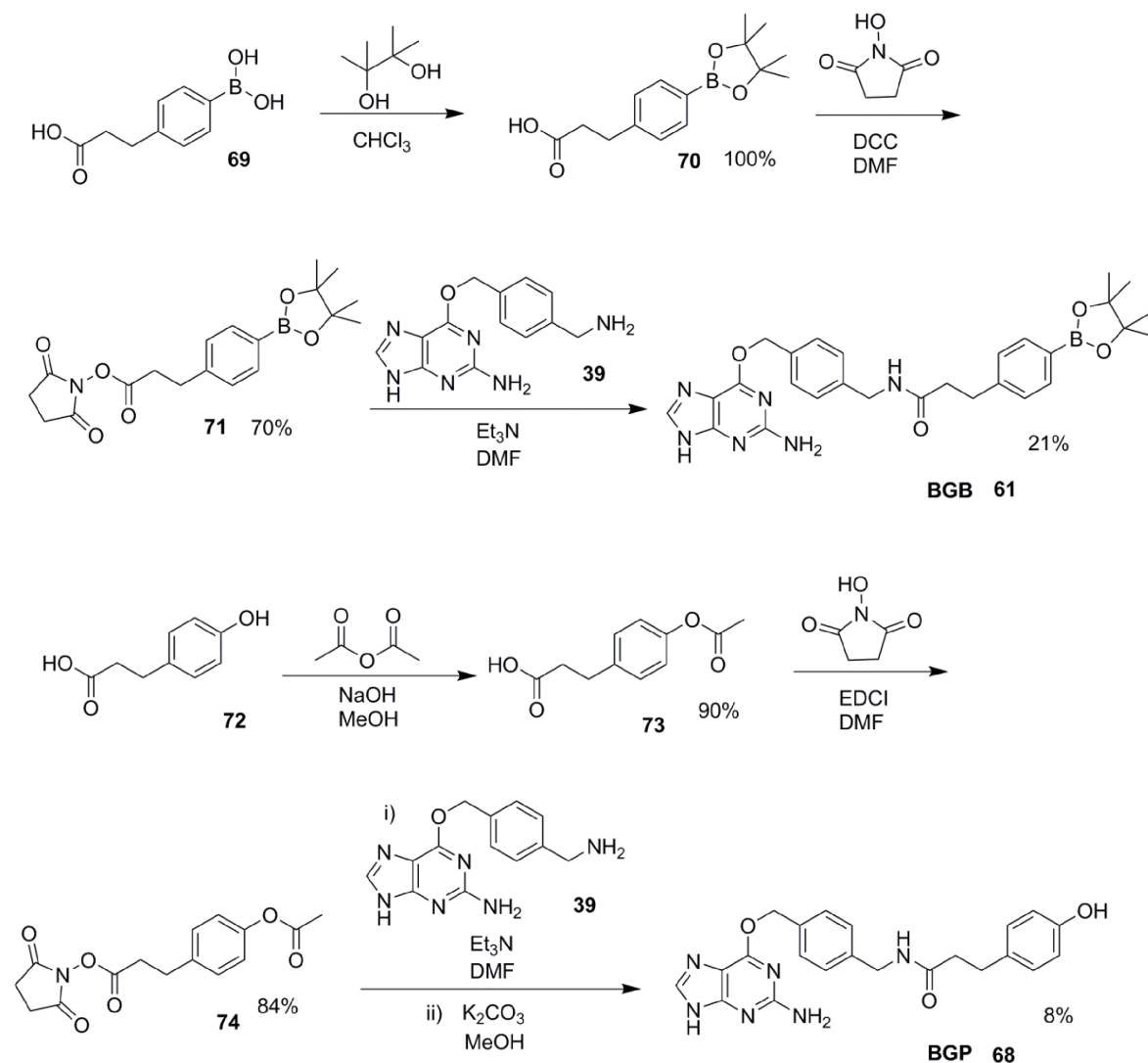
Figure 43 – The syntheses of the probes BGB and BGP. The syntheses incorporated the SNAP-tag substrate and H$_2$O$_2$ reactive boronate ester for BGB with the corresponding phenol for BGP.

The synthesis of BGB began with a protection of 4-(2-carboxyethyl)benzeneboronic acid **69** with pinacol yielding pinacol ester **70** in a quantitative yield. The pinacol ester is used for synthetic ease as the polarity of the boronic acid can lead to issues in purification and the formation of stable trimers via the acid [73]. The pinacol ester is in equilibrium with the boronic acid in aqueous solutions so is likely to be hydrolysed when used at high dilution in a biological system. This was followed by activation of the carboxylic acid via a carbodiimide coupling with *N*-hydroxysuccinimide in a high yield. Succinimidyl esters are reactive towards amine groups [141] and so succinimidyl ester **71** was chosen because it was expected to react with *O*[6]-(4-aminomethyl)benzylguanine

39 without the use of a coupling agent that would give side products that may be difficult to remove.

BGB **61** was produced by coupling the activated succinimidyl ester with the SNAP-tag substrate **39** with triethylamine as the base. There was a low yield for this reaction. The coupling itself was fairly efficient but loss of material occurred in the purification steps. O^6-(4-aminomethyl)benzylguanine is insoluble in most solvents and once formed, BGB also maintained this level of insolubility. Unfortunately this rendered the purification by column chromatography a fairly tricky process where a lot of material was lost on the silica of the column. Nevertheless enough material was produced for the required purposes. Since the aim of the process was just to produce enough material for biological testing, it was not deemed worthwhile to spend further synthetic time in improving this process.

The synthesis of the corresponding phenol, BGP **68**, also began with a protection. 3-(4-Hydroxyphenyl)propanoic acid **72** was protected as the acetate **73** with acetic anhydride in a high yield. Again the carboxylic acid was activated as a succinimidyl ester **74** for amide bond formation using N-hydroxysuccinimide and a carbodiimide coupling, also in a high yield. In a mirroring of the BGB synthesis, the coupling to O^6-(4-aminomethyl)benzylguanine **39** also proved troublesome for the same reasons. The coupling of the two halves of the molecule was followed by the deprotection of the phenolic hydroxyl group without purifying the intermediate. The yield of BGP **68** over these two steps was low due to the difficulty of working with such compounds, but enough was produced for biological testing purposes.

10.2.2 Confirmation of Probe Binding and Visualisation in MALDI-TOF Mass Spectra

With both BGB and BGP in hand from a relatively short and effective synthesis, the first step was to achieve the proof of concept which was lacking for BG-Fura-B.

HT SNAP ER cells where treated with DMEM with or without 5 µM BGB for 30 min. After 30 min cells were washed to remove any excess unbound probe. Cells were then lysed and prepared for SDS-PAGE as usual. Samples were run on a 15% gel

and transferred to a nitrocellulose membrane. The membrane was blotted with anti-SNAP-tag and anti-GAPDH (Fig. 44).
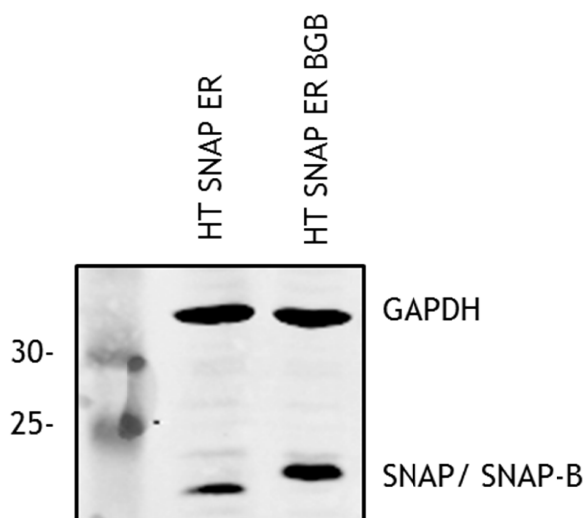
Figure 44 - Western blot from a 15% SDS-PAGE of lysates from HT SNAP ER cells and HT SNAP ER cells treated with BGB. Modified SNAP runs slower and shows SNAP is modified quantitatively in the ER.

As seen in the western blot (Fig. 44), the band for SNAP-tag from cells which had been treated with probe runs slightly slower through the gel. The difference is not vast as the mass addition is 296 Da to a 23.5 kDa protein; however it clearly shows there is a mass difference and also suggests quantitative labelling as in the sample from treated cells there is no lower band at the SNAP-tag level. The lysates were also blotted with GAPDH as a control. This shows that BGB can successfully navigate the cell membrane and the ER membrane and efficiently label SNAP-tag in 30 min.

After confirming that labelling of SNAP-tag was successful with BGB, the possibility of analysis using MALDI-TOF mass spectrometry was investigated. From the *in silico* digest (Table. 1) the expected peak mass for the peak containing the active site cysteine was 1688 for SNAP-tag and with the addition of BGP to form SNAP-P this was calculated as 1955 (Fig. 45).
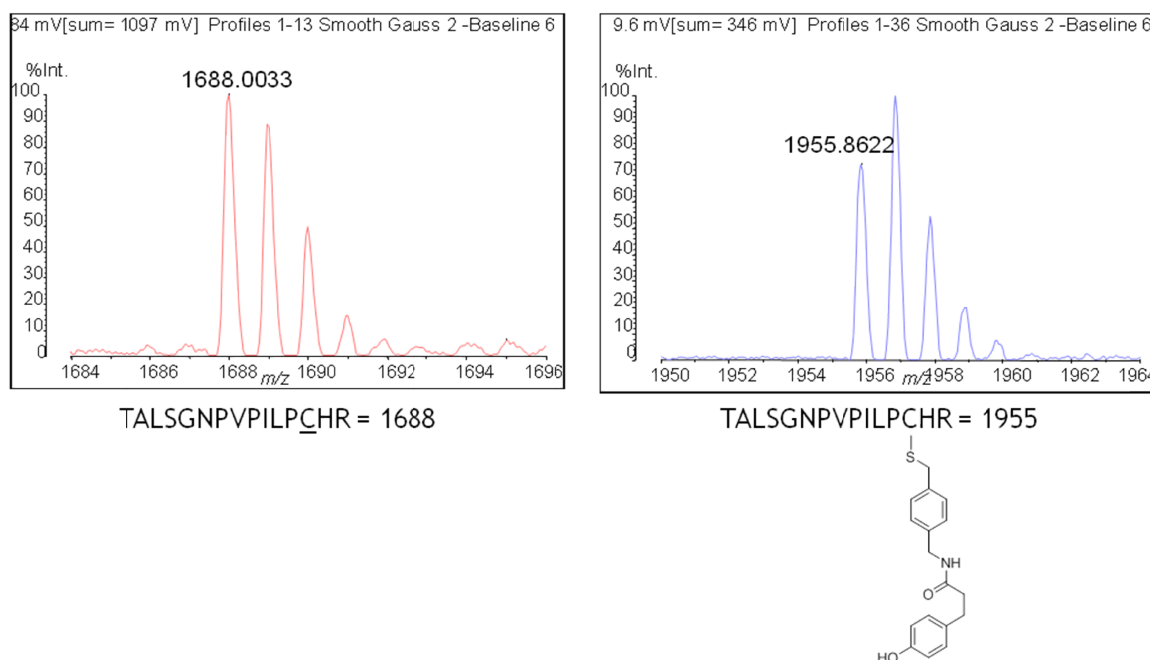
Figure 45 - MALDI-TOF spectra of unmodified and modified SNAP-tag. The left-hand spectrum shows the SNAP-tag active site peptide with a mass of 1688 and the right-hand spectrum shows the SNAP-tag active site peptide with the phenol BGP conjugated at a mass of 1955.

In Fig. 45 spectra were collected of the SNAP-tag and SNAP-P derived peptides created by trypsin digestion of purified recombinant protein. The left-hand spectrum shows a peak at 1688, the expected mass of the peptide containing the active site cysteine and in the right-hand spectrum there is a peak at 1955, the expected mass for SNAP-P derived peptide with a modified active site. These spectra confirm that the desired peptides fly by MALDI-TOF and can be successfully detected. There are no other SNAP-tag or system peaks which interfere with these peaks, a benefit as this would cause the intensities to be non-representative. These preliminary spectra suggested that the method of trypsin digestion of the protein and subsequent analysis by MALDI-TOF may be successful.

To further confirm that the peak at 1955 was in fact due to the addition of BGP some further control experiments were carried out. Samples of recombinant SNAP-tag were either treated with iodoacetamide, which alkylates any available cysteine residues [142], and subsequently with BGP or alternatively, with first

BGP then iodoacetamide. The calculated mass of the active site peptide with the iodoacetamide modification was 1745 (Fig. 46).
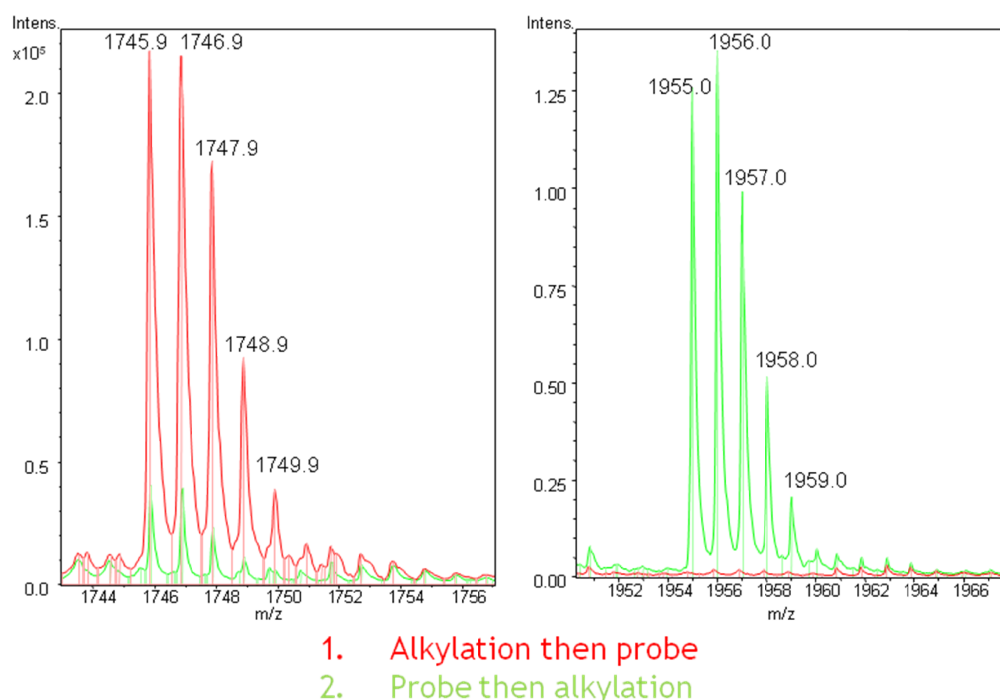
Figure 46 - Overlay of two MALDI-TOF spectra. To allow easier comparison the masses at 1745 and 1955 have been enlarged with the intervening masses removed. The red spectrum arises from alkylating SNAP-tag with iodoacetamide then treating with BGP. The green spectrum results from first treating with BGP and then subsequently alkylating with iodoacetamide.

In Fig. 45 two spectra are overlaid. The red spectrum is the sample which was first treated with iodoacetamide. There is a strong peak at 1745, the mass of the active site peptide after alkylation, and at 1955 there is no peak. The green spectrum was the result of first treating with BGP, then iodoacetamide and shows a strong peak at 1955, the mass of the active site peptide with BGP modification and a weaker peak at 1745. This confirmed that the peak at 1955 was due to the modification of SNAP-tag by BGP, as in spectrum 1, the addition of iodoacetamide prevented any BGP from binding as the cysteine was blocked. The fact that there is still a weak alkylation peak at 1745 in spectrum 2 shows that not all of the protein was modified with BGP. The SNAP-tag used was expressed in *E.coli* and so it is possible that some of the protein may not have been folded correctly, so the active site may not have been in the correct

conformation for reaction with the O^6-(4-aminomethyl)benzylguanine derivative. If this was the case then the cysteine would still be available for alkylation with iodoacetamide after the addition of BGP.

Tandem mass spectrometry, performed out of house also confirmed the sequence of the peptides and the mass of the modification of the peak at 1955.

A stock of SNAP-tag conjugated to BGB (SNAP-B) had been prepared and this was digested with trypsin in order to confirm that the mass peak for the active site peptide derived from SNAP-B could also be visualised by MALDI-TOF. The use of mass spectrometric analysis was based on the fact that the intensities of the starting material and product peaks could be compared to measure the reactivity of the probe and hence hydrogen peroxide levels. The probe had been synthesised as the boronate ester, however, in the dilute aqueous conditions used for biological experimentation this was expected to be hydrolysed and for the unreacted probe to be in the boronic acid form. The expected mass for the SNAP-B peptide was therefore 1984 (2066 for the boronic ester).

Any boron containing peak in the mass spectrum was easy to identify as boron produces a very distinct splitting pattern due to the presence of the ^{10}B and ^{11}B isotopes (Fig. 47).

Molecular Formula:	$C_{92}H_{145}N_{23}O_{23}BS$
Molecular Weight:	1984.152000
Exact Mass:	1983.069745
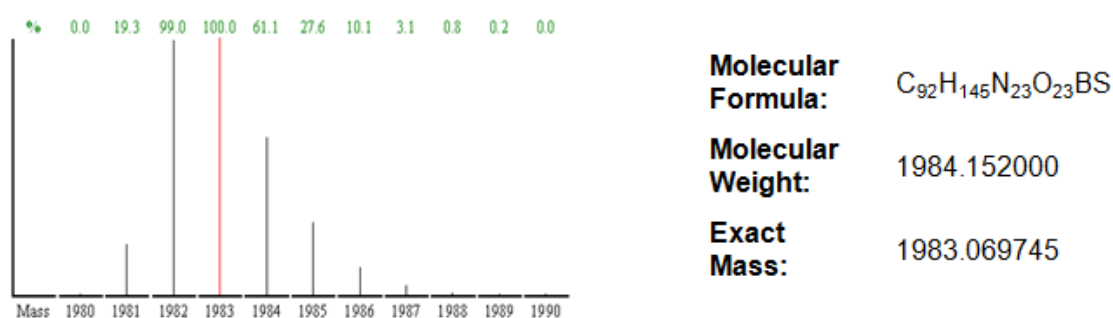
Figure 47 – The calculated mass and splitting pattern of the peak representing the active site peptide from SNAP-B. The peak was calculated using SNAP-B in the boronic acid form as this is expected to be dominant in highly aqueous conditions.

Unfortunately a peak at 1984 was not observed. On some occasions a small peak that did display the characteristic splitting pattern was observed at 2066, suggesting some of the SNAP-B derived peptide was still in the ester form. With

the aqueous conditions used it was known that most of the probe would be in the acid form and it became evident that this form did not fly by MALDI-TOF. Other peaks were also occasionally observed in the spectra that contained the boron splitting pattern but were not at expected masses (Fig. 48).
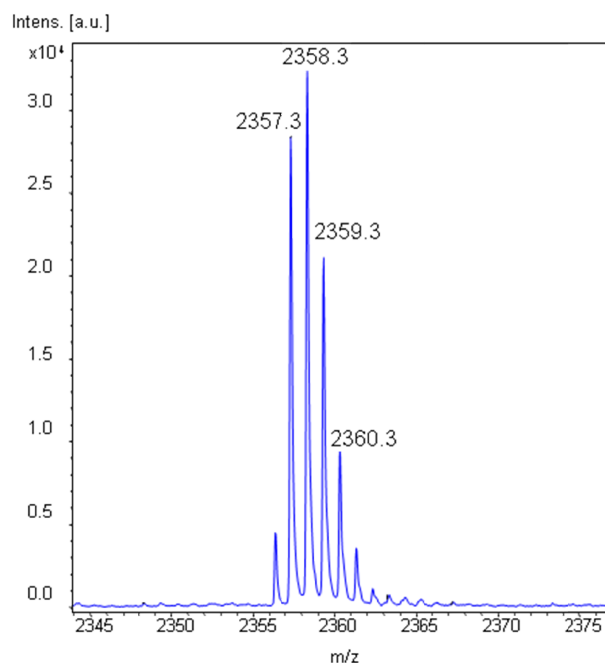
Figure 48 – A peak with mass 2357 displaying the characteristic boron splitting pattern.

In Fig. 48 a peak was recorded with mass 2357 which seemed to contain boron as seen by the splitting pattern. This was not a mass at which anything should have contained boron and had not been calculated from the *in silico* digest. The presence of high mass boron containing peaks suggested that adducts may be being formed. This was disappointing as the planned method had been to compare intensities of the unreacted boronic acid peak to the reacted phenol peak. The facts that the boronic acid did not fly and other high mass boron containing adducts were present meant that this simple method of analysis would not be possible.

Other ways of processing the data were considered in order to overcome the issue. The phenol peak at 1955 successfully flew in the MALDI-TOF and did not produce any problematic adducts. It was decided that an internal standard could be used as a method to measure against so the increase in the intensity of the peak at 1955 as the probe reacted could be determined. Another SNAP-tag derived peptide was chosen as the internal standard. This peptide had a mass of

1247 and consistently showed good intensity in all spectra. Tandem mass spectrometry performed out-of-house confirmed that this was in fact a SNAP-tag derived peptide. Even with the use of the internal standard the total amount of SNAP-tag conjugated probe present in each sample still needed to be known. Since the amount of probe in the boronic acid form could not be calculated, this was circumvented by the inclusion of samples in each experiment which had been completely saturated with hydrogen peroxide. This meant all probe in the saturated samples was in the phenol form which could be measured in the MALDI-TOF spectra (Equation 1).

$$\left. \frac{\text{Reacted probe}}{(SNAP-P)} \middle/ \frac{\text{Total probe}}{(SNAP-B+SNAP-P)} \right. = \frac{\text{Intensity at 1955}/\text{Intensity at 1247 in experimental sample}}{\text{Intensity at 1955}/\text{Intensity at 1247 in saturated sample}}$$

Equation 1 – The equation devised to calculate the reaction of SNAP-B to SNAP-P. This incorporated the use of a SNAP-tag derived internal standard and saturated sample to account for the inability to measure the boronic acid using MALDI-TOF mass spectrometry.

In Equation 1 the method of calculation is shown that allowed the determination of the fraction of SNAP-B that had reacted without direct measurement of the boronic acid. This had not been the original plan; however, it allowed the development of the BGB system to continue to advance.

10.2.3 *In Vitro* Results

After deciding to use the internal standard and saturated sample system as a means of overcoming the fact that studying SNAP-B directly by MALDI-TOF was not possible, the next step was to test this system using the purified recombinant protein.

As mentioned a stock of SNAP-B had previously been prepared and was used to test the new system. SNAP-B was mixed with varying concentrations of hydrogen peroxide for varying times at room temperature. For the saturated samples used to calculate the total amount probe, SNAP-B was mixed with 10 mM hydrogen

peroxide. The reactions between SNAP-B and hydrogen peroxide were stopped by adding a five times volume of cold acetone to each reaction, which precipitated the protein. The samples were stored at -20 °C for a further one hour before they were centrifuged and supernatants removed. Samples were resuspended in trypsin solution and incubated overnight at 37 °C before analysis by MALDI-TOF and the peak intensities produced, used in Equation 1 to measure the reaction of SNAP-B to SNAP-P.

Fig. 49 shows an experiment displaying the effects of a range of hydrogen peroxide concentrations on the phenol (SNAP-P) to total probe ratio (SNAP-B + SNAP-P).
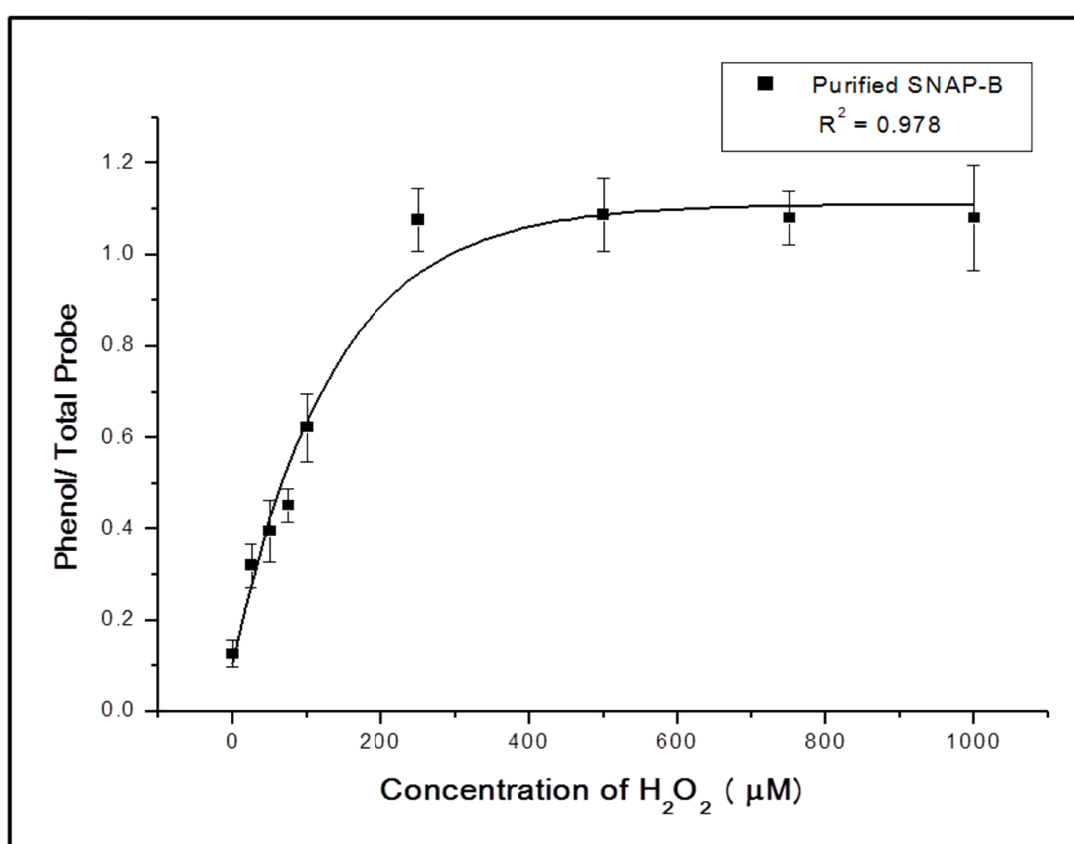
Figure 49 - SNAP-B concentration range experiment. Recombinant SNAP-B was mixed with different concentrations of hydrogen peroxide for 30 min at 37˚C in 100 mM Tris-HCl. Reactions were stopped by the addition of -20˚C acetone. The y axis values were calculated using the internal standard and by including samples completely saturated with hydrogen peroxide to determine total amount of probe.

In Fig. 49 the results from the concentration range studied show that Equation 1 can be used as a method of calculating the reaction of SNAP-B with hydrogen peroxide. SNAP-B was mixed with the varying concentrations of hydrogen peroxide for 30 minutes. Interestingly the graph does not go through zero. This suggests that after 30 minutes in buffer the probe is around 10% oxidised. Saturation is reached at around 250 µM hydrogen peroxide and sensitivity is achieved even in the low micromolar concentrations.

The reaction of SNAP-B to hydrogen peroxide with fixed concentrations over time was also studied (Fig. 50).
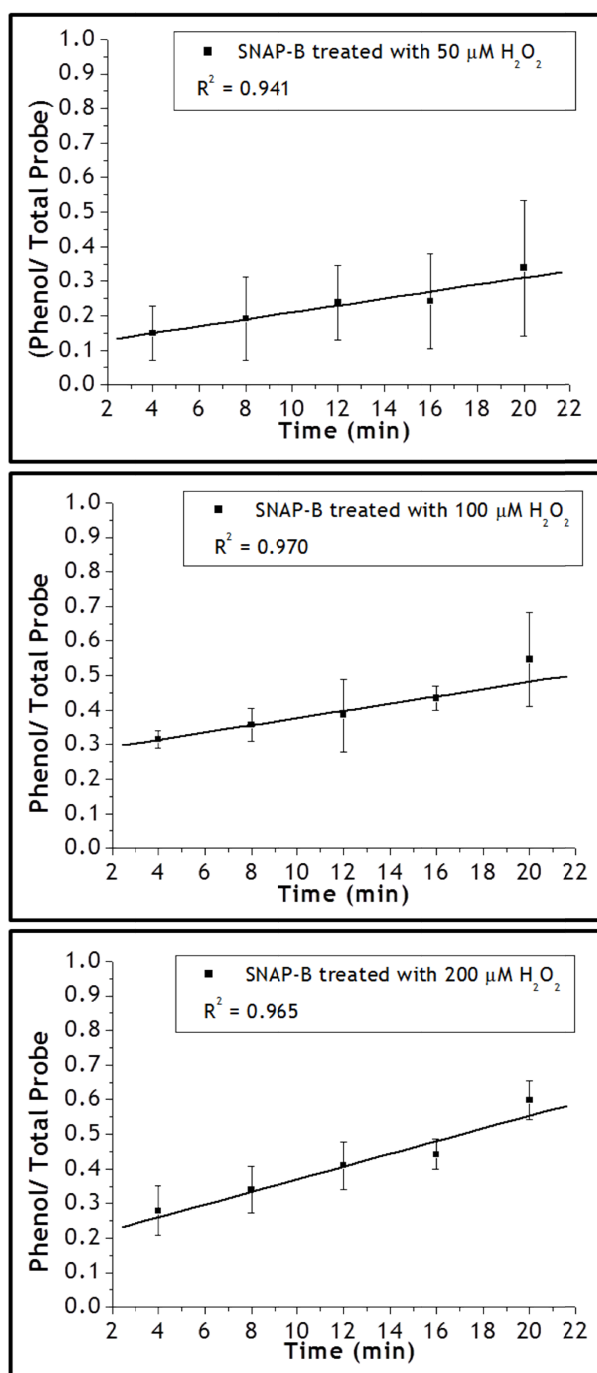
Figure 50 - SNAP-B time courses. Recombinant SNAP-B was mixed with 50 μM, 100 μM and 200 μM hydrogen peroxide for different times up to 20 min in 100 mM Tris-HCl. Reactions were stopped by the addition of -20˚C acetone. The y axis values were calculated using the internal standard and by including samples completely saturated with hydrogen peroxide to determine total amount of probe.

The *in vitro* time courses (Fig. 50) show reactivity at low micromolar concentrations with increasing reactivity at the higher concentrations. The error bars are smaller at 100 µM and 200 µM than for the 50 µM timecourse but the change in the SNAP-B to SNAP-P ratio can still be measured. The first time point was recorded at four minutes at which point the probe has already been oxidised to varying extents. Both the time courses and concentration range showed SNAP-B *in vitro* reacted with hydrogen peroxide and the reaction could be measured without direct detection of SNAP-B in the MALDI-TOF mass spectra.

In the experiments hydrogen peroxide was in a vast excess over SNAP-B. This means pseudo first order kinetics are expected where the value of k when the molarity is 200 µM is four times that of the value of k when the molarity is 50 µM. The rate of reaction clearly increases when the hydrogen peroxide concentration increases; however, pseudo first order kinetics are not apparent from Fig. 50. This is possibly due to some variability as a consequence of the choice of analysis technique.

10.2.4 *In Cellulo* Experimental Method Development

The preliminary experiments showed that the probe was capable of binding to SNAP-tag *in vitro* and *in cellulo*. The mass spectrometry experiments confirmed that the trypsin digestion was successful and produced the expected peaks, including the active site peptide. The use of SNAP-P in mass spectrometry experiments showed that the phenol product of the probe after hydrogen peroxide reaction was visible by MALDI-TOF and the development of Equation 1 allowed for the fact that SNAP-B could not be directly measured from the mass spectra. These experiments were carried out on recombinant protein only so the next requirement was a method for use of the probe in cells to prove that the previous method development was applicable *in cellulo* (Fig. 51).
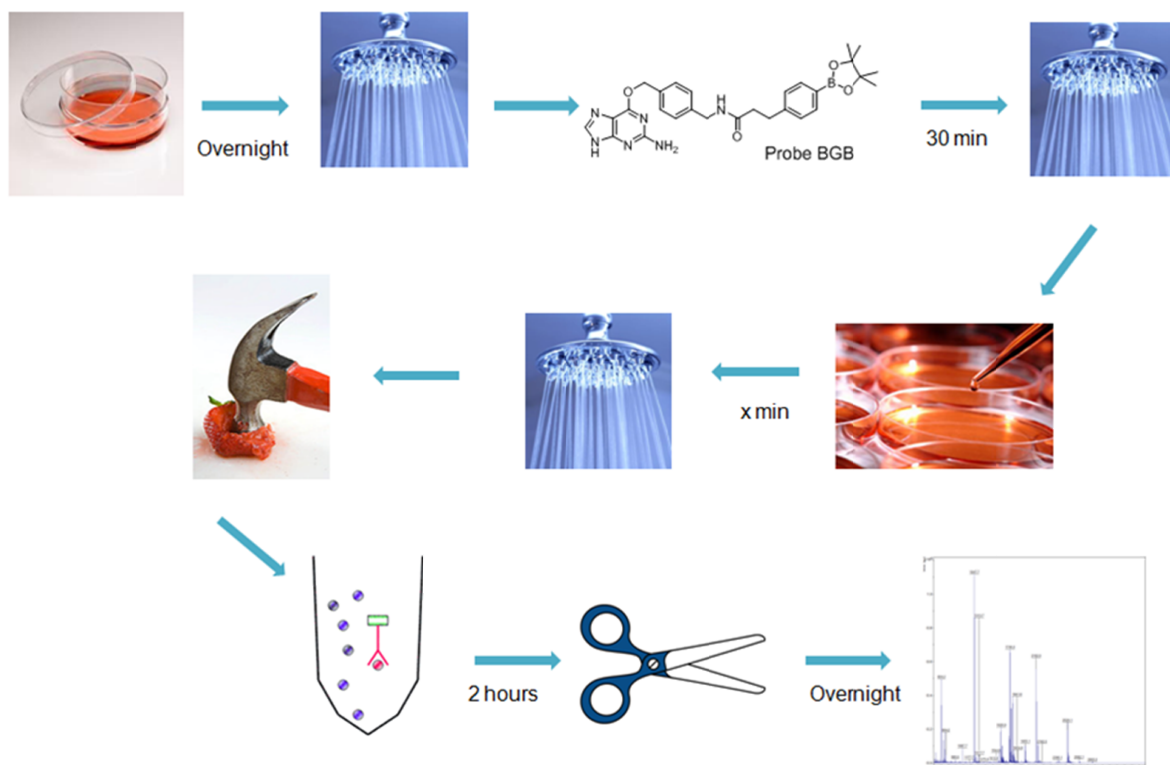
Figure 51 - BGB method for use in cells. Cells are seeded, then the following day washed with PBS, and treated with 5 µM BGB for 30 min. Excess unbound probe is washed out with PBS and the cells are then treated with H$_2$O$_2$ for the desired time. Cells are again washed with PBS and lysed. SNAP is immunoisolated with anti-FLAG M2 affinity gel (Sigma-Aldrich) then digested with trypsin prior to analysis by MALDI-TOF.

HT SNAP cells were seeded into 10 cm dishes until 70-90% confluent. Cells were then washed with PBS before treatment with 5 µM BGB in medium for 30 minutes. This was judged as the optimal time from the western blot experiment (Fig. 44) which had shown complete labelling. Cells were then washed again to remove any excess unbound BGB. Cells were treated with varying levels of hydrogen peroxide for varying times. The hydrogen peroxide was added to the cells as a solution in medium.

At the end of the desired treatment time cells were again washed and lysed using a detergent based lysis buffer. The SNAP-B and SNAP-P mixture was isolated from the rest of the lysate by immunoisolation performed under native conditions. SNAP-tag was expressed in mammalian cells with a FLAG-tag. Various

products are available for use with this tag and include the anti-FLAG affinity gel which was utilised in this procedure.

After isolation the SNAP-B and SNAP-P mixture was then denatured using 8M urea, to remove the protein from the agarose beads of the affinity gel and to unfold the protein so the trypsin digest was more effective and subsequently diluted with buffer to a 1M solution in preparation for the trypsin digestion. Trypsin was then incubated with the protein overnight to produce the peptides. At this point samples of the peptides were mixed with 10 mM hydrogen peroxide and stored on the bench for 30 minutes to completely oxidise the probe and make the saturation samples.

The use of SNAP-tag ensured that BGB was maintained in either the ER or the cytosol and washing steps were included in the procedure to ensure that any BGB not bound to SNAP-tag was removed from the cells. Cells were treated with hydrogen peroxide after the washing steps to ensure that the reaction that occurred between the probe and hydrogen peroxide was only experienced by probe which had bound to SNAP-tag and was, therefore, in the ER. Immunoisolating SNAP-tag after lysis and studying the probe bound to the immunoisolated SNAP-tag ensured that only the levels of hydrogen peroxide in the ER were studied.

The peptides were purified and concentrated using a chromatography step. This was required since the presence of urea has a negative effect on the quality of the mass spectrum produced and the peptides had been diluted in order to reduce the urea concentration sufficiently for the trypsin to work, which could also cause a reduction in spectrum quality. There was however an advantage to including the denaturation step as the denatured protein was more susceptible to trypsin digestion. The combination of these steps was found to produce a higher quality spectrum and greater peak intensities. With the analysis method used, the greater the peak intensities, the lower the variability in the results as essentially a better signal to noise ratio was produced. At this point the samples were ready for analysis by MALDI-TOF.

10.2.5 *In Cellulo* Results

Fig. 51 and Fig. 52 show the results of treatment of HT SNAP ER and HT SNAP Cyto with hydrogen peroxide. Cells were seeded into 10 cm dishes and once 70

to 90% confluent, treated with 5 µM BGB in medium for 30 min to allow complete binding and saturation of SNAP-tag with BGB. Cells were then washed to remove any excess probe. Medium or medium containing either 500 µM or 1 mM hydrogen peroxide was then added to the dishes. Cells were washed and lysed at 0 min, 20 min, 40 min and 60 min. All time points were carried out in triplicate. Immunoisolation was used to purify the SNAP-tag from the lysates by the FLAG-tag which the protein was expressed with. Samples were denatured once immunoisolated and trypsin digested. Saturated samples were prepared by treating peptides with 10 mM hydrogen peroxide for 30 min at 37 °C, also in triplicate, prior to the analysis. Peptides were purified and concentrated before analysis by MALDI-TOF with CHCA used as the matrix compound. Results were calculated using Equation 1.
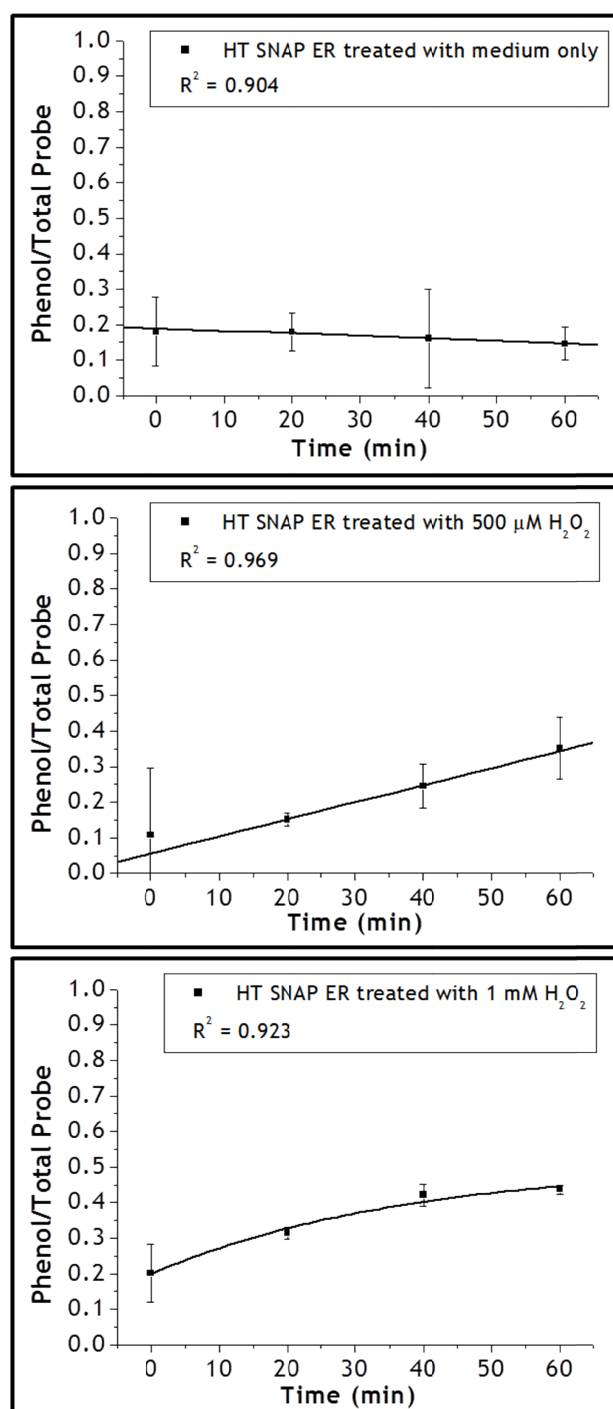
Figure 52– Mammalian cell ER-targeted SNAP-B time courses. HT SNAP ER cells were first treated with 5 µM BGB for 30 min. Excess unbound probe was washed out and cells were treated with medium or medium containing either 500 µM or 1 mM hydrogen peroxide. Cells were lysed at 0 min, 20 min, 40 min and 60 min after the medium and hydrogen peroxide treatments. SNAP-B/ SNAP-P mix was immunoisolated, trypsinised and analysed using MALDI-TOF.

In Fig. 52 the results from the treatment of HT SNAP ER cells are seen. The top graph displays the results measured when no hydrogen peroxide was added to the medium. The graph displays no increase in the ratio of phenol to total probe over the 60 min of the experiment. It was expected that an increase would occur as though there was no exogenous hydrogen peroxide added; there is endogenous hydrogen peroxide in the ER which SNAP-B is capable of reacting with. This result suggests that the analysis method as a whole is not sensitive enough to detect endogenous levels of hydrogen peroxide. Some of the error bars are larger than optimal which also prevents sensitive reaction measurements. The experiments displayed in the graphs middle and bottom of Fig. 51 show the results when cells were treated with 500 µM and 1 mM hydrogen peroxide respectively. Both of these experiments showed increases in the phenol to total probe ratio over the course of 60 min. It is intriguing that the graphs do not go further than around 50% phenol to total probe. The graph showing the results from treatment with 1 mM hydrogen peroxide plateaus by 60 min. There is evidence [44] that hydrogen peroxide cannot move freely around cells and is controlled by aquaporins. It is not possible to know how much of the hydrogen peroxide added to the cells reaches the ER, but it is likely that it is only a fraction. 1 mM hydrogen peroxide is a very high concentration and certainly by 60 min cell death occurred due to its toxicity.

With regards to the expected pseudo first order kinetics, the graph showing the results from cells treated with 1 mM hydrogen peroxide increases at a faster rate than that of the graph showing results from cells treated with 500 µM hydrogen peroxide. It is possible that the pseudo first order kinetics are occurring but are obscured by variability. What can be concluded is that BGB can react with exogenously added hydrogen peroxide in the ER.
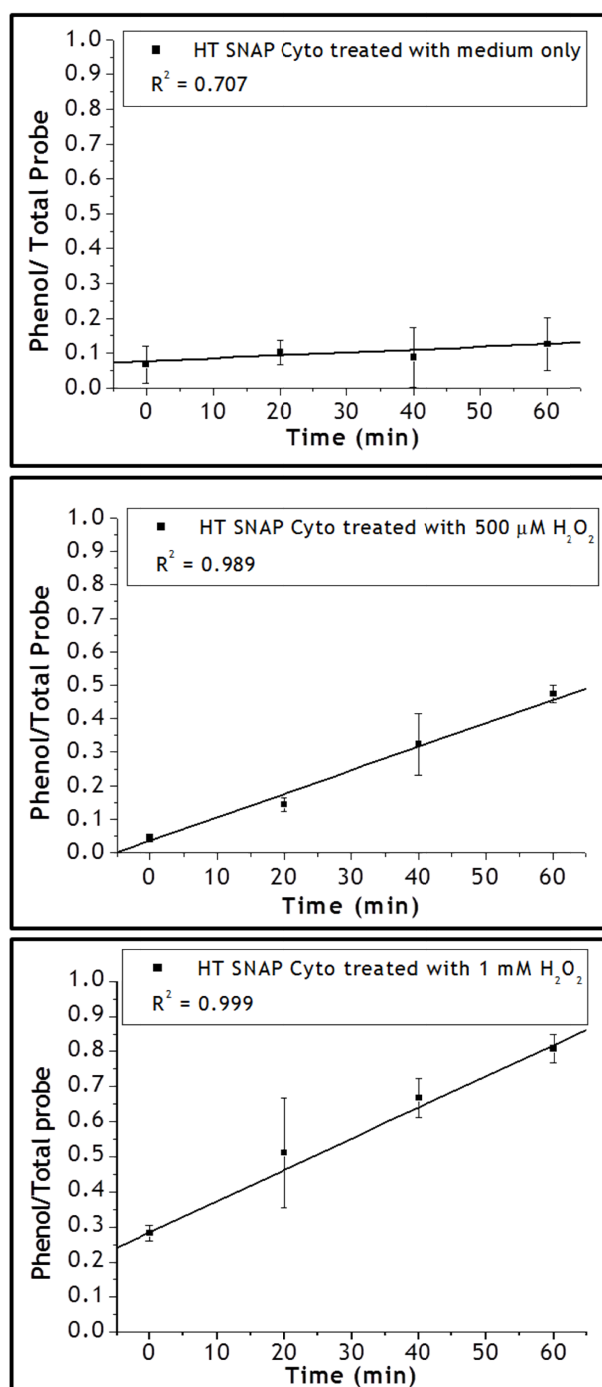
Figure 53 - Mammalian cell cytosol-targeted SNAP-B time courses. HT SNAP Cyto cells were first treated with 5 µM BGB for 30 min. Excess unbound probe was washed out and cells were treated with medium or medium containing either 500 µM or 1 mM hydrogen peroxide. Cells were lysed at 0 min, 20 min, 40 min and 60 min after the medium and hydrogen peroxide treatments. SNAP-B/ SNAP-P mix was immunoisolated, trypsinised and analysed using MALDI-TOF.

In Fig. 53 the equivalent experiments were carried out on HT SNAP Cyto cells as were carried out on HT SNAP ER cells in Fig. 51. As with the HT SNAP ER experiment there was no significant increase over time in the SNAP-P level when the cells were incubated with medium only for 60 min. In the cytosol it is also expected that the probe would come into contact with hydrogen peroxide so again this is likely to be due to the lack of sensitivity of the method. Increases in the level of SNAP-P are seen in both the 500 µM and 1 mM hydrogen peroxide samples. The level of increase is greater than that of the HT SNAP ER samples. This is perhaps due to the fact that more of the hydrogen peroxide reaches the SNAP-B conjugate as it only has to cross the cell membrane rather than both the cell and ER membranes. Again some of the error bars are fairly large, possibly an indication that MALDI-TOF as a quantification technique is not ideal. As with Fig. 51 there is no clear representation of pseudo first order kinetics however it is likely that MALDI-TOF may be the source of the lack of representation rather than anything on a molecular level.

10.2.6 Trapping the Boronic Acid

It was considered that the issues with variability and lack of sensitivity in the results in Figs. 52 and 53 could be at least in part due to the fact that a direct measurement of starting material to product could not be taken as the boronic acid did not fly by MALDI-TOF. It was hypothesised that if this problem could be overcome and all the boronic acid could be trapped in one measurable form then variability in the final data would be reduced.

Boronic acids often come in the form of pinacol esters as it makes them easier to handle, but this also illustrates an important type of reactivity. Boronic acids are capable of forming reversible covalent complexes with a range of compounds including sugars, hydroxamic acids and amino acids, which allow bidentate binding. They have even been exploited as detectors of sugar transport in cells [143].

It was known that the pinacol ester form of SNAP-B flew by MALDI-TOF but that the majority of the probe was not in this form. If, for example, a large excess of pinacol could be added to the sample as it was crystallised on the MALDI plate then perhaps this would trap all the boronic acid as the boronate ester when the water evaporated and crystals formed. In theory this would work, however

MALDI-TOF is a very sensitive process and the addition of large amounts of any compound is likely to have a detrimental effect on the quality of the spectrum. However, there would be a danger that if you lowered the pinacol concentration sufficiently to negate any disadvantages then the concentration would not be high enough to trap all the boronic acid present.

There are a range of different matrix compounds that can be used when performing MALDI-TOF. The most suitable one depends on the analyte being studied and often trial and error is used to find the best one. CHCA is perhaps the best all round choice as it provides good sensitivity for peptides, proteins and glycans, however, there are a wide range of others possibilities.

2,5-Dihydroxybenzoic acid is also known as one of the most efficient matrices and has been shown to be able to act as both the matrix and derivatising agent for boronic acid containing peptides [144]. When the analyte is co-crystallised with the matrix, the matrix is in such a huge excess that as the water evaporates all boronic acids are trapped in an on-plate esterification procedure. It was proposed that this would trap any SNAP-B derived boronic acid (Fig. 54).
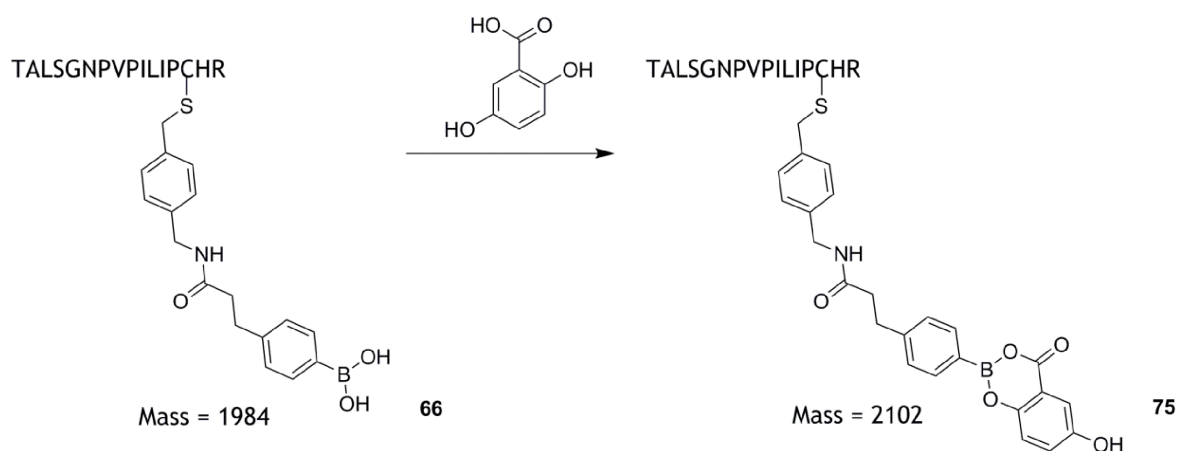
Figure 54 – SNAP-B trapped with DHB. The SNAP-B derived peptide in the boronic acid form 66 has a mass of 1984. Once derivatised with DHB 75 which also acts as the matrix compound, the expected mass is 2102.

Once the SNAP-B derived peptide had been derivatised with DHB the expected mass would be 2102. This is also a sufficient distance from the phenol mass at 1955 that no interference would occur.

Samples of SNAP-B and SNAP-P were first trypsinised and then prepared for MALDI-TOF as normal, except DHB was used instead of CHCA as the matrix compound (Fig.55).
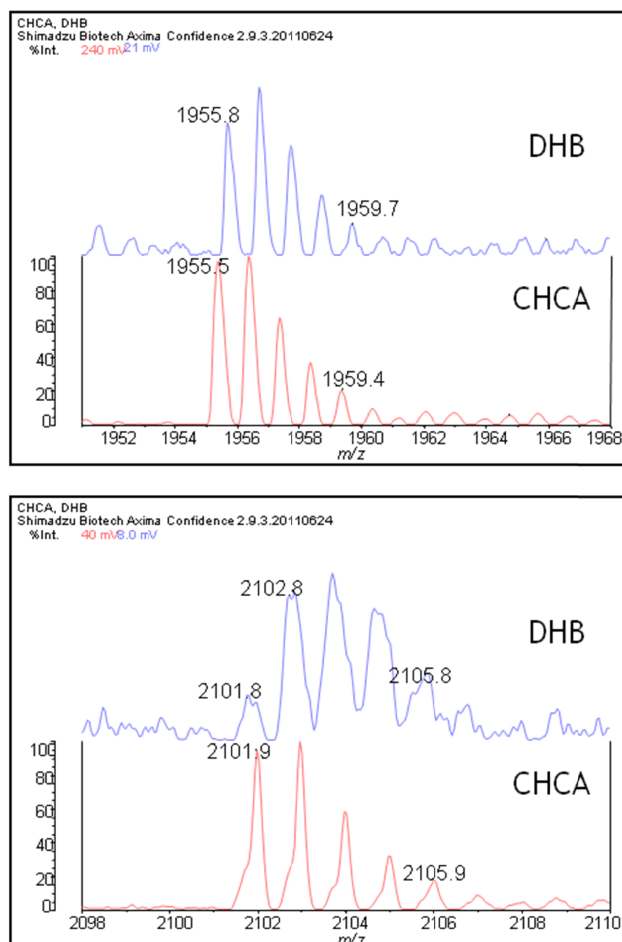
Figure 55 – Comparison of MALDI-TOF spectra with different matrices. The top spectra show the peak representing SNAP-P derived peptide ionized with DHB and CHCA. The bottom spectra show the peak representing SNAP-B ionized with DHB and CHCA.

In Fig. 54 the top spectra show the peptide derived from SNAP-P (mass 1955) ionized with both DHB and CHCA. The peak is strong and shows good signal to noise with both matrices. The bottom spectra show the calculated mass for the SNAP-B derived peptide (mass 2102). There is a peak in the CHCA sample. This is not the BGB containing peptide as there is no DHB there to derivatise it. In the DHB spectrum it can be seen that there are two peaks overlapping at the same mass. One of these does appear to contain boron, as can be seen from the splitting pattern, which suggests that using DHB as the matrix does derivatise the boron and allows it to be detected. The presence of an overlapping peak

134

would prevent this peak being used for quantification, however; as the intensity measured would not be the true intensity of that peak. An *in silico* digest which accounted for one missed cleavage by trypsin did calculate for a peptide with mass 2102. Previous work had optimized the trypsin digest conditions so the use of other digestion enzymes was investigated. From further *in silico* work it was reasoned that the combination of trypsin and AspN world prevent this peptide from being produced. AspN is an endoproteinase that hydrolyses peptide bonds N-terminal to aspartic acid residues (Fig. 56).
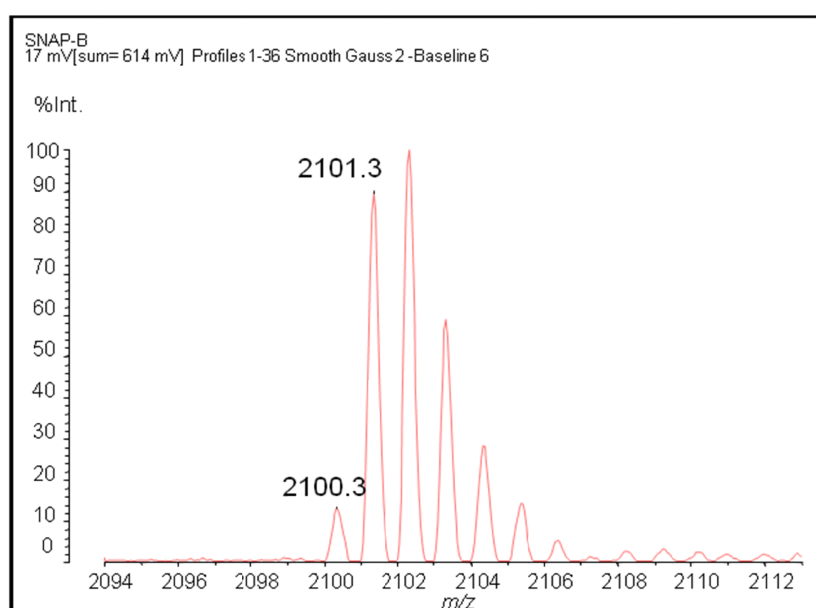
Figure 56 - Direct detection of SNAP-B. When SNAP-B was digested using a combination of trypsin and Asp-N the only peak that appeared at the mass of 2101 was that representing the active site peptide containing the boronic acid derivatised by DHB.

The combination of enzymes was found to prevent the overlapping peptide and so meant the intensity of both the SNAP-P peak at 1955 and the SNAP-B peak at 2102 could be used to measure the reaction of the probe with hydrogen peroxide.

With the SNAP-B peptide detectable *in vitro* experiments were carried out to assess whether the reactivity of the probe could be measured (Fig. 57).
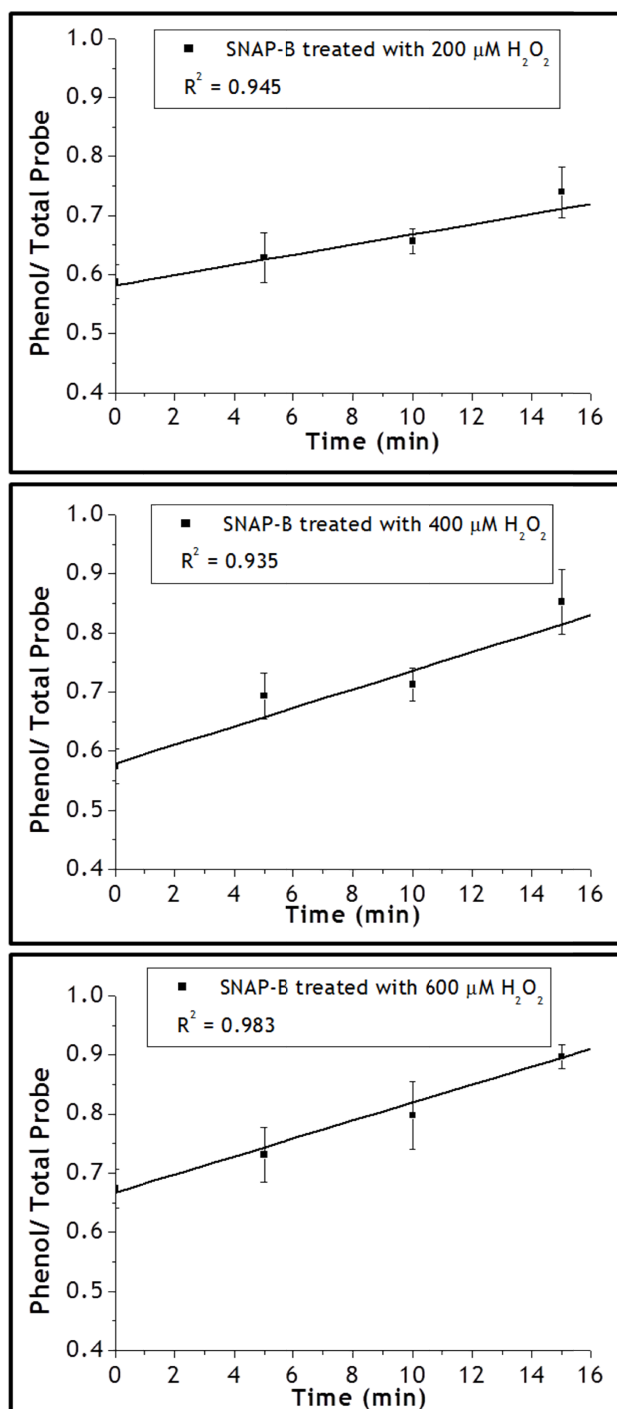
Figure 57 - SNAP-B time courses analysed with a DHB matrix.
Recombinant SNAP-B was mixed with 200 µM, 400 µM and 600 µM
hydrogen peroxide for different times up to 16 min in 100 mM Tris-
HCl. Reactions were stopped by the addition of -20°C acetone.
Samples were analysed by MALDI-TOF using DHB as the matrix. The
y axes were calculated using the peak at 1955 representing the
phenol and the sum of the peaks at 1955 and 2102 representing
the unreacted probe as total probe.

The graphs produced show the reaction of SNAP-B with 200 μM, 400 μM and 600 μM hydrogen peroxide over 15 min. The results are comparable to the *in vitro* results produced using the previous method of including saturated samples and Equation 1, however, the background is noticeably higher. This is due to the fact that the peak at 2102 representing SNAP-B did not fly as well as the SNAP-P peak at 1955. This meant that the peak at 2102 was always far lower in intensity than 1955 and so when these values were used it lead to a high value for the zero timepoint and prevented the results from displaying pseudo first order kinetics.

It was hoped that the real impact would be seen from experiments carried out in the HT SNAP cells however when these were attempted the peak at 2102 was either not seen at all or barely above baseline. This is likely to be due to the combination of the fact that the peak at 2102, representing SNAP-B, did not fly well and a concentration effect as the concentration of peptides produced from cellular SNAP-tag is far lower than that produced from an *in vitro* digestion of purified material. This unfortunately prevented further use of this method.

10.3 Conclusions

10.3.1 Syntheses and Conjugations

The syntheses of both BGB and BGP were by and large successful. The lower yielding reactions were due to the difficulty of working with the fairly insoluble O^6-(4-aminomethyl)benzylguanine, the insolubility of which did not improve once conjugated to the boronate and phenol moieties. Purifications were attempted using column chromatography however higher yields may be achieved using an HPLC system. Even with the low yields resulting from the purification of the final compounds, enough material was produced for biological testing, the aim of the syntheses.

Initial testing was successful with the probes conjugating efficiently to both purified SNAP-tag and protein in HT SNAP cells. Comprehensive labelling was evident from the western blot showing SNAP-tag running slower through the gel after labelling (Fig. 44).

10.3.2 *In Vitro* Experiments

The initial MALDI-TOF experiments showed that the peptide derived from SNAP-P could be detected and this was confirmed to be the correct peptide by a number of different experiments. Unfortunately the peptide derived from SNAP-B could not be detected but a solution was found with the use of the internal standard and inclusion of hydrogen peroxide saturated samples in every experiment. The *in vitro* experiments which showed the reaction of SNAP-B over concentration and time courses showed that this method was capable of demonstrating the reactivity of SNAP-B down to low micromolar concentrations of hydrogen peroxide. It is assumed that the lack of pseudo first order kinetics displayed in the results is due to variability caused by the use of MALDI-TOF as an analysis technique.

10.3.3 *In Cellulo* Experiments

The experiments then carried out in cells did show reactivity towards exogenous hydrogen peroxide but there were a number of issues encountered. The error bars produced were in some cases large and this prevented lower concentrations of hydrogen peroxide, which would be more akin to those produced

endogenously, from being studied. There is evidence that hydrogen peroxide cannot diffuse freely though cells and so when it is added as a solution in the medium there is no way of determining how much reaches the inner compartments, particularly the ER. The method developed for use with BGB was not particularly simple and so with the number of steps involved, the chance of variability was increased. The variability and the lack of pseudo first order kinetics observed were likely to be due to the use of MALDI-TOF. Though as a technique it is capable of detecting analytes in the femtomolar range, for quantification the concentration must be far higher.

When doing the analysis of SNAP-tag derived from cells the concentration of SNAP-tag depends on a number of things. The expression of the protein inside the cells must be high. As discussed in Chapter I, it was found that the HT SNAP cell line had an issue with losing expression, often at low passage number. This meant that on a number of occasions the protein levels were less than optimal and so the final peptide concentration that was analysed would also be less than optimal. The expression level of the HT SNAP ER cell line was also far lower than that of the HT SNAP Cyto cell line (Results I, Fig. 24). The peptide intensity is also dependent on both the immunoisolation procedure and the trypsin digest.

10.3.4 Changing the Matrix

The use of DHB as the matrix compound, in theory, would have allowed the direct comparison of starting material to product. It was hoped that this would provide greater sensitivity. The *in vitro* results were comparable to those calculated using CHCA and Equation 1; however there was no major improvement. When DHB was used with material produced from the HT SNAP cell lines it became evident that the peak representing SNAP-B was not differentiated enough from the baseline to provide useful information.

It has been shown that BGB can be localised to the desired cell compartment and reacts with hydrogen peroxide in the desired manner, but the analysis of the probe was the limiting factor in the overall success of the method. It is potentially possible to use MALDI-TOF for quantification, but many factors can influence its ability to provide the sensitivity required for measurements of endogenous factors within cells. The aim was to develop an effective and user-friendly method and though the method has shown some success, in particular

with the short and effective synthesis which allowed the biological experiments to be tackled very quickly, the process of using the probe in cells was not wholly user-friendly. With BG-Fura-B the synthesis had been the issue and with BGB this was overcome, but the difficulties with the method had been troublesome. This was a consideration which was taken into account for the next development in the project.

11.0 Results III

11.1 Introduction

The main lesson learned from the synthesis of BG-Fura-B was that the focus should be on the biological utility of the probe rather than the complexity of synthesis. This was applied in the synthesis and design of BGB. BGB was fairly successful as a design and this allowed method development in cells to occur. The method developed did show the reaction of BGB in cells, but not at the sensitivity required and it was time consuming to quantify SNAP-B and SNAP-P by mass spectrometry. This led to a reconsideration of the possible analysis techniques. The chemistry of BGB was effective and so the aim was still to incorporate this into the next phase of the project.

For the greatest chance of success it was decided that a double pronged approach would be used. One of the downfalls of the analysis method of BGB experiments was that it required many steps and each experiment required these steps done over a period of three days. It was reasoned that if this process could be simplified then the method would be more effective.

SNAP-tag targeting, though effective, did affect the process as there were issues with loss of expression in cells. The use of SNAP-tag also required immunoisolation and trypsin digestion, both of which added length to the time required for an experiment to be carried out. An alternative method of targeting a synthetic peptide to a cellular locale would be to use a targeting peptide. Peptides have been used before to target to the ER [145] and this technology was chosen to be developed for use with a boronate based probe.

A previous example of peptide targeting to the ER used the peptide Ac-NYTC [108]. This peptide is not a targeting sequence to the ER as such, but it contains a site that is glycosylated by enzymes in the ER, and once glycosylated the peptide is trapped within the ER lumen. Originally, the peptide was used as a means of measuring the redox state in the ER by measurement of the ratio of reduced glutathione to glutathione disulfide. The peptide diffused in to the ER then underwent *N*-linked glycosylation at the Asn-Y-Thr sequence (Fig. 58). This prevented the peptide from diffusing back out of the ER since the hydrophilic nature of the oligosaccharide prevented it from crossing the ER membrane [146]

and so a local concentration built up in the organelle. The terminal cysteine underwent SH-SS exchange reactions. The peptides were purified from the cell lysates by isolation with immobilized Concanavalin A (ConA), a carbohydrate binding protein, which bound to the oligosaccharide of the peptide produced from *N*-linked glycosylation [147]. This ensured that only peptide that had been in the ER was isolated and analysed. The peptides were released from the immobilized ConA by the use of Endoglycosidase H (EndoH), an enzyme which cleaves asparagine linked oligosaccharides [148].
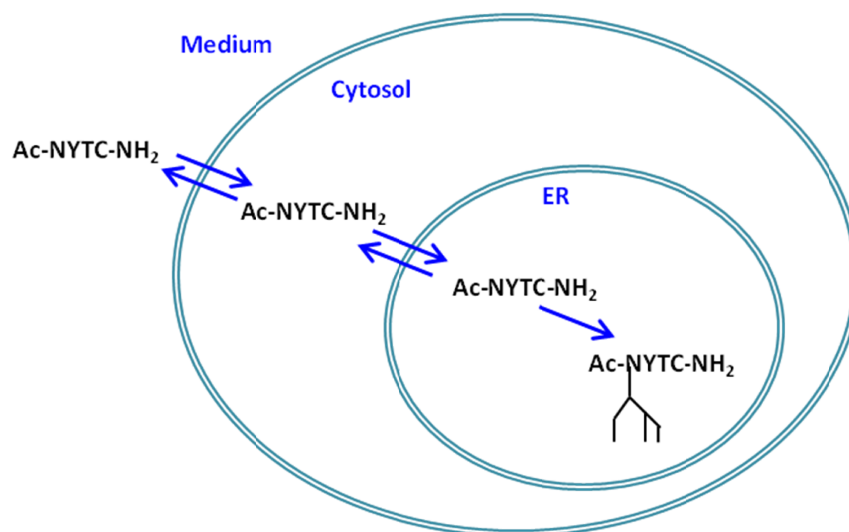
Figure 58 – The peptide NTYC diffuses from the medium into the cytosol and the ER. In the ER it becomes glycosylated and the hydrophilic nature of the oligosaccharide prevents it from diffusing back out, leading to a local build-up in concentration of the peptide.

The aim here was to incorporate this glycosylation sequence into the peptide as it would provide a mechanism of keeping the peptide in the ER and act both as a handle for purification from the cell lysate and an indication that the peptide studied was only that which had been in the ER. One of the main advantages of the peptide system is that any cell line could be used, which gave the possibility of comparison of hydrogen peroxide in different types of cells. It was decided that the peptide sequence would be extended to incorporate the KDEL sequence. The KDEL sequence is the ER retention sequence. The KDEL sequence is recognised by the KDEL receptor which is a seven transmembrane domain protein which acts to retrotransport proteins from the Golgi to the ER by

recognition of the four amino acid sequence [149]. It was felt that this would provide an extra measure of keeping the peptide in the ER. The glycosylated peptide may not be able to diffuse back through the ER membrane, but that does not prevent it from being packaged into a transport vesicle and traversing the secretory pathway.

Hwang et al. utilised a cysteine residue to react with glutathione and glutathione disulfide in the ER. This cysteine was not necessary for the use of the peptide as a method of boronate probe targeting so it was decided that it could be used as a reactive group to conjugate the boronate to the peptide. Various chemical groups are reactive to cysteine residues including maleimides and alkyl halides. The design of the probe therefore incorporated a benzylic bromide in the arylboronate, required for hydrogen peroxide reactivity. The benzylic bromide was placed in the *meta* position to the boronate (Fig. 59). The positioning avoids any potential fragmentation when the electron-withdrawing boronate is converted into an electron-donating hydroxyl group by hydrogen peroxide.
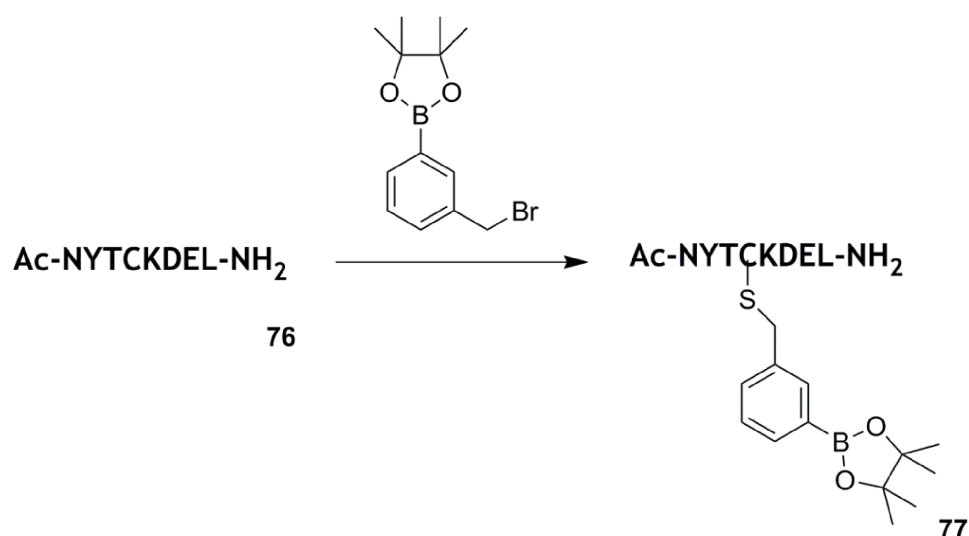
Figure 59 – The formation and design of Pep-B. The peptide 76 which incorporates the site for N-linked glycosylation, ER retention sequence and probe binding site reacts with the boronate via the maleimide moiety to form Pep-B 77.

Once formed, the theory was that Pep-B would be added to cells where it would diffuse into the ER. There it would become glycosylated and the combination of the hydrophilic nature of the oligosaccharide preventing diffusion back across

143

the membrane and the KDEL receptor retrieving any that reached the secretory pathway would cause the probe to build up in the ER. When Pep-B encountered any hydrogen peroxide the boronate would be converted into the corresponding phenol, Pep-P (Fig. 60).
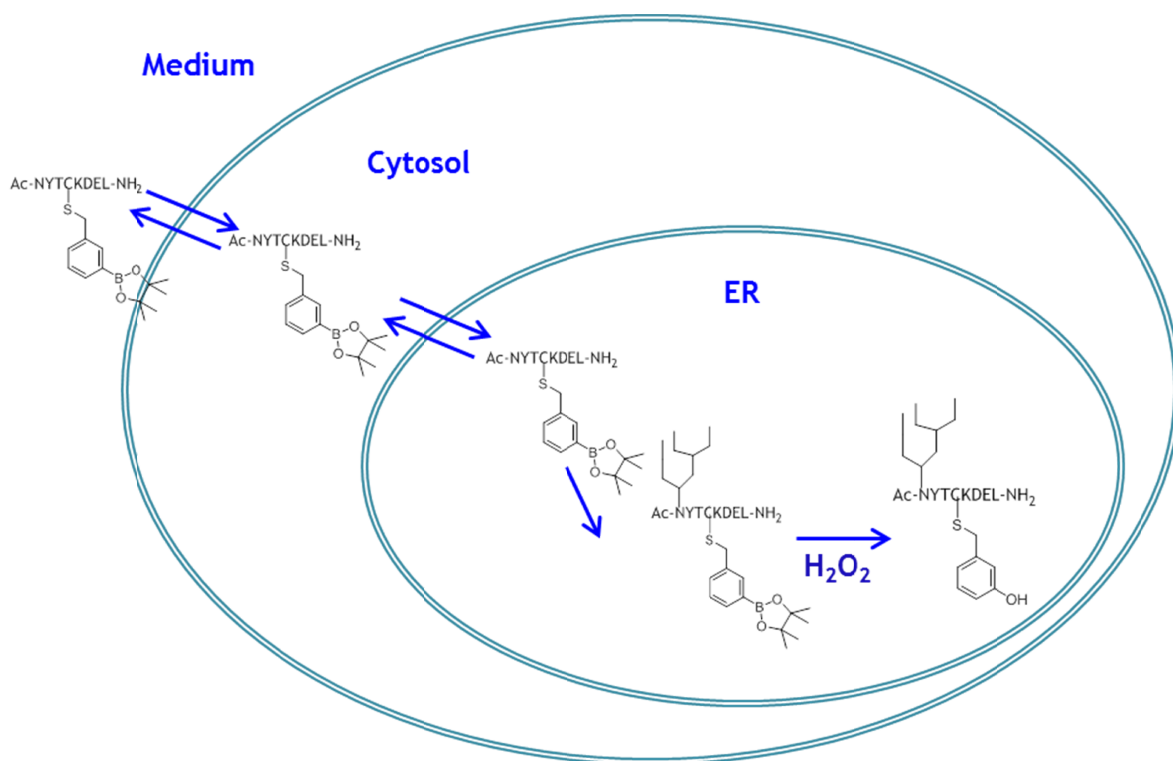
Figure 60 – Pep-B is added to the medium and from there diffuses through the cytosol into the ER of a mammalian cell. Once in the ER, it becomes glycosylated and cannot diffuse out. The KDEL sequence causes retention of any Pep-B which traverses the secretory pathway. When hydrogen peroxide is encountered Pep-B is converted to Pep-P, the phenolic equivalent.

After the experiment the planned method was to purify Pep-B from the cell lysate using immobilized ConA and removal from ConA by EndoH. Analysis was to be performed using MALDI-TOF. The matrix chosen to be used was DHB so that a direct comparison of Pep-B to Pep-P could be carried out (see 10.2.6).

The second approach we decided to take involved using a different method of analysis. As discussed the chemistry of both the synthesis and workings of BGB with regard to SNAP-tag and hydrogen peroxide worked as desired but analysis by MALDI-TOF did present some problems and was not the most efficient and rapid method. The aim of the project was essentially technology development

and so it was hoped that the method would go on to be used by others in a wider setting. It was considered that not all labs have access to MALDI-TOF or the training to use it but all labs have access to and use western blotting successfully. It was reasoned that if a Western blotting method could be used for experiments involving the probe BGB, then the issues stemming from the use of MALDI-TOF would be resolved and the method would have the ability to reach a much wider audience.

In order to use Western blotting an antibody would be required to recognise either SNAP-B or SNAP-P. An antibody which recognised either SNAP-B or SNAP-P would also be useable in ELISA and in-cell Western systems as well, providing further options. It was decided that an antibody to recognise SNAP-P, the phenol product, would be a more attractive choice as it was known that SNAP-B was not always fully in the boronic acid form.

In order to raise an antibody against a small molecule a hapten is required. This is a compound which is non-immunogenic itself, but must be attached to a carrier protein and once in this adduct form can elicit an immune response [150]. Most antibodies produced for bioscience purposes are raised against proteins but there are previous examples of antibodies specific for protein modifications by small molecules. There are, for example, commercially available antibodies to recognise phosphorylation of proteins. The first phosphor-antibody was produced in 1981 by the conjugation of *p*-azobenzyl phosphonate to keyhole limpet hemocyanin (KLH) [151]. Rabbits were immunised with the small molecule-KLH adduct and an immune response elicited. The antibody produced was capable of recognising proteins containing phosphotyrosine.

The design of the hapten was of utmost importance as antibody production is both slow and expensive as months and repeated immunisation are required for the animal to produce the antibodies. The animals are bled at various timepoints throughout the process to check the sera for an immune response and are terminated and bled at the end of the process.

The hapten must be conjugated to a carrier protein; however, it was not possible to use SNAP-P as the hapten-protein conjugate as antibodies would likely be produced that recognised SNAP-tag rather than the chemical

modification. It was, therefore, decided that the hapten analogue of BGP would be conjugated to KLH. The hapten could not be BGP itself as BGP contained the derivatised O^6-(4-aminomethyl)benzylguanine which reacted with the active site of SNAP-tag and which would have no reactivity towards KLH. It was decided that the same method of conjugation would be used as for Pep-B (Fig. 60) with a benzylic bromide group providing cysteine reactivity. The design of the hapten is shown in Fig. 61.
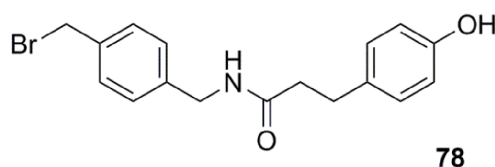
Figure 61 – The design of the hapten 78 used to create the anti-SNAP-P antibody. The hapten contains a benzylic bromide for cysteine reactivity, with the rest of the molecule being the same as the modification to SNAP-tag produced when BGP 68 reacts to form SNAP-P 63.

The design of the hapten incorporated the benzylic bromide to give reactivity towards cysteine residues. KLH is an extremely large multi subunit protein with a size of approximately 390 KDa. It therefore has a large number of available cysteine residues and many haptens will bind to the one protein structure, increasing the immune response. It is the most widely used protein for antibody generation. Since KLH comes from a gastropod, it is phylogenetically distinct enough that when used in mammalian systems the chances of producing non-specific antibodies is reduced. It can be notoriously difficult to work with, however, as the large size means aggregation and precipitation is fairly common [152]. Once conjugated to KLH the hapten modification exactly mirrors the modification of BGP on SNAP-tag, therefore, giving the best chance of good antibody recognition (Fig. 62).
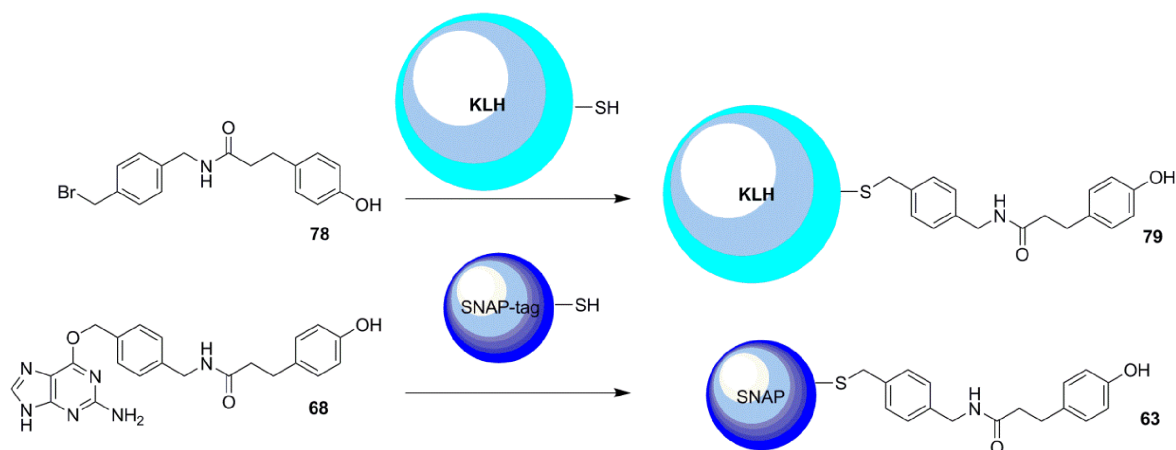
Figure 62 – Hapten structure similarity to SNAP-P. The hapten 78 binds to KLH via a nucleophilic substitution of the thiol onto the hapten structure with the loss of HBr. The conjugate 79 mirrors the modification of SNAP-tag by BGP, SNAP-P 63.

Once the hapten KLH conjugate is formed and binding is confirmed, the procedure involves injection into two rabbits for the production of a polyclonal antibody for a 70 day protocol. Once crude sera are collected they can be tested for reactivity by Western blot or ELISA.

11.2 Results

11.2.1 Syntheses of Pep-B and Pep-P

Of the two alternative methods discussed, the first to be investigated was the peptide probe, Pep-B. The first step was the synthesis of benzylic bromides **80** and **81** which were conjugated to the peptide Ac-NYTCKDEL to form the boronate probe Pep-B and the phenol product Pep-P (Fig. 63).
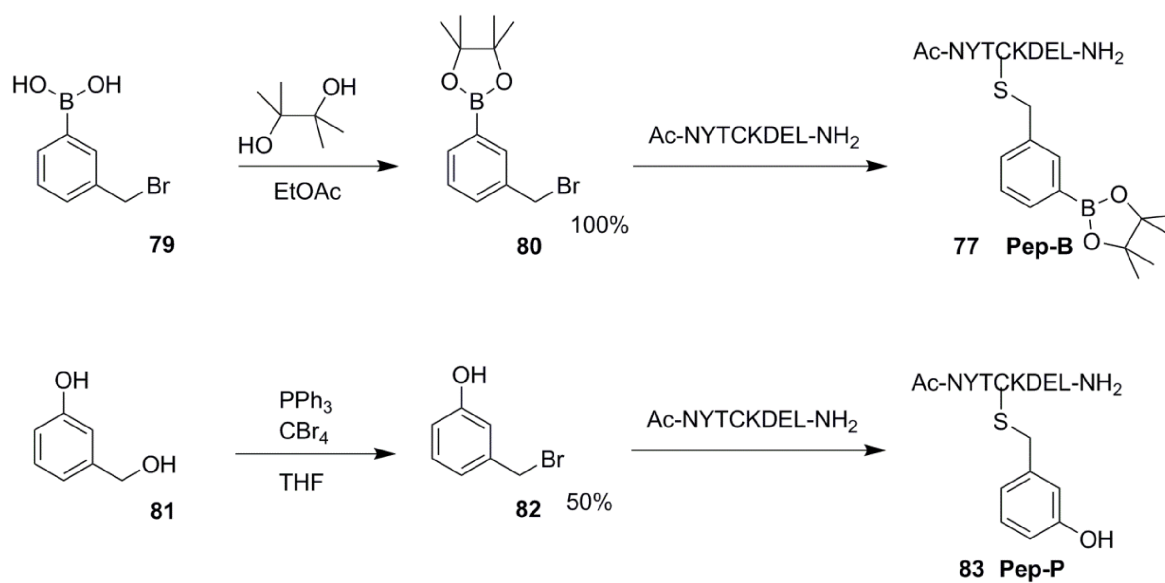
Figure 63 – The syntheses of Pep-B 77 and Pep-P 82. Pep-B was synthesised as the boronate ester as with BGB and both probes were conjugated to the cysteine residue of the peptide via a nucleophilic substitution reaction.

The syntheses of Pep-B and Pep-P were both simple and effective. For Pep-B the first step was to protect 3-(bromobenzyl)boronic acid as the boronate ester boronate ester **80**, which was achieved in quantitative yield. The benzylic bromide **80** was then stirred in Tris-HCl pH 7.5 buffer with the peptide to form Pep-B **77**. With regards to Pep-P the first reaction was to brominate 3-(hydroxymethyl)phenol via an Appel reaction, which yielded benzyl bromide **81** in a moderate yield [153]. The coupling to the peptide to form Pep-P **82** was performed in the same manner as for Pep-B.

11.2.2 Purification and Detection of Pep-B and Pep-P

After the couplings had taken place the reaction mixtures were prepared for HPLC to separate unreacted benzylic bromide **80** or **81** and peptide from the

final products, Pep-B and Pep-P. The chromatograms of the peptide alone, Pep-B and Pep-P are shown in Fig. 63. The different peaks in the chromatograms were assessed by MALDI-TOF to determine which ones contained the probes. DHB was used as the matrix to trap the boronic acid as the aqueous conditions of the peptide conjugation and purification meant that the pinacol ester was likely to have been removed (Fig. 65).

Figure 64 - The HPLC traces produced from reverse phase chromatography of Ac-NYTCKDEL, Pep-P and Pep-B. The peak contents were determined by MALDI-TOF (Fig. 65). The top spectrum is that of the unreacted peptide. The highlighted peak is the peptide. The middle spectrum shows that of the crude mixture produced by reaction of Ac-NYTCKDEL with phenol 81. The peak at around 35 min is that of the unreacted peptide. The highlighted peak at 36 min is the desired product. The bottom spectrum shows the crude mixture produced by reaction of Ac-NYTCKDEL with boronate 80. The peak at around 24 min is the unreacted peptide. The two peaks highlighted at around 25 and 29 min are the desired product in the boronic acid and boronate ester forms.

Figure 65 – MALDI-TOF peaks showing peptide alone, Pep-P and Pep-B modified with DHB. The analyses were of the highlighted peaks in Fig. 64 and confirmed the conjugations had been successful and that Pep-P and Pep-B both were detectable by mass spectrometry.

11.2.3 *In Vitro* Reactivity

After confirming the conjugation reactions to form Pep-B and Pep-P had been successful and that the probe and its product could be detected by MALDI-TOF the reactivity of the probe was assessed *in vitro*. Pep-B was mixed with hydrogen peroxide and then analysed by MALDI-TOF (Fig. 66). The increase in the ratio of Pep-P to total probe confirmed that the boronic acid of Pep-B was capable of reacting with hydrogen peroxide and formed Pep-P after reaction. The small error bars were an indication of good reproducibility of the method.
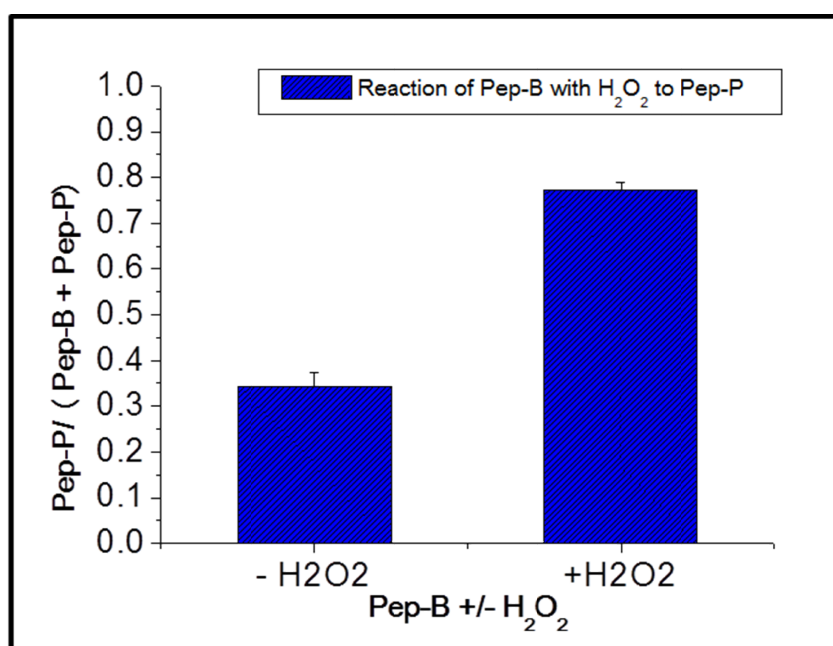
Figure 66 – The effect of hydrogen peroxide on Pep-B. The solution was analysed by MALDI-TOF with DHB matrix before and after reaction to show that Pep-P was formed from the reaction of Pep-B with hydrogen peroxide.

Different ratios of Pep-B and Pep-P were mixed and analysed by MALDI-TOF in order to confirm that the method of analysis was accurate and the same ratios that had been mixed could then be calculated back from the data gathered in the spectra (Fig. 67). This confirmed that MALDI-TOF was capable of providing an accurate analysis of the reaction of Pep-B to Pep-P. The ratios fairly accurately represented the mixtures created and the small error bars showed good reproducibility over the triplicate samples. It should be noted that the line

does not go through the origin of the graph as in the Pep-B stock there will always be some of the oxidised form as well.
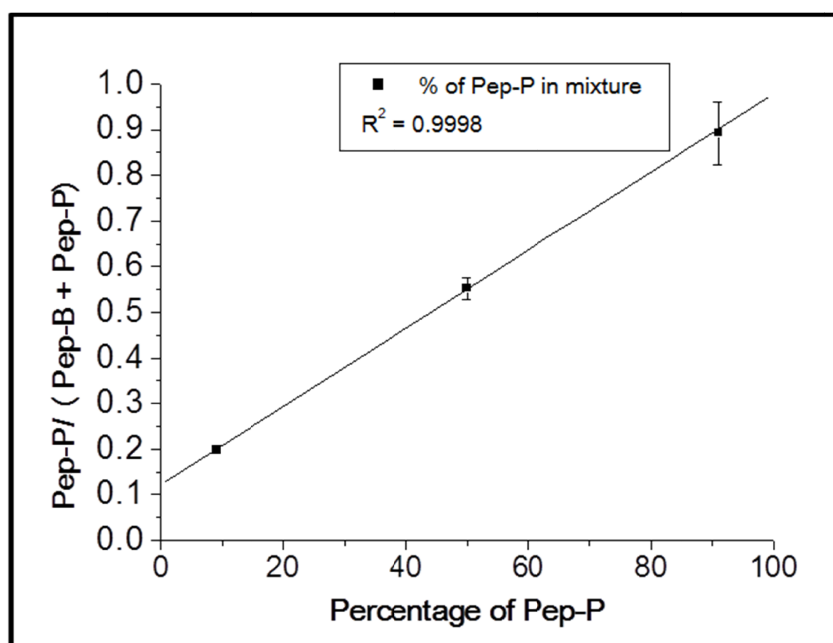
Figure 67 – Analysis of Pep-B and Pep-P. Different ratios of Pep-B and Pep-P were mixed then those solutions analysed by MALDI-TOF with DHB matrix to determine whether the analysis would give an accurate response. The linear response showed that it was possible to analyse Pep-B and Pep-P by mass spectrometry.

11.2.4 *In Cellulo* Detection

After confirming *in vitro* that Pep-B was reactive towards hydrogen peroxide and that this reaction could be studied by MALDI-TOF mass spectrometry, the next step was to add the probe to cells to assess whether it was possible to recover the probe, detect whether glycosylation had occurred and if the probe was reacting with hydrogen peroxide inside cells.

Pep-P (final concentration 5 μM in medium) was added to HT1080 cells. A control dish was also prepared in which the cells were treated with medium only. The cells were incubated with medium with or without Pep-P for 1 hour to allow for time for the peptide to reach the ER and become glycosylated. The aim of this experiment was to confirm that glycosylation occurred and the peptide could be detected. After the incubation cells were lysed and ConA agarose used to isolate any glycopeptides. EndoH was then used to elute the peptides and the eluate

was analysed by MALDI-TOF. No peaks were seen which did not appear in the control. It was hypothesised that this could have been due to a number of different reasons. Pep-P may not have been capable of crossing the cell membrane or ER membrane, glycosylation may not have occurred which would have prevented isolation from the lysate by ConA or if Pep-P was reaching the ER and becoming glycosylated then perhaps the concentration doing so was so small that after the isolation procedure it was not detectable by mass spectrometric methods.

11.2.5 Control Experiment

In order to determine what the exact issue with the system was a number of steps were taken. The peptide Ac-NYTC was ordered from an external company as this peptide had been shown to be capable of reaching the ER and of becoming glycosylated from the work of Hwang et al [108]. The idea was that this would be used as a control to test out the theories for the lack of detection of Pep-P.

An experiment was devised that would incorporate Ac-NYTC as a control and that would show if the peptide Ac-NYTCKDEL was capable of crossing the ER membrane. An *in vitro* translation system was used which consisted of dog pancreas microsomes, rabbit reticulocyte lysate and an appropriate mRNA and in which protein translation, co-translational insertion and glycosylation occurred [154]. It has been shown that upon the addition of peptides containing the glyosylation site, Asn-X-Ser/Thr, the glycosylation of the translated protein is inhibited as the peptide is glycosylated instead [155].

It was decided that an *in vitro* translation system which incorporated ^{35}S methionine amongst the amino acids would be used as the addition of Ac-NYTC or Ac-NYTCKDEL should prevent glycosylation of the translated protein if the peptides are capable of crossing the ER membrane of the microsomes. The use of ^{35}S methionine in the amino acid mixture meant the experiment could be analysed by phosphorimaging if the translated protein was run on an SDS-PAGE gel. Glycosylation of a protein produces a noticeable shift in mobility. The mRNA chosen coded for influenza virus hemagglutinin (HA).

Rabbit reticulocyte lysate, dog pancreas microsomes, mRNA encoding for HA and amino acids including ^{35}S methionine were mixed with Ac-NYTC, Ac-NYTCKDEL or water as a control and the translation incubated for 1 hour. Samples were also prepared to include a translation without microsomes and one in which the translated and glycosylated protein was digested with EndoH to remove any oligosaccharides. Samples were run on an SDS-PAGE gel to assess levels of glycosylation (Fig. 68).
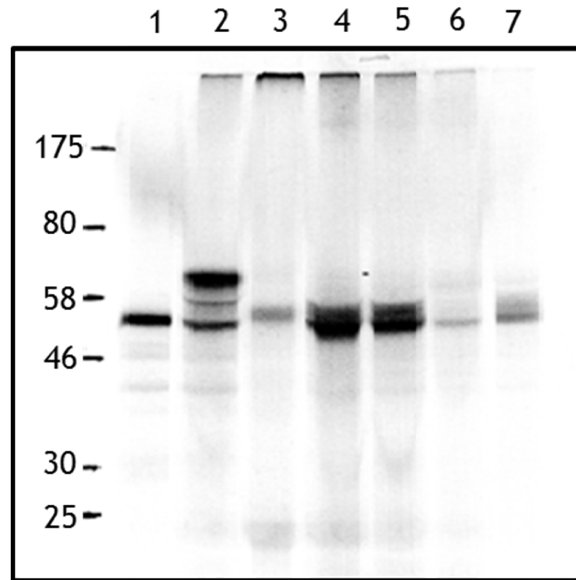
Figure 68 – *In vitro* translation. Lane 1 did not contain any microsomes or peptides. The HA has been translated but not translocated. Lane 2 contained microsomes but no peptides. The lower band is some remaining untranslocated HA. The upper band is translocated and glycosylated. Lane 3 was as lane 2 but the material was treated with EndoH which removed any oligosaccharides and so the band runs lower. Lane 4 was treated with 1 mM Ac-NYTC. There is no glycosylation band. Lane 5 was treated with 0.5 mM Ac-NYTC. Again no glycosylation band is visible. In lanes 4 and 5 there are two bands. The lower band is material which has been translated and translocated with signal peptide cleavage occurring which causes the protein to migrate faster through the gel. The upper band has been translated but not translocated, as in lane 1, meaning the signal peptide is still attached so the protein migrates slightly slower through the gel. In lane 6 1 mM Ac-NYTCKDEL was added to the translation. There is

one band which is fairly weak but at the level of the signal peptide cleaved material. Again no glycosylation has occurred. In lane 7 the translation was treated with 0.5 mM Ac-NYTCKDEL. There is a stronger band at the level of the signal peptide cleaved material and a weaker band above as for the samples treated with AC-NYTC.

The *in vitro* translation suggested that Ac-NYTCKDEL was in fact capable of crossing the ER membrane. The lack of glycosylated HA appearing in the gel suggests this. The control Ac-NYTC which has previously been shown to be capable of reaching the ER of cells and becoming glycosylated showed the same bands in the gel as for the translations treated with Ac-NYTCKDEL. The experiment does not prove that AC-NYTCKDEL was capable of crossing the cell membrane and it was *in vitro* rather than in cells but it was a positive result in suggesting that Ac-NYTCKDEL was capable of behaving as hypothesized.

11.2.6 Treatment of Cells with High Concentration of Peptide

The *in vitro* translation suggested that Ac-NYTCKDEL would be capable of crossing the ER membrane and of being glycosylated. One of the other possible reasons for lack of success when cells were treated with Pep-P was that the final concentration of peptide being analysed by MALDI-TOF was too low for detection. It was decided that cells would be treated with a higher concentration of peptide and that the process of recovering the peptide would be simplified in order to increase the chance of detection. HT1080 cells were treated with 1 mM Ac-NYTCKDEL for 1 hour before cells were washed and a cold solution of 10% trichloroacetic acid (TCA) added to cells. The acid acted to precipitate all proteins but left the peptides in solution. The solutions were centrifuged to remove all precipitated protein and any peptides in the supernatants concentrated and purified by the use of C18 ZipTips. Cells were treated with either Ac-NYTC or Ac-NYTCKDEL. Control samples which were not treated were also included. By not including the ConA sepharose isolation and EndoH digest to remove oligosaccharides, any evidence of glycosylation occurring was visible in the analysis (Fig. 69).
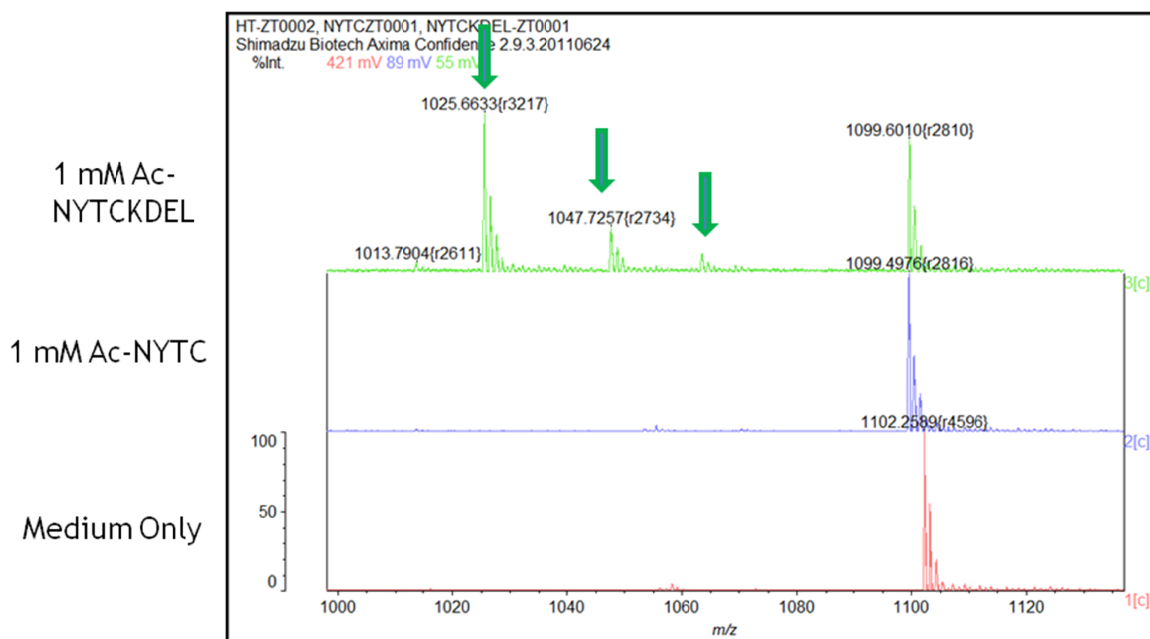
Figure 69 – MALDI-TOF analysis of HT1080 lysates. The lysates were from cells which had been treated with 1 mM Ac-NYTCKDEL, 1 mM Ac-NYTC or medium only for the control. The cells treated with 1 mM Ac-NYTCKDEL displayed a peak at 1026 which corresponded to the mass of the peptide. Two further peaks appeared in the spectrum which were not in the control and corresponded to Ac-NYTCKDEL plus sodium and potassium respectively. The cells treated with 1 mM Ac-NYTC displayed no peaks that were not in the control.

The MALDI-TOF analysis of treatment of cells with Ac-NYTCKDEL confirmed that the peptide was capable of getting into cells. However it was not possible to determine whether the peptide was within the cytosol or the ER as no evidence of glycosylation was observed. This was at odds with the *in vitro* translation which suggested that Ac-NYTCKDEL was in fact capable of crossing the ER membrane and of becoming glycosylated. It is possible that that amount of peptide being glycosylated is too small for the analysis method to detect. The analysis of cells treated with Ac-NYTC detected no peaks that were not present in the control. This is also at odds with both the previous literature [108] and the *in vitro* translation which suggest that this peptide is capable of reaching the ER and of glycosylation. Hwang et al. found that only 1.5% of Ac-NYTC added to cells was recovered and of this only 5% bound to ConA via the oligosaccharide modification. Using these figures it can be calculated that approximately 60 nM

of Ac-NYTC, from a 1 mM concentration in the 4 mL of medium used, entered the cells and 3 nM would have been glycosylated. Considering this and the fact that any peptides would have been further diluted by the addition of 10% TCA, it may have meant that the final amount of peptide deposited on the MALDI-TOF plate for analysis may not have been enough for detection.

The preliminary experiments with Pep-B showed the reactivity of the probe was reliable but once *in cellulo* the practicality of such a system was not so efficient. This further propagated the idea for a different method of analysis.

11.2.7 Synthesis of Hapten for Anti-SNAP-P

The design of the hapten incorporated a benzylic bromide for reactivity towards cysteine residues on KLH, the carrier protein chosen to be used in the antibody production, and the rest of the molecule which mirrored the structure of BGP once conjugated to SNAP-tag (Fig. 70).
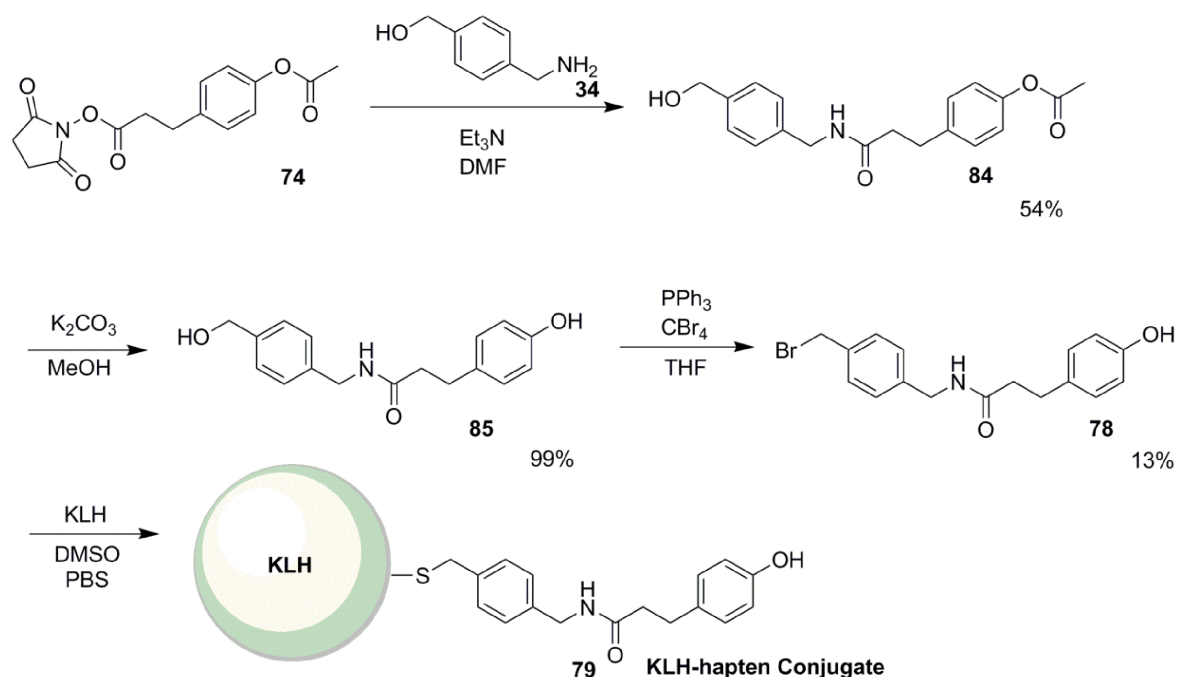
Figure 70 – The synthesis of the hapten. The hapten was conjugated to KLH, the carrier protein, to induce an antibody response in rabbits for the generation of a polyclonal anti-SNAP-P antibody. The key intermediate 78 included a benzylic bromide for reactivity towards cysteine residues on KLH and the *para*-xylyl group linked through a nitrogen atom to 4-(4-hydroxyphenylpropanamide), which mirrors the structure of BGP after conjugation to SNAP-tag.

158

The synthesis of the hapten began with the coupling of the previously synthesised succinimidyl ester **74** with the also previously synthesised amine **34** to form amide **84**. This reaction proceeded in a moderate yield. The acetate was then deprotected using potassium carbonate in a high yield. The final small molecule reaction was an Appel reaction to prepare the alkyl bromide of the hapten **78** [153]. The hapten was then used with KLH to prepare the conjugate **79** ready for inoculation.

11.2.8 Hapten-KLH Conjugation

After synthesising the hapten molecule, the subsequent step was to couple it to KLH. KLH was bought as a solution in PBS. KLH fairly easily precipitates out of solution due to its large size and it is not possible to get it back into solution once this has happened. The hapten was not soluble in aqueous solution so finding a solvent system in which both the hapten and KLH remained in solution involved some trial and error. The most suitable system involved dissolving the hapten in DMSO and then adding this to the solution of KLH in a dropwise manner so that not more than 50% of the final solution was DMSO. The solution was left to stir for 24 hours before analysis was carried out to determine whether the binding of the hapten to KLH was successful.

It was decided that the most successful way of determining whether the conjugation had occurred was to assay for free cysteine residues on KLH. If the hapten had conjugated then the number of available cysteine residues would have decreased. Fluorescein maleimide was chosen for the assay. Fluorescein maleimide reacts with any available cysteine residue and can be analysed by its fluorescence. KLH and KLH-hapten were reacted with fluorescein maleimide and run on a gel as well as KLH-hapten alone and the gel analysed on a fluorescence imager (Fig. 71).
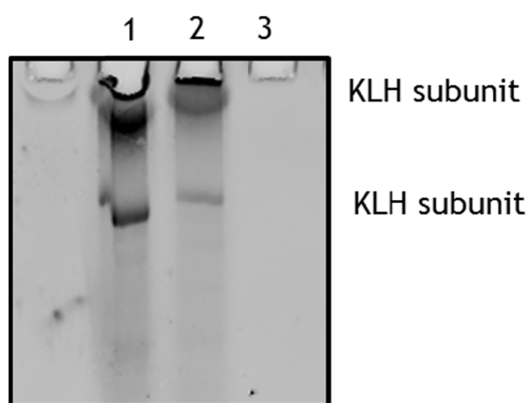
Figure 71 – 8% SDS-PAGE scanned on a fluorescence scanner confirming the binding of the hapten to KLH. Lane 1 shows KLH after reaction with fluorescein maleimide. There is strong fluorescence confirming fluorescein maleimide has reacted with available cysteines in the protein. Lane 2 shows a sample of KLH which was reacted with fluorescein maleimide after undergoing conjugation to the hapten. The fluorescence is weaker than that of lane 1. Lane 3 shows a sample of KLH which has undergone the hapten conjugation but no reaction with fluorescein maleimide. There is no fluorescence emitted.

From the fluorescent gel the KLH-hapten conjugate was confirmed. The fluorescence of KLH-hapten after reaction with fluorescein maleimide was present, showing there were still some available cysteine residues after the hapten conjugation, but it was far reduced compared to the sample of KLH alone after reaction with fluorescein maleimide.

The KLH-hapten conjugate was then freeze dried in preparation for immunization of two rabbits which was carried out by an external company.

11.2.9 Anti-SNAP-P Testing

After receiving a selection of sera produced from bleeds at different timepoints in the antibody production process, they were first tested using SNAP, SNAP-P and SNAP-B produced from overexpression in *E.coli* (Fig. 72).
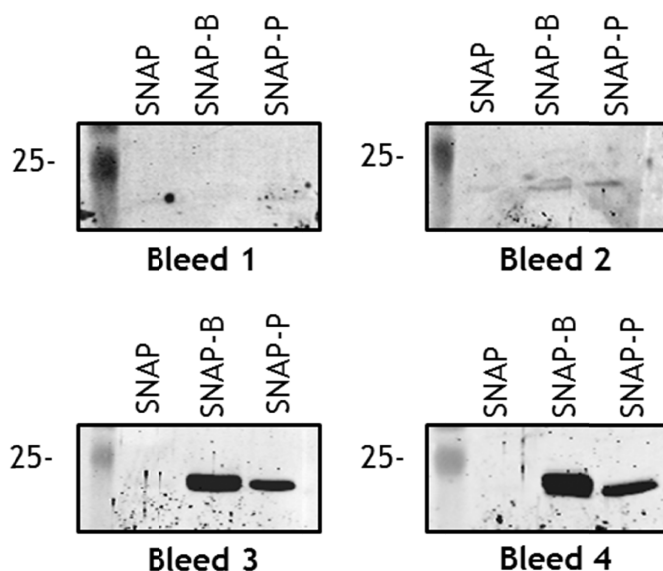
Figure 72 – Western blot from a 12.5% SDS-PAGE showing testing of anti-SNAP-P sera produced from four different stages of the antibody production process. The sera were tested with SNAP-tag, SNAP-B and SNAP-P to assess recognition. The antibody showed positive recognition for both SNAP-B and SNAP-P, but not SNAP-tag.

Western blots were used to assess the efficacy of anti-SNAP-P. A weak positive result is seen in bleed 2 and far stronger in bleeds 3 and 4. There is no recognition of unmodified SNAP-tag but there is strong recognition for both SNAP-B and SNAP-P. This was unfortunate as the hope was that the antibody would only recognise SNAP-P so that as the amount of SNAP-P increased, this increase could be studied by western blot. If the antibody recognises both SNAP-B and SNAP-P then it is not possible to use it for quantification. The antibody was also tested with samples from HT SNAP ER and HT SNAP Cyto cell lines (Fig. 73).
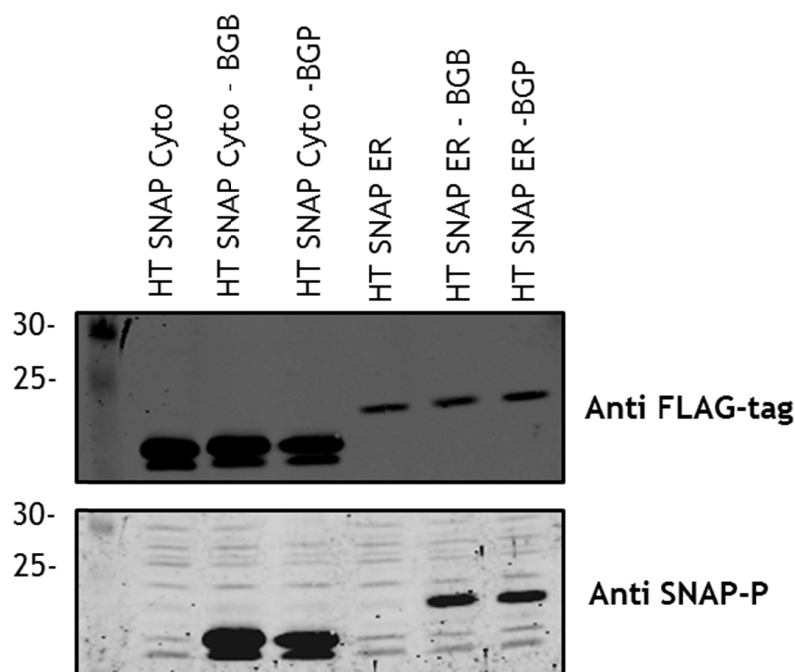
Figure 73 – Western blot from a 12.5% SDS-PAGE showing testing of anti-SNAP-P sera against material from mammalian cells. SNAP-tag from HT SNAP Cyto and ER cells was either untreated or treated with BGB or BGP prior to analysis by western blot. The gel was also probed with anti-FLAG-tag as a control. SNAP-tag expressed in mammalian cells has a FLAG-tag. As with the in vitro data anti-SNAP-P does not recognise SNAP-tag alone but recognises both SNAP-B and SNAP-P.

The results from the testing of anti-SNAP-P with material from HT SNAP Cyto and HT SNAP ER cells mirrors the results when it was tested with purified protein (Fig. 72). This suggests that the antibody cannot differentiate between SNAP-B and SNAP-P. Unfortunately this prevents its use as originally planned. It was hypothesised that the antibody could be used if it was possible to separate SNAP-B and SNAP-P on a gel. At this stage only SDS-PAGE gels had been used which did not show a difference in mobility between SNAP-B and SNAP-P. Isoelectric focussing (IEF) separates proteins on a gel by pH. Proteins are applied to a polyacrylamide gel with a fixed pH gradient and an electric current is applied. The proteins move through the gel until they find their isoelectric point (pI). IEF is known to be capable of detecting post-translational modifications so it was decided that separation of SNAP-B and SNAP-P would be attempted using this method (Fig. 74).
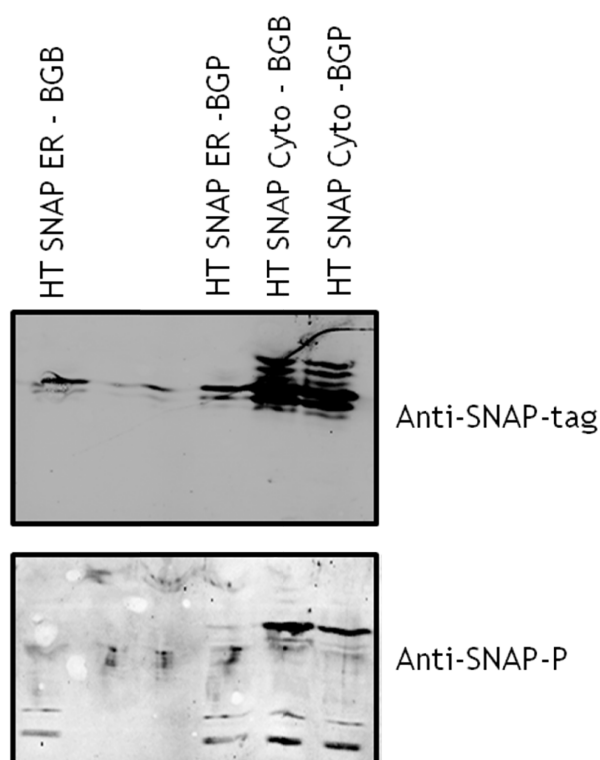
Figure 74 - IEF gel showing SNAP-B and SNAP-P from HT SNAP ER and HT SNAP Cyto cells. The gel was also treated with anti-SNAP-tag as a control. The material from HT SNAP ER cells was only detected by the anti-SNAP-tag antibody. The material from HT SNAP Cyto cells was detected by both anti-SNAP-tag and anti-SNAP-P but showed no difference between the cells treated with BGB and the cells treated with BGP.

The IEF gel did not appear to be capable of separating SNAP-B and SNAP-P. There were a number of possible reasons as to why anti-SNAP-P recognised both SNAP-P and SNAP-B. It was possible that the boronic acid and the phenol of BGB and BGP did not look different enough from each other for the antibodies to be able to differentiate. It was also possible that the antibodies were recognising the parts of the probes that are the same, rather than the end where BGB and BGP are either a boronic acid or a phenol respectfully. Anti-SNAP-P was a polyclonal antibody and so consisted of a range of different antibody populations. It was decided that a purification of the sera would be attempted in order to separate any antibodies which recognised SNAP-B. SNAP-P was conjugated to cyanogen bromide (CNBr) activated sepharose. The CNBr grouping on the sepharose reacts with available NH_2 groups and so couples proteins. The

hypothesis was that when the sera were passed over SNAP-P immobilized on sepharose any antibodies which recognised the phenol group would bind and those which recognised the boronate or boronic acid would pass over. SNAP-P was chosen for binding rather than SNAP-B as it was known that SNAP-B would be in a mixture of forms. Binding of SNAP-P to the sepharose was confirmed by checking the absorbance reading of the SNAP-P solution before and after the binding reaction. There was a reduction in absorbance which confirmed the binding was successful. Antibody sera (1 mL) were passed through the SNAP-P modified sepharose which had been packed into a column. The sepharose was washed and fractions collected. The fractions were tested for SNAP-B and SNAP-P affinity in an ELISA experiment (Fig. 75). The fractions collected were used as the primary antibodies and goat anti-rabbit HRP conjugate used as the secondary. *O*-phenylenediamine dihydrochloride was used as the substrate to produce readouts for the levels of antibody which was measurable via the absorbance at 490 nm.
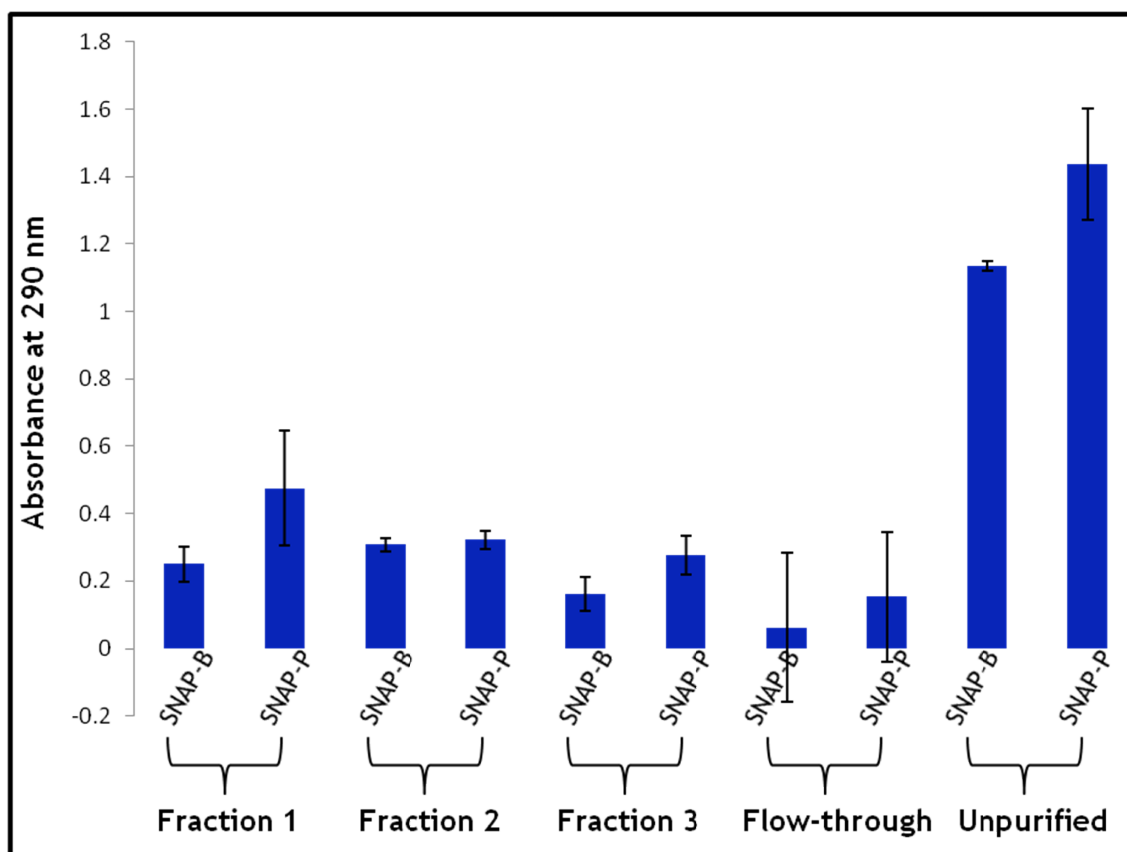
Figure 75 – Purification of anti-SNAP-P. SNAP-B and SNAP-P adsorbed onto the wells of a 96 well plate for testing with the sera after purification. The eluate was collected in three fractions. The ELISA was performed using each of the three fractions collected as well as the flow-through and the unpurified material. The fractions collected did not show any different recognition to SNAP-B and SNAP-P when compared to the unpurified material. The absorbance is weaker for the fractions than for the unpurified material as dilution of the antibodies occurred as part of the process.

The purification attempt was not successful in creating any differential recognition of the antibody towards SNAP-B and SNAP-P. The antibody sera do show intrinsic increased recognition for SNAP-P as can be seen in both the unpurified material and the collected fractions; however this is not great enough to be used practically. This does suggest that there is at least a population of antibodies which recognise the phenol specifically as if all of the antibody population was recognising the linker part of the probe such a difference would not be seen.

11.3 Conclusions

11.3.1 Pep-B

The syntheses and purifications of Pep-B and Pep-P were successful and the reactivity *in vitro* was as expected. When added to cells no peptide could be detected; however, the *in vitro* translation suggested that the peptide was capable of crossing the ER membrane and of also being glycosylated. When used at a concentration of 1 mM the peptide could be detected from the lysate but since no oligosaccharides were detected it cannot be confirmed that this material was ever in the ER. From the work of Hwang et al. it may be that the amounts of peptide actually reaching the ER and being glycosylated are beyond the limit of detection of the analysis method.

The hypothesis behind Pep-B was that by bypassing the need for the probe to react with SNAP-tag certain problems with the use of BGB would be overcome. HT SNAP cells were shown to lose expression following 10-15 passages. SNAP-B and SNAP-P were analysed in the BGB method and this requires conjugation to SNAP-tag. If the expression of SNAP-tag was low then the amount of SNAP-B/SNAP-P would also be low, leading to poor reproducibility and sensitivity. By using a system that did not require conjugation with an endogenous protein, it was believed that the concentration of probe in the ER would be higher and therefore when analysed by MALDI-TOF the concentration of peptides would be higher, leading to the quality of results seen *in vitro* experiments. The other obvious advantage to the Pep-B system was that different cell lines could be used without the need for any kind of transfection. This would have meant that cell lines with either overexpressed or knocked down proteins involved in hydrogen peroxide production and removal in the ER could be used in experiments easily.

Recovery and analysis by MALDI-TOF proved problematic. This was for different reasons than had been the case for BGB but perhaps confirmed the need for a different analysis method. MALDI-TOF can be used for quantification analysis and was successfully shown to do so for the *in vitro* experiments; however what has been shown is that to be successful in quantification MALDI-TOF requires fairly high concentrations of analyte which cannot be produced from *in cellulo* samples.

11.3.2 Anti-SNAP-P

The synthesis of the hapten required for the antibody production was successful and this was shown to bind to KLH. The process itself of producing an antibody against a small molecule was also a successful one and the sera showed a strong response in the western blots performed with both SNAP-probe conjugates produced by overexpression of the protein in *E.coli* and mammalian cells. There was also relatively little in the way of background or non-specific bands in the western blots.

The problem lay in the differential recognition of SNAP-B and SNAP-P. The hypothesis had been that the antibody would recognise SNAP-P and so a gradual increase in the antibody response would be seen as the levels of hydrogen peroxide increased either *in vitro* or *in cellulo*. When the aim of a project is method development then one of the most important factors to consider is ease of use and the change of analysis method from MALDI-TOF to western blot or other antibody technique would have represented a step forward in achieving such an aim. Anti-SNAP-P would have likely also provided a more sensitive analysis of SNAP-P and so allowed investigation of more endogenous conditions when compared to the addition of highly toxic concentrations of hydrogen peroxide to cells.

It has not been possible to assess exactly what part of SNAP-B/SNAP-P, the antibody is recognising. This could be the whole modification of perhaps just the part which actually reacts with hydrogen peroxide. There is not a huge difference between the arylboronic acid of SNAP-B and the phenol of SNAP-P and so it is certainly possible that this is not enough for the antibody to differentiate.

Though it was certainly disappointing that the antibody recognised SNAP-B and SNAP-P and that attempts to separate the forms by IEF and to purify the antibody sera were not successful many parts of this approach were successful. With that in mind the use of an antibody for analysis is something that could be developed further. If a modification could be made to SNAP-B that changed the structure to make it bulkier or different to SNAP-P then the antibody might well differentiate between them, and this would also likely be the most sensitive and reproducible method of analysing hydrogen peroxide in the ER.

12.0 General Discussion

12.1 Hydrogen Peroxide as a Signalling Molecule and a Toxin

Historically viewed as a dangerous toxin, hydrogen peroxide has come to be acknowledged as an important signalling molecule that affects many cellular processes [156]. The use of such a molecule requires careful regulation in order to avoid the acceleration of associated physiological diseases and aging.

As discussed (5.2, 5.3, 5.4), the cell produces hydrogen peroxide from a number of sources. The Nox group of enzymes is the only enzyme family that produces reactive oxygen species as the main function. Other sources are produced as a by-product of the enzymes main function. The fact that such a ubiquitously expressed group of proteins as the Nox enzymes exists, alludes to the importance of hydrogen peroxide [157].

One of the other sources of hydrogen peroxide is the electron transport chain in the mitochondria and occurs as part of respiration. Most reactive oxygen species that are produced in the mitochondria come from complexes I and II when electrons from NADH and $FADH_2$ are leaked and react with molecular oxygen. It is not possible to estimate accurately the levels of hydrogen peroxide produced from this process, but it has been found that in isolated mitochondria that up to 2% of oxygen consumption is diverted into the production of hydrogen peroxide [158].

Within the ER, sources of hydrogen peroxide are the enzymes, Ero1 and Nox4. When PDI catalyses the formation of a disulfide bond in a newly formed protein, the active site becomes reduced and so requires to be reoxidised in order to continue the catalytic cycle. Ero1 acts as a source of disulfides for the reoxidation of PDI and couples this oxidation with the reduction of molecular oxygen, forming a molecule of hydrogen peroxide. Therefore, one molecule of hydrogen peroxide is formed for every new disulfide [159]. Combined with the production from the mitochondrial electron transport chain and the Nox enzymes, this is a substantial amount being released into the cell. Without mechanisms for removing this hydrogen peroxide the amount would far exceed that required for signalling and rapidly result in irreparable damage to the contents of the cell.

The cell employs a range of tactics to protect itself from the dangers of oxidative stress. Antioxidant enzymes play a vital role in protecting the cell from such dangers [5]. Catalase is present in most organisms exposed to oxygen and has one of the highest enzyme turnover numbers. It is capable of converting millions of hydrogen peroxide molecules to water and oxygen every second [30]. The efficiency and ubiquitous expression indicate the importance of its position in the cellular defence against reactive oxygen species.

It has been shown that under conditions of oxidative stress in the ER, glutathione synthesis is increased [160]. Glutathione itself is capable of scavenging reactive oxygen species but also acts in conjunction with the GPx group of enzymes, two of which are resident in the ER. The GPxs contain a cysteine residue reactive towards hydrogen peroxide [161]. This results in the formation of a selenenic acid intermediate which is resolved by formation of a disulfide between the enzyme and glutathione. The disulfide can be reduced by a second molecule of glutathione.

Also at work in defending the cell from excess hydrogen peroxide are the Prx enzymes. The Prxs contain a cysteine residue, known as the peroxidatic cysteine which is reactive to hydrogen peroxide and forms a sulfenic acid, as with the GPxs. However unlike the GPxs this is resolved by another cysteine residue within the protein, known as the resolving cysteine, resulting in a disulfide. It has also been shown the within the ER, PrxIV is capable of *de novo* disulfide bond formation by acting as a source of oxidising equivalents to PDI [37]. Prxs are also capable of hyperoxidation. That is once the sulfenic acid is formed, rather than being resolved it can go on to form sulfinic acid (SO_2H) and sulfonic acid (SO_3H). This only occurs in times of high oxidative stress and is perhaps an indication of when hydrogen peroxide concentrations increase enough that it loses its role as a signalling molecule and becomes an instigator of cell death by apoptosis or necrosis [162].

It is the occasions that the role of hydrogen peroxide changes from signaller to toxin that are less well understood. With regards to the ER, it would be of great benefit to measure hydrogen peroxide and provide a greater understanding of the mechanisms involved in protein folding. By studying hydrogen peroxide levels in the ER when cells are placed under various stresses or when the expression of

proteins involved in disulfide bond formation is either increased or reduced that a greater understanding of the role that hydrogen peroxide plays in the ER could be garnered.

12.2 Different Ways to Measure Hydrogen Peroxide

Within the cell there are two ways by which it is possible to measure hydrogen peroxide: a protein based method or a small molecule based method. As previously described (5.9), one protein based method to have been used was HyPer [67].

HyPer consists of a cpYFP inserted into the regulatory domain of the bacterial protein OxyR. OxyR is a hydrogen peroxide sensing protein that undergoes a conformational change after reaction with hydrogen peroxide [163]. A cysteine residue within OxyR reacts with hydrogen peroxide to form a sulfenic acid which then goes onto form a disulfide with another cysteine residue within the active site. Since HyPer is a protein based method it is possible to express the protein within mammalian cells and target it to various organelles by incorporating signal sequences. It is also possible to express HyPer as an ER located sensor by use of the ER retention sequence, KDEL. Upon oxidation the fluorescence of HyPer at 500 nm increases and the excitation peak at 420 nm decreases.

The advantage of HyPer lies in the fact that it can be expressed within the cell at the organelle of choice. There are however a number of disadvantages with such a method. As with most circularly permuted proteins, HyPer is pH sensitive, so any local changes in the pH of the cell will lead to an alteration in the fluorescence of HyPer [70]. By relying on a protein to assess changes, there is always the possibility that cellular factors will affect the readout. When HyPer becomes oxidised it forms a disulfide bond, this disulfide could be reduced either by other proteins or by glutathione, which would again affect the readout. Therefore, the danger of using a protein based methodology lies in the fact that it is in a cell full of other proteins affecting a range of processes, which could include the very process being used to assess hydrogen peroxide levels.

Another protein based method developed was the probe Orp1-roGFP2. This works in a similar method to Hyper in that a redox sensitive protein was coupled to a fluorescent one. Orp1 is a thioredoxin dependant protein with two cysteines

within the active site. The peroxidatic cysteine reacts with hydrogen peroxide to form a sulfenic acid. This can be resolved by forming a disulfide with the resolving cysteine. When coupled to roGFP2, this results in a measurable fluorescence change [164].

With regards to small molecule probes there have been a number of different probes used. One of the earlier and widely used probes was DCF. This relies on oxidation to induce the change from non-fluorescent to fluorescent compound. As a simple and quick method for looking at oxidation changes, DCF could provide what is required but if a more specific answer is desired it is not suitable. This is due to lack of specificity for hydrogen peroxide over other reactive oxygen species. It is an OFF-ON probe, so it only indicates a general increase in oxidation rather than something that can be quantified accurately, which would require a ratiometric method [165].

Since DCF, the field of small molecule probes has shown a remarkable improvement, chiefly with regards to the reactivity towards hydrogen peroxide. The use of boronate esters as the hydrogen peroxide reactive moiety created the specificity that DCF lacked. Boronates have been shown to be selective for hydrogen peroxide over other reactive oxygen species and have since been used widely in hydrogen peroxide sensors. Most sensors have been fluorescent with the exception of MitoB, a mass spectrometry probe for the mitochondria [166].

Fluorescent boronate based probes have been developed with a wide range of spectral properties. Change and co-workers created a suite of three probes, Peroxyresorufin-1 (PR1), Peroxyfluor-1 (PF1) and Peroxyxanthone-1 (PX1) [82]. PR1, PF1 and PX1 emitted red, green and blue fluorescence respectively, upon oxidation by hydrogen peroxide. By using the boronate, which provided the desired specificity lacking in previous small molecule probes and which was immune to the cellular factors that affected HyPer it meant that the research focus could shift to further developing the best spectral qualities.

Therefore, when it came to decide on the approach to take when designing our own probes it was firmly believed a small molecule probe would provide the greatest chance of success. HyPer's downfall was perhaps that it was a protein that was susceptible to endogenous metabolic processes. It was reasoned that whatever hydrogen peroxide reactive protein construct chosen, whether OxyR or

another hydrogen peroxide reactive protein, it would be subject to cellular pressures that would be difficult to predict. In order to offer a significant improvement on HyPer, there would need to be some guarantee that the reactive protein would not be affected by anything other than hydrogen peroxide, something which would have been difficult to predict. This led us to believe that the future of hydrogen peroxide sensitive probes was in the field of small molecules.

When designing the probes BG-Fura-B, BGB and Pep-B there was no debate over whether or not to utilise the boronate as the hydrogen peroxide reactive moiety. The literature has shown that it is a good choice and extensive work carried out previously within the group on mitochondrial probes substantiated this evidence.

Unfortunately with regards to BG-Fura-B, the testing stage was never reached but with regards to BGB and Pep-B the *in vitro* tests confirmed that the reactivity of the probes was as desired. When compared to the most similar probe previously published, the fluorescent SPG1 synthesised by the Chang group, the reactivity was similar. The boronate provided a reliable and selective reaction mechanism, shown in the MALDI-TOF experiments carried out. The probes were capable of showing a measurable change down to low micromolar concentrations of hydrogen peroxide. Though this is perhaps still higher than steady state concentrations of hydrogen peroxide inside cells, this is likely to be akin to what cells experience under times of oxidative stress. This was what was desired as the aim of the project had been to create probes to aid understanding of the mechanism of protein folding in times of such stress. Another advantage of the boronate is that the reaction rate is conveniently measurable [166]. It can, therefore, be concluded that the reactivities of BGB and Pep-B could potentially have provided a successful measure of the likely conditions felt by mammalian cells during oxidative stress.

12.3 Methods of Targeting Probes

As previously discussed there are a number of different methods of targeting small molecule probes. Small molecule probes can be targeted to the mitochondrial matrix due to the existence of the membrane potential. If a charged group such as a TPP cation is used, then a concentration builds up in the matrix. If other areas of the mitochondria are to be studied then a different

method of targeting that is not purely small molecule based is required. Probes targeted to the ER also require some assistance from either a protein or peptide-based method.

The most utilised methods for targeting to the ER are protein based labelling methods. The SNAP-tag system involves the use of a mutated version of AGT which is a DNA repair protein. SNAP-tag specifically reacts with O^6-(4-aminomethyl)benzylguanine derivatives [93]. The mutation ensures that a covalent bond is formed between the substrate and protein in an irreversible reaction.

SNAP-tag was the system chosen for BG-Fura-B and BGB. In order to be reactive to SNAP-tag BG-Fura-B and BGB required the incorporation of the O^6-(4-aminomethyl)benzylguanine moiety into the structures, though never realised for BG-Fura-B. The steps in the synthesis required to incorporate such a functionality did create some difficulty due to the lack of solubility of the moiety in most solvents. Even when conjugated to the rest of the probe for BGB, the solubility did not improve. However, the final probe was produced in a suitable quantity, though material was undoubtedly lost due to the difficulty of working with such a substrate.

Both the *in vitro* and *in cellulo* testing of BGB showed successful labelling of SNAP-tag. The evidence provided from the western blot of unlabelled and labelled SNAP-tag from the HT SNAP ER cell line (Fig. 44) suggested quantitative labelling in 30 min with a 5 μM solution of the probe in medium. The reaction between probe and SNAP-tag proceeds with a fast and efficient rate. The *in cellulo* experiments with BGB also showed the addition of the O^6-(4-aminomethyl)benzylguanine moiety to the structure did not hamper the ability of the probe to cross both the cell and ER membranes. This was concordant with previous literature examples which had used SNAP-tag as a targeting method.

With regards to peptide-based targeting systems, it was hypothesised that by using such a system some of the problems associated with SNAP-tag would be overcome. Peptide based targeting has been used successfully to target fluorophores, drugs and imaging agents to various organelles and it was believed that this would offer a viable alternative to the SNAP-tag system [104]. It was found that the SNAP-tag cell lines lost expression at low passage number and

since the method for BGB was very dependent on concentration, this affected the quality of the results produced. The peptide chosen for use in Pep-B, Ac-NYTCKDEL, incorporated a glycosylation site and the ER retention sequence. The peptide incorporated both glycosylation and ER retention to create the best chance of a suitable concentration building up within the ER.

Initial experiments failed to detect any peptide recovered from cells so an in vitro translation was carried out which suggested that the peptide was capable of crossing the ER membrane and of becoming glycosylated once having done so. Some recovery of the peptide was seen by MALDI-TOF when cells were treated with a millimolar concentration of the peptide, though no evidence of glycosylation, so it cannot be said whether the recovery seen was from ER or cytosol located peptide.

It is likely that though some of the peptide was entering the cell and perhaps diffusing into the ER, the concentration that was doing so was too low to achieve reasonable results using MALDI-TOF.

The evidence shows that SNAP-tag is the more successful of the two targeting techniques investigated. Peptide targeting may be of more use in a system which is not so sensitive to concentration, such as one which uses fluorescence as the method of analysis.

12.4 Analysis Techniques of Probes

The original aim of the project had been to develop a fluorescent and targetable probe for hydrogen peroxide in the ER. It was felt that the fluorescent properties of previous probes such as SPG1, which also utilised SNAP-tag and a boronate for hydrogen peroxide reactivity, could be improved upon.

Since SPG1 used the same targeting system and reactive moiety, it was vital that any probe synthesised greatly improved upon this. SPG1 is mildly fluorescent before reaction and emits much greater fluorescence after reaction, but importantly it is not ratiometric as the fluorescence prior to reaction is too weak for detection. Therefore, it was imperative that a new fluorescent probe offered a significant improvement, and so we designed a probe to be fully ratiometric.

It was believed that by incorporating the fluorophore used in the calcium sensor, Fura-Red™, into the structure then this ratiometricity could be achieved. It can be difficult to achieve ratiometricity when using boronates, as the empty p orbital of the boron atom acts as a quencher of fluorescence. Therefore, the structure of BG-Fura-B was developed so that the boron was a suitable distance away from the fluorescent core of the molecule. It was hypothesised that the large Stokes shift of Fura-Red would also be observed in a hydrogen peroxide sensitive probe and that the structural change that would have occurred upon reaction of the probe with hydrogen peroxide would lead to a significant red-shift in the absorption frequency. Thus, BG-Fura-B would offer full ratiometricity, and therefore, a significant improvement on the previously published probes.

Unfortunately, due to the instability of a precursor analogue to BG-Fura-P, the synthesis was not completed. However, gratifyingly, the large Stokes shift was observed (9.2.6 Fig.39). Since it was unlikely that by synthesising a different fluorescent probe the desired property of ratiometricity would be achieved, a different method of analysis was considered.

BGB offered something significantly different from other hydrogen peroxide probes targetable to the ER, in that it is a mass spectrometry probe. Mass spectrometry provides the guarantee of ratiometricity that the present fluorescent probes cannot. By deciding on a different technique of analysis it allowed a much quicker synthesis and the opportunity to develop a completely novel method of studying hydrogen peroxide in the ER. BGB was, therefore, still perceived to offer the same improvement as BG-Fura-B on all the previously published probes.

The *in vitro* experiments analysed by MALDI-TOF using SNAP-B, BGB conjugated to recombinant SNAP-tag, showed repeatable reactivity with sensitivity to low micromolar concentrations. When experiments were carried out in HT SNAP ER and HT SNAP Cyto cells, the repeatability and sensitivity were not as good as the *in vitro* experiments. However, what could be seen was that there was reactivity and the level of SNAP-P increased over time. The fact that the increase in the level of SNAP-P in the cell line which expressed SNAP-tag in the cytosol was greater than that in the cell line which expressed SNAP-tag in the ER showed

that less exogenously added hydrogen peroxide reaches the ER than reaches the cytosol. This is in agreement with research into the transport of hydrogen peroxide through specific aquaporins, which showed that the movement of hydrogen peroxide is tightly regulated by the cell [167].

MALDI-TOF, the technique used for analysis of BGB, has rarely been used for such a purpose as it is mostly used for qualitative rather than quantitative results. This presented a challenge with regards to method development for use of BGB in cells. When it was discovered that the boronic acid did not fly using MALDI-TOF, a formula was developed to overcome this by using an internal standard which allowed this issue to be overcome to some extent. It was attempted to improve the quality of the results by using DHB as the matrix, rather than CHCA though this was found to offer no advantage.

It has been shown that MALDI-TOF can in fact be used as a quantitative method of analysis though there are caveats to its use. The main one being that the concentration of the analyte must be fairly high in order to achieve data with low variability. It is also imperative that the MALDI-TOF conditions be developed specifically for the analyte in order to collect results. Nevertheless, the development of BGB has offered a completely novel way of analysing hydrogen peroxide in specific organelles. Though BGB was only targeted to the ER and cytosol it would be possible to utilise it in other organelles.

The development of the polyclonal antibody, Anti-SNAP-P, was carried out in order to provide a further method of analysis which would allow for a more widespread use of BGB. Anybodies have been used successfully for recognition of a range of small molecules including fluorogenic dyes as well as protein modifications such as sulfotyrosine [168], [169]. This was to provide an advantage over the MALDI-TOF analysis method of BGB and all the previously published fluorescent probes as it meant a way of analysing the reactivity of BGB without the use of costly equipment such as mass spectrometers and confocal microscopes that require specialist knowledge. Though unfortunately, the antibody was not able to distinguish between SNAP-B and SNAP-P, it was certainly the first attempt at developing such a method of analysing hydrogen peroxide and is perhaps one which merits further attention in the future.

12.5 Summary Table of Probe Qualities

The following table summarizes the different probes developed during the course of the project:
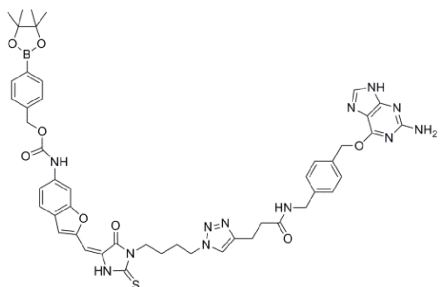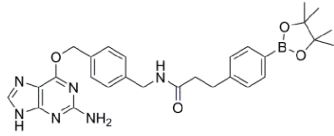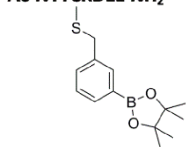
Probe	Method of Targeting	Method of Detection	Comments
BG-Fura-B	SNAP-tag – protein reactive to benzylguanine derivatives, can be expressed in ER	Fluorescence-different fluorescence expected before and after reaction	Target structure not synthesised due to instability of core structure
BGB	SNAP-tag – protein reactive to benzylguanine derivatives, can be expressed in ER	MALDI-TOF mass spectrometry	Successful targeting and measurement of H_2O_2 in ER, MALDI-TOF a source of variability
Pep-B	Peptide-including glycosylation site and ER retention sequence	MALDI-TOF mass spectrometry	Probe not detectable from cell lysate by MALDI-TOF

Table 2 – Summary of the probes developed.

13.0 Future Work

13.1 HT SNAP Cell Lines

As discussed, it was found that the stably transfected HT SNAP cell lines were found to lose expression after a low passage number. This was inconvenient as it can cause delays to an experimentation plan. Cells stocks were made at low passage number and stored so in the event of currently cultured cells losing expression, more cells could be brought into culture from -80°C storage. This, however, takes time as cells are often slow to grow just after being brought out of storage.

Cells can sometimes lose expression of a protein that has been transfected in to create an overexpression cell line. This can occur when the protein being expressed causes a detrimental effect on the vital processes of the cell. It would not be advantageous to use transient transfection of SNAP-tag since this would add a lot of time onto every experiment. Therefore, an important step for the future would be to create inducible cell lines. The tetracycline system utilises the tetracycline repressor protein to generate a very efficient regulatory system for the expression of the desired protein [170]. If these cell lines were created then the expression of SNAP-tag could be induced prior to the experiment, doubtless saving time and preventing the discovery that the expression had dropped only after the experiment was carried out.

13.2 O^6-(4-Aminomethyl)benzylguanine Solubility

The synthesis of BGB was somewhat complicated by the fact that the SNAP-tag substrate O^6-(4-aminomethyl)benzylguanine was insoluble in most solvents. This meant that purification of the substrate and final probe became an inefficient procedure whereby a lot of material was lost and high purity was difficult to achieve. If the substrate was to be more soluble this would make the synthesis of BGB and any future SNAP-tag substrates simpler and higher yielding.

Adding poly(ethyleneglycol) (PEG) units to organic compounds does have the ability to improve the solubility of some insoluble compounds. Risseeuw et al. synthesised compounds though not O^6-(4-aminomethyl)benzylguanine but with a similar structure that were soluble in dichloromethane: methanol 93:7 (Fig. 76) [171].

178
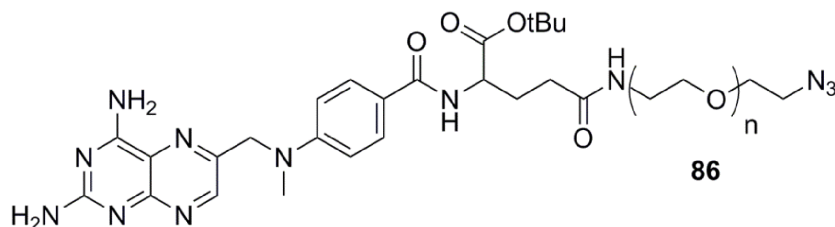
Figure 76 – The compound synthesised by Risseeuw et al. which encorporated PEG units (n = 5). Though a different compound, the structure shares some similarities with O^6-(4-aminomethyl)benzylguanine. The incorporation of PEG units into the SNAP-tag structure may increase the solubility in standard solvents used in column chromatography.

PEG units of varying lengths were incorporated into the structure by Risseeuw et al. and possibly aided the solubility. The incorporating of PEG units into O^6-(4-aminomethyl)benzylguanine may increase the solubility enough to allow an easier and more efficient synthesis. The proposed structure (Fig. 77) allows the addition of the PEG units and maintains the amine moiety used for conjugation to the active part of the probe, therefore no other alterations in synthesis would be required [99].
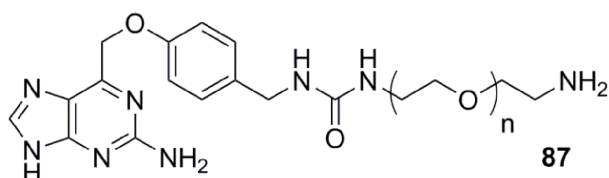
Figure 77 – The proposed SNAP-tag substrate incorporating PEG units (n = 5). It is hypothesised that the PEG units would increase solubility and so lead to a more efficient synthesis and purification of BGB and future probes for use with SNAP-tag.

13.3 New Probes for Use with Anti-SNAP-P

The hypothesis behind Anti-SNAP-P was that by developing an antibody for use with BGB then the method of analysis could be by western blot or ELISA, thus eliminating the requirement for MALDI-TOF and overcoming the associated issues. Unfortunately it was found that the antibody could not differentiate between SNAP-B and SNAP-P. One possibility would be to attempt to produce a new antibody that would be able to differentiate between the two. Instead of

raising the antibody against the phenol form of the probe it could be raised against the boronic acid. When devising the plan for the antibody this was decided against as the boronic acid is known to take different forms, i.e. the boronate ester.

Another possibility would be to alter the structure of BGB itself to prevent the antibody recognising the boronic acid form. If an extra aryl ring was incorporated into the structure and a similar fragmentation reaction to that proposed for SNAP-Fura-B designed in, then it could be possible to form SNAP-P from a significantly different SNAP-conjugate. The positioning of the aryl boronate cage may make the unreacted structure bulky enough that the interaction between the probe and the antibody is prevented (Fig. 78). Further variation in the caging group would be possible, e.g. the boronate could be positioned at either the *ortho* or *para* position and other bulky or polar groups attached.
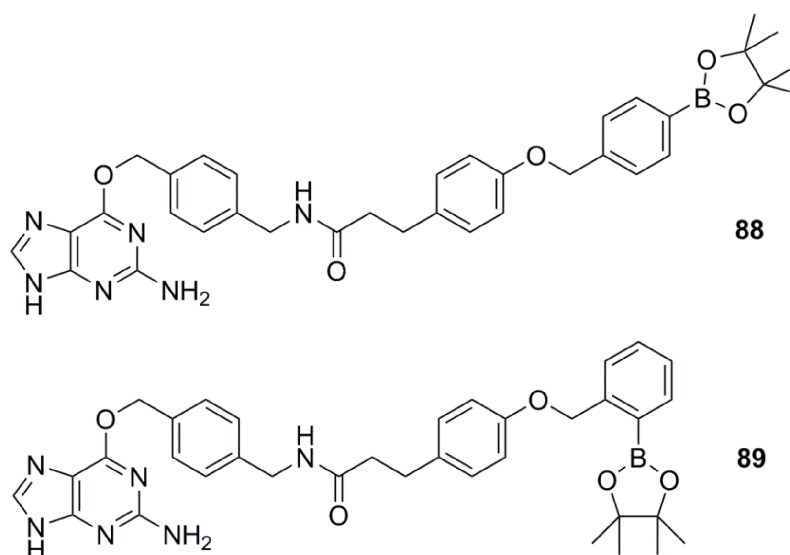
Figure 78 – Proposed structures for second generation probes 88 and 89. After reaction with hydrogen peroxide the boronate would be converted to a phenol which would lead to lose the phenyl ring upon which the boronate is located. This would produce the same phenol compound as that produced from the reaction of BGB with hydrogen peroxide. It is hypothesised that this may prevent the interaction between unreacted probe and antibody.

Once conjugated to SNAP-tag the second generation probes would likely equilibrate to the boronic acid form, as happened with SNAP-B, and the reaction with hydrogen peroxide would occur leading to the same product, SNAP-P, as produced by the original SNAP-B conjugate (Fig. 79).
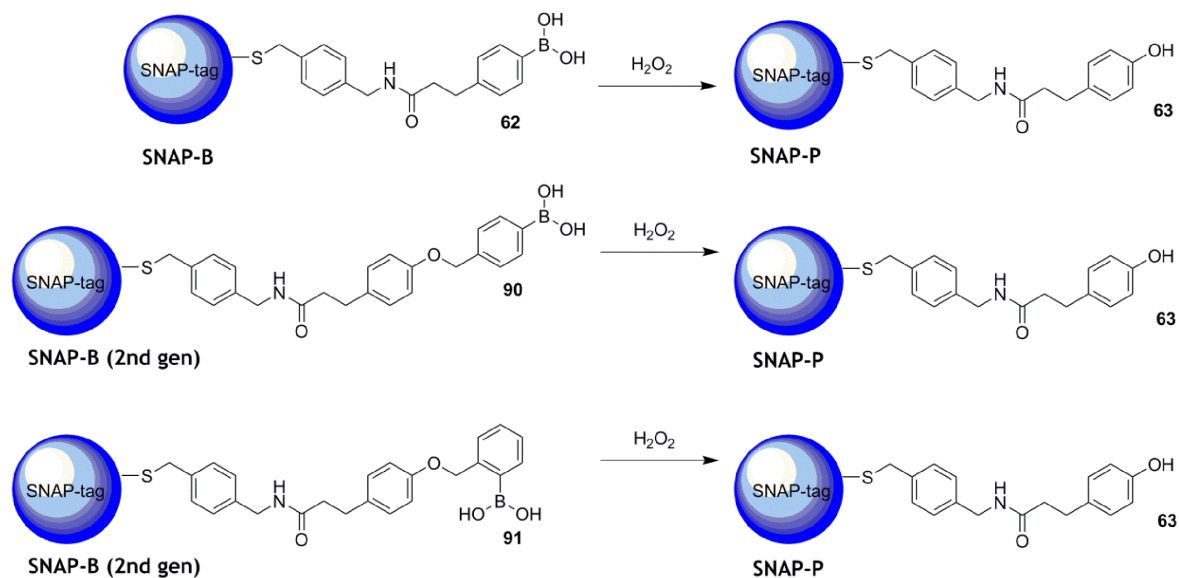
Figure 79 – The reactions of SNAP-B 62 and the two second generation SNAP-B (*para* and *ortho*) conjugates, 90 and 91 with hydrogen peroxide. With all three conjugates, the same product, SNAP-P 63, is produced.

14.0 Summary

It is clear that a method of studying hydrogen peroxide in the ER would aid the understanding of the processes of protein folding and oxidative stress. It is only in recent years that the full plethora of roles hydrogen peroxide plays has begun to be appreciated. The data described have shown the development and use of a probe, BGB which can be successfully targeted to the ER and react with hydrogen peroxide. The method developed for use with BGB has demonstrated the use of quantitative MALDI-TOF and, therefore, does not require the incorporation of any fluorescent moieties, which often show sensitivity to other factors such as environment and the surrounding molecular structure. The development of the antibody, anti-SNAP-P has provided a further opening into novel methods of analysis of hydrogen peroxide probes and hopefully further development of this will provide a new a simple technique to aid the understanding of oxidative stress.

15.0 References

1   Veal, E. A., Day, A. M. and Morgan, B. A. (2007) Hydrogen peroxide sensing and signaling. Mol Cell. **26**, 1-14

2   Bedard, K. and Krause, K. H. (2007) The NOX family of ROS-generating NADPH oxidases: physiology and pathophysiology. Physiological reviews. **87**, 245-313

3   Boveris, A., Oshino, N. and Chance, B. (1972) The cellular production of hydrogen peroxide. Biochem J. **128**, 617-630

4   Tavender, T. J. and Bulleid, N. J. (2010) Peroxiredoxin IV protects cells from oxidative stress by removing H2O2 produced during disulphide formation. Journal of cell science. **123**, 2672-2679

5   Mates, J. M., Perez-Gomez, C. and Nunez de Castro, I. (1999) Antioxidant enzymes and human diseases. Clinical biochemistry. **32**, 595-603

6   Bray, R. C., Cockle, S. A., Fielden, E. M., Roberts, P. B., Rotilio, G. and Calabrese, L. (1974) Reduction and inactivation of superoxide dismutase by hydrogen peroxide. Biochem J. **139**, 43-48

7   Thannickal, V. J. and Fanburg, B. L. (2000) Reactive oxygen species in cell signaling. American journal of physiology. Lung cellular and molecular physiology. **279**, L1005-1028

8   Gough, D. R. and Cotter, T. G. (2011) Hydrogen peroxide: a Jekyll and Hyde signalling molecule. Cell death & disease. **2**, e213

9   Touyz, R. M., Briones, A. M., Sedeek, M., Burger, D. and Montezano, A. C. (2011) NOX isoforms and reactive oxygen species in vascular health. Molecular interventions. **11**, 27-35

10   Wong, J. L., Creton, R. and Wessel, G. M. (2004) The oxidative burst at fertilization is dependent upon activation of the dual oxidase Udx1. Developmental cell. **7**, 801-814

11   Rossi, F. and Zatti, M. (1964) Biochemical aspects of phagocytosis in polymorphonuclear leucocytes. NADH and NADPH oxidation by the granules of resting and phagocytizing cells. Experientia. **20**, 21-23

12   Chen, J. X., Zeng, H., Lawrence, M. L., Blackwell, T. S. and Meyrick, B. (2006) Angiopoietin-1-induced angiogenesis is modulated by endothelial NADPH oxidase. American journal of physiology. Heart and circulatory physiology. **291**, H1563-1572

13   Segal, A. W. and Jones, O. T. (1978) Novel cytochrome b system in phagocytic vacuoles of human granulocytes. Nature. **276**, 515-517

14   Ni, Z., Hou, S., Barton, C. H. and Vaziri, N. D. (2004) Lead exposure raises superoxide and hydrogen peroxide in human endothelial and vascular smooth muscle cells. Kidney international. **66**, 2329-2336

15   Hasegawa, T., Kikuyama, M., Sakurai, K., Kambayashi, Y., Adachi, M., Saniabadi, A. R., Kuwano, H. and Nakano, M. (2002) Mechanism of superoxide anion production by hepatic sinusoidal endothelial cells and Kupffer cells during short-term ethanol perfusion in the rat. Liver. **22**, 321-329

16   Jiang, F., Zhang, Y. and Dusting, G. J. (2011) NADPH oxidase-mediated redox signaling: roles in cellular stress response, stress tolerance, and tissue repair. Pharmacological reviews. **63**, 218-242

17   Liu, H., Nishitoh, H., Ichijo, H. and Kyriakis, J. M. (2000) Activation of apoptosis signal-regulating kinase 1 (ASK1) by tumor necrosis factor receptor-associated factor 2 requires prior dissociation of the ASK1 inhibitor thioredoxin. Molecular and cellular biology. **20**, 2198-2208

18   Tonks, N. K. (2006) Protein tyrosine phosphatases: from genes, to function, to disease. Nature reviews. Molecular cell biology. **7**, 833-846

19   Turrens, J. F. (2003) Mitochondrial formation of reactive oxygen species. The Journal of physiology. **552**, 335-344

20   Han, D., Antunes, F., Canali, R., Rettori, D. and Cadenas, E. (2003) Voltage-dependent anion channels control the release of the superoxide anion from mitochondria to cytosol. The Journal of biological chemistry. **278**, 5557-5563

21   Simonson, S. G., Zhang, J., Canada, A. T., Jr., Su, Y. F., Benveniste, H. and Piantadosi, C. A. (1993) Hydrogen peroxide production by monoamine oxidase during ischemia-reperfusion in the rat brain. Journal of cerebral blood flow and metabolism : official journal of the International Society of Cerebral Blood Flow and Metabolism. **13**, 125-134

22   Sideris, D. P. and Tokatlidis, K. (2010) Oxidative protein folding in the mitochondrial intermembrane space. Antioxid Redox Signal. **13**, 1189-1204

23   Gilbert, H. F. (1998) Protein disulfide isomerase. Methods in enzymology. **290**, 26-50

24   Wilkinson, B. and Gilbert, H. F. (2004) Protein disulfide isomerase. Biochimica et biophysica acta. **1699**, 35-44

25   Lappi, A. K. and Ruddock, L. W. (2011) Reexamination of the role of interplay between glutathione and protein disulfide isomerase. J Mol Biol. **409**, 238-249

26   Tu, B. P. and Weissman, J. S. (2002) The FAD- and O-2-dependent reaction cycle of Ero1-mediated oxidative protein folding in the endoplasmic reticulum. Molecular Cell. **10**, 983-994

27   Gross, E., Sevier, C. S., Heldman, N., Vitu, E., Bentzur, M., Kaiser, C. A., Thorpe, C. and Fass, D. (2006) Generating disulfides enzymatically: reaction products and electron acceptors of the endoplasmic reticulum thiol oxidase Ero1p. Proceedings of the National Academy of Sciences of the United States of America. **103**, 299-304

28   Appenzeller-Herzog, C., Riemer, J., Christensen, B., Sorensen, E. S. and Ellgaard, L. (2008) A novel disulphide switch mechanism in Ero1alpha balances ER oxidation in human cells. EMBO J. **27**, 2977-2987

29   Baker, K. M., Chakravarthi, S., Langton, K. P., Sheppard, A. M., Lu, H. and Bulleid, N. J. (2008) Low reduction potential of Ero1alpha regulatory disulphides ensures tight control of substrate oxidation. EMBO J. **27**, 2988-2997

30   Alfonso-Prieto, M., Biarnes, X., Vidossich, P. and Rovira, C. (2009) The molecular mechanism of the catalase reaction. Journal of the American Chemical Society. **131**, 11751-11761

31   Groves, J. T., Haushalter, R. C., Nakamura, M., Nemo, T. E. and Evans, B. J. (1981) High-valent iron-porphyrin complexes related to peroxidase and cytochrome P-450. Journal of the American Chemical Society. **103**, 2884-2886

32   Purdue, P. E. and Lazarow, P. B. (1996) Targeting of human catalase to peroxisomes is dependent upon a novel COOH-terminal peroxisomal targeting sequence. J Cell Biol. **134**, 849-862

33   Brigelius-Flohe, R. and Maiorino, M. (2013) Glutathione peroxidases. Biochimica et biophysica acta. **1830**, 3289-3303

34   Nguyen, V. D., Saaranen, M. J., Karala, A. R., Lappi, A. K., Wang, L., Raykhel, I. B., Alanen, H. I., Salo, K. E., Wang, C. C. and Ruddock, L. W. (2011) Two endoplasmic reticulum PDI peroxidases increase the efficiency of the use of peroxide during disulfide bond formation. J Mol Biol. **406**, 503-515

35   Barranco-Medina, S., Lazaro, J. J. and Dietz, K. J. (2009) The oligomeric conformation of peroxiredoxins links redox state to function. FEBS letters. **583**, 1809-1816

36   Woo, H. A., Chae, H. Z., Hwang, S. C., Yang, K. S., Kang, S. W., Kim, K. and Rhee, S. G. (2003) Reversing the inactivation of peroxiredoxins caused by cysteine sulfinic acid formation. Science. **300**, 653-656

37   Cao, Z., Tavender, T. J., Roszak, A. W., Cogdell, R. J. and Bulleid, N. J. (2011) Crystal structure of reduced and of oxidized peroxiredoxin IV enzyme reveals a stable oxidized decamer and a non-disulfide-bonded intermediate in the catalytic cycle. The Journal of biological chemistry. **286**, 42257-42266

38   Antunes, F. and Cadenas, E. (2000) Estimation of H2O2 gradients across biomembranes. FEBS letters. **475**, 121-126

39   Bienert, G. P., Schjoerring, J. K. and Jahn, T. P. (2006) Membrane transport of hydrogen peroxide. Biochimica et biophysica acta. **1758**, 994-1003

40   Sousa-Lopes, A., Antunes, F., Cyrne, L. and Marinho, H. S. (2004) Decreased cellular permeability to H2O2 protects Saccharomyces cerevisiae cells in stationary phase against oxidative stress. FEBS letters. **578**, 152-156

41   Verkman, A. S., Anderson, M. O. and Papadopoulos, M. C. (2014) Aquaporins: important but elusive drug targets. Nat Rev Drug Discov. **13**, 259-277

42   Henzler, T. and Steudle, E. (2000) Transport and metabolic degradation of hydrogen peroxide in Chara corallina: model calculations and measurements with the pressure probe suggest transport of H(2)O(2) across water channels. Journal of experimental botany. **51**, 2053-2066

43   Fu, D., Libson, A., Miercke, L. J., Weitzman, C., Nollert, P., Krucinski, J. and Stroud, R. M. (2000) Structure of a glycerol-conducting channel and the basis for its selectivity. Science. **290**, 481-486

44   Bienert, G. P., Moller, A. L., Kristiansen, K. A., Schulz, A., Moller, I. M., Schjoerring, J. K. and Jahn, T. P. (2007) Specific aquaporins facilitate the diffusion of hydrogen peroxide across membranes. The Journal of biological chemistry. **282**, 1183-1192

45   Calamita, G., Ferri, D., Gena, P., Liquori, G. E., Cavalier, A., Thomas, D. and Svelto, M. (2005) The inner mitochondrial membrane has aquaporin-8 water channels and is highly permeable to water. The Journal of biological chemistry. **280**, 17149-17153

46   Sauer, H., Rahimi, G., Hescheler, J. and Wartenberg, M. (2000) Role of reactive oxygen species and phosphatidylinositol 3-kinase in cardiomyocyte differentiation of embryonic stem cells. FEBS letters. **476**, 218-223

47   Foreman, J., Demidchik, V., Bothwell, J. H., Mylona, P., Miedema, H., Torres, M. A., Linstead, P., Costa, S., Brownlee, C., Jones, J. D., Davies, J. M. and Dolan, L. (2003) Reactive oxygen species produced by NADPH oxidase regulate plant cell growth. Nature. **422**, 442-446

48   Ushio-Fukai, M. (2006) Redox signaling in angiogenesis: role of NADPH oxidase. Cardiovascular research. **71**, 226-235

49   Cai, H. (2005) Hydrogen peroxide regulation of endothelial function: origins, mechanisms, and consequences. Cardiovascular research. **68**, 26-36

50   Sablina, A. A., Budanov, A. V., Ilyinskaya, G. V., Agapova, L. S., Kravchenko, J. E. and Chumakov, P. M. (2005) The antioxidant function of the p53 tumor suppressor. Nat Med. **11**, 1306-1313

51   Bossis, G. and Melchior, F. (2006) Regulation of SUMOylation by reversible oxidation of SUMO conjugating enzymes. Mol Cell. **21**, 349-357

52   Kim, J. R., Yoon, H. W., Kwon, K. S., Lee, S. R. and Rhee, S. G. (2000) Identification of proteins containing cysteine residues that are sensitive to oxidation by hydrogen peroxide at neutral pH. Analytical biochemistry. **283**, 214-221

53   Bae, Y. S., Kang, S. W., Seo, M. S., Baines, I. C., Tekle, E., Chock, P. B. and Rhee, S. G. (1997) Epidermal growth factor (EGF)-induced generation of hydrogen peroxide. Role in EGF receptor-mediated tyrosine phosphorylation. The Journal of biological chemistry. **272**, 217-221

54   Clement, M. V., Ponton, A. and Pervaiz, S. (1998) Apoptosis induced by hydrogen peroxide is mediated by decreased superoxide anion concentration and reduction of intracellular milieu. FEBS letters. **440**, 13-18

55   Fan, T. J., Han, L. H., Cong, R. S. and Liang, J. (2005) Caspase family proteases and apoptosis. Acta biochimica et biophysica Sinica. **37**, 719-727

56   Gilbert, H. F. (1995) Thiol/disulfide exchange equilibria and disulfide bond stability. Methods in enzymology. **251**, 8-28

57   Tochigi, M., Inoue, T., Suzuki-Karasaki, M., Ochiai, T., Ra, C. and Suzuki-Karasaki, Y. (2013) Hydrogen peroxide induces cell death in human TRAIL-resistant melanoma through intracellular superoxide generation. International journal of oncology. **42**, 863-872

58   Ramming, T. and Appenzeller-Herzog, C. (2013) Destroy and Exploit: Catalyzed Removal of Hydroperoxides from the Endoplasmic Reticulum. International Journal of Cell Biology. **2013**, 13

59   Oslowski, C. M. and Urano, F. (2011) Chapter Four - Measuring ER Stress and the Unfolded Protein Response Using Mammalian Tissue Culture System. In Methods in enzymology (Conn, P. M., ed.). pp. 71-92, Academic Press

60   Votyakova, T. V. and Reynolds, I. J. (2004) Detection of hydrogen peroxide with Amplex Red: interference by NADH and reduced glutathione auto-oxidation. Archives of biochemistry and biophysics. **431**, 138-144

61   Zhao, B., Summers, F. A. and Mason, R. P. (2012) Photooxidation of Amplex Red to resorufin: implications of exposing the Amplex Red assay to light. Free radical biology & medicine. **53**, 1080-1087

62   Winterbourn, C. C. (2014) The challenges of using fluorescent probes to detect and quantify specific reactive oxygen species in living cells. Biochimica et biophysica acta. **1840**, 730-738

63   Bass, D. A., Parce, J. W., Dechatelet, L. R., Szejda, P., Seeds, M. C. and Thomas, M. (1983) Flow cytometric studies of oxidative product formation by neutrophils: a graded response to membrane stimulation. J Immunol. **130**, 1910-1917

64   LeBel, C. P., Ischiropoulos, H. and Bondy, S. C. (1992) Evaluation of the probe 2',7'-dichlorofluorescin as an indicator of reactive oxygen species formation and oxidative stress. Chemical research in toxicology. **5**, 227-231

65   Burkitt, M., Jones, C., Lawrence, A. and Wardman, P. (2004) Activation of cytochrome c to a peroxidase compound I-type intermediate by H2O2: relevance to redox signalling in apoptosis. Biochemical Society symposium, 97-106

66   Schaferling, M. G., D. B. M.; Schreml, S. (2011) Luminescent probes for detection and imaging of hydrogen peroxide. Microchim Acta. **174**, 18

67   Belousov, V. V., Fradkov, A. F., Lukyanov, K. A., Staroverov, D. B., Shakhbazov, K. S., Terskikh, A. V. and Lukyanov, S. (2006) Genetically encoded fluorescent indicator for intracellular hydrogen peroxide. Nature methods. **3**, 281-286

68   Christman, M. F., Storz, G. and Ames, B. N. (1989) OxyR, a positive regulator of hydrogen peroxide-inducible genes in Escherichia coli and Salmonella typhimurium, is homologous to a family of bacterial regulatory proteins. Proceedings of the National Academy of Sciences of the United States of America. **86**, 3484-3488

69   Mishina, N. M., Markvicheva, K. N., Bilan, D. S., Matlashov, M. E., Shirmanova, M. V., Liebl, D., Schultz, C., Lukyanov, S. and Belousov, V. V.

(2013) Visualization of intracellular hydrogen peroxide with HyPer, a genetically encoded fluorescent probe. Methods in enzymology. **526**, 45-59

70   Quatresous, E., Legrand, C. and Pouvreau, S. (2012) Mitochondria-targeted cpYFP: pH or superoxide sensor? The Journal of general physiology. **140**, 567-570

71   Frankland, E., Duppa, B. F. (1860) Vorläufige Notiz über Boräthyl European Journal of Organic Chemistry. **115**, 319-322

72   Bull, S. D., Davidson, M. G., van den Elsen, J. M., Fossey, J. S., Jenkins, A. T., Jiang, Y. B., Kubo, Y., Marken, F., Sakurai, K., Zhao, J. and James, T. D. (2013) Exploiting the reversible covalent bonding of boronic acids: recognition, sensing, and assembly. Accounts of chemical research. **46**, 312-326

73   Hall, D. G. (2005) Boronic Acids: Preparation and Applications in Organic Synthesis, Medicine and Materials. Wiley-VCH Verlag GmbH & Co, New Jersey

74   Thomas, S. E. (1991) Organic Synthesis: The Roles of Boron and Silicon. Oxford University Press, Oxford

75   Kuivila, H. G. and Armour, A. G. (1957) Electrophilic Displacement Reactions. IX. Effects of Substituents on Rates of Reactions between Hydrogen Peroxide and Benzeneboronic Acid1-3. Journal of the American Chemical Society. **79**, 5659-5662

76   Lippert, A. R., Van de Bittner, G. C. and Chang, C. J. (2011) Boronate oxidation as a bioorthogonal reaction approach for studying the chemistry of hydrogen peroxide in living systems. Accounts of chemical research. **44**, 793-804

77   Atkins, P., de Paula, J.,. (2006) Atkins' Physical Chemistry. Oxford University Press, Oxford

78   Johnson, I. (1998) Fluorescent probes for living cells. The Histochemical journal. **30**, 123-140

79   Crosby, G. A. and Demas, J. N. (1971) Measurement of photoluminescence quantum yields. Review. The Journal of Physical Chemistry. **75**, 991-1024

80   Lichtman, J. W. and Conchello, J. A. (2005) Fluorescence microscopy. Nature methods. **2**, 910-919

81   Chang, M. C. Y., Pralle, A., Isacoff, E. Y. and Chang, C. J. (2004) A Selective, Cell-Permeable Optical Probe for Hydrogen Peroxide in Living Cells. Journal of the American Chemical Society. **126**, 15392-15393

82   Miller, E. W., Albers, A. E., Pralle, A., Isacoff, E. Y. and Chang, C. J. (2005) Boronate-Based Fluorescent Probes for Imaging Cellular Hydrogen Peroxide. Journal of the American Chemical Society. **127**, 16652-16659

83   Miller, E. W., Tulyathan, O., Isacoff, E. Y. and Chang, C. J. (2007) Molecular imaging of hydrogen peroxide produced for cell signaling. Nat Chem Biol. **3**, 263-267

84   Murphy, M. P. (2008) Targeting lipophilic cations to mitochondria. Biochimica et biophysica acta. **1777**, 1028-1031

85   Mukhopadhyay, P., Rajesh, M., Yoshihiro, K., Hasko, G. and Pacher, P. (2007) Simple quantitative detection of mitochondrial superoxide production in live cells. Biochemical and biophysical research communications. **358**, 203-208

86   Baier, G., Baier-Bitterlich, G., Couture, C., Telford, D., Giampa, L. and Altman, A. (1994) An efficient expression, purification and immunodetection system for recombinant gene products. BioTechniques. **17**, 94, 96, 98-99

87   Chalfie, M., Tu, Y., Euskirchen, G., Ward, W. W. and Prasher, D. C. (1994) Green fluorescent protein as a marker for gene expression. Science. **263**, 802-805

88   Wang, L. and Schultz, P. G. (2004) Expanding the genetic code. Angew Chem Int Ed Engl. **44**, 34-66

89   Gronemeyer, T., Godin, G. and Johnsson, K. (2005) Adding value to fusion proteins through covalent labelling. Current opinion in biotechnology. **16**, 453-458

90   Sletten, E. M. and Bertozzi, C. R. (2011) From mechanism to mouse: a tale of two bioorthogonal reactions. Accounts of chemical research. **44**, 666-676

91   Adams, S. R., Campbell, R. E., Gross, L. A., Martin, B. R., Walkup, G. K., Yao, Y., Llopis, J. and Tsien, R. Y. (2002) New biarsenical ligands and tetracysteine motifs for protein labeling in vitro and in vivo: synthesis and biological applications. Journal of the American Chemical Society. **124**, 6063-6076

92   Daniels, D. S. and Tainer, J. A. (2000) Conserved structural motifs governing the stoichiometric repair of alkylated DNA by O(6)-alkylguanine-DNA alkyltransferase. Mutation research. **460**, 151-163

93   Keppler, A., Gendreizig, S., Gronemeyer, T., Pick, H., Vogel, H. and Johnsson, K. (2003) A general method for the covalent labeling of fusion proteins with small molecules in vivo. Nature biotechnology. **21**, 86-89

94   Toft, N. J., Sansom, O. J., Brookes, R. A., Arends, M. J., Wood, M., Margison, G. P., Winton, D. J. and Clarke, A. R. (2000) In vivo administration of O(6)-benzylguanine does not influence apoptosis or mutation frequency following DNA damage in the murine intestine, but does inhibit P450-dependent activation of dacarbazine. Carcinogenesis. **21**, 593-598

95   Magull-Seltenreich, A. Z., W. (1995) Inhibition of O6-alkylguanine-DNA alkyltransferase in animal and human ovarian tumor cell lines by O6-benzylguanine and sensitization to BCNU. Cancer Chemother. Pharmacol. **35**, 262-266

96   Xu-Welliver, M., Leitao, J., Kanugula, S., Meehan, W. J. and Pegg, A. E. (1999) Role of codon 160 in the sensitivity of human O6-alkylguanine-DNA alkyltransferase to O6-benzylguanine. Biochemical pharmacology. **58**, 1279-1285

97   Damoiseaux, R., Keppler, A. and Johnsson, K. (2001) Synthesis and applications of chemical probes for human O6-alkylguanine-DNA alkyltransferase. Chembiochem : a European journal of chemical biology. **2**, 285-287

98   Pick, H., Jankevics, H. and Vogel, H. (2007) Distribution plasticity of the human estrogen receptor alpha in live cells: distinct imaging of consecutively expressed receptors. J Mol Biol. **374**, 1213-1223

99   Kindermann, M., George, N., Johnsson, N. and Johnsson, K. (2003) Covalent and selective immobilization of fusion proteins. Journal of the American Chemical Society. **125**, 7810-7811

100   Lemercier, G., Gendreizig, S., Kindermann, M. and Johnsson, K. (2007) Inducing and sensing protein--protein interactions in living cells by selective cross-linking. Angew Chem Int Ed Engl. **46**, 4281-4284

101   Srikun, D., Albers, A. E., Nam, C. I., Iavarone, A. T. and Chang, C. J. (2010) Organelle-targetable fluorescent probes for imaging hydrogen peroxide in living cells via SNAP-Tag protein labeling. Journal of the American Chemical Society. **132**, 4455-4465

102   Los, G. V., Encell, L. P., McDougall, M. G., Hartzell, D. D., Karassina, N., Zimprich, C., Wood, M. G., Learish, R., Ohana, R. F., Urh, M., Simpson, D., Mendez, J., Zimmerman, K., Otto, P., Vidugiris, G., Zhu, J., Darzins, A., Klaubert, D. H., Bulleit, R. F. and Wood, K. V. (2008) HaloTag: a novel protein labeling technology for cell imaging and protein analysis. ACS chemical biology. **3**, 373-382

103   Newman, J., Peat, T. S., Richard, R., Kan, L., Swanson, P. E., Affholter, J. A., Holmes, I. H., Schindler, J. F., Unkefer, C. J. and Terwilliger, T. C. (1999) Haloalkane dehalogenases: structure of a Rhodococcus enzyme. Biochemistry. **38**, 16105-16114

104   Pap, E. H., Dansen, T. B., van Summeren, R. and Wirtz, K. W. (2001) Peptide-based targeting of fluorophores to organelles in living cells. Experimental cell research. **265**, 288-293

105   Cabrera, M., Muniz, M., Hidalgo, J., Vega, L., Martin, M. E. and Velasco, A. (2003) The retrieval function of the KDEL receptor requires PKA phosphorylation of its C-terminus. Molecular biology of the cell. **14**, 4114-4125

106   Lee, S., Xie, J. and Chen, X. (2010) Peptide-based probes for targeted molecular imaging. Biochemistry. **49**, 1364-1376

107   Radford, R. J., Chyan, W. and Lippard, S. J. (2013) Peptide-based Targeting of Fluorescent Zinc Sensors to the Plasma Membrane of Live Cells. Chem Sci. **4**, 3080-3084

108   Hwang, C., Sinskey, A. J. and Lodish, H. F. (1992) Oxidized redox state of glutathione in the endoplasmic reticulum. Science. **257**, 1496-1502

109   Schwarz, F. and Aebi, M. (2011) Mechanisms and principles of N-linked protein glycosylation. Current opinion in structural biology. **21**, 576-582

110 Mohorko, E., Glockshuber, R. and Aebi, M. (2011) Oligosaccharyltransferase: the central enzyme of N-linked protein glycosylation. Journal of inherited metabolic disease. **34**, 869-878

111   Kowarik, M., Numao, S., Feldman, M. F., Schulz, B. L., Callewaert, N., Kiermaier, E., Catrein, I. and Aebi, M. (2006) N-linked glycosylation of folded proteins by the bacterial oligosaccharyltransferase. Science. **314**, 1148-1150

112   Quin, C., Robertson, L., McQuaker, S. J., Price, N. C., Brand, M. D. and Hartley, R. C. (2010) Caged mitochondrial uncouplers that are released in response to hydrogen peroxide. Tetrahedron. **66**, 2384-2389

113   Gracia Ferrer, J. B. A., M. A.; Moreno Mollo, I. M.; Pages Santacana, L. M.; Roberts, R. S.; Sevilla Gome, S.; Taltavull Moll, J. (2010) (3-Oxo)pyridazin-4-ylurea derivatives as PDE4 inhibitors. (Office, E. P., ed.)^eds.), Almirall, S. A.

114   Adlington, R. M. B., J. E.; Becker, G. W.; Chen, B.; Cheng, L.; Cooper, S. L.; Hermann, R. B.; Howe, T. J.; McCoull, W.; McNulty, A. M.; Neubauer, B. L.; Pritchard, G. J. (2001) Design, Synthesis, and Proposed Active Site Binding

Analysis of Monocyclic 2-Azetidinone Inhibitors of Prostate Specific Antigen. Journal of medicinal chemistry. **44**, 1491-1508

115   Cocheme, H. M., Quin, C., McQuaker, S. J., Cabreiro, F., Logan, A., Prime, T. A., Abakumova, I., Patel, J. V., Fearnley, I. M., James, A. M., Porteous, C. M., Smith, R. A., Saeed, S., Carre, J. E., Singer, M., Gems, D., Hartley, R. C., Partridge, L. and Murphy, M. P. (2011) Measurement of H2O2 within living Drosophila during aging using a ratiometric mass spectrometry probe targeted to the mitochondrial matrix. Cell metabolism. **13**, 340-350

116   McQuaker, S. J. (2013) Functional molecules to test the free radical theory of aging. In Chemistry ed.)^eds.), University of Glasgow, Glasgow

117   Majoul, I. V., Bastiaens, P. I. and Soling, H. D. (1996) Transport of an external Lys-Asp-Glu-Leu (KDEL) protein from the plasma membrane to the endoplasmic reticulum: studies with cholera toxin in Vero cells. J Cell Biol. **133**, 777-789

118   Kurebayashi, N., Harkins, A. B. and Baylor, S. M. (1993) Use of fura red as an intracellular calcium indicator in frog skeletal muscle fibers. Biophysical journal. **64**, 1934-1960

119   Takahashi, A., Camacho, P., Lechleiter, J. D. and Herman, B. (1999) Measurement of intracellular calcium. Physiological reviews. **79**, 1089-1125

120   Heagy, M. D. (2011) New Fluorophore Design. In Chemosensors. pp. 253-273, John Wiley & Sons, Inc.

121   Kolb, H. C., Finn, M. G. and Sharpless, K. B. (2001) Click Chemistry: Diverse Chemical Function from a Few Good Reactions. Angew Chem Int Ed Engl. **40**, 2004-2021

122   Srikun, D., Miller, E. W., Domaille, D. W. and Chang, C. J. (2008) An ICT-Based Approach to Ratiometric Fluorescence Imaging of Hydrogen Peroxide Produced in Living Cells. Journal of the American Chemical Society. **130**, 4596-4597

123   Oslowski, C. M. and Urano, F. (2011) Measuring ER stress and the unfolded protein response using mammalian tissue culture system. Methods in enzymology. **490**, 71-92

124   Sevier, C. S. and Kaiser, C. A. (2008) Ero1 and redox homeostasis in the endoplasmic reticulum. Biochimica et biophysica acta. **1783**, 549-556

125   Kimura, Y., Matsuura, D., Hanawa, T. and Kobayashi, Y. (2012) New preparation method for Vilsmeier reagent and related imidoyl chlorides. Tetrahedron letters. **53**, 1116-1118

126   Aramendía, M. A., Lafont, F., Moreno-Mañas, M., Pleixats, R. and Roglans, A. (1999) Electrospray Ionization Mass Spectrometry Detection of Intermediates in the Palladium-Catalyzed Oxidative Self-Coupling of Areneboronic Acids. The Journal of organic chemistry. **64**, 3592-3594

127   Meth-Cohn, O. S., S. P. (1991) The Vilsmeier-Haack Reaction. ed.)^eds.). pp. 777-794, Pergamon: Oxford, UK

128   Hansen, T. V., Skatterbol, L. (2005) Ortho-Fomylation of Phenols; Preparation of 3-Bromosalicylaldehyde. Organic Syntheses. **82**, 64-68

129   Aldred, R. J., R.; Levin, D.; Neilan, J. (1994) Magnesium-mediated ortho-Specific Formylation and Formaldoximation of Phenols. J. Chem. Soc. Perkin. Trans. **1**, 1823-1831

130   Bellur, E., Yawer, M. A., Hussain, I., Riahi, A., Fatunsin, O., Fischer, C. and Langer, P. (2009) Synthesis of 3-Acylpyrroles, 3-(Alkoxycarbonyl)pyrroles, 1,5,6,7-Tetrahydro-4H-indol-4-ones and 3-Benzoylpyridines Based on Staudinger-Aza-Wittig Reactions of 1,3-Dicarbonyl Compounds with 2-and 3-Azido-1,1-dialkoxyalkanes. Synthesis-Stuttgart, 227-242

131   Wang, Z. (2010) Lemieux-Johnson Oxidation. In Comprehensive Organic Name Reactions and Reagents, John Wiley & Sons, Inc.

132   Schroeder, M. (1980) Osmium tetraoxide cis hydroxylation of unsaturated substrates. Chemical reviews. **80**, 187-213

133   Demko, Z. P. and Sharpless, K. B. (2002) A click chemistry approach to tetrazoles by Huisgen 1,3-dipolar cycloaddition: Synthesis of 5-acyltetrazoles from azides and acyl cyanides. Angew Chem Int Edit. **41**, 2113-2116

134   Jones, G. (2004) The Knoevenagel Condensation. In Organic Reactions, John Wiley & Sons, Inc.

135   Gibson, M. S. and Bradshaw, R. W. (1968) Gabriel Synthesis of Primary Amines. Angew Chem Int Edit. **7**, 919-&

136   Gomez-Martinez, M., Schmitz, D. and Hergovich, A. (2013) Generation of stable human cell lines with Tetracycline-inducible (Tet-on) shRNA or cDNA expression. Journal of visualized experiments : JoVE, e50171

137 Bergen, J. M., Kwon, E. J., Shen, T. W. and Pun, S. H. (2007) Application of an Environmentally Sensitive Fluorophore for Rapid Analysis of the Binding and Internalization Efficiency of Gene Carriers. Bioconjugate chemistry. **19**, 377-384

138 Lin, V. S., Dickinson, B. C. and Chang, C. J. (2013) Boronate-based fluorescent probes: imaging hydrogen peroxide in living systems. Methods in enzymology. **526**, 19-43

139 Ho, C. S., Lam, C. W., Chan, M. H., Cheung, R. C., Law, L. K., Lit, L. C., Ng, K. F., Suen, M. W. and Tai, H. L. (2003) Electrospray ionisation mass spectrometry: principles and clinical applications. The Clinical biochemist. Reviews / Australian Association of Clinical Biochemists. **24**, 3-12

140 Marvin, L. F., Roberts, M. A. and Fay, L. B. (2003) Matrix-assisted laser desorption/ionization time-of-flight mass spectrometry in clinical chemistry. Clinica chimica acta; international journal of clinical chemistry. **337**, 11-21

141 Montalbetti, C. A. G. N. and Falque, V. (2005) Amide bond formation and peptide coupling. Tetrahedron. **61**, 10827-10852

142 Sechi, S. and Chait, B. T. (1998) Modification of Cysteine Residues by Alkylation. A Tool in Peptide Mapping and Protein Identification. Analytical chemistry. **70**, 5150-5158

143 Kawanishi, T., Romey, M. A., Zhu, P. C., Holody, M. Z. and Shinkai, S. (2004) A study of boronic acid based fluorescent glucose sensors. Journal of fluorescence. **14**, 499-512

144 J, B. C., Zhang, W. and W, L. S. (2011) Facile analysis and sequencing of linear and branched peptide boronic acids by MALDI mass spectrometry. Analytical chemistry. **83**, 3548-3554

145 Yu, H. C., Lu, M. C., Li, C., Huang, H., Huang, K. Y., Liu, S. Q., Lai, N. S. and Huang, H. B. (2013) Targeted Delivery of an Antigenic Peptide to the Endoplasmic Reticulum: Application for Development of a Peptide Therapy for Ankylosing Spondylitis. PloS one. **8**, e77451

146 Wieland, F. T., Gleason, M. L., Serafini, T. A. and Rothman, J. E. (1987) The rate of bulk flow from the endoplasmic reticulum to the cell surface. Cell. **50**, 289-300

147 Ogata, S., Muramatsu, T. and Kobata, A. (1975) Fractionation of glycopeptides by affinity column chromatography on concanavalin A-sepharose. Journal of biochemistry. **78**, 687-696

148   Chien, S. F., Weinburg, R., Li, S. C. and Li, Y. T. (1977) Endo-β-N-acetylglucosaminidase from fig latex. Biochemical and biophysical research communications. **76**, 317-323

149   Capitani, M. and Sallese, M. (2009) The KDEL receptor: new functions for an old protein. FEBS letters. **583**, 3863-3871

150   Singh, K. V., Kaur, J., Varshney, G. C., Raje, M. and Suri, C. R. (2004) Synthesis and characterization of hapten-protein conjugates for antibody production against small molecules. Bioconjugate chemistry. **15**, 168-173

151   Ross, A. H., Baltimore, D. and Eisen, H. N. (1981) Phosphotyrosine-containing proteins isolated by affinity chromatography with antibodies to a synthetic hapten. Nature. **294**, 654-656

152   Varshney, A., Rabbani, G., Badr, G. and Khan, R. H. (2014) Cosolvents induced unfolding and aggregation of keyhole limpet hemocyanin. Cell biochemistry and biophysics. **69**, 103-113

153   Wang, Z. (2010) Appel Reaction. In Comprehensive Organic Name Reactions and Reagents, John Wiley & Sons, Inc.

154   Jackson, A. M., Boutell, J., Cooley, N. and He, M. (2004) Cell-free protein synthesis for proteomics. Briefings in functional genomics & proteomics. **2**, 308-319

155   Lau, J. T., Welply, J. K., Shenbagamurthi, P., Naider, F. and Lennarz, W. J. (1983) Substrate recognition by oligosaccharyl transferase. Inhibition of co-translational glycosylation by acceptor peptides. The Journal of biological chemistry. **258**, 15255-15260

156   Finkel, T. (2011) Signal transduction by reactive oxygen species. J Cell Biol. **194**, 7-15

157   Dupuy, C., Virion, A., Ohayon, R., Kaniewski, J., Deme, D. and Pommier, J. (1991) Mechanism of hydrogen peroxide formation catalyzed by NADPH oxidase in thyroid plasma membrane. The Journal of biological chemistry. **266**, 3739-3743

158   Kembro, J. M., Aon, M. A., Winslow, R. L., O'Rourke, B. and Cortassa, S. (2013) Integrating mitochondrial energetics, redox and ROS metabolic networks: a two-compartment model. Biophysical journal. **104**, 332-343

159   Bulleid, N. J. and Ellgaard, L. (2011) Multiple ways to make disulfides. Trends in biochemical sciences. **36**, 485-492

160   Lu, S. C. (2009) Regulation of glutathione synthesis. Molecular aspects of medicine. **30**, 42-59

161   Arthur, J. R. (2000) The glutathione peroxidases. Cellular and molecular life sciences : CMLS. **57**, 1825-1835

162   Saito, Y., Nishio, K., Ogawa, Y., Kimata, J., Kinumi, T., Yoshida, Y., Noguchi, N. and Niki, E. (2006) Turning point in apoptosis/necrosis induced by hydrogen peroxide. Free radical research. **40**, 619-630

163   Aslund, F., Zheng, M., Beckwith, J. and Storz, G. (1999) Regulation of the OxyR transcription factor by hydrogen peroxide and the cellular thiol-disulfide status. Proceedings of the National Academy of Sciences of the United States of America. **96**, 6161-6165

164   Gutscher, M., Sobotta, M. C., Wabnitz, G. H., Ballikaya, S., Meyer, A. J., Samstag, Y. and Dick, T. P. (2009) Proximity-based protein thiol oxidation by H2O2-scavenging peroxidases. The Journal of biological chemistry. **284**, 31532-31540

165   Chen, X., Zhong, Z., Xu, Z., Chen, L. and Wang, Y. (2010) 2',7'-Dichlorodihydrofluorescein as a fluorescent probe for reactive oxygen species measurement: Forty years of application and controversy. Free radical research. **44**, 587-604

166   Cocheme, H. M., Logan, A., Prime, T. A., Abakumova, I., Quin, C., McQuaker, S. J., Patel, J. V., Fearnley, I. M., James, A. M., Porteous, C. M., Smith, R. A., Hartley, R. C., Partridge, L. and Murphy, M. P. (2012) Using the mitochondria-targeted ratiometric mass spectrometry probe MitoB to measure H2O2 in living Drosophila. Nature protocols. **7**, 946-958

167   Bienert, G. P. and Chaumont, F. (2014) Aquaporin-facilitated transmembrane diffusion of hydrogen peroxide. Biochimica et biophysica acta. **1840**, 1596-1604

168   Szent-Gyorgyi, C., Schmidt, B. F., Creeger, Y., Fisher, G. W., Zakel, K. L., Adler, S., Fitzpatrick, J. A., Woolford, C. A., Yan, Q., Vasilev, K. V., Berget, P. B., Bruchez, M. P., Jarvik, J. W. and Waggoner, A. (2008) Fluorogen-activating single-chain antibodies for imaging cell surface proteins. Nature biotechnology. **26**, 235-240

169   Hoffhines, A. J., Damoc, E., Bridges, K. G., Leary, J. A. and Moore, K. L. (2006) Detection and purification of tyrosine-sulfated proteins using a novel anti-

sulfotyrosine monoclonal antibody. The Journal of biological chemistry. **281**, 37877-37887

170   Orth, P., Schnappinger, D., Hillen, W., Saenger, W. and Hinrichs, W. (2000) Structural basis of gene regulation by the tetracycline inducible Tet repressor-operator system. Nature structural biology. **7**, 215-219

171   Risseeuw, M. D., De Clercq, D. J., Lievens, S., Hillaert, U., Sinnaeve, D., Van den Broeck, F., Martins, J. C., Tavernier, J. and Van Calenbergh, S. (2013) A "clickable" MTX reagent as a practical tool for profiling small-molecule-intracellular target interactions via MASPIT. ChemMedChem. **8**, 521-526